VOLUME 102

OCT 3 0 1945

NUMBER 2

THE ASTROPHYSICAL JOURNAL

AN INTERNATIONAL REVIEW OF SPECTROSCOPY AND ASTRONOMICAL PHYSICS

Founded in 1895 by GEORGE E. HALE *and* JAMES E. KEELER

SEPTEMBER 1945

ON THE RADIAL PULSATION OF GASEOUS STARS . . . . . *P. Ledoux* 143

CHEMICAL COMPOUNDS IN THE SUN . . . . . *Harold D. Babcock* 154

T TAURI VARIABLE STARS . . . . . *Alfred H. Joy* 168

PRELIMINARY COLOR INDICES FOR STARS OF LARGE PROPER MOTION. II *Willem J. Luyten and Martin Dartayet* 196

THE PHOTOMETRIC ORBIT OF QY AQUILAE . . . . . *Balfour S. Whitney* 202

COMMENTS ON CAPTAIN WHITNEY'S PAPER . . . . . *Henry Norris Russell* 207

ON THE INTERNAL CONSTITUTION OF STARS OF SMALL MASSES ACCORDING TO BETHE'S LAW OF ENERGY GENERATION . . . *N. R. Sen and U. R. Burman* 208

A STELLAR MODEL WITH A GRAVITATIONAL SOURCE OF ENERGY *Marjorie Hall Harrison* 216

ON THE CONTINUOUS ABSORPTION COEFFICIENT OF THE NEGATIVE HYDROGEN ION . . . . . *S. Chandrasekhar* 223

THE VELOCITY-CURVES OF SEVEN CEPHEID VARIABLES . . . *Otto Struve* 232

PHYSICAL PROCESSES IN GASEOUS NEBULAE. XVIII. THE CHEMICAL COMPOSITION OF THE PLANETARY NEBULAE . *Lawrence H. Aller and Donald H. Menzel* 239

REVIEWS 264

THE UNIVERSITY OF CHICAGO PRESS
CHICAGO, ILLINOIS, U.S.A.

September 1945 Vol. 102, No. 2

THE ASTROPHYSICAL JOURNAL

AN INTERNATIONAL REVIEW OF SPECTROSCOPY AND ASTRONOMICAL PHYSICS

The Astrophysical Journal is published bimonthly by the University of Chicago at the University of Chicago Press, 5750 Ellis Avenue, Chicago, Illinois, during July, September, November, January, March, and May. ¶The subscription price is $10.00 a year; the price of single copies is $2.00. Orders for service of less than a full year will be charged at the single-copy rate. ¶Postage is prepaid by the publishers on all orders from the United States and its possessions, Argentina, Bolivia, Brazil, Chile, Colombia, Costa Rica, Cuba, Dominican Republic, Ecuador, Guatemala, Haiti, Republic of Honduras, Mexico, Morocco (Spanish Zone), Nicaragua, Panama, Paraguay, Peru, Rio de Oro, El Salvador, Spain (including Balearic Islands, Canary Islands, and the Spanish Offices in Northern Africa; Andorra), Spanish Guinea, Uruguay, and Venezuela. ¶Postage is charged extra as follows: for Canada and Newfoundland, 42 cents on annual subscriptions (total $10.42); on single copies, 7 cents (total $2.07); for all other countries in the Postal Union, 96 cents on annual subscriptions (total $10.96), on single copies 16 cents (total $2.16). ¶Patrons are requested to make all remittances payable to The University of Chicago Press, in United States currency or its equivalent by postal or express money orders or bank drafts.

The following are authorized agents:

For the British Empire, except North America, India, and Australasia: The Cambridge University Press, Bentley House, 200 Euston Road, London, N.W. 1, England. Prices of yearly subscriptions and of single copies may be had on application.

Claims for missing numbers should be made within the month following the regular month of publication. The publishers expect to supply missing numbers free only when losses have been sustained in transit, and when the reserve stock will permit.

Business correspondence should be addressed to The University of Chicago Press, Chicago 37, Illinois.

Communications for the editors and manuscripts should be addressed to: Otto Struve, Editor of THE ASTROPHYSICAL JOURNAL, Yerkes Observatory, Williams Bay, Wisconsin.

Line drawings and photographs should be made by the author, and all marginal notes such as co-ordinates, wave lengths, etc., should be included in the cuts. It will not be possible to set up such material in type.

One copy of the corrected galley proof should be returned as soon as possible to the editor, Yerkes Observatory, Williams Bay, Wisconsin. Authors should take notice that the manuscript will not be sent to them with the proof.

The cable address is "Observatory, Williamsbay, Wisconsin."

The articles in this journal are indexed in the *International Index to Periodicals*, New York, N.Y.

Applications for permission to quote from this journal should be addressed to The University of Chicago Press, and will be freely granted.

Entered as second-class matter, July 31, 1940, at the Post-Office at Chicago, Ill., under the act of March 3, 1879.
Acceptance for mailing at special rate of postage provided for in United States Postal Act of October 3, 1917, Section 1103, amended February 28, 1925.

[PRINTED IN U.S.A.]

THE ASTROPHYSICAL JOURNAL

AN INTERNATIONAL REVIEW OF SPECTROSCOPY AND ASTRONOMICAL PHYSICS

VOLUME 102 SEPTEMBER 1945 NUMBER 2

ON THE RADIAL PULSATION OF GASEOUS STARS

P. LEDOUX

F/L.R.A.F., Stanleyville, Belgian Congo

Received May 22, 1945

ABSTRACT

An application of the virial theorem to the radial pulsation of gaseous stars leads to a simple derivation of the approximate formula

$$\tau = 2\pi\left(\frac{I_0}{-[3\Gamma_1 - 4]\,\Omega_0}\right)^{1/2} \qquad \text{(i)}$$

for the period found earlier (*Ap. J.*, **94**, 124, 1941) by a variational method. In the foregoing formula I_0 denotes the moment of inertia and Ω_0 the potential energy of the star, and Γ_1 is the adiabatic exponent assumed constant through the star.

If the star is in steady uniform rotation, in the same approximation, the theorem gives

$$\tau = 2\pi\left(\frac{I_0}{-[3\Gamma_1 - 4]\Omega_0 + [5 - 3\Gamma_1]\omega_0\mathfrak{M}}\right)^{1/2}, \qquad \text{(ii)}$$

where ω_0 denotes the angular velocity and $\mathfrak{M}$ is the total angular momentum of the star. In the case of a homogeneous distribution of mass, equation (ii) reduces to a formula which can be derived directly from one of Poincaré's theorems. When $\frac{4}{3} < \Gamma_1 < \frac{5}{3}$ and under the circumstances of validity of the approximations used, the decrease in period due to the rotation is small.

1. *The application of the virial theorem to the steady pulsations of a gaseous star.*—For a cloud of particles which act on each other only by gravitational attraction or shocks we have the Lagrangian identity

$$\frac{1}{2}\frac{d^2I}{dt^2} = 2T + \Omega\,, \qquad (1)$$

where I is the moment of inertia with respect to the origin, T the kinetic energy, and Ω is the gravitational potential energy of the star. Equation (1) is the form given by Jacobi to a theorem originally due to Lagrange for three bodies. For a spherical distribution of mass

$$I = \int_0^M r^2 dm\,(r) \qquad \text{and} \qquad \Omega = -G\int_0^M \frac{m\,(r)\,dm\,(r)}{r}\,, \qquad (2)$$

where $m(r)$ denotes the mass interior to r and M is the total mass of the configuration.

In this paper we shall consider the application of equation (1) to the steady radial pulsations of a gaseous star. In studying this problem we shall adopt the Lagrangian mode of description, in which we follow each particle (or element of mass) during its mo-

tion. Let the distance r from the center of symmetry be used as such a Lagrangian coordinate. Further, let δr denote the displacement from the "equilibrium" position r_0. The conservation of mass clearly requires that

$$m(r_0+\delta r) = m(r_0). \tag{3}$$

Let δI, δT, and $\delta\Omega$ denote the changes from their equilibrium values in the respective quantities at time t. Equation (1) gives

$$\frac{1}{2}\frac{d^2\delta I}{dt^2} = 2\delta T + \delta\Omega. \tag{4}$$

To a first order in δr we have (cf. eq. [2])

$$\delta I = 2\int_0^M r\,\delta r\,dm(r) \simeq 2\int_0^M \frac{\delta r}{r_0}\,dI_0 \tag{5}$$

and

$$\delta\Omega = G\int_0^M \frac{m(r)\,\delta(r)}{r^2}\,dm(r) \simeq -\int_0^M \frac{\delta r}{r_0}\,d\Omega_0, \tag{5'}$$

where we have used the suffix zero to indicate that the quantities refer to the instant when $r = r_0$.

For small periodic oscillations we may write

$$\frac{\delta r}{r_0} = \xi = \xi_0 e^{i\sigma t}, \tag{6}$$

where $2\pi/\sigma$ denotes the period. Equations (5) and (5') now become

$$\delta I = 2e^{i\sigma t}\int_0^M \xi_0 dI_0 \quad \text{and} \quad \delta\Omega = -e^{i\sigma t}\int_0^M \xi_0 d\Omega_0. \tag{7}$$

Considering next the evaluation of δT, we may first observe that T consists of two parts: the kinetic energy due to thermal motions and the kinetic energy due to the vibrations. It is evident that the latter is of the second order in ξ and can therefore be ignored in a first-order theory. Accordingly, we need to consider only the variation in the total kinetic energy T, stored in the form of thermal motions. If the radiation pressure is negligible, we have the relation

$$2T_1 = 3\int_0^M \frac{p_g}{\rho}\,dm(r), \tag{8}$$

where p_g denotes the gas pressure and ρ the density. On the other hand, if the radiation pressure is included, the usual argument which leads to equation (1) shows that equation (8) has to be replaced by (cf. eq. [66], below)

$$2T_1 = 3\int_0^M \frac{P}{\rho}\,dm(r). \tag{9}$$

where P is the total pressure, including the gas and the radiation pressures. Thus, to the first order

$$2\delta T = 2\delta T_1 = 3\int_0^M \delta\left(\frac{P}{\rho}\right) dm(r_0). \tag{10}$$

We shall now suppose that the pulsations are adiabatic, in which case

$$\delta\left(\frac{P}{\rho}\right) = \frac{P_0}{\rho_0}(\Gamma_1 - 1)\frac{\delta\rho}{\rho_0}, \tag{11}$$

where Γ_1 is the adiabatic exponent properly defined. Moreover, if $d\xi/dr_0$ is further assumed to be a small quantity of the first order everywhere, the equation of continuity leads to the relation

$$\frac{\delta\rho}{\rho_0} = -\left(3\xi_0 + r_0\frac{d\xi_0}{dr_0}\right)e^{i\sigma t}. \tag{12}$$

Combining equations (10), (11), and (12), we obtain

$$2\delta T = -9e^{i\sigma t}\int_0^M \frac{P_0}{\rho_0}(\Gamma_1-1)\,\xi_0 dm(r_0) - 3e^{i\sigma t}\int_0^{R_0} 4\pi P_0(\Gamma_1-1)\frac{d\xi_0}{dr_0}r_0^3 dr_0. \tag{13}$$

Integrating by parts the second of the two integrals on the right-hand side of equation (13), we find

$$\left.\begin{aligned} 4\pi\int_0^{R_0} P_0(\Gamma_1-1)\,r_0^3\frac{d\xi_0}{dr_0}\,dr_0 &= 4\pi P_0(\Gamma_1-1)\,r_0^3\xi_0\Big|_0^{R_0} - 4\pi\int_0^{R_0} P_0\xi_0 r_0^3\,d\Gamma_1 \\ &\quad - 4\pi\int_0^{R_0}(\Gamma_1-1)\,\xi_0\frac{dP_0}{dr_0}r_0^3 dr_0 - 12\pi\int_0^{R_0} P_0(\Gamma_1-1)\,\xi_0 r_0^2 dr_0. \end{aligned}\right\} \tag{14}$$

The integrated part vanishes at both limits, and we are left with (cf. eq. [2])

$$\left.\begin{aligned} 4\pi\int_0^{R_0} P_0(\Gamma_1-1)\,r_0^3\frac{d\xi_0}{dr_0}\,dr_0 &= -\int_0^M \frac{P_0}{\rho_0}\xi_0 r_0\frac{d\Gamma_1}{dr_0}\,dm(r_0) \\ &\quad - 3\int_0^M \xi_0\frac{P_0}{\rho_0}(\Gamma_1-1)\,dm(r_0) - \int_0^M \xi_0(\Gamma_1-1)\,d\Omega_0, \end{aligned}\right\} \tag{15}$$

where in transforming the second of the three integrals on the right-hand side of equation (14) we have used the relation

$$4\pi r_0^3\frac{dP_0}{dr_0} = -4\pi r_0^3\frac{Gm(r_0)}{r_0^2}\rho_0 = -\frac{Gm(r_0)\,dm(r_0)}{r_0 dr_0} = \frac{d\Omega_0}{dr_0}. \tag{16}$$

Equations (13) and (15) now give

$$2\delta T = 3e^{i\sigma t}\int_0^M \frac{P_0}{\rho_0}\xi_0 r_0\frac{d\Gamma_1}{dr_0}\,dm(r_0) + 3e^{i\sigma t}\int_0^M \xi_0(\Gamma_1-1)\,d\Omega_0. \tag{17}$$

Finally, introducing equations (7) and (17) into equation (4), we obtain

$$-\sigma^2\int_0^M \xi_0 dI_0 = 3\int_0^M \frac{P_0}{\rho_0}\xi_0 r_0\frac{d\Gamma_1}{dr_0}\,dm(r_0) + 3\int_0^M \xi_0(\Gamma_1-1)\,d\Omega_0 - \int_0^M \xi_0 d\Omega_0, \tag{18}$$

or

$$\sigma^2 = -\frac{\displaystyle\int_0^M (3\Gamma_1-4)\,\xi_0 d\Omega_0 + 3\int_0^M \frac{P_0}{\rho_0}\xi_0 r_0\frac{d\Gamma_1}{dr_0}\,dm(r_0)}{\displaystyle\int_0^M \xi_0 dI_0}. \tag{19}$$

Equation (19) for the period is of the same general form as the one obtained in an earlier paper.[1] However, in that paper σ^2 was defined, in accordance with the Ritz principle, as the minimum of a similar expression which included terms of the second order in ξ_0.

[1] P. Ledoux and C. L. Pekeris, *Ap. J.*, **94**, 124, 1941. This paper will be referred to as "I."

If Γ_1 is assumed to be independent of r_0, equation (19) reduces to

$$\sigma^2 = -\frac{(3\Gamma_1 - 4)\int_0^M \xi_0 d\Omega_0}{\int_0^M \xi_0 dI_0}. \tag{20}$$

If we further suppose that ξ_0 is a constant, we recover the formula

$$\sigma^2 = -\frac{(3\Gamma_1 - 4)\,\Omega_0}{I_0}, \tag{21}$$

obtained in paper I. As has been shown in paper I, equation (21) already provides a fair approximation to the true periods if the central condensation of the star is not too high.

The extension of the foregoing analysis to include second-order terms is feasible and may give indications as to the manner in which σ^2 may be expected to change when the amplitudes of the pulsation become large. However, in such cases the assumption that the pulsations are adiabatic will require reconsideration.

2. *Application of one of Poincaré's theorems*[2] *to the pulsation of a rotating configuration.*— The problem of a rotating gaseous configuration in pulsation is a difficult one. But we may expect that a general theorem such as the one we have referred to will give us some idea as to the effect of rotation on the period.

Consider, then, the case of a uniformly rotating gaseous configuration in which at any given instant the angular velocity is the same throughout the mass. Since we have in view the pulsation of such a configuration, we must allow $\boldsymbol{\omega}$ to be a function of time. Under these conditions the equation of motion in a frame of reference rotating with an angular velocity $\boldsymbol{\omega}$ is

$$\frac{d\boldsymbol{v}}{dt} = -\frac{1}{\rho}\operatorname{grad} P + \operatorname{grad} \mathfrak{V} - \boldsymbol{\omega} \times (\boldsymbol{\omega} \times \boldsymbol{r}) - 2(\boldsymbol{\omega} \times \boldsymbol{v}) - \left(\frac{d\boldsymbol{\omega}}{dt} \times \boldsymbol{r}\right), \tag{22}$$

where P denotes the total pressure, ρ the density, and $\mathfrak{V}$ the gravitational potential governed by Poisson's equation,

$$\nabla^2 \mathfrak{V} = -4\pi G\rho\,. \tag{23}$$

Under the circumstances envisaged,

$$\boldsymbol{v} = \frac{d\,\delta\boldsymbol{r}}{dt}, \tag{24}$$

where $\delta\boldsymbol{r}$ denotes the displacement, at time t, of an element of gas whose equilibrium position is $\boldsymbol{r}_0$ (say). Since the problem admits of an axial symmetry, it would appear that $\delta\boldsymbol{r}$ will lie in the meridian plane. If we assume that this is the case, $\boldsymbol{v}$ will also lie in this plane, and the two last terms on the right-hand side of equation (22) are the only vectors in this equation which are normal to the meridian plane. Accordingly, we must require that

$$2(\boldsymbol{\omega} \times \boldsymbol{v}) + \frac{d\boldsymbol{\omega}}{dt} \times \boldsymbol{r} \equiv 0\,. \tag{25}$$

In spherical polar co-ordinates (with the z-axis along the axis of rotation) equation (25) takes the form

$$2\left(\omega r \cos\vartheta \frac{d\vartheta}{dt} + \omega \sin\vartheta \frac{dr}{dt}\right) + r \sin\vartheta \frac{d\omega}{dt} = 0\,, \tag{26}$$

[2] *Leçons sur les hypothèses cosmogoniques*, p. 22, Paris, 1911.

or, somewhat differently,

$$\frac{1}{\omega}\frac{d\omega}{dt} = -\frac{2}{r}\frac{dr}{dt} - 2\cot\vartheta\,\frac{d\vartheta}{dt}. \tag{27}$$

Equation (27) admits of immediate integration, and we have

$$\omega r^2 \sin^2\vartheta = \text{constant}. \tag{28}$$

The foregoing equation (28) expresses merely the conservation of angular momentum. We must, of course, expect this to be an integral of our problem. Thus, for pulsations in which the angular momentum is identically conserved, the displacements $\delta\boldsymbol{r}$ lie in the meridian planes, and the equation of motion (22) simplifies to

$$\frac{d\boldsymbol{v}}{dt} = -\frac{1}{\rho}\operatorname{grad} P + \operatorname{grad}\mathfrak{V} - \boldsymbol{\omega}\times(\boldsymbol{\omega}\times\boldsymbol{r}). \tag{29}$$

On the other hand,

$$\boldsymbol{\omega}\times(\boldsymbol{\omega}\times\boldsymbol{r}) = -\tfrac{1}{2}\omega^2 \operatorname{grad}(x^2+y^2) = -\tfrac{1}{2}\omega^2 \operatorname{grad}(r^2\sin^2\vartheta). \tag{30}$$

We can, accordingly, re-write equation (29) in the standard form

$$\frac{d\boldsymbol{v}}{dt} = -\frac{1}{\rho}\operatorname{grad} P + \operatorname{grad}\phi, \tag{31}$$

where

$$\phi = \mathfrak{V} + \tfrac{1}{2}\omega^2(x^2+y^2). \tag{32}$$

At the equilibrium position, $\boldsymbol{v} = 0$; and equation (31) reduces to

$$\frac{1}{\rho_0}\operatorname{grad}_0 P_0 = \operatorname{grad}_0 \phi_0, \tag{33}$$

where, as in § 1, the suffix zero is used to indicate that the quantities are assigned their equilibrium values.

Proceeding as in Poincaré's analysis, we take the divergence of equation (31) and integrate over the entire volume occupied by the configuration. We obtain

$$\int_V \frac{d}{dt}(\operatorname{div}\boldsymbol{v})\,dV = \int_V (2\omega^2 - 4\pi G\rho)\,dV - \int_V \operatorname{div}\left(\frac{1}{\rho}\operatorname{grad} P\right)dV, \tag{34}$$

use having been made of the relation (cf. eq. [23])

$$\left.\begin{aligned}\operatorname{div}\operatorname{grad}\phi &= \nabla^2\mathfrak{V} + \frac{\omega^2}{2}\nabla^2(x^2+y^2)\\ &= -4\pi G\rho + 2\omega^2.\end{aligned}\right\} \tag{35}$$

The first of the two integrals on the right-hand side of equation (34) is readily evaluated; and, transforming the second into a surface integral by Gauss's theorem, we find

$$\int_V \frac{d}{dt}(\operatorname{div}\boldsymbol{v})\,dV = 2\omega^2 V - 4\pi GM - \int_S \frac{1}{\rho}\operatorname{grad} P\cdot \mathbf{1}_{dS}\,dS, \tag{36}$$

where the surface integral is extended over the entire bounding surface S of the configuration and $\mathbf{1}_{dS}$ is a unit vector normal to element of surface dS of S.

Now, in virtue of equation (24), we may regard $\boldsymbol{v}$ as a quantity of the first order of smallness. Hence, in an approximation in which we ignore all quantities of the second

order of smallness we may interchange the differentiation with respect to t and an integration over the spatial co-ordinates. Thus, in this approximation equation (36) becomes

$$\frac{d^2V}{dt^2} = 2\omega^2 V - 4\pi GM - \int_S \frac{1}{\rho} \operatorname{grad} P \cdot \mathbf{1}_{dS} dS \,. \tag{37}$$

Writing $V = V_0 + \delta V$, etc., in equation (37), we obtain

$$\frac{d^2\delta V}{dt^2} = 2\delta(\omega^2 V) - \delta \int_S \frac{1}{\rho} \operatorname{grad} P \cdot \mathbf{1}_{dS} dS \,. \tag{38}$$

We shall now suppose that δr is along r and that $\delta r/r_0$ can again be represented as in equation (6). Under these circumstances equation (28) allows us to conclude that

$$\frac{\delta\omega}{\omega_0} = -2\frac{dr}{r_0} = -2\xi_0 e^{i\sigma t} \,. \tag{39}$$

Moreover, it is clear that, to be consistent with our assumption of uniform rotation (ω independent of spatial co-ordinates), we should also suppose that

$$\xi_0 = \text{constant} \tag{40}$$

throughout the entire configuration. As we have seen in § 1, this assumption leads, in most cases, to a fair approximation for the period and is therefore to be regarded as not too restrictive. On the assumption (40)

$$\frac{\delta\rho}{\rho_0} = -3\xi_0 e^{i\sigma t} \quad \text{and} \quad \frac{\delta V}{V_0} = 3\xi_0 e^{i\sigma t} \,. \tag{41}$$

Further, according to equations (39) and (41),

$$2\delta(\omega^2 V) = 2\omega_0^2 V_0 \left(2\frac{\delta\omega}{\omega_0} + \frac{\delta V}{V_0}\right) = -2\omega_0^2 V_0 \xi_0 e^{i\sigma t} \,. \tag{42}$$

Again, to a first approximation, we have

$$\delta \int_S \frac{1}{\rho} \operatorname{grad} P \cdot \mathbf{1}_{dS} dS = \int_{S_0} \delta\left(\frac{1}{\rho} \operatorname{grad} P\right) \cdot \mathbf{1}_{dS_0} dS_0 + \int \frac{1}{\rho_0} \operatorname{grad}_0 P_0 \cdot \delta(\mathbf{1}_{dS} dS) \,. \tag{43}$$

As in § 1, we shall assume that during the pulsations the changes of state take place adiabatically. Then

$$\delta\left(\frac{1}{\rho} \operatorname{grad} P\right) = -\frac{\delta\rho}{\rho_0}\frac{1}{\rho_0} \operatorname{grad}_0 P_0 + \frac{1}{\rho_0} \operatorname{grad}_0\left(\Gamma_1 P_0 \frac{\delta\rho}{\rho_0}\right) + \frac{1}{\rho_0}(\delta \operatorname{grad}) P_0 \,. \tag{44}$$

Now the components proportional to $\partial/\partial r$ and $\partial/r\partial\vartheta$ of the gradient operator at time t have the values

$$\frac{1}{1+\xi}\frac{\partial}{\partial r_0} \quad \text{and} \quad \frac{1}{1+\xi}\frac{1}{r_0}\frac{\partial}{\partial\vartheta} \,. \tag{45}$$

Accordingly,

$$\delta(\operatorname{grad}) = -\xi_0 e^{i\sigma t} \operatorname{grad}_0 \,. \tag{46}$$

Restricting ourselves further to the case where Γ_1 is a constant, we have

$$\frac{1}{\rho_0} \operatorname{grad}_0\left(\Gamma_1 P_0 \frac{\delta\rho}{\rho_0}\right) = \frac{\Gamma_1 P_0}{\rho_0} \operatorname{grad} \frac{\delta\rho}{\rho_0} + \frac{\Gamma_1}{\rho_0}\frac{\delta\rho}{\rho_0} \operatorname{grad}_0 P_0 \,, \tag{47}$$

or, since $\delta\rho/\rho_0$ is independent of spatial co-ordinates (cf. eqs. [40] and [41]),

$$\frac{1}{\rho_0}\operatorname{grad}_0\left(\Gamma_1 P_0\frac{\delta\rho}{\rho_0}\right)=-3\xi_0 e^{i\sigma t}\frac{\Gamma_1}{\rho_0}\operatorname{grad}_0 P_0\,. \tag{48}$$

Combining equations (44), (46), and (48) and after some further minor reductions, we find

$$\delta\left(\frac{1}{\rho}\operatorname{grad}P\right)=\xi_0 e^{i\sigma t}(2-3\Gamma_1)\frac{1}{\rho_0}\operatorname{grad}_0 P_0\,. \tag{49}$$

Now, since the bounding surface S of the configuration must be an equipotential surface,

$$1_{dS}=\frac{\operatorname{grad}\phi}{|\operatorname{grad}\phi|}\,. \tag{50}$$

Also, we may write

$$dS=2\pi r^2\sin\vartheta\,d\vartheta\,. \tag{50'}$$

Further, under the assumptions made concerning δr, it is evident that the direction of the normal is left unchanged during the pulsation. Hence,

$$\delta\,(1_{dS}dS)\;=2\xi_0 e^{i\sigma t}\,(1_{dS_0}dS_0)\,. \tag{51}$$

Introducing equations (49) and (51) into equation (43), we have

$$\delta\int_S\frac{1}{\rho}\operatorname{grad}P\cdot 1_{dS}dS=(4-3\Gamma_1)\,\xi_0 e^{i\sigma t}\int_{S_0}\frac{1}{\rho_0}\operatorname{grad}_0 P\cdot 1_{dS_0}dS_0\,. \tag{52}$$

The foregoing equation can be further simplified by the use of equations (32) and (33). Thus,

$$\left.\begin{aligned}\delta\int_S\frac{1}{\rho}\operatorname{grad}P\cdot 1_{dS}dS&=(4-3\Gamma_1)\,\xi_0 e^{i\sigma t}\int_V\operatorname{div}_0\operatorname{grad}_0\phi_0 dV_0\\&=(4-3\Gamma_1)\,\xi_0 e^{i\sigma t}\,(2\omega_0^2V_0-4\pi GM)\,.\end{aligned}\right\} \tag{53}$$

Equation (38) now reduces to (cf. eqs. [41], [42], and [53])

$$\sigma^2=\tfrac{4}{3}\pi G(3\Gamma_1-4)\,\bar\rho+\tfrac{2}{3}\omega_0^2(5-3\Gamma_1)\,, \tag{54}$$

where $\bar\rho$ denotes the mean density. For a mass devoid of rotation, equation (54) gives

$$\sigma^2=\tfrac{4}{3}\pi G(3\Gamma_1-4)\,\bar\rho\,. \tag{55}$$

In this case of no rotation a better approximation, taking into account the variation of ξ_0 with r_0, can readily be found. The final result can be expressed in the form

$$\sigma^2=\frac{4}{3}\pi G\bar\rho\left[(3\Gamma_1-4)+\Gamma_1 R\left(\frac{1}{\xi_0}\frac{d\xi_0}{dr_0}\right)_R\right], \tag{56}$$

where R is the radius of the spherical star considered. However, equation (56) has the disadvantage that it makes σ^2 spuriously sensitive to the boundary values.

According to equation (54) for $\frac{4}{3}<\Gamma_1<\frac{5}{3}$, the effect of rotation is to increase σ^2, and this implies a decrease in the period. But this can only be regarded as a qualitative indication. For equation (55) predicts for the standard model, for example, a value of σ which is smaller than the true value by a factor 3.6. On the other hand, equation (55) predicts a value which approaches the true one in the limit of a uniform distribution. As

our discussion in paper I has shown, the effect of the central condensation is to multiply the value of σ^2 given by equation (54) by a factor of the order of

$$-\frac{3\Omega_0}{4\pi G\bar{\rho}I_0}. \tag{57}$$

We may assume that this is true of the first term of equation (54). But to find the corresponding factor for the second term we need a more detailed discussion, which is undertaken in the following section.

3. *The application of the virial theorem to the pulsation of a rotating star.*—The statement of the virial theorem for a rotating configuration can be deduced from (1) if proper allowance is made for the fact that in this equation T refers to the kinetic energy in a fixed frame of reference. However, we shall derive the necessary formulation of the theorem more directly from the equation of motion (31). Re-writing this equation in the form

$$\frac{d\boldsymbol{v}}{dt}\,dm = -\,(\text{grad}\,P)\,dV + (\text{grad}\,\mathfrak{V})\,dm + [\tfrac{1}{2}\omega^2\,\text{grad}\,(x^2+y^2)\,]\,dm\,, \tag{58}$$

we resolve it into its Cartesian components. We have

$$\left.\begin{aligned}
\frac{d^2x}{dt^2}\,dm &= -\frac{\partial P}{\partial x}\,dV + \frac{\partial \mathfrak{V}}{dx}\,dm + \omega^2 x\,dm\,,\\
\frac{d^2y}{dt^2}\,dm &= -\frac{\partial P}{\partial y}\,dV + \frac{\partial \mathfrak{V}}{\partial y}\,dm + \omega^2 y\,dm\,,\\
\frac{d^2z}{dt^2}\,dm &= -\frac{\partial P}{\partial z}\,dV + \frac{\partial \mathfrak{V}}{\partial z}\,dm\,.
\end{aligned}\right\} \tag{59}$$

Multiplying the foregoing equations by x, y, and z, respectively, adding them together, and integrating the result over the entire configuration, we obtain

$$\left.\begin{aligned}
\frac{1}{2}\int_0^M \frac{d^2}{dt^2}(x^2+y^2+z^2)\,dm = \int_0^M \left[\left(\frac{dx}{dt}\right)^2+\left(\frac{dy}{dt}\right)^2+\left(\frac{dz}{dt}\right)^2\right]dm\\
+\int_0^M \left(x\frac{\partial \mathfrak{V}}{\partial x}+y\frac{\partial \mathfrak{V}}{\partial y}+z\frac{\partial \mathfrak{V}}{\partial z}\right)dm + \int_0^M \omega^2(x^2+y^2)\,dm\\
-\int_0^V \left(x\frac{\partial P}{\partial x}+y\frac{\partial P}{\partial y}+z\frac{\partial P}{\partial z}\right)dm\,,
\end{aligned}\right\} \tag{60}$$

where use has been made of the relations

$$x\frac{d^2x}{dt^2} = \frac{1}{2}\frac{d^2x^2}{dt^2} - \left(\frac{dx}{dt}\right)^2, \quad \text{etc.} \tag{61}$$

Equation (60) can be written alternatively in the form

$$\frac{1}{2}\frac{d^2I}{dt^2} = 2T_2 + \Omega - \int_V \boldsymbol{r}\cdot\text{grad}\,P\,dV + \int_0^{\mathfrak{M}} \omega\,d\mathfrak{M}\,, \tag{62}$$

where I and Ω have the same meanings as in § 1, T_2 is the kinetic energy with respect to the chosen axis, and $\mathfrak{M}$ is the total angular momentum ($d\mathfrak{M} = \omega^2[x^2 + y^2]dm$). Since

$$\text{div}\,(\boldsymbol{r}P) = \boldsymbol{r}\cdot\text{grad}\,P + 3P\,, \tag{63}$$

we have

$$\left.\begin{aligned}
\int_V \boldsymbol{r}\cdot\text{grad}\,P\,dV &= \int_V \text{div}\,(\boldsymbol{r}P)\,dV - 3\int_V P\,dV\\
&= \int_S (\boldsymbol{r}P)\cdot\boldsymbol{1}_{dS}\,dS - 3\int_V P\,dV\,.
\end{aligned}\right\} \tag{64}$$

But as P vanishes on the bounding surface, we have

$$\int_V \mathbf{r}\cdot\operatorname{grad} P\,dV = -3\int_V P\,dV\,. \tag{65}$$

Equation (62) therefore becomes

$$\frac{1}{2}\frac{d^2I}{dt^2} = 2T_2+\Omega+3\int_V P\,dV+\int_0^{\mathfrak{M}}\omega\,d\mathfrak{M}\,. \tag{66}$$

In considering the variation of this equation we shall (as in § 2) consider displacements δr, which lie in the meridian planes and which can further be represented as

$$\frac{\delta r}{r_0} = \xi_0 e^{i\sigma t} \qquad (\xi_0 = \text{constant})\,. \tag{67}$$

Also, ξ_0 is assumed to be a quantity of the first order of smallness. For such variations T_2 is of the second order of smallness and can be ignored. We can therefore write

$$\frac{1}{2}\frac{d^2\delta I}{dt^2} = \delta\Omega+3\int_0^M \delta\left(\frac{P}{\rho}\right)dm\,(r)+\delta\int_0^{\mathfrak{M}}\omega\,d\mathfrak{M}\,. \tag{68}$$

Remembering that ξ_0 is assumed to be a constant, we have

$$\delta I = 2\xi_0 e^{i\sigma t} I_0 \qquad \text{and} \qquad d\Omega = -\xi_0 e^{i\sigma t}\Omega_0\,. \tag{69}$$ [3]

Moreover, for adiabatic pulsations under our present conditions we have (cf. eqs. [11] and [12])

$$\delta\left(\frac{P}{\rho}\right) = \frac{P_0}{\rho_0}(\Gamma_1-1)\frac{\delta\rho}{\rho_0} = -3\,\xi_0 e^{i\sigma t}(\Gamma_1-1)\frac{P_0}{\rho_0}. \tag{70}$$

Assuming, further, that Γ_1 is a constant, we have

$$\int_0^M \delta\left(\frac{P}{\rho}\right)dm\,(r) = -3\,(\Gamma_1-1)\,\xi_0 e^{i\sigma t}\int_{V_0} P_0\,dV_0\,, \tag{71}$$

and equation (68) becomes

$$-\sigma^2\xi_0 e^{i\sigma t} I_0 = -\xi_0 e^{i\sigma t}\Omega_0 - 3\,(\Gamma_1-1)\,\xi_0 e^{i\sigma t}\int_{V_0} 3P_0\,dV_0+\delta\int_0^{\mathfrak{M}}\omega\,d\mathfrak{M}\,. \tag{72}$$

On the other hand, for the equilibrium position equation (66) gives

$$\Omega_0+3\int_{V_0} P_0\,dV_0+\int_0^{\mathfrak{M}}\omega_0\,d\mathfrak{M} = 0\,. \tag{73}$$

Combining equations (72) and (73), we have

$$-\sigma^2\xi_0 e^{i\sigma t} I_0 = (3\Gamma_1-4)\,\xi_0 e^{i\sigma t}\Omega_0+3\,(\Gamma_1-1)\,\omega_0\mathfrak{M}\,\xi_0 e^{i\sigma t}+\delta\int_0^{\mathfrak{M}}\omega\,d\mathfrak{M}\,. \tag{74}$$

Now the conservation of angular momentum insures that $\mathfrak{M}$ and $d\mathfrak{M}$ remain constant during the pulsation. Hence,

$$\delta\int_0^{\mathfrak{M}}\omega\,d\mathfrak{M} = \int_0^{\mathfrak{M}}\frac{\delta\omega}{\omega_0}\,\omega_0\,d\mathfrak{M}\,; \tag{75}$$

or, using equation (39),

$$\delta\int_0^{\mathfrak{M}}\omega\,d\mathfrak{M} = -2\,\xi_0 e^{i\sigma t}\int_0^{\mathfrak{M}}\omega_0\,d\mathfrak{M} = -2\,\xi_0 e^{i\sigma t}\omega_0\mathfrak{M}\,. \tag{76}$$

[3] The relation for $\delta\Omega$ follows from the fact that Ω is of dimension -1 in the relative distances.

Substituting this in equation (74), we finally obtain

$$\sigma^2 = -\frac{(3\Gamma_1 - 4)\,\Omega_0}{I_0} + \frac{(5 - 3\Gamma_1)\,\omega_0 \mathfrak{M}}{I_0}. \tag{77}$$

Just as equation (21) for the period is superior to equation (55), we may expect that equation (77) is a correspondingly better approximation for the period when there is rotation than equation (54). On the other hand, equations (77) and (54) become identical in the limit of a homogeneous distribution.

Now the factor introduced by our present method in the second term of (77) is never very different from $2\omega_0/3$, while Ω_0/I_0 can be much larger than $4\pi G\bar{\rho}/3$. For instance, in the case of the standard model, $\Omega_0/I_0 = 13.26 \times 4\pi G\bar{\rho}/3$. If we consider a star having the same distribution of density as the standard model but rotating with an angular velocity ω and neglect its deviations from spherical shape, we have

$$\sigma^2 = 13.26\,(3\Gamma_1 - 4)\frac{g}{R} + \frac{2}{3}(5 - 3\Gamma_1)\frac{f}{R}, \tag{78}$$

where we have used g to denote the gravitational attraction at the surface and f the centrifugal force at the equator. If we take its spheroidal shape into consideration, Ω_0/I_0 will decrease and $\mathfrak{M}/I_0$ will increase. However, the maximum value of $\mathfrak{M}/I_0$ is 1; and Ω_0/I_0 is not likely to become much smaller for stable configurations than its spherical value, since the central condensation will persist; and $\Omega_0/I_0 = 10 \times 4\pi G\bar{\rho}/3$ is likely to be a minimum value. With these values (78) becomes

$$\sigma^2 \simeq 10\,(3\Gamma_1 - 4)\frac{g}{R} + (5 - 3\Gamma_1)\frac{f}{R}. \tag{79}$$

Now let us consider more closely the implications of our assumptions concerning δr. For displacements of the kind we have considered, isosteric as well as isobaric, surfaces will remain as such, since $\delta\rho/\rho_0 =$ constant and $\delta P/P_0 = \Gamma_1\delta\rho/\rho_0 =$ constant. But on such a surface ϕ will not remain a constant, and grad ϕ and grad P will not continue to be parallel and there will be a tendency to create a current causing circulation. To the first order of approximation the restoring force along r is

$$F_r = \xi\,(3\Gamma_1 - 4)\frac{\partial \mathfrak{V}_0}{\partial r_0} - \xi\,(5 - 3\Gamma_1)\,\omega_0^2 r_0 \sin^2\vartheta\,. \tag{80}$$

But there is a component along ϑ as well, and this has the value

$$F_\vartheta = \xi\,(3\Gamma_1 - 4)\frac{1}{r_0}\frac{\partial \mathfrak{V}}{\partial \vartheta} - \xi\,(5 - 3\Gamma_1)\,\omega_0^2 r \sin\vartheta\cos\vartheta\,. \tag{81}$$

For a spheroid of revolution flattened at the poles F_ϑ vanishes at the poles and at the equator. Comparing F_r and F_ϑ at 45° for masses which have reached their critical configurations (maximum rotation compatible with steady rotation), we shall obtain an idea of the maximum effect of F_ϑ. If we take $\Gamma_1 = \frac{5}{2}$, the ratio of F_ϑ to F_r at 45° on the surface of the critical Roche's model is equal to $\frac{1}{5}$, and on the Maclaurin's spheroid it is equal to $\frac{1}{6.5}$. On the other hand, what happens in the external layers of the star is not likely to have a great bearing on the problem and in any case would not be expected to affect the proper period of the star, so that we should really compare the values of F_ϑ and F_r at some distance inside the surface. Actually, the ratio decreases rapidly with r. Thus, if we suppose ω_0 to be reasonably far from its critical value, the component of force along ϑ will be small, compared to the component along r; and the transfer of energy from the pulsation to the currents due to F_ϑ will be slow, compared to the period of pulsation. Therefore, it is the stability, rather than the period, which will be affected.

However, if Γ_1 approaches $\frac{4}{3}$, equations (54) and (55) become equal at 45° and our approximation breaks down altogether, whatever the rotation. If Γ_1 becomes smaller than $\frac{4}{3}$, it is seen that the star becomes unstable at the poles along r and that currents will be set up rapidly in the rest of the star, increasing its instability.

Returning to equation (79), we see that, if its validity is assumed also when f and g are of the same order of magnitude, the contribution of rotation to σ^2 amounts to only about 10 per cent if $\Gamma_1 = \frac{5}{3}$. The corresponding change in the period will be about 5 per cent. However, as the central condensation decreases, the effect of rotation on the period increases. Thus for a polytrope n = 2, under similar circumstances the contribution of rotation to σ^2 can amount to 20 per cent.

It is a pleasure to record my indebtedness to Dr. S. Chandrasekhar for his help in recasting the original paper in a more presentable form and for seeing the paper through the press.

CHEMICAL COMPOUNDS IN THE SUN*

HAROLD D. BABCOCK
Mount Wilson Observatory
Received May 15, 1945

ABSTRACT

Sunspot and solar-disk spectrograms, λλ 3000–11500, when compared with laboratory data compiled by Pearse and Gaydon, show that 18 chemical compounds are recognizable in both spot and disk. Criteria for identification are mainly qualitative and physical rather than statistical. Observed vibrational transitions are summarized; maximum excitation potentials for spots are well over 1 volt. A finding list of solar bands is given.

The compounds *NH* and probably *MgH* appear in electronically excited states as well as in the normal state. The red system of *CN* is weak but extensive in both spot and disk. Newly identified compounds are *BH*, *MgF*, *SrF*, *YO*, *ScO*, *MgO*, and O_2, the last being observed in high vibrational levels of the ground term. For 14 others, nearly all considered present by previous observers, no evidence is found.

Agreement between abundance estimated from the appearance of bands and computed from the theory of dissociative equilibrium by Russell's method is improved and extended.

The abundance of chemical compounds in the atmospheres of the cooler stars has been investigated theoretically by Miss Cambresier and Rosenfeld,[1] by Rosenfeld,[2] and by H. N. Russell.[3] From atomic abundance, the properties of molecules, and the temperatures and pressures characteristic of stellar atmospheres these writers computed the numbers of molecules, on an arbitrary scale, above unit area of the photospheres of the later-type stars. The difficulties are serious, requiring the introduction of numerous assumptions, and the molecular data are incomplete; yet the results exhibit a general agreement with the observed abundance.

Miss Cambresier and Rosenfeld concluded that the observed intensity variations of molecular bands in stellar spectra may be accounted for on the theory of dissociative equilibrium; and, with some quite different assumptions, Russell not only reached the same conclusion but incorporated many additional details. His method and the observational data for the sun, which he took from the compilation by R. S. Richardson,[4] are a convenient point of departure for the present work.

Progress in the laboratory analysis of molecular spectra, together with new solar observations, now permits a broader survey of compounds in the sun than was formerly possible. With the aid of G. Herzberg's *Molecular Spectra and Molecular Structure*[5] and Pearse and Gaydon's *Identification of Molecular Spectra*[6] this paper presents a synopsis of the molecular components of the sun's atmosphere, both computed and observed.

No claim to completeness is advanced; indeed, unidentified molecular absorption bands in sunspots are more numerous and extensive than those now accounted for. The identification of solar bands is rendered difficult by their superposition on a rich atomic spectrum, by extensive overlapping among themselves, and by the dearth of laboratory data. The impressive spectral complexity associated in some molecules with a single electronic transition, the phenomena of molecular absorption continua, well known in the laboratory but not yet recognized in the sun, and the probability that molecules and

* *Contributions from the Mount Wilson Observatory, Carnegie Institution of Washington*, No. 708.

[1] *M.N.*, **93**, 710, 1933.

[2] *M.N.*, **93**, 724, 1933.

[3] *Mt. W. Contr.*, No. 490; *Ap. J.*, **79**, 317, 1934.

[4] *Mt. W. Contr.*, No. 422; *Ap. J.*, **73**, 216, 1931.

[5] New York: Prentice Hall, 1939.

[6] London: Chapman & Hall, 1941.

radicals not yet produced in the laboratory may be observable under solar conditions have all to be taken into account. The solar bands not yet interpreted will doubtless reveal the presence of additional compounds, but much further study must precede a truly comprehensive knowledge of the molecular constituents of the sun's atmosphere.

Most of the spectrograms for the present investigation were obtained during the last sunspot maximum at the Hale Solar Laboratory in Pasadena. With the 150-foot reflecting telescope and various orders of a 21-foot concave grating (Eagle mounting) more than 100 spectrograms were made of the solar disk between λ 2950 and λ 12200 and of spots between λ 3000 and λ 11500. In addition, a few plates procured by the late Ferdinand Ellerman with the equipment on Mount Wilson have been used.

Earlier workers depended mainly on coincidences between solar and laboratory wave lengths of individual lines for the identification of compounds in the sun, a method which yields conclusive results when the solar absorption is sufficiently strong, as in Fowler's work on *OH* and *NH*. In the case of bands of less favorable intensity, additional evidence from the occurrence of band heads and from the statistical criterion of Russell and Bowen[7] is especially valuable.

For very weak solar bands the line-coincidence method alone, or even in combination with the Russell-Bowen test, may lead to erroneous results, some of which are set forth in the notes to Table 3. When observed under the best conditions, extensive regions of the sunspot spectrum present no true continuous background but show, instead, innumerable faint absorption "lines," many of which are not discrete. Such "lines" result from superposition of real lines, too faint to be perceived separately, associated with molecules whose band spectra overlap. Measurements on such an array of "lines" have little accuracy and less meaning. There is always a coincidence, within errors of observation, with any arbitrarily chosen wave length in the region; and the statistical test fails because the total number of real lines within a given interval cannot be determined. The microphotometer gives no help in disentangling the individual lines. It does, however, show plainly the broader fluctuations in such a background, sometimes surpassing the eye when the gradient of density is very slight, the region extended.

The foregoing remarks apply also, in part, to the background of the disk spectrum, where irregularities occur, although less obviously than in spots. These features of the disk spectrum defy attempts to measure them but clearly match the positions of the similar stronger variations in the spot. As would be expected, the perception of such details is favored in the observations under discussion by the width of the spectrum and by its freedom from dust lines and from obscurations due to a compound quarter-wave plate.

The physical method of identification is analogous to that which has proved effective for atomic spectra. It rests upon the electronic and vibrational analysis of the molecular spectrum; reckons with band heads having the type of degradation, position, and relative intensity within a given vibrational transition reported from the laboratory; recognizes that, among the members of a system of bands, the distribution of intensity may be very different in absorption and in emission; and questions the identification of any absorption band (unless the relative probabilities of transition favor it) if others of the same molecule having lower excitation potential are absent.

The dependence of visibility of a head on molecular abundance may be illustrated by the A band of atmospheric oxygen. With an air path of about 100 km, as at low sun, the head of this band is sharply defined on the violet edge and forms a black break in the solar spectrum. But with an air path of 3 meters the spectrum of any continuous source shows only two doublets in the P branches of the band, about 40 A to the red of the normal position of the head, since, line for line, the R branches, in which the head occurs, are weaker than the P branches and thus disappear first with diminishing abundance, leaving the two strongest P doublets as *raies ultimes*.

[7] *Ap. J.*, **69**, 196, 1929.

Such an observation shows that the absence of a compound is not necessarily a valid inference from the absence of its band heads and indicates that many faint lines in the solar spectrum may be ultimate remnants of ground-state bands associated with rare molecules or with abundant molecules in excited states, of which numerous varieties must be present.

For the present purpose no measurements of individual lines have been used except in the case of *CN*, O_2, *NH*, and a group of unknown lines in the red which will be discussed later. Positions of band heads have been derived from adjacent atomic lines, with due allowance for uncertainties, since the heads are not susceptible of precise measurement. Intensities of heads have been designated; 0, barely discernible; 1, weak; 2, medium; 3, strong—a logarithmic scale corresponding to that used by Russell[8] for the intensity of bands, as determined by the individual lines. Although my intensities are not always strictly identical in meaning with Russell's values, the distinction is unimportant for our purpose.

Tables 1 and 3 list relative numbers, S, of molecules above unit area of photosphere for both disk and spot in descending order of computed spot abundance. All numbers followed by "R" have been taken from Table III of Russell's paper; other numbers, except as noted below for *OH*, are newly computed or observed by the writer.

Details of the method of computation will be found in Russell's paper. For our present purpose it will suffice to state that if A and B are any two atoms that may be associated in a diatomic molecule or radical, and if S_A and S_B are their atomic abundances in the sun, the abundance, S_{AB}, of the molecule AB is given by

$$\log S_{AB} = \log S_A + \log S_B - \log K_{AB} - 12.6 ,$$

where K_{AB} is the dissociation constant for AB corresponding to the solar temperature. With a few exceptions the atomic abundances are those derived by Russell from the intensities of atomic solar lines; K is computed as a function of the dissociation potential, the fundamental frequency of vibration, the statistical weight, other less effective molecular constants, and the temperature.

Taking, for example, the molecular constants for *CH* from compilations by Jevons or Herzberg and putting $T = 5740°$ for the solar disk, we have

$$\log_{10} K_{CH} = -\frac{5040}{5740}\cdot 4.0 + \tfrac{1}{2}\log 5740 - \frac{0.286}{5740}\cdot 2851 + \tfrac{1}{2}\log 0.92$$
$$- 2\log 1.13 + \log 2851 + \log 3 + 0.24$$
$$= 2.3 .$$

The abundance of *CH* in the disk follows from

$$\log S_{CH} = 7.5 + 10.5 - 2.3 - 12.6 = 3.1 ,$$

as tabulated.

For disk and spot, respectively, $\log S = 4$ and 5 has been adopted for both B and F. As compared with the early estimates of Russell, these lower values seem more consistent with current opinion on terrestrial abundance—a fair index of solar abundance. For Y and Sc the abundance found by Russell[9] has been used.

In Table 1, the sixth column, "Observed Δv in Spot," shows all the values of $\Delta v = v'' - v'$, where v'' and v' are the vibrational quantum numbers in the states of lower and higher electronic excitation, respectively, as observed in the spot spectrum. Thus, if 0 stands alone here, it signifies that only vibrational transitions such as 0, 0; 1, 1; 2, 2 . . . . ,

[8] *Op. cit.*, p. 324.

[9] *Mt. W. Contr.*, No. 383; *Ap. J.*, **70**, 11, 1929.

TABLE 1

CHEMICAL COMPOUNDS IN THE SUN

COMPOUND	LOG S				OBSERVED $\Delta v = v'' - v'$ IN SPOT	OBS. MAX. v''	OBS. MAX. E.P. IN SPOT (VOLTS)	NO. OF GROUND-STATE SYSTEMS IN SPOT	NO. OF OTHER GROUND-STATE SYSTEMS KNOWN	REMARKS
	Disk		Spot							
	Comp.	Obs.	Comp.	Obs.						
OH	1.7	2	3.2	2.5	0, +1	2	1.09	1	0	2 more transitions inaccessible
NH	4.0R	2.5	5.3R	3	0	1	0.6	1	0	Simple system $^3\Pi \leftarrow ^3\Sigma$ ground state
NH	2.9	0	3.9	1	0	0	1.2	.....	.....	$^1\Pi \leftarrow ^1\Delta$
NH	1.4	0	2.1	0	0	0	2.3	.....	.....	$^1\Pi \leftarrow ^1\Sigma$
O_2	2.9R	.....	4.4R	.....	.....	.....	.....	.....	.....	Inaccessible in ultraviolet
O_2	−0.8	0	0.2	1	+13 .... +19	21	4.2	2	1*	Extension of Schumann-Runge system
O_2	−1.5	0?	0	0	+ 4, +5	8	1.5	.....	.....	Extension of Herzberg system
CH	3.1R	3R	4.1R	3.5	− 1, 0	1	0.51	3	0	See note at end of paper
CN	2.3R	3	3.9R	3.5	− 1, 0, +1	6	1.6	2	0	Violet *CN*
CN	0.4	0	2.0	1	− 4, −3, −2, −1, 0, +1?	3	0.87	.....	.....	Red *CN*
SiH	2.2R	1R	3.5R	1.5	0	1?	0.39	1	0	
MgH	1.4R	1R	2.9R	2	− 1, 0, +1	3	0.6	1		
C_2	0.9R	1.3R	2.4R	2R	− 2?, −1, 0, +1	5	1.08	1	2†	
TiO	−0.6R	0	2.2R	3R	0, +1	1	0.13	3	0	
MgO	0.2	0?	2.0	1?	0	3?	(0.28)	.....	.....	Analysis incomplete
CaH	−0.4R	0	1.5R	2	0	1	0.24	2	3†	
BH	−1.3	0	0.6	1	0	0	0.15	1	0	Q and R heads observed
ScO	−0.6	0	0.5	0	0	0	0.06	1, 2?	0	
AlO	−1.9R	0	0.4R	1R	0	1	0.18	1	0	See note at end of paper
ZrO	−2.4R	0	0.3R	1	0	0, 1?	0.17	2, 3?	0	Yellow system not certain
YO	−1.6	0	−0.1	1	0	1	0.16	2	0	Log S_Y assumed: disk, 1; spot, 2
MgF	−1.8	0?	−1.0	0	− 1?, 0	0	0.04	1	2†	
SrF	.....	0	.....	0	0	0	0.03	2	1	Heat of dissociation unknown

* The forbidden atmospheric system. † Weak.

have been found; a positive number means that the vibrational energy of the lower state exceeds that of the upper, and vice versa.

The seventh column states the vibrational quantum number, v'', for the observed band having the highest excitation potential, while the eighth gives this potential as calculated from the relation

$$\text{E.P. (volts)} = \frac{\omega\,(v''+\tfrac{1}{2}) - \omega x\,(v''+\tfrac{1}{2})^2}{8067}.$$

Molecular constants of vibration for the lower electronic state are here written ω and x without subscript, and v'' is taken from the seventh column. The small additions (maximum $\sim$0.1 volt) that should be made to some of the tabulated excitation potentials to allow for the rotational energy of the lower electronic state are ignored.

The ninth and tenth columns give the numbers, respectively, of ground-state systems observed in the spot and of other ground-state systems known in the laboratory. A molecule with only one system involving the ground state is more likely to be seen in absorption than one with several such systems. Similarly, complexity of a system may reduce its visibility as compared to that of an equally probable electronic transition which produces a system having fewer branches.

The abundance computed for *OH* has been taken from R. J. Dwyer [10] but reduced one thousand fold in accordance with R. S. Mulliken's[11] calculation of the ratio of absolute intensities of *OH* and *CN*. This procedure removes much of the discrepancy found for *OH* by Russell, who suggested that faulty calibration of Rowland's solar intensities near λ 3000 might be responsible. I have given special study to the intensities of individual *OH* lines in this region and find them consistent with the scale of intensities in the region λ 3600, about which no doubts have appeared. It is true, however, that Rowland's intensities of many other lines near λ 3000 require revision, a task now in progress.

For *NH*, O_2, and *CN*, multiple entries appear in Table 1. The first line for *NH* contains Russell's computed abundances and my observed values, with added data. These entries refer to the only known system of ground-state bands. The second and third lines for *NH* show results for two systems arising from electronic levels $^1\Delta$ and $^1\Sigma$, approximately 1.2 and 2.3 volts, respectively, above the ground state. The computed abundance here requires reduction by some factor expressing the relative probability, as compared to that of the ground-state system; but it seems unlikely[12] that the logarithmic abundance would be changed by 1, and the factor is ignored. No other celestial absorption bands from electronically excited levels are known.

The first line for O_2, showing only Russell's computed abundance in disk and spot, refers to the lowest vibrational level of the ground state, i.e., bands of the Schumann-Runge system having $v'' = 0$. These are inaccessible in the ultraviolet. The second line for O_2 shows computed abundance for bands in the same system having $v'' = 21$, with observations for several vibrational transitions involving similar high values of v''. The corresponding bands extend into the visible region as far as λ 4452, having been observed in the laboratory in both absorption and emission. Solar identifications have been made by comparing the laboratory wave lengths of H. Fesefeldt,[13] as analyzed by Lochte-Holtgreven and Dieke,[14] with the wave lengths in the *Revised Rowland*. Over 200 lines of O_2 belonging to 6 bands, λλ 3230–4452, coincide with weak unidentified solar lines, while nearly as many more fall upon atomic solar lines previously identified. Of 14 band heads, 6 are probably present, 2 are masked, and 6 are uncertain.

[10] *Ap. J.*, **100**, 300, 1944.

[11] *Ap. J.*, **89**, 287, 1939.

[12] Suggestion of Dr. Swings.

[13] *Zs. f. wiss. Photographie*, **25**, 33, 1927.

[14] *Ann. d. Phys.*, **3**, 937, 1929.

In Table 1, the third line for O_2 refers to the extension of the Herzberg system of ultraviolet bands, whose stronger members are also beyond λ 3000. The vibrational analysis and the positions of many heads are due to P. Swings,[15] who has identified them in the spectrum of the night sky. The abundance has been computed for $v'' = 8$, allowance being made for the lower probability of this forbidden transition by subtracting 3 from the computed logarithm. No rotational details are available for the identification of individual lines, but 9 of the heads appear to be faintly present in spots between λ 3200 and λ 3700. The evidence appears sufficient to establish O_2 as an abundant constituent of the solar atmosphere in accord with computation. The recognition of O_2 may have added significance because this molecule has enormous opacity in the ultraviolet and also because it is paramagnetic.

The first line for *CN* refers to the violet system and the second to the red system, now for the first time observed in spot and disk. Thanks to A. S. King and P. Swings, who kindly made available the manuscript of their paper, "A Comparative Study of the Red and Violet Systems of *CN* Bands,"[16] before its publication, the 1, 0 band of the red system could be identified by the line-coincidence method. Of the laboratory wave lengths for 112 lines, λλ 7873–8161, which these writers have observed in both absorption and emission, 74 coincide with lines of solar intensity −3 to −1 in the disk, 35 are masked by stronger lines, and only 3 of the weakest are unaccounted for. Spot effects for 16 of the lines amount to a general strengthening of about one intensity unit, while no Zeeman effects have been seen.

This evidence alone would establish the existence of the red system in the sun. It is reinforced, however, by the recognition of weak heads belonging to many other bands in the system, for some of which no rotational details are available. Jenkins, Roots, and Mulliken[17] observed parts of this extensive system in the laboratory and made a vibrational and rotational analysis. Each vibrational transition gives rise to eight branches, three of which show heads more or less distinctly. If we bear in mind these facts as well as the conclusion of King and Swings[16] that in absorption the violet *CN* system has 87 times as high a probability of occurrence as the red system, it is somewhat surprising that the latter can be observed in a star as hot as the sun. But a search for the heads recorded by Jenkins, Roots, and Mulliken, as well as for others now computed from their analysis, shows that 15 vibrational transitions are more or less certainly represented in spots. Only the stronger of these are seen in the disk. The results are summarized in Table 2, which leaves no question that the strong *CN* absorption observed for $\lambda < 9000$ in cooler stars is, in fact, only a fraction of the total effect due to this molecule. Since the opacity of *C* and *N* atoms is insignificant, compared to that of *CN*, the formation and dissociation of this compound may well play an important role in the atmospheres of N-type stars.

For red *CN*, log *S* is obtained by subtracting log 87 = 1.9 from log *S* for violet *CN*, in accordance with the results of King and Swings. Since this molecule, as well as *CH* and *TiO*, appears in more than one ground-state system, the computed abundance is slightly too large for comparison with observations on any one system alone.

Seven compounds now for the first time identified in the sun are *BH*, *MgF*, *SrF*, *YO*, *ScO*, *MgO*, and O_2. The first three of these are of interest because they present the only evidence for the occurrence of *B* and *F* (*BO* and *SiF* now being rejected; cf. Table 3). Richardson[18] reported *BH* absent; but as he appears to have examined only one spectrogram for this purpose, the discrepancy may be accounted for by the remarks which follow on real variations in the appearance of bands. No solar evidence for halogens other than *F*, either atomic or in chemical combination, has been reported. The head of *SrF* at

[15] *McDonald Obs. Contr.*, No. 63; *Ap. J.*, **97**, 72, 1943.

[16] *Mt. W. Contr.*, No. 700; *Ap. J.*, **101**, 6, 1945.

[17] *Phys. Rev.*, **39**, 16, 1932.

[18] *Pub. A.S.P.*, **47**, 275, 1935.

λ 3712 is scarcely recognizable on ordinary disk and spot spectrograms because of confusion with atomic lines. The space λλ 3713–3715 is, however, practically free of atomic absorption; and here are found weak lines, strengthened in spots, whose arrangement indicates rotational fine structure. This apparent rotational structure is still better developed in absorption in the spectrum of the extreme solar limb, where it can be traced to the head at λ 3712. Two heads in the deep-red system are faintly present in spots.

TABLE 2*

THE RED SYSTEM OF CN BANDS IN THE SUN

v'	v'' = 0		v'' = 1		v'' = 2		v'' = 3	
	Disk	Spot	Disk	Spot	Disk	Spot	Disk	Spot
0	R_2	$\underline{R_2}$	R_2?	R_2?				
	λ 9140		λ 11240C		λ 14600C			
1	R_2	$\underline{R_2}$	R_2	R_2	R_2?	...		
	λ 7873		λ 9393		λ 11574C		λ 15240C	
2	a	R_2	R_2	$\underline{R_2}$	R_2	R_2	R_2?	...
	a	R_1	R_1?	$\underline{R_1}$				
	a	Q_1						
	λ 6920		λ 8067		λ 9635C		λ 11922C	
3	a	R_2	a	R_2	a	R_2?		
	a	R_1	a	(R_1)			R_2	$\underline{R_2}$
	a	Q_1	a	Q_1				
	λ 6192		λ 7091		λ 8272		λ 9901C	
4	a	R_1	R_2	R_2				
			(R_1)†	R_1	a	a	a	a
			a	Q_1				
	λ 5619		λ 6332		λ 7259		λ 8485	
5		†		†	a	R_2?		
					(R_1)	(R_1)	a	a
					Q_1	Q_1		
	λ 5140		λ 5731		λ 6478		λ 7440	

* a = absent; ( ) = masked; underscoring indicates strengthening; C = computed; leaders indicate no observation; † = confused by other bands.

For H_2, *CO*, *NO*, *SiO*, and N_2, not shown in Table 1, Russell's computation (E.P. = 0) indicates great abundance; but the evidence, as he remarked, is inaccessible. On further examination for higher vibrational states, the computed abundances for *CO*, *NO*, and N_2 show that in sunspots these compounds might become observable. Thus far they have not been found. Even in the most favorable excited state, H_2 was shown by Swings[19] and by Russell[3] to be too weak for detection.

In Table 3 are listed compounds which I do not find in the sun, although most of them have been identified there by other observers. The notes amplify the tabular entries with observations from other sources, confirming or explaining my observations.

[19] *Pub. Inst. d'Astron. Liége*, No. 120, 1934.

TABLE 3

COMPUTED ABUNDANCE OF COMPOUNDS NOT FOUND IN THE SUN

COMPOUND	Log S			
	Disk		Spot	
	Comp.	Obs.	Comp.	Obs.
SiN	1.3R	a	3.2R	masked
BO	−0.8	a	1.7	a
AlH	−0.7R	a	1.4R	a?
CuH	−0.7R	a	0.7R	a
ZnH	−1.3R	.....	−0.5R	masked
SiF	−3.1	a	−0.6	a
BN	.....	a	.....	.....
FeH	.....	a	.....	a
PH	−4.0	a	−1.5	a
CP	−4.7	a	−2.3	a
FeO	.....	a	.....	a
CaO	−1.8	a	+0.6	a
NaH	.....	a	.....	a
CdH	.....	a	.....	a

NOTES TO TABLE 3

As in Table 1, the computed log S is followed by "R" when taken from Russell's paper; numbers not so marked have been computed by the writer.

SiN. One complex ground-state system is known.

BO. Identified by Nicholson and Perrakis (*Mt. W. Contr.*, No. 370; *Ap. J.*, **58**, 489, 1928). Bands studied by them have E.P. ~ 0.6 volt. Two strong complex ground-state systems are known. Tanaka, Nagasawa, and Saito found no evidence for *BO* in the sun (*Proc. Phys.-Math. Soc. Japan*, **21**, 421, 1939).

AlH. Identified by Richardson (*Mt. W. Contr.*, No. 422; *Ap. J.*, **73**, 216, 1931) from bands with E.P. 0.3 volt and 2.9 volt. Three ground-state systems are known. Not found by Tanaka, Nagasawa, and Saito (*op. cit.*) or by Stenvinkel, Svenson, and Olson (*Arkiv mat., astron., fysik, Stockholm*, **26A**, 10, 1938).

CuH. Six ground-state systems are known.

ZnH. Two ground-state systems are known. Stenvinkel, Svenson, and Olson (*op. cit.*) concluded that this compound is not established in the spectrum of the disk.

SiF. Identified by Richardson (*op. cit.*) from band having E.P. = 0.47 volt. Three very complex ground-state systems are known.

BN. No analysis is available. In a personal communication Professor Swings reports that *BN* is absent from the spectrum of the solar disk.

FeH. Analysis incomplete.

PH. Identified by Nicolet (*Pub. Inst. d'Astron. Liége*, No. 205, 1937), a result shown by Miss Davis (*Ap. J.*, **94**, 276, 1941) to be due to chance. The system is very complex.

CP. See remarks for *PH*, which apply here.

FeO. No analysis available. The familiar emission bands in the visual region are absent.

CaO. Analysis incomplete, ground state not yet determined. Six band systems are known.

NaH. Stenvinkel, Svenson, and Olson (*op. cit.*) consider Nicolet's identification improbable. Energy of dissociation uncertain but probably about 2.2 volts.

CdH. Energy of dissociation only 0.678 volt. Two ground-state systems are known, each with multiple branches. Stenvinkel, Svenson, and Olson find no evidence for it.

In Table 4 approximate wave lengths of band heads that have been recognized in spot spectra are shown for the molecules listed in Table 1. For each system the type of transition is stated, and the symbols "R" and "V" show that the heads degrade toward the red or the violet. In two cases where the degradation is more or less symmetrical in both directions, "R" and "V" are used together. Vibrational quantum numbers—v' for the excited state and v'' for the lower state—are given for most of the bands. Parentheses inclose the more doubtful heads. Data assembled here are taken mainly from Pearse and Gaydon.[6]

Table 5 collects a group of lines whose origin is unknown. The wave lengths in column 1 are from spot spectra, where their intensity and sharpness make them very well measurable. Some of these lines appear to have extremely weak counterparts in the spectrum of the disk, but several of those strongest in the spot are absent in the disk; the apparent correspondence is probably in part fortuitous.

It is not certain that the lines of Table 5 constitute a physically related group or part of one, but their similarity in character, small range of intensity, and localization in a comparatively narrow spectral range indicate that they are related. Even in the magnetic fields of the largest sunspots, these lines show no trace of Zeeman effect but remain exceptionally narrow and black. To postulate a molecular origin for them seems inescapable. Their open spacing (average distance apart = 3.9 A) and the apparent absence of any regularity in their arrangement suggest that they belong to a band spectrum like that of H_2, of which the members in Table 5 may be only a few of the strongest individuals.

DISCUSSION

A new feature of the data in Table 1 is the occurrence in the normal disk spectrum of all 18 compounds found in spots, whereas only about one-third of them had been recognized there before. Numerous weak unidentified bands, however, have thus far been seen only in spots.

In the normal spectrum of the solar disk variations have rarely been noted in the appearance of any molecular band, but among sunspot spectrograms marked differences occur. Such differences, when they affect both atomic and molecular lines, are usually only apparent and result from technical difficulties all tending to submerge the spectrum of the umbra in that of the penumbra and the disk. Imperfect seeing, errors in guiding, and the scattering of light by atmospheric and instrumental causes all impair the true sunspot spectrum.

But sunspot spectrograms are sometimes obtained, usually from different spots, on which clear differences in the molecular bands cannot be accounted for by observational limitations, since the atomic lines on each spectrogram exhibit, fully developed, the familiar magnetic and thermal effects associated with the spot spectrum. The observed differences in the strength of molecular bands are occasionally so marked as to indicate real variations in the abundance of compounds from spot to spot.

In Table 1 the mean systematic difference, observed *minus* computed, is, for spots, $\Delta \log S = -0.3$; and the mean without regard to sign is ± 0.9. As Russell remarked, many of the computed values of $\log S$ are uncertain by 0.5 or more, on account of inadequate laboratory data. It is probable, therefore, that errors in the observed values of $\log S$ in Table 1 are, on the average, about ± 0.5. In the special case where variations in the strength of the same band are studied on spectrograms of equal quality, effects corresponding to an appreciably smaller change in $\log S$ should be readily distinguished. Russell's computations[20] for *TiO* show that in stars like the sun a change, $\Delta \log S = -1.0$, corresponds to an increase of about 500° in the temperature. Differences of temperature from spot to spot amounting to only 200° or 300° should therefore be observable, and it should not be surprising if a band barely discernible in one spot were invisible in another.

[20] *Mt. W. Contr.*, No. 490; *Ap. J.*, **79**, 332, 1934.

TABLE 4

WAVE LENGTHS OF BAND HEADS IN SUNSPOT SPECTRA

Molecule	Transition	Degradation	v', v''	λ
OH.....	$^2\Sigma \leftarrow {}^2\Pi$	R	0, 0	3063, 3078, 3089
			1, 1	3121, 3126
			2, 2	3185, 3190, 3195, 3209
			0, 1	3428, 3432, 3458, 3472
NH.....	$^3\Pi \leftarrow {}^3\Sigma$	R V	0, 0	3360
			1, 1	3370
	$^1\Pi \leftarrow {}^1\Delta^*$	R	0, 0	3240, 3253
	$^1\Pi \leftarrow {}^1\Sigma^*$	R	0, 0	4502, 4523
O_2.....	$B^3\Sigma \leftarrow X^3\Sigma$	R	1, 18	3913
			1, 19	4096
			2, 21	4373
			2, 19	3987
			2, 20	4173
			1, 20	(4292)
			0, 18	(4021)
	$A^1\Sigma \leftarrow X^3\Sigma$	R	7, 6	
			0, 3	3211
			2, 4	
			4, 5	3233
			2, 5	
			0, 4	3378
			4, 6	
			6, 7	3425
			1, 5	3460
			3, 6	
			2, 6	
			0, 5	3556
			4, 7	
			6, 8	3598
			5, 8	3664
			7, 9	3707
CH.....	$^2\Delta \leftarrow {}^2\Pi$	V	0, 0	4312, 4315
	$^2\Sigma \leftarrow {}^2\Pi$	R	0, 0	3889, 3872
			1, 0	3628
	$^2\Sigma \leftarrow {}^2\Pi$	V R	1, 1	3157
			0, 0	3145
CN.....	$^2\Sigma \leftarrow {}^2\Sigma$	V	1, 0	3590
			2, 1	3586
			3, 3	3854
			2, 2	3862
			1, 1	3871
			0, 0	3883
			5, 6	4152
			4, 5	4158
			3, 4	4167
			2, 3	4181
			1, 2	4197
			0, 1	4216

* The $^1\Delta$ and $^1\Sigma$ terms of *NH* are electronically excited, as discussed in the text. All other transitions listed in Table 4 are from ground states.

TABLE 4—*Continued*

Molecule	Transition	Degradation	v′, v″	λ
CN (cont.)	$^2\Pi \leftarrow {}^2\Sigma$	R	.....	See Table 2 for red *CN*
SiH.....	$^2\Delta \leftarrow {}^2\Pi$	R	0, 0 1, 1	4142, 4128 4184
MgH.....	$^2\Pi \leftarrow {}^2\Sigma$	V	1, 0 0, 0 1, 1 2, 2 2, 3 1, 2 0, 1	4845 5211 5182 5155 5516 5568 5621
C_2.....	$^3\Pi \leftarrow {}^3\Pi$	V	4, 2 3, 1 1, 0 2, 2 1, 1 0, 0 3, 4 2, 3 1, 2 0, 1 4, 5	4365 4371 4737 5097 5129 5165 5501 5540 5585 5635 (5470)
TiO.....	$A^3\Sigma \leftarrow X^3\Pi$	R	0, 0 1, 1 0, 1	7054, 7088, 7125 7197 7672
	$? \leftarrow X^3\Pi$	R	0, 0 1, 1	5598 5629
	$? \leftarrow X^3\Pi$	R	?	4955
MgO.....	.....	V	0, 0 1, 1 2, 2 3, 3	5007† 4997† 4986† 4974
CaH.....	$A^2\Pi \leftarrow {}^2\Sigma$	V	0, 0 1, 1	6920, 7035 6903
	$B^2\Sigma \leftarrow {}^2\Sigma$	V	0, 0	6382, 6389
BH.....	$^1\Pi \leftarrow {}^1\Sigma$	R	0, 0	4246, 4332
ScO.....	$A^2\Pi \leftarrow X^2\Sigma$	R	0, 0	6036
	$B^2\Sigma \leftarrow X^2\Sigma$	R	0, 0	4858
AlO.....	$B^2\Sigma \leftarrow {}^2\Sigma$	R	0, 0 1, 1	4842 4866
ZrO.....	$C^3\Pi \leftarrow X^3\Pi$	R	0, 0	4640
	$A^3\Sigma \leftarrow X^3\Pi$	R	0, 0 1, 1	6345, 6473 (6508)

† Heads of *MgO* at λ 5007, λ 4997, and λ 4986 are masked.

TABLE 4—*Continued*

Molecule	Transition	Degradation	v', v''	λ
YO.....	$^2\Sigma \leftarrow {}^2\Sigma$	R	0,0	4817
			1,1	(4842)
	$^2\Pi \leftarrow {}^2\Sigma$	R	0,0	5972, 6132
			1,1	6148
MgF.....	$A^2\Pi \leftarrow {}^2\Sigma$	V	0,0	3594
			1,0	(3503)
SrF.....	$A^2\Pi \leftarrow {}^2\Sigma$	R	.....	This red system masked
	$C^2\Pi \leftarrow {}^2\Sigma$	R	.....	3712

Near the solar limb, *OH*, *CH*, *SrF*, and possibly some other compounds appear in greater strength than at the center of the disk, indicating that the effective level of absorption is fairly high. In their study of the chromospheric spectrum, W. S. Adams and Miss Burwell[21] noted that near λ 5000 the limb spectrum has a peculiar appearance, quite different from that of the normal disk. My spectrograms show the same effect and suggest the emergence of molecular absorption as the cause.

Instead of being restricted to zero, as Russell supposed, the excitation potential in Table 1 ranges well above 1 volt for abundant molecules, as a result of the appreciable population of higher vibrational levels in the ground state. The vibrational transitions now recognized include marked changes in the quantum number instead of being always 0 or ± 1.

Absorption from the electronically excited states, $^1\Delta$ and $^1\Sigma$, of the abundant molecule, *NH*, appears plausible because their excitation potentials are comparable with others in Table 1 and also because combinations of these two terms with the ground state are forbidden. This last circumstance must operate, as in the case of metastable atomic terms, to increase the population of $^1\Delta$ and $^1\Sigma$.

Magnesium hydride, *MgH*, has an excited level, $^2\Pi$, E.P. $\sim$ 2.4 volts, from which absorption would be possible; in fact, weak absorption in the disk at λ 4372, notably strengthened in spots, may correspond to one of the only two strong heads known to be associated with this term. The other head is confused with a strong atomic line, λ 4405. Since for sunspots calculation gives a value of $\log S = 0.4$ for *MgH* in this state of excitation and since other molecules recognized in spots have similar computed abundance, the absorption at λ 4372 is probably valid evidence of a transition from a level well above the ground state.

Molecular oxygen, O_2, has a $^1\Delta$ state with E.P. < 1 volt, but no system of absorption bands is known to arise from this term.

Among other investigations of molecular abundance in the sun, only the work of F. E. Roach[22] will be mentioned here. Assuming equal absolute intensity factors for five molecu'es, he obtained their abundance in the reversing layer from equivalent widths of resolved lines. His values of log *S* are, on the average, greater by 4.0 than those given here in Table 1; since our scale is in arbitrary units, this discrepancy is less disturbing than the fact that the differences range from 1.9 to 5.5.

Much further work remains to be done, both in cataloging the features of solar spectra that appear to be due to molecular absorption and in interpreting such data in terms of laboratory experience—a task in which more observation of absorption bands in the labo-

[21] *Mt. W. Contr.*, No. 95; *Ap. J.*, **41**, 116, 1915.

[22] *Ap. J.*, **89**, 99, 1939.

TABLE 5

SOME PECULIAR SUNSPOT LINES

Spot		Disk				Remarks
λ I.A.	Int.	*R.R.* λ	Int.	Atlas λ*	Int.	
6007.09	−1	0.04	−3			
6009.24	0					
6020.63	0	.66	−3			
6021.02	0					
6025.21	−1	.21	−3	0.20	−3	
6028.44	−2					
6030.31	−1	.34	−3			
6040.18	0					
6040.92	0					
6043.88	−1					
6049.68	−2					
6049.80	−2	.80	−3N			Atm? in *R.R.*
6053.48	−1	.48	−2	.48	−2	Disk line probably not related to spot line
6056.82	−1					
6061.01	−1			.00	−3	
6068.65	0					
6074.04	1	.02	−3	.00	−3	
6075.08	0					
6076.14	0	15	−2d?	.13	−3	
6079.86	0					
6087.85	−1	.84	0N	.83	0N	Disk line not related to spot line
6088.29	−1	.28	−3N	.28	−3	
6091.50	−1	.51	−3			
6092.11	−2					
6095.09	0					
6100.48	−1					
6104.91	−2					
6108.50	0	.47	−3d?	.50	−3	
6108.88	−2	.90	−3	.92	−3	
6109.39	−2	.34	−3			
6115.74	−2	.75	−2N	.73	−3	
6116.70	0	.70	−3d?	.75	−3	
6117.78	0	0.82	−3			
6123.81	0					
6140.08	−1					
6146.84	−1			0.85	−3	

* Minnaert, Mulders, and Houtgast, *Photometric Atlas of the Solar Spectrum*, Amsterdam, 1940.

ratory would help materially. In the meantime, perhaps the results collected here will lend added weight to conclusions derived from the theory of dissociative equilibrium and at the same time emphasize the importance of physical criteria in the interpretation of molecular phenomena in the sun and other stars.

It is a pleasure to express my thanks to Dr. P. Swings for many instructive conversations and to Mrs. H. A. Coffeen for assistance in some phases of the work.

NOTE ADDED IN PROOF

Through the kindness of Dr. Swings I have learned of a paper by B. Rosen, to appear in the *Physical Review*, in which the analysis of the *AlO* bands is revised. As a result, the identification of *AlO* in the sun is open to question. Swings has also called attention to Dufay's identification in the solar disk of the 1, 1 band of the $^2\Sigma \leftarrow {}^2\Pi$ system of *CH*. This work probably appeared in *Comptes rendus* about 1940 or 1941, but the reference is not available. A review appeared in *Bulletin* No. 3 (n.d.), published by the Committee for the Continued Distribution of Astronomical Literature.

T TAURI VARIABLE STARS*

ALFRED H. JOY
Mount Wilson Observatory
Received June 9, 1945

ABSTRACT

Eleven irregular variable stars have been observed whose physical characteristics seem much alike and yet are sufficiently different from other known classes of variables to warrant the recognition of a new type of variable stars whose prototype is T Tauri. The distinctive characteristics are: (1) irregular light-variations of about 3 mag., (2) spectral type F5–G5 with emission lines resembling the solar chromosphere, (3) low luminosity, and (4) association with dark or bright nebulosity. The stars included are RW Aur, UY Aur, R CrA, S CrA, RU Lup, R Mon, T Tau, RY Tau, UX Tau, UZ Tau, and XZ Tau. They are situated in or near the Milky Way dark clouds in the direction either of the center or of the anticenter of the galaxy.

The light-curves.—The total light-changes are about 3 mag., the variations being extremely irregular as to range and time. The light-curves are not unique.

The individual variables.—The spectrographic observations of the variables are described and the significant features of the spectra pointed out.

Discussion of the spectra.—The spectral types of the T Tauri stars are estimated to be between F5 and G5, although for many of them the absorption lines generally used in classification are lacking. A small variation of type with phase was found for T Tau and RY Tau. Bright hydrogen has been found in all stars of the group, and bright *Ca* II (H and K) in all except R CrA. Most of the stars show an emission spectrum composed of many bright lines of low excitation. The strongest lines are those of *Ca* II, *H*, *Fe* II, *Ca* I, *Sr* II, *Fe* I, and *Ti* II. The identification and relative maximum intensities of 160 lines of the different stars are shown in Table 16. The intensity of the emission spectrum varies greatly from time to time in each star, the bright lines becoming more prominent at maximum light of the variable.

The lines λ 4063 and λ 4132 of the $a^3F-y^3F^0$ multiplet of *Fe* I are greatly enhanced in strength in the stars showing strong emission spectra. This distortion is probably the result of fluorescent effects.

The marked similarity of the bright-line spectrum of the T Tauri stars to that of the upper solar chromosphere is shown in Table 17.

Absolute magnitudes and color indices.—Spectroscopic absolute magnitudes of three stars of the group, together with meager indirect evidence, indicate that the T Tauri stars are dwarfs of the main sequence. Color indices for five stars show some color excess, which is probably the result of selective absorption by surrounding nebulosity.

Radial velocities.—Radial-velocity measures from absorption lines are difficult when the emission spectrum is present. Lack of agreement in the measures of both absorption and emission spectra indicates irregular atmospheric motions. In the mean the emission lines are displaced toward the violet with respect to the absorption lines.

The criteria distinguishing variable stars included in the T Tauri class are: (1) rapid irregular light-variations of about 3 mag.; (2) spectral type F5–G5, with emission lines resembling those of the solar chromosphere, particularly in the great strength of H and K of calcium; (3) low luminosity; (4) association with dark or bright nebulosity. Although little or nothing is known as to the cause of the light-variation, characteristics 1–4 are probably physically interrelated and together form a distinct stellar type which may be readily recognized. These stars differ from other known variables, especially in their low luminosity and the high intensity of bright H and K in their spectra. The well-known variable T Tauri is one of the brightest stars of the group and may properly be considered as the prototype, although there are marked differences among the stars and no two are exactly alike.

Eleven stars (Table 1) make up the list of variables whose characteristics are sufficiently alike to entitle them to membership in this class. Heretofore, they have generally been classed as "irregular" variables, and their unpredictable light-changes indicate that

* *Contributions from the Mount Wilson Observatory, Carnegie Institution of Washington*, No. 709.

they well deserve the title. Four stars (R CrA, R Mon, T Tau, and RY Tau) are definitely involved in surrounding nebulosity (Pl. XII), and all stars of the group are situated in or near large areas of heavy obscuration by Milky Way clouds. In the course of this investigation, five others (RW Aur, UY Aur, S CrA, UX Tau, and UZ Tau) were discovered[1] to be visual double stars, leaving only two of the group (XZ Tau and RU Lup) which appear to be uninvolved either with local nebulosity or with near-by companion stars.

The galactic co-ordinates are in the fifth and sixth columns of Table 1. The peculiar distribution of these stars is evident and is shown in Figure 1. Three are in the Milky Way clouds near the direction of the center of the galaxy, and the others form a group

TABLE 1

T TAURI VARIABLES

Star	α (1900)	δ (1900)	Magnitude Range	Galactic		Remarks
				l	b	
RW Aur	$5^h\ 1^m.4$	+30° 16′	9.0–12.0	142°	− 6°	Double
UY Aur	4 45.4	+30 37	*11.6–14.0*	139	− 8	Double
R CrA	18 55.1	−37 6	9.7–13.5	328	−19	Nucleus of variable comet-like nebula, NGC 6729
S CrA	18 54.4	−37 5	9.5–13	328	−19	Double
RU Lup	15 50.1	−37 32	*9.0–11.0*	307	+11	
R Mon	6 33.7	+ 8 50	9.3–14.0	171	+ 3	Nucleus of variable comet-like nebula, NGC 2261
T Tau	4 16.2	+19 18	9.0–12.8	148	−22	Near Hind's variable nebula, NGC 1555, and surrounded by a small shell
RY Tau	4 15.6	+28 12	8.8–11.1	136	−14	Nucleus of a fan nebula
UX Tau	4 24.2	+18 0	*10.5–13.4*	146	−19	Double
UZ Tau	4 26.6	+25 40	9.2–<13	140	−14	Double
XZ Tau	4 25.9	+18 1	*10.4–13.5*	146	−19	

about the anticenter in the opposite direction; but, unlike the distant Cepheids, they do not lie closely along the galactic equator as seen from the sun. The mean latitude (disregarding signs) is 14°. The mean median apparent magnitude of these two groups is practically the same, indicating equal distances from the earth if all the stars are of equal absolute magnitude and suffer equal amounts of obscuration.

THE LIGHT-CURVES

The variations in light of the T Tauri stars are so irregular and unpredictable that classification by means of their light-curves is practically impossible. Thus far, observations have been insufficient to determine definite sequences of light-changes which are uniquely characteristic of the group. The light-curves vary greatly from year to year and from star to star. Figure 2, showing light-curves of RW Aur by S. Enebo[2] and E. Zinner[3] in different years, illustrates the complicated nature of the light-variations. Other stars such

[1] A. H. Joy and G. van Biesbroeck, *Pub. A.S.P.*, **56**, 123, 1944.

[2] *A.N.*, **175**, 205, 1907.

[3] *A.N.*, **195**, 456, 1913.

as RR Tau and certain variables in Orion have similar light-changes, yet their spectra are very different. The color index for several of the stars has been determined (Table 18), but changes in color have not yet been studied. If the fluctuations in light result from the interposition of obscuring clouds, changes in color due to scattering or selective absorption might be expected.

The magnitude ranges in Table 1 are from Schneller's Catalogue.[4] The total variation is large, averaging over 3 mag. The brightness of RU Lup and RY Tau at the time of some of the spectrographic observations was certainly a magnitude or more fainter than the minimum given by Schneller.

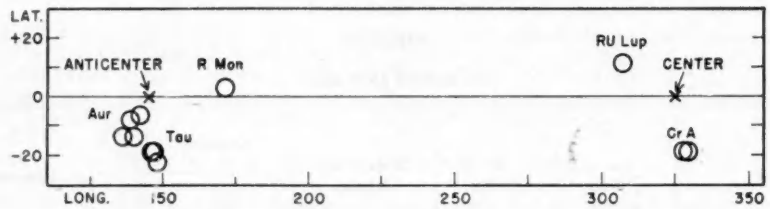

FIG. 1.—The galactic distribution of the T Tauri stars

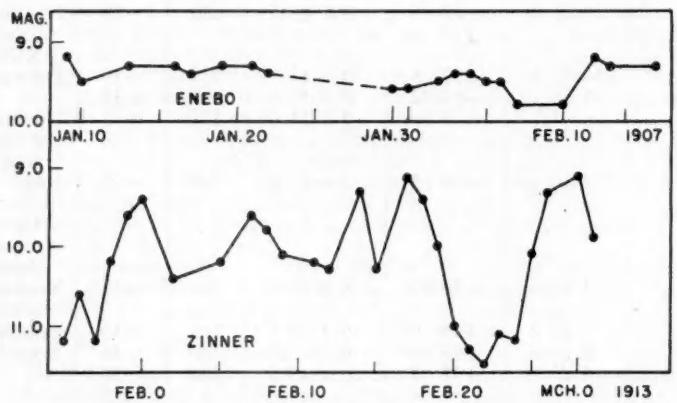

FIG. 2.—Light-curves of RW Aur by Enebo (*above*) and Zinner (*below*)

THE INDIVIDUAL VARIABLES

On account of the peculiarities of the individual variables, separate descriptions of their behavior, characteristics, and spectra are desirable. For each star the table of observations gives the plate number ("γ" signifies 60-inch one-prism spectrograph; "C," 100-inch one-prism; and "E," 100-inch two-prism); the date; the magnitude; the dispersion (a = 35 A/mm at Hγ, b = 75, c = 115, and d = 220, approximately); the velocities, together with the number of lines measured; and the relative prominence of the emission spectrum as a whole ("str" = strong, "m" = medium, and "wk" = weak). The estimated magnitudes are those recorded in the observing-record book when the spectrograms were made and have little photometric value. They are entered in the table only because no other magnitudes are available. No comparison stars were used, and the effect of haze, moonlight, and seeing may have introduced errors of the order of a magnitude on nights when the observing conditions were unfavorable.

[4] *Kleinere Veröff. Sternwarte Berlin-Babelsberg*, No. 21, 1939.

PLATE XII

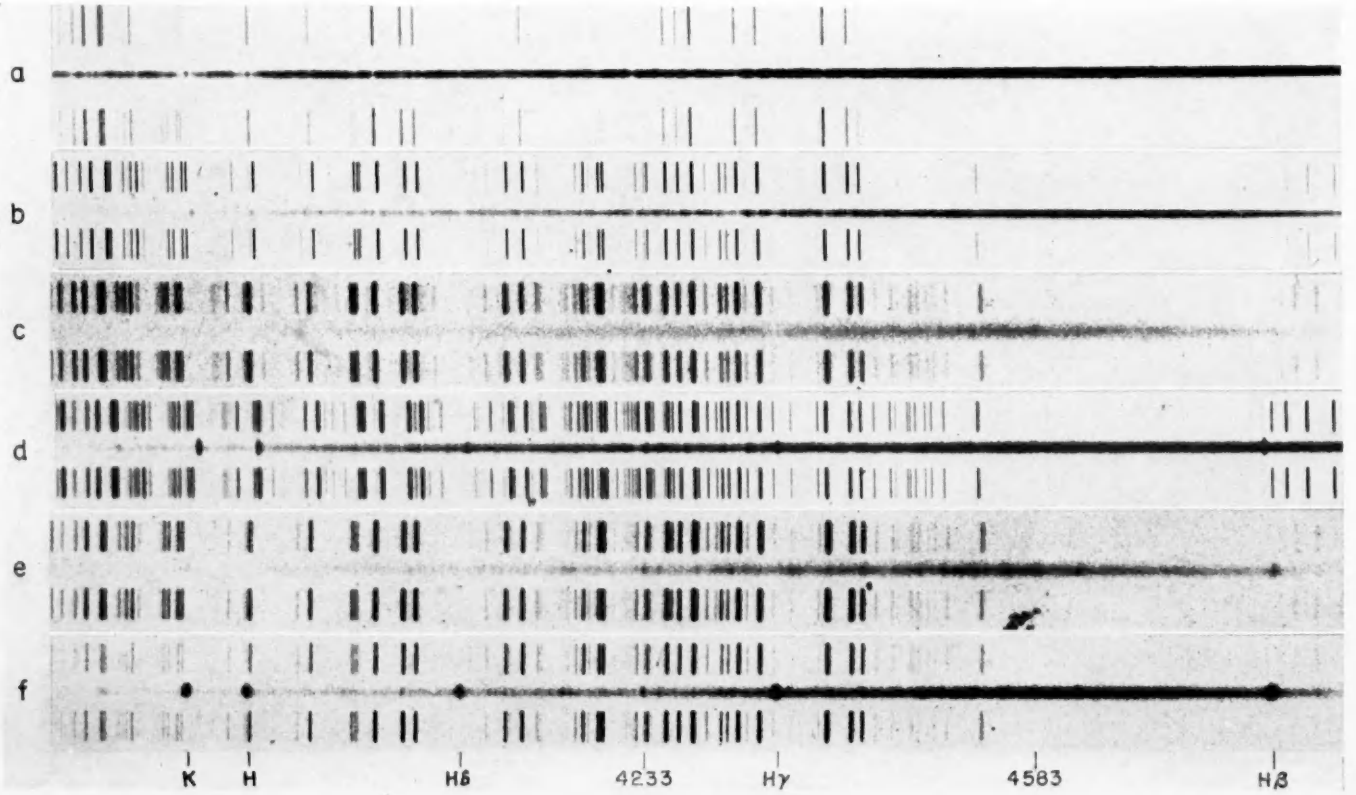

SPECTRA OF T TAURI STARS

(*a*) UX Tau, E1299, 1944 December 9; (*b*) RY Tau, E560, 1942 August 31; (*c*) R CrA, E474, 1942 June 3; (*d*) T Tau, E344, 1941 November 26; (*e*) R Mon, E319, 1941 October 30; (*f*) UY Aur, E322, 1941 October 31.

PLATE XIII

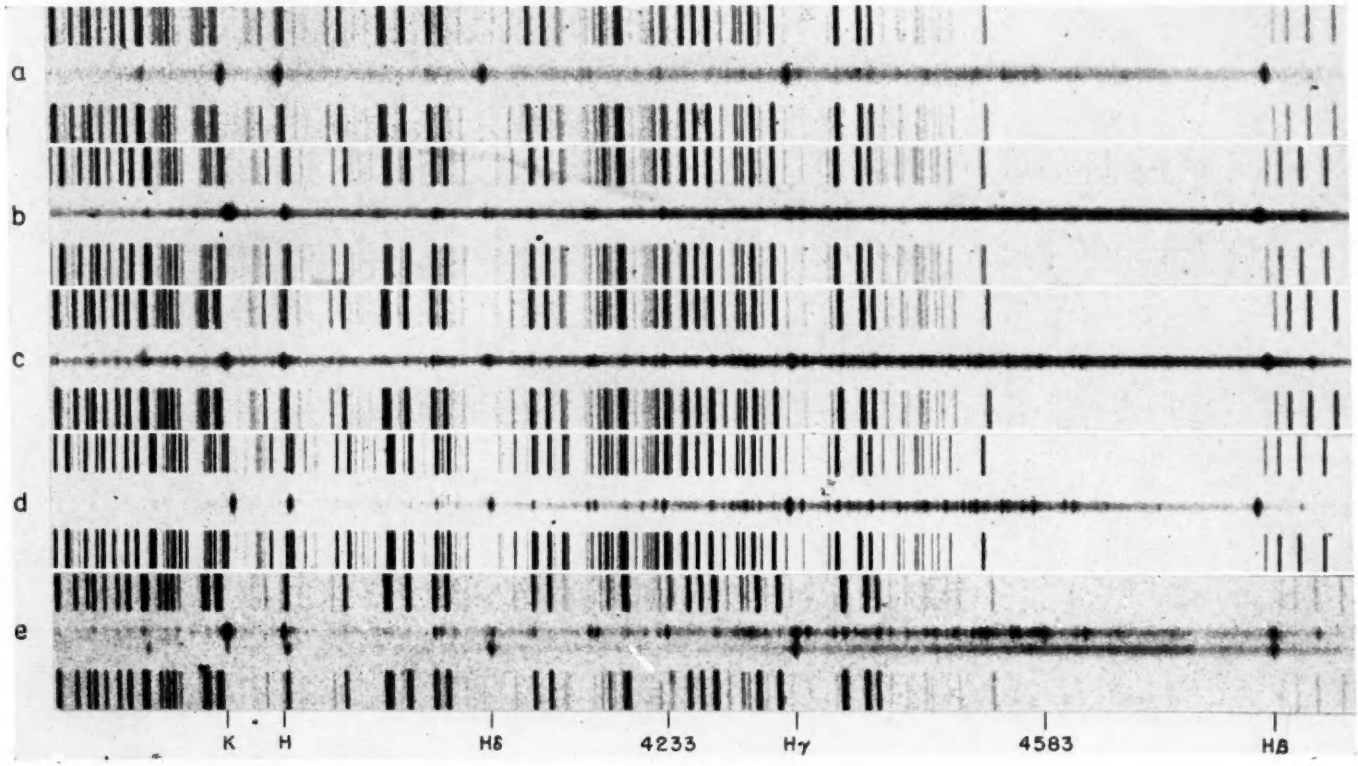

SPECTRA OF T TAURI STARS

(*a*) S CrA, E1106, 1944 June 28; (*b*) RW Aur, E1196, 1944 August 27; (*c*) XZ Tau, E1202, 1944 August 28; (*d*) RU Lupi, E833, 1943 May 11; (*e*) UZ Tau with companion below, E617, 1942 October 17.

PLATE XIV

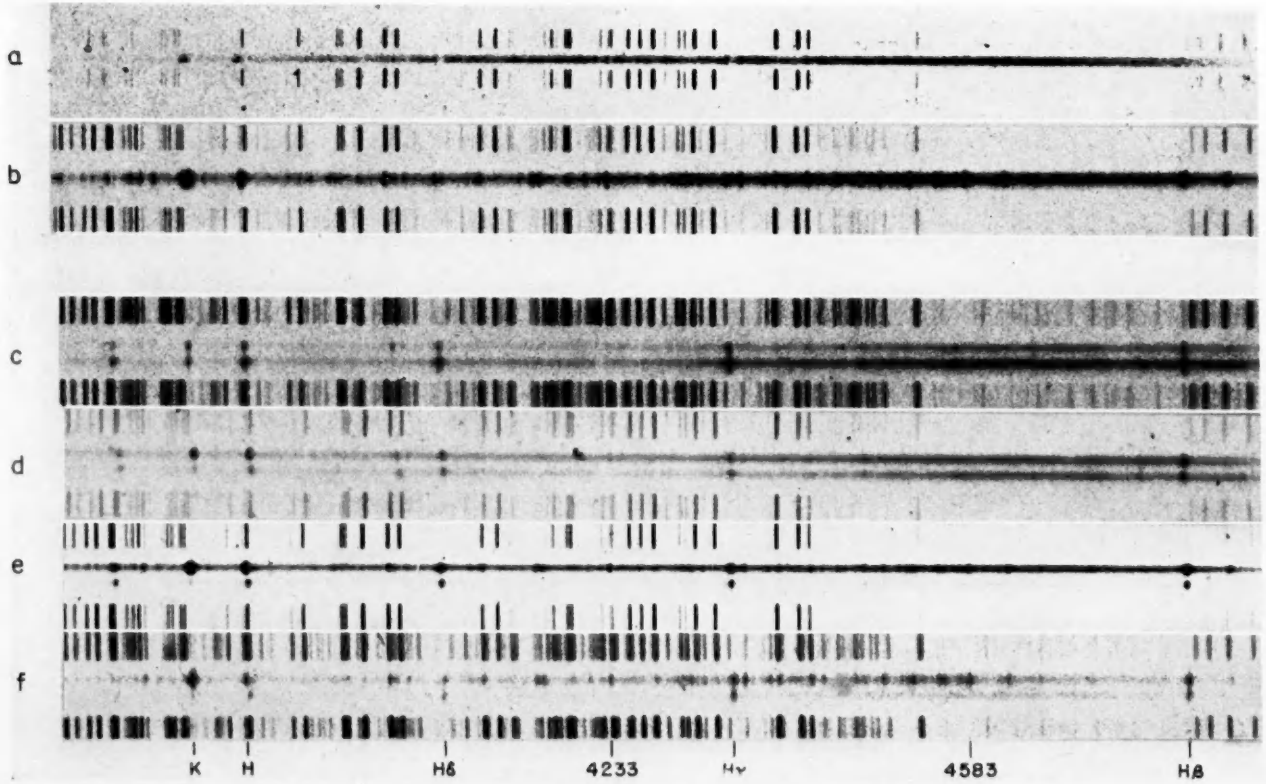

SPECTRA OF RW AUR AND UZ TAU AT DIFFERENT PHASES

RW Aur: (*a*) γ23841, November 2, 1941; (*b*) E1229, September 25, 1944.

UZ Tau with dMe companion below: (*c*)E1224, September 23, 1944; (*d*) E1047, January 4, 1944; (*e*) E1318, January 8, 1945; (*f*) E720, December 28, 1942.

PLATE XV

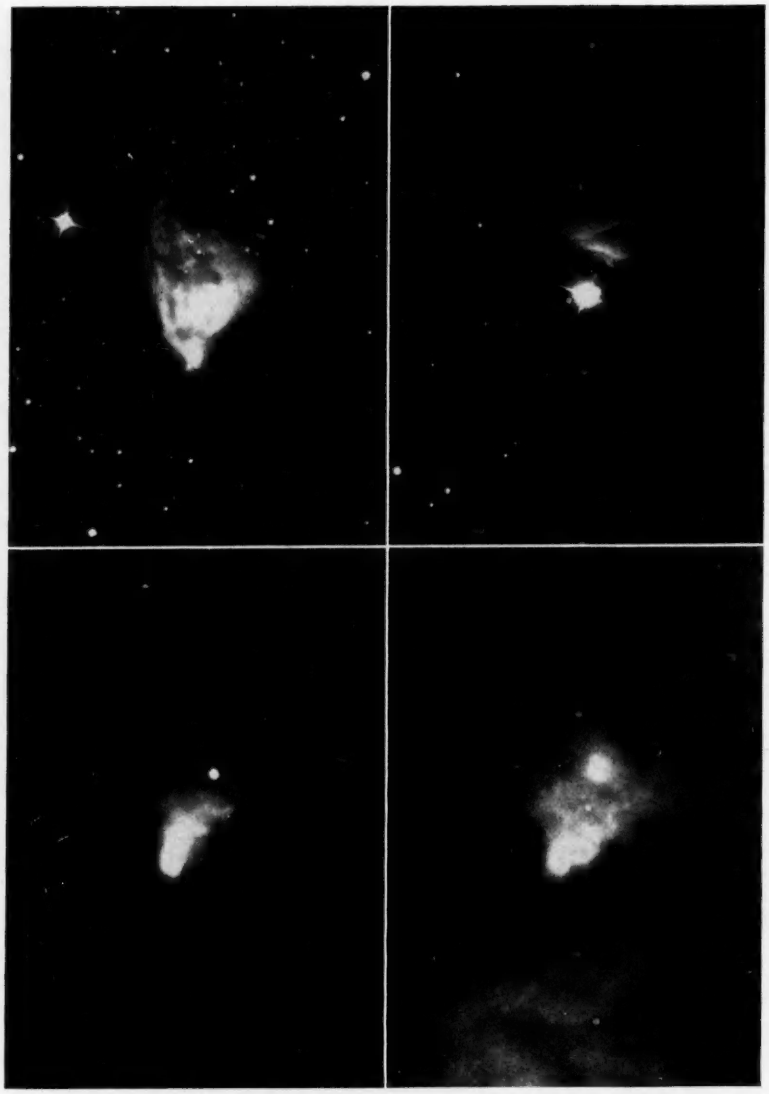

PHOTOGRAPHS OF VARIABLE STARS WITH ASSOCIATED VARIABLE NEBULAE

R Mon with NGC 2261 (*upper left*), 1920 January 26, photographed by E. Hubble; T Tau with NGC 1555 (*upper right*), 1940 September 30, photographed by W. Baade; R CrA with NGC 6729 (*lower left*), 1920 August 15, and (*lower right*), 1941 August 17, photographed by E. Hubble. 100-inch reflector.

RW Aurigae 050130

In 1906, Mme Ceraski[5] discovered from Moscow photographs the variation in light of RW Aur. Many variable-star observers have followed its rapid and unpredictable fluctuations without finding any trace of regularity. Large changes in brightness may take place within a few days or even a few hours. The total range is 3.0 mag. (9.0-12.0 vis.). The spectral class in the *Henry Draper Extension Catalogue* is G0.

Ten spectrograms of RW Aur, listed in Table 2, have been obtained. One of these, E342, was reproduced for comparison with other variable stars in the *Publications of the Astronomical Society of the Pacific*, **54**, 17, 1942. The outstanding peculiarities of the spectrum are well shown in this illustration. H and K of *Ca* II and the hydrogen lines are strong in emission and are distorted by broad, deep, central reversals. Numerous bright lines of other elements are also present, but the absorption spectrum is weak. The estimated spectral type is G5.

TABLE 2

OBSERVATIONS OF RW AURIGAE

Plate	Date	Est. Mag.	Disp.	Metallic Lines					*H* and *Ca* II Lines					
				Emission			Absorption		Emission (V. Comp.)		Emission (R. Comp.)		Absorption	
				No	Vel.	Int.	No.	Vel.	No.	Vel.	No.	Vel.	No.	Vel.
					km/sec			km/sec		km/sec		km/sec		km/sec
γ21234	1937 Oct. 14	11.5	c	1	− 94	wk	...	.....	3	−168	...	.....	2	+32
E286	1941 Sept. 30	10	c	6	− 185	str	7	+ 52	10	−220	1	+ 80	9	−31
γ23841	Nov. 2	11.5	c	3	− 5	wk	6	+ 63	5	−161	1	+103	4	+36
E342	Nov. 25	9.0	b	38	− 51	str	9	+ 11	5	−177	3	+ 97	5	− 2
E349	Nov. 27	9.5	b	60	− 43	str	...	.....	4	−197	4	+109	3	−35
γ24541	1942 Oct. 3	11.5	b	34	+ 2	m	...	.....	5	−165	3	+159	4	−23
E624	Oct. 19	9.0	b	28	− 10	m	13	+118	5	−115	2	+189	4	+61
E1048	1944 Jan. 4	9.5	c	...	.....	...	...	.....	...	.....	...	.....	...	.....
E1196	Aug. 27	11.0	c	37	+ 39	str	...	.....	9	−108	3	+160	4	+29
E1229	Sept. 25	10.0	c	56	− 39	str	...	.....	12	−173	7	+108	7	−32
Weighted mean	.....	.....	...	...	− 25	.....	...	+ 59	...	−166	...	+125	...	− 5

The red emission components of H (*Ca* II) and of *Hγ*, *Hδ*, and *Hε* are too weak to be seen except on the strongest exposures. The bright violet component of *Hε* falls near the absorption reversal of *H*(*Ca* II) and is practically obliterated; *Hβ* appears as a strong double emission line on all plates; *Hα* is a single bright line on plates E349 and E624, but the D(*Na* I) lines show only in absorption; *He* I is present on some of the plates but is too weak for reliable measurement.

Both absorption and emission lines of RW Aur lack the sharpness necessary for good measurement of radial velocity, and the accordance of the results both for individual lines and for the plate means leaves much to be desired. The discrepancies, however, are much greater than can be attributed to errors of measurement alone. A large part of the difficulty is probably due to the presence of the absorption reversals, which lie somewhat to the red of the centers of the stronger emission lines. These absorption components are especially strong in H and K (*Ca* II) and the hydrogen lines, but they are also present with varying intensity on the red side of many other lines.

[5] *A.N.*, **170**, 339, 1906.

The dark lines obviously originate in a stratum lying above that region of the stellar atmosphere in which the emission lines are formed. Variations in the intensities or positions of the dark lines tend to shift the bright components. Examples of the varying intensities of the emission components resulting from relative shift of the superposed absorption line may be found in $H\beta$. The ratios of the intensities of the violet to the red components on the spectrograms listed in Table 2 are, in order, 3 to 1, 4 to 4, 2 to 1, 3 to 1, 4 to 3, 4 to 4, 4 to 2, 3 to 2, 5 to 5, and 4 to 4. The decrement of the violet component from $H\beta$ to $H\delta$ is gradual, but the increasing width of the absorption line causes a steep decrement of the red component.

The conditions in the atmosphere seem far from stable, and no simple correlation of motion with light-variation can be drawn from the observations. A comparison of the mean velocity deduced from the few measurable low-level absorption lines with that from *Ca* II and hydrogen indicates that the upper layer is expanding with reference to the lower. The velocities from the bright lines are not readily comparable because of the interference of the absorption reversals.

The variable star RW Aur has an 11.5-mag. visual companion ($d = 1''.2$; $p = 254°$). A spectrogram of the companion was obtained on January 4, 1944, but on account of the proximity of the principal star its interpretation is uncertain. Additional observations are needed before its spectrum can be described with confidence. No strong bright lines are present, but in the region of $H\beta$ some emission is suspected.

Although obscured areas may be found near by, the sky in the immediate vicinity of RW Aur seems practically free from absorbing clouds.

UY Aurigae 044530

The variation of UY Aur was discovered in 1913 as a result of studies of Moscow photographs by Mme Ceraski.[6] Later observers have reported rapid irregular changes in brightness within intervals of a few days. The photographic-magnitude range is from 11.6 to 14.0. The spectrum was first observed[7] at Mount Wilson in 1932 and found to be like that of T Tau except that the lines of enhanced iron were comparatively weak at that time.

Ten spectrograms of UY Aur (Table 3) have been obtained. The spectrum is outstanding in the T Tauri group for strength of the bright lines of hydrogen and helium. On plate E619, *Hα* is extremely strong, and on most of the spectrograms λ 4026 and λ 4471 of *He* I are well marked. The line λ 4685 of *He* II was measured on one plate; D_1 and D_2 of *Na* I are fairly strong in absorption, but emission is weak or absent; D_3 (5875 *He* I) is probably present in emission. The extraordinary strength of the hydrogen series may result from the combined emission of both stars of the visual pair.

Considerable variation in the intensities of the emission lines of the metallic elements is indicated in the seventh column of Table 3. The hydrogen, calcium, and helium lines are not greatly affected by these changes and maintain about the same intensity at all phases. On plate E606 seven hydrogen lines were measured to the violet of $H\zeta$. As in the other stars of the group, the metallic emission lines are stronger and more numerous when the star is brighter. The absorption spectrum of UY Aur is poor; the lines are few and diffuse; the spectral type is not far from G5; and the absolute magnitude is that of the main sequence, λ 4435 and λ 4454 being well marked. Titanium oxide bands are suspected on some of the plates, but they may originate in the companion star.

On September 30, 1941, a twelfth-magnitude visual companion was discovered ($d = 0''.8$; $p = 212°$). The spectrogram of UY Aur obtained at that time indicated that some of the bright lines were displaced slightly along the length of the lines as if they had their origin in the companion star. This appearance is also present on several other plates with more or less certainty, depending upon the seeing and the accuracy of guid-

[6] *A.N.*, **193**, 439, 1913.

[7] A. H. Joy, *Pub. A.S.P.*, **44**, 385, 1932.

ing. On account of the proximity of the two stars, it has not thus far been possible to resolve the images sufficiently to separate the two spectra entirely. Further observations are needed before an adequate description of the two stars can be given.

R Coronae Australis 185537

The variable star, R CrA (CD−37°13027, mag. 9.7), is situated in the nucleus, near the preceding edge of the variable nebula, NGC 6729. The nebula is about 1.5 minutes of arc in length and extends beyond the neighboring star T CrA. Variation of both star and nebula was found by J. F. J. Schmidt in Athens and later confirmed photographically by R. Innes[8] and H. Knox-Shaw.[9] The remarkable changes in the form and appear-

TABLE 3

Observations of UY Aurigae

Plate	Date	Vis. Mag.	Disp.	Emission Lines			Absorption Lines	
				No.	Vel.	Int.	No.	Vel.
					km/sec			km/sec
C6135	1932 Sept. 12	12.0	c	5	+18	wk	.....	.....
6150	Oct. 10	11.7	c	6	−19	m	3	+38
E285	1941 Sept. 30	11.6	c	29	+ 7	str	12	+34
322	Oct. 31	11.6	c	16	−40	m	2	−15
345	Nov. 26	11.6	c	25	−15	str	.....	.....
606	1942 Oct. 1	12	c	16	+ 3	m	6	+38
619	Oct. 18	12	c	29	+19	str	.....	.....
677	Nov. 16	11.5	c	11	−18	wk	.....	.....
726	Dec. 29	12.5	c	12	+10	wk	3	+11
1233	1944 Sept. 26	12	c	15	−14	wk	2	+39
Weighted mean	.....	.....	.....	.....	− 3	.....	.....	+30

ance of the nebula are shown in Plate XV, but the relationship between the variations of star and nebula has not yet been satisfactorily determined. The nebula so enshrouds the star that, except with the lowest magnification, the object resembles the head of a comet rather than a stellar point and measures of the brightness of the variable are affected by the adjacent nebulosity. The extreme range in the brightness of the star as recorded by various observers is nearly 4 mag. The Harvard plates [10] indicate rapid irregular changes of about 2 mag. within a few days, superposed on slower changes over several years.

The spectrum was photographed in 1917 by V. M. Slipher,[11] who suspected that it was like that of R Mon. Observations by E. Hubble[12] in 1920–21 showed "bright unsymmetrically reversed hydrogen and enhanced iron lines on an absorption spectrum that is approximately G-type but which has contradictory characteristics" and led to the conclusion that "the spectrum resembles that of T Tauri except that it has no bright H and K."

[8] *Union Obs. Circ.*, No. 36, p. 282, 1916.

[9] *Bull. Helwan Obs.*, **1**, 141, 1920.

[10] S. Gaposchkin, *Harvard Ann.*, **105**, 514, 1937.

[11] *Bull. Lowell Obs.*, **3**, 66, 1918.

[12] *Mt. W. Contr.*, No. 241; *Ap. J.*, **56**, 181, 1922.

All the Mount Wilson spectrographic observations are included in Table 4.

The emission lines are not sharp, and few absorption lines can be distinguished with the dispersion used. On no plate are H and K definitely present in emission; but the exposures in that region are not adequate to make it certain that the lines are absent, although they are evidently weaker than in any other star of the group. This may be a sufficient reason for excluding R CrA; on the other hand, its connection with the variable nebula, its location in a dark lane, and its spectrum, in general, make it probable that it is related in some way to the T Tauri variables. The line $H\beta$ is fairly strong in emission, and the decrement of the hydrogen series toward the violet is rapid. As in the spectrum of RW Aur, the 1920–1921 plates show a strong absorption reversal in the normal position dividing the emission of $H\beta$ unsymmetrically, the violet component being the stronger. Later plates are quite different in this respect. On D1213 and E474 the absorption is weak or absent, and the emission is in the normal position. On plates C7509 and E539 the emission at $H\beta$ is weak, and $H\gamma$ is an absorption line about as strong as in an early F star with no emission showing. The bright *Fe* II lines vary in intensity. They are best

TABLE 4

OBSERVATIONS OF R CORONAE AUSTRALIS

PLATE	DATE	VIS. MAG.	SPEC.	DISP.	EMISSION LINES			ABSORPTION LINES		OBSERVER
					No.	Vel.	Int.	No.	Vel.	
C583.....	1920 Aug. 21	.....	F5	b	.....	.....	wk	.....	.....	E. P. Hubble
588.....	Aug. 22	.....	.....	b	.....	.....	wk	.....	.....	E. P. Hubble
1099.....	1921 June 28	.....	F5	b	.....	.....	m	.....	.....	E. P. Hubble
7509.....	1940 June 26	12.5	F5	c	.....	.....	wk	.....	.....	.....
D1213.....	Aug. 10	14±	F5	d	.....	.....	wk	.....	.....	E. P. Hubble
E474.....	1942 June 3	12	F5	c	2	−97	m	2	−36	.....
539.....	Aug. 3	13.5	F5	d	.....	.....	wk	.....	.....	.....

seen on plates C1099, June 28, 1921, and E474, June 3, 1942. Helium is not present, and no other chromospheric lines are recognized on our plates, but further observation at other times might be more favorable for their appearance. On plate E539, August 3, 1942, the bright lines are very weak; even $H\beta$ is hardly visible. The absorption components of hydrogen are present, however, in considerable strength. The spectrum on this plate somewhat resembles that of T CrA. Other than the lines of hydrogen, few absorption lines can be distinguished in the spectrum of R CrA.

Partly because of the strong hydrogen absorption lines, $H\gamma$ and $H\delta$, the spectral type of R CrA appears to be earlier than that of R Mon and might be estimated as F5. The spectroscopic absolute magnitude cannot be determined on account of the absence of absorption lines. Since it is embedded in nebulous matter, the apparent magnitude of the star may be considerably diminished.

The spectral type of T CrA, which lies in the direction of the tail of the cometary nebula, 5 seconds of time following and 0.8 minutes of arc south of R CrA, is F0. Three spectrograms taken at minimum light show no bright lines or abnormal spectrographic features. On the other hand, S CrA, 12.5 minutes of arc distant in the same lane of dark nebulosity as R CrA, is one of the most advanced of the T Tauri stars.

S CORONAE AUSTRALIS 18543*7*

The variability of S CrA, which is 43 seconds of time preceding and 0.3 minutes of arc south of R CrA, was discovered by J. F. J. Schmidt in Athens in 1866. He followed its

light-changes for nearly twenty years but was unable to find any regularity in its behavior. Suspected periods were of the order of 6 days.

Since 1925 the star has been observed by members of the American Association of Variable Star Observers, and magnitude estimates have been published yearly in *Harvard Circulars*. The variation has usually been between 11.5 and 12.5 mag., but in 1933 and 1941 estimates brighter than 11.0 mag. were reported.

Six spectrograms of S CrA (Table 5) were obtained at Mount Wilson in the years 1941–1944. The first spectrogram, which was obtained when the star was one or more magnitudes brighter than at the dates of later exposures, shows a rich emission spectrum characteristic of the T Tauri class. The bright lines of *Ca* II, *Fe* I, *Sr* II, and *Ca* I are nearly as well shown as in RU Lup. These lines are much reduced in intensity on later plates. The strong lines of *Ca* II (H and K) and hydrogen remain practically unchanged. Weak absorption reversals, which are not readily measurable, are superposed upon the strong emission; *He* I (λ 4026 and λ 4471) and *He* II (λ 4685) are stronger than in any other star

TABLE 5

OBSERVATIONS OF S CORONAE AUSTRALIS

Plate	Date	Vis. Mag.	Disp.	Emission Lines		
				No.	Vel.	Int.
					km/sec	
E287	1941 Oct. 1	11.4*	c	50	−24	str
510	1942 July 4	12.5	c	21	−39	m
556	Aug. 31	13	c	7	−39	wk
859	1943 June 21	13	c	26	−27	wk
881	July 11	12.5	c	9	−19	wk
1106	1944 June 28	12	c	25	−56	m
Weighted mean					−33	

* A.A.V.S.O. estimate.

of the group. None of the observations cover the red portion of the spectrum. No absorption lines are visible, and estimates of spectral type and spectroscopic absolute magnitude are impossible.

A companion of S CrA of magnitude 13.5 was observed on July 4, 1942 ($d = 1''$; $p = 135°$–$140°$). On account of its faintness it probably has little effect on the spectrum of the brighter star.

RU Lupi 155037

The variation in brightness of this star (HD 142560, CoD−37°10602) was detected by Miss J. C. Mackie[13] on Harvard photographs after Miss Cannon[14] had noted bright lines of hydrogen and calcium in its spectrum. The survey plates show irregular changes in brightness from 1893 to 1912 with a magnitude range from 9 to 11. Probably on account of its southern declination, it has been neglected by variable-star observers for nearly thirty years. No further observations are recorded until 1940, when P. W. Merrill[15] photographed its spectrum and called attention to the presence of strong emission of *Fe* II and *Ti* II, as well as of *H* and *Ca* II. He also found weak lines corresponding to *Fe* I, *Mg* II, *Cr* II, and *Sc* II. The appearance of bright lines of *Fe* I and strong H and K of *Ca* II indicated at once that the spectrum was related to that of T Tauri. Dr. Merrill

[13] *Harvard Circ.*, No. 196, 1916.

[14] *Harvard Circ.*, No. 201; *A.N.*, **207**, 215, 1918.

[15] *Pub. A.S.P.*, **53**, 342, 1941.

has been kind enough to place at my disposal two spectrograms of RU Lup, together with his line identifications and velocity measures for discussion in this paper.

Ten additional spectrograms, listed in Table 6, were obtained at the 100-inch telescope. The magnitude estimates may be influenced by atmospheric absorption, since the minimum zenith distance of RU Lup at Mount Wilson is 72°. The star was certainly much fainter in March and April, 1942, than at the other dates of observation.

With the dispersion used, no absorption lines can be distinguished, although the distribution of light in the continuous spectrum suggests a temperature lower than G0. No titanium oxide bands are present. The lack of absorption lines may be accounted for, in part, by the great number of emission lines of neutral, as well as ionized, atoms. Probably many lines having insufficient emission to show above the continuous spectrum have enough radiation to fill up the absorption in the lines. On one plate, E878, however, a faint central absorption line appears within the emission of both H and K.

TABLE 6

OBSERVATIONS OF RU LUPI

Plate	Date	Vis. Mag.	Disp.	Emission Lines			Observer
				No.	Vel.	Int.	
					km/sec		
C7535	1940 July 20	11	b	13	−22.5	m	P. W. Merrill
7680	1941 May 16	10.5	b	44	− 7.1	str	P. W. Merrill
E424	1942 Mar. 25	12	c	4	− 8.5	wk	
447	Apr. 24	12	c	18	−13.0	wk	
465	May 22	11	c	29	+ 8.5	m	
469	May 23	11	b	10	− 5.1	m	
496	June 21	10.5	b	78	− 9.0	str	
833	1943 May 11	11	b	70	− 6.7	m	
854	June 19	11.5	b	64	− 8.1	m	
878	July 10	11	b	52	− 1.8	str	
1393	1945 Apr. 20	11	d	.....	.....	m	
1407	May 21	10.5	c	.....	.....	m	
Weighted mean	.....	.....	.....	.....	− 6.4	.....	.....

The bright lines of RU Lup as well as of other stars of the T Tauri group are much wider than those of the Me variables or of stars like Z And, and the accuracy of measurement is correspondingly decreased. The apparent width of *H* and *Ca* II lines is about 4.5 A. Lines of other elements are, perhaps, one-half as wide, but none can be called sharp.

In the spectral region λλ 3900–6500, 120 emission lines have been measured and identified. The 15 elements represented, together with the number of lines, are shown in Table 7 in order of their line intensities. Many other blended lines are probably present in RU Lup, but they are not resolved on account of the width of the lines and the low dispersion. This list, however, will be sufficient to give a general idea of the characteristics of the emission spectrum of the T Tauri stars. The metallic lines were greatly weakened in March and April, 1942, when the light of the star diminished.

The radial velocities (Table 6) from the emission lines were practically constant during the period of observation. The weighted mean velocity is −6.4 km/sec. Likewise, the range in velocity among the different elements is small, as indicated by Table 8, in which the elements are arranged in order of atomic weight. For most of the elements the agreement of the individual lines is satisfactory, but for *Ca* II the measures indicate a dis-

crepancy of 36 km/sec between H and K. The effect is systematic and is seen on all plates measured, K being displaced 21 km/sec toward the red and H 15 km/sec toward the violet with reference to the mean of all lines. Both lines appear to be quite symmetrical. The faint emission of $H\epsilon$ would have little influence on the position of H, but it is possible that absorption in the hydrogen line might decrease the intensity of H on the red edge and tend to shift the line toward the violet. No explanation for the displacement of K, however, seems evident.

RU Lup is located in one of the dark lanes of the southern Milky Way but is not known to have any companion or to be enveloped in local nebulosity.

R Monocerotis 063308

The variable star R Mon (BD+8°1427) is the nucleus of the comet-shaped variable nebula, NGC 2261. Its light-changes were detected by J. F. J. Schmidt[16] in Athens in

TABLE 7

ELEMENTS REPRESENTED IN RU LUPI

Atom	No. Lines	Atom	No. Lines	Atom	No. Lines	Atom	No. Lines	Atom	No. Lines	Atom	No. Lines
H.....	5	*Ti* II....	35	*Ca* I....	1	*He* I....	1	*Ni* II...	1	*Na* I...	2
Ca II....	5	*Sr* II....	2	*Sc* II....	5	*Cr* I.....	3	*Mg* II...	1	*He* II...	1
Fe II....	28	*Fe* I.....	24	*Cr* II....	6						

TABLE 8

RADIAL VELOCITIES OF ELEMENTS IN RU LUPI

Element	Vel.	No. Lines	Element	Vel.	No. Lines	Element	Vel.	No. Lines	Element	Vel.	No. Lines
	km/sec			km/sec			km/sec			km/sec	
H.....	−10.7	4	*Sc* II....	− 3.6	5	*Cr* II....	+ 4.0	6	*Ni* II....	− 7.2	1
Ca I.....	−12.0	1	*Ti* II....	− 8.5	35	*Fe* I.....	− 6.7	22	*Sr* II....	+11.5	2
Ca II....	− 3.0	2	*Cr* I.....	− 3.0	2	*Fe* II....	−11.0	28			

1861, and later observations indicated that the variations were irregular, with a range of at least 4 mag. It is difficult to make precise estimates of brightness on account of the surrounding nebulosity. With high magnification the star resembles the nucleus of a comet near the sun.

From direct photographs taken with the 24-inch reflector of the Yerkes Observatory, E. Hubble[17] in 1916 discovered that marked changes in the outline of the nebula occurred within a period of a few months. In size and general form it is similar to NGC 6729, except that the outer parts of NGC 2261 are longer, extending to a distance of 2.5 minutes of arc.

The spectrum of the star and that of the nebula were photographed by V. M. Slipher[18] at the Lowell Observatory in 1917 and found to be identical, indicating that the light of the nebula is reflected radiation from the star. He suggested that the emission spectrum resembled that of Nova Aurigae. The lines that can be identified from his measures are those of *H*, *Ti* II, and *Fe* II, which do not necessarily pertain to novae, although, soon

[16] *A.N.*, **55**, 91, 1861.

[17] *Proc. Nat. Acad.*, **2**, 230, 1916; *Ap. J.*, **44**, 190, 1916, and **45**, 351, 1917.

[18] *Op. cit.*, p. 63.

after maximum, bright lines of ionized metals are prominent in most novae and at minimum they may appear in such stars as RS Oph.[19] The high-excitation features characteristic of the spectra of novae are entirely lacking in R Mon. On the other hand, the Mount Wilson spectra of R Mon and probably the Lowell spectrum, as well, correspond closely with the spectra of the T Tauri variables. The bright hydrogen lines are accompanied by moderately strong dark lines on the violet side as in T Tau, and the decrement of the series toward the violet is steep. The H and K lines are present in emission but are not nearly so strong as in T Tau. Helium and the nebular lines are definitely lacking. The normal absorption spectrum is extremely weak.

By attributing the formation of cometary nebulae to the action of radiation pressure from the star upon the surrounding material particles, R. Minkowski[20] finds that the radiation of dwarf stars is insufficient to produce nebular forms such as NGC 2261 or NGC 6729 from surrounding material and concludes that if the spectrum is G-type, as appears from the distribution of light in its spectrum and from analogy with other stars of

TABLE 9

OBSERVATIONS OF R MONOCEROTIS

Plate	Date	Vis. Mag.	Disp.	Emission Lines			Absorption Lines		Observer
				No.	Vel.	Int.	No.	Vel.	
					km/sec			km/sec	
D1158	1939 Nov. 13	.....	d	.....	.....	wk	.....	.....	E. Hubble
1159	Nov. 13	.....	d	.....	.....	wk	.....	.....	E. Hubble
E319	1941 Oct. 30	13	c	19	+18	m	7	+12	
727	1942 Dec. 29	13	c	7	+28	wk	.....	.....	
Weighted mean	.....	.....	.....	.....	+21	.....	.....	+12	.....

the group, the stars must be giants with absolute magnitudes of +0.7 or brighter. Since the absorption lines are poorly shown in the spectra, the spectroscopic absolute magnitudes cannot be well determined. A. van Maanen[21] estimates the trigonometric parallax of R Mon to be smaller than 0".005, which, without allowance for obscuration, would indicate an absolute magnitude brighter than +2.8 at maximum and +7.5 at minimum.

The Mount Wilson spectrographic observations of R Mon are listed in Table 9. Plates D1158 and D1159, taken with the 3-inch camera, are excellent, but the dispersion is too low to allow accurate measurement. On plate E319 the stronger chromospheric lines are well represented, and the resemblance of the emission spectrum to that of T Tau is beyond question.

The K line is three or four times as strong as H, and both are considerably weaker than in any of the other stars of the group except R CrA and UX Tau. None of the observations, however, were made at maximum light.

Although R Mon is deeply imbedded in nebulosity, its spectrum shows no marked effect of selective absorption, as far as can be estimated by visual inspection of the distribution of the continuous spectrum.

T Tauri 041619

The variable T Tau (BD+19°706) has been chosen as the typical star of this group of peculiar variable stars because it is the best known, is among the brightest, and rep-

[19] Adams, Joy, and Humason, *Pub. A.S.P.*, **39**, 366, 1927.

[20] *Pub. A.S.P.*, **54**, 190, 1942.

[21] *Mt. W. Contr.*, No. 237, 1922.

resents the group with respect to both emission and absorption spectra. It has an extended history, its variation in light having been discovered by Hind in 1852. It is 2.3 seconds of time following, 37 seconds of arc north of, the faint irregular patch of nebulosity well known as Hind's variable nebula (NGC 1555). The star itself is surrounded by faint variable shell, 4″ in diameter, observed by S. W. Burnham[22] in 1890 and by H. D. Curtis[23] in 1899. On Dr. Baade's remarkable photograph of T Tau, reproduced on Plate XV, this shell appears as a semicircular protuberance between the two diffraction rays on the right-hand side.

TABLE 10

OBSERVATIONS OF T TAURI

Plate	Date	Est. Mag.	Spec.	Disp.	Emission Lines			Absorption Lines		Observer
					No.	Vel.	Int. Metal. Lines	No.	Vel.	
						km/sec			km/sec	
P76	1915 Jan. 12	11	G5	d	5	(+86)	str	...	...	F. G. Pease
γ4479	Nov. 18	...	G5	b	2	+ 0.7	wk	7	+ 3.9	W. S. Adams
Σ24	1918 Oct. 5	10	G4	d	...	...	str	...	...	R. F. Sanford
C121	1919 Oct. 13	...	G5	a	10	+23	wk	35	+29	R. F. Sanford
C3128	1925 Jan. 11	10	G6	b	5	+26.4	str	7	+21.6	R. F. Sanford
C5350	1929 Oct. 21	9.5	G7	b	...	...	wk	...	...	R. F. Sanford
G1554	1940 Sept. 20	9	...	b	1	+21	wk	9	+41.4	R. F. Sanford
G1555	Sept. 20	9	...	b	...	...	wk	...	...	R. F. Sanford
γ23821	1941 Oct. 12	9.0	G8	c	4	+15.0	wk	5	− 8.9	
E321	Oct. 31	9.0	G5	c	19	− 5.8	str	15	+ 6.6	
E344	Nov. 26	9.0	G4	b	45	+36.2	m	22	+18.3	
γ23928	Dec. 4	10	G8	b	15	− 2.0	wk	17	+21.7	
E366	Dec. 26	9.0	G3	b	5	+34.5	wk	11	+41.7	
γ24022	1942 Feb. 6	9.2	G5	c	4	+18.2	wk	4	+23.3	
E596	Sept. 29	9	G5	b	8	+10.9	wk	19	+10.2	
E620	Oct. 18	9	G6	c	11	+11.9	m	6	+10.2	
E752	1943 Jan. 15	9.0	G6	b	12	+18.6	wk	4	+46.0	
G1838	Sept. 12	9	...	c	...	...	...	...	...	
E1237	1944 Sept. 27	11.0	G8	c	33	+25.8	m	10	+41.4	
Weighted mean	...	...	...	...	...	+19.6	...	...	+24.6	

The brightness of T Tau changes erratically from magnitude 9.0 to magnitude 12.8. It may vary rather quickly in the course of a few weeks, or the fluctuations may be delayed for months. In the last three years the brightness, at the time of observation, has remained near maximum.

The spectrograms show emission and absorption lines, both of which lack the sharpness needed for accurate measurement. The spectral type is about G5, and the spectroscopic absolute magnitude based on the Mount Wilson system of 1935 is +5.0.

The Mount Wilson observations are collected in Table 10. I am greatly indebted to Dr. W. S. Adams and Dr. R. F. Sanford for the use of their plates and measures in this study. The first known slit-spectrogram of T Tau was obtained in 1915 by F. G. Pease, and many of the interesting features of the spectrum were described by Adams and

[22] *M.N.*, 51, 94, 1890.

[23] *Pub. A.S.P.*, 27, 242, 1915.

Pease.[24] On account of the low dispersion used, the published radial velocity and some of the identifications of lines have little weight. Fifteen emission lines were measured, H and K being the most intense. The *Fe* I lines, λ 4063 (probably blended with λ 4068 [*S* II]) and λ 4132, which they did not identify, are stronger than the lines of *Fe* II. Lines of *Ti* II are too weak for measurement. The metallic lines are extremely weak on the second plate taken ten months later, and only a few lines of *Fe* II were measured in addition to those of *H* and *Ca* II. Dr. Sanford's low-dispersion spectrogram of 1918 is very similar to that of 1915.

Higher dispersion was used for C121 than for any other plate of this series, but unfortunately it was obtained at a time when the emission lines were comparatively weak. Sanford[25] measured 11 bright and 35 absorption lines, which he estimated to be 3–4 A in width. The metallic bright lines measured were without exception the strongest lines of *Fe* II.

The region of the D lines is well shown on G1554. Sodium is doubtless present in emission in T Tau, although the strength of the lines is not much greater than that of the adjacent continuous background. Bright D_1 and D_2 show, according to Dr. Sanford's measures, approximately normal velocities, but they are accompanied by strong absorption, which is displaced 165 km/sec to the violet, as compared with the mean of the bright lines. Similar violet displacements of absorption adjacent to the strong emission lines of hydrogen and *Ca* II (H and K) appear on plates showing the violet regions of the spectrum. On G1554, the bright lines of *Fe* II are distinctly weak, and the hydrogen lines *Hβ* and *Hα*, only moderately strong as compared with the continuous spectrum.

The infrared region, λλ 6400–8700, of the spectrum is shown on plate G1838. Although the spectrogram is underexposed, it shows that the $3^2D - 4^2P^0$ triplet of *Ca* II (λλ 8498, 8542, 8662) cannot be present in any great strength either in emission or in absorption.

In general, the *Ca* II (H and K) emission lines of T Tau appear with an intensity unsurpassed by any star of the group; the hydrogen lines are strong, *Hγ* being only slightly fainter than *H* (*Ca* II), but the metallic lines are weaker than those of most of the other stars of the group. The metallic bright lines are not prominent features of the spectrum of T Tau on most of our spectrograms.

Although the absorption lines are wide, they are not greatly affected by the emission spectrum, and measures of radial velocity based on a considerable number of lines should give reliable results. The mean velocities of the emission and absorption lines agree closely, but the range in both is more than can reasonably be attributed to errors of measurement. The scatter among the mean velocities of the various elements is comparatively small and probably is not significant.

RY Tauri 041528

The variation in brightness of RY Tau (BD+28°645; 9.1 mag.) was discovered from Harvard photographs by Miss Leavitt[26] in 1907. The range was estimated to be 1 mag. with slow and irregular changes. Few photometric observations have been reported since its discovery.

The star RY Tau is at the head of a faint fan-shaped nebula about 7 minutes of arc in length, which spreads out in two tails toward the dark nebula, Barnard 214. The close connection between the star and the bright nebula is apparent from photographs by E. E. Barnard[27] and by O.C. Collins.[28] The image of the star at the telescope appears stellar because of the faintness of the nebulosity.

[24] *Pub. A.S.P.*, **27**, 132, 1915.

[25] *Pub. A.S.P.*, **32**, 59, 1920.

[26] *Harvard Circ.*, No. 130, 1907.

[27] *Atlas of the Milky Way*, Pl. 5, 1927.

[28] *Ap. J.*, **86**, 543, 1937.

The Mount Wilson observations and velocities are listed in Table 11. The first three spectrograms were obtained by E. Hubble, who estimated the spectral type to be F8±.[29] These plates are, unfortunately, not suitable for radial-velocity determinations. Later spectrograms show some evidence of variation in type between F8 and G2. The absorption lines are only slightly widened and should give good measures of radial velocity and spectroscopic absolute magnitude.

The four lower members of the hydrogen series and the calcium lines H and K are the only emission lines found in RY Tau. As indicated in the eighth column of Table 11, the strength of the bright H and K lines varies considerably. They appear in emission on all fully exposed plates but are especially strong on plate E272, where they are about 5 A in width and K is much stronger than H. On plates E560 and E1273, H and K are divided

TABLE 11

OBSERVATIONS OF RY TAURI

Plate	Date	Est. Mag.	Spec.	Disp.	Ca II Emission Lines			Absorption Lines		Observer
					No.	Vel.	Int.	No.	Vel.	
						km/sec			km/sec	
C587	1920 Aug. 21	.....	.....	b	.....	.....	.....	.....	.....	E. Hubble
934	1921 Mar. 9	9.6	G0	b	.....	.....	.....	.....	.....	E. Hubble
2526	1923 Nov. 11	11.0	G0	b	.....	.....	.....	.....	.....	E. Hubble
γ21100	1936 Dec. 5	10	F8	b	.....	.....	wk	12	+25	
E272	1941 Sept. 28	10	G2	c	1	0	str	13	+32	
γ23840	Nov. 2	9	G0	b	.....	.....	wk	6	+23	
23922	Dec. 4	9	G2	c	.....	.....	wk	10	+32	
E407	1942 Feb. 22	10	.....	b	.....	.....	.....	6	+18	
560	Aug. 31	8.8	G0	b	2	+ 15	str	15	+32	
621	Oct. 18	9	F8	c	2	− 20	str	13	+26	
γ24669	Nov. 13	8.8	F8	b	.....	.....	m	14	+22	
E1273	1944 Nov. 7	9.5	G0	b	2	−116 + 44	m	14	+24	
Weighted mean	.....	.....	.....	.....	.....	− 8	.....	.....	+26.2	.....

by deep absorption. The violet component of K has about twice the intensity of the red component, but the strong absorption of $H\epsilon$ greatly weakens the red component of H. The violet emission components of $H\gamma$ and $H\delta$ appear as faint bright edges of the wide absorption lines. On the red-sensitive plate E621, $H\alpha$ is a strong bright line and $H\beta$ is faintly visible.

The radial velocities from the absorption lines show little or no variation. Measurements of bright H and K are uncertain on account of the width of these lines and of insufficient exposure on some plates.

UX TAURI 042418

The variability of UX Tau (BD+17°736; 9.5 mag.) was discovered from Harvard photographs by Miss H. Locke in 1917.[30] Photographic observations by P. P. Parenago,[31] H. Rugemer,[32] and M. Esch[33] indicate that the light-changes are rapid and con-

[29] *Mt. W. Contr.*, No. 241; *Ap. J.*, **56**, 182, 1922.

[30] *Harvard Circ.*, No. 201, 1918.

[31] *Nishni-Novgorod, Veränderliche Sterne*, **4**, 154, 1933.

[32] *A.N.*, **255**, 180, 1935.

[33] *Valkenburg Obs. Veröff.*, No. 7, p. 13, 1937.

tinuous. Periods of a few days were, at first, suggested but have not been confirmed by later observers. The extreme photographic range was found to be nearly 3 mag., from 10.5 to 13.4 mag. The spectral type was estimated as G5 by Miss Cannon.[34]

Eight spectrograms of UX Tau were obtained at Mount Wilson, as listed in Table 12. The star was near maximum light at the time of observation. In this star H and K are faintly bright on all plates sufficiently exposed in the violet region. On the red-sensitive plate, E622, *Hα* is a moderately strong emission line, and *Hβ* is faintly bright. On the remaining plates of the series, *Hβ* is present in absorption but appears to be somewhat weakened on E309 and E568. No other lines appear in emission in UX Tau.

The absorption spectrum indicates that the spectral type is dG5. The range in velocity shown in the last column is somewhat larger than would be expected for stars of constant velocity.

TABLE 12

OBSERVATIONS OF UX TAURI

Plate	Date	Vis. Mag.	Spec.	Disp.	*Ca* II Emission Lines		Absorption Lines	
					No.	Vel	No.	Vel
						km/sec		km/sec
E309	1941 Oct. 28	10.5	G6	c	.....	.....	17	+27
425	1942 Mar. 25	10.5	G5	c	.....	.....	6	+42
568	Sept. 2	10.5	G6	c	2	− 6	13	+ 9
622	Oct. 19	10.5	G6	c	3	− 5	10	+ 2
676	Nov. 16	10.5	G5	c	.....	.....	9	+16
995	1943 Oct. 14	10	G0	c	.....	.....	6	+27
γ26339	1944 Dec. 6	10.5	G5	b	2	+31	17	+30
E1299	Dec. 9	10.5	G5	c	2	+20	11	+22
Weighted mean	.....	.....	.....	.....	.....	+18	.....	+24

UX Tau is situated in the center of a densely obscured area. A thirteenth-magnitude companion, 5.7 seconds of arc preceding, shows a spectrum whose type is dM2e, with bright hydrogen and *Ca* II (H and K). Its radial velocity agrees with the mean for the variable star, and they probably form a physical double.

UZ TAURI 042625

The variable star UZ Tau, whose light-changes were first noticed by K. Bohlin[35] on photographs taken in 1921, has been described as "nova-like." Maxima brighter than 9.5 were observed on October 4, 1921, by Bohlin and on January 6, 1924, by M. Esch.[36] P. P. Parenago[37] reported photographic magnitudes as faint as 15.0 in 1934, and K. Himpel[38] estimated the visual magnitude to be about 13.2. On 148 Harvard photographs from January, 1890, to November, 1900, and from September, 1913, to January, 1941,[39] Miss Dorrit Hoffleit found that the magnitudes generally varied irregularly from 13.5 to 14.5 and no maximum was brighter than 11.7.

[34] *Harvard Bull.*, No. 897, 1934.

[35] *A.N. Beob.-Zirk.*, **3**, 55 (No. 32), 1921.

[36] *A.N. Beob.-Zirk.*, **6**, 5 (No. 2), 1924.

[37] *Nishni-Novgorod, Veränderliche Sterne*, **4**, 228, 1934.

[38] *A.N.*, **270**, 185, 1940.

[39] *Pub. A.S.P.*, **54**, 33, 1942.

The star UZ Tau is 53 seconds of time following and 1 minute of arc south of BD+24°719. At the time of the first Mount Wilson observation,[40] the star was discovered to be double ($d = 3''.7$; $p = 92°$; mag. 13.0 and 13.3, vis.). Since, on the first spectrograms, both stars appeared to be of class dMe, the conclusion was erroneously drawn that the variation previously observed pertained to a dwarf M-type star with emission lines of hydrogen and *Ca* II. Later observations[41] made in October and December, 1942, revealed that the following star had increased in relative brightness by half a magnitude or more and its spectrum had so changed that it became clear that the star belonged to the T Tauri group, although the titanium bands remained faintly visible on most of the plates. Further observations are needed to determine with certainty whether two or three stars are involved and whether the variable star and the preceding dMe star are physical companions.

TABLE 13

OBSERVATIONS OF UZ TAURI

Plate	Date	Vis. Mag.	Disp.	Emission Lines			Observer
				No.	Vel.	Int.	
					km/sec		
E341	1941 Nov. 25	13.5	c	4	− 5	wk	
367	1942 Jan. 12	13.3	d	.....	.....	wk	M. L. Humason
396	Feb. 3	13.2	d	.....	.....	wk	
571	Sept. 3	13.2	c	5	+ 6	wk	
617	Oct. 17	13.0	c	83	− 6	str	
633	Oct. 21	12.5	d	.....	.....	str	
711	Dec. 15	13.0	c	.....	.....	.....	
720	Dec. 28	12.5	c	59	−16	str	
1047	1944 Jan. 4	12.8	c	11	− 1	wk	
1224	Sept. 23	14.0	c	6	+25	wk	
1318	1945 Jan. 8	12.5	c	81	+ 1	str	
Weighted mean	.....	.....	.....	.....	− 5	.....	.....

Eleven spectrograms of UZ Tau have been obtained (Table 13). Since the position angle of the stars is nearly 90°, images of both fall on the slit of the spectrograph and may be photographed at the same exposure. On account of the faintness of the stars, observations can be made only with low dispersion and with favorable seeing. Three plates—E367, E396, and E633—were made with the 3-inch Schmidt camera and, on account of low dispersion, were not used for radial-velocity determinations. Plate E711, which was sensitive to the red portion of the spectrum, is weak but shows the hydrogen *Hα* emission line in both stars, that of the variable being the fainter of the two, although the stars were estimated to be of equal visual brightness at the time of observation.

Absorption lines in the spectrum of UZ Tau are weak and cannot be measured with certainty. The changes in the spectrum are extraordinary (Pl. XIV), varying from close resemblance to that of BD+20°2465 (dM3) with indistinct absorption lines (E341) to a spectrum with a strong continuous background upon which are superposed, at different times, few (E1047) or many (E720) emission lines. In general, a greater number of bright lines appears when the star is more luminous. However, E1047 shows distinct peculiarities. The magnitude, according to the estimate made at the time this spectrogram was

[40] A. H. Joy, *Pub. A.S.P.*, **54**, 33, 1942.

[41] A. H. Joy, *Pub. A.S.P.*, **55**, 38, 1943.

taken, was somewhat brighter than the mean, and the titanium bands are obliterated, yet bright lines, other than hydrogen, H and K, *Fe* II, and λ 4068 [*S* II] are few and weak. The peculiar features of E1047 have not been detected in spectrograms of any other star of the group, although E677 and E726 of UY Aur are similar in certain respects. The *He* I line, λ 4471, and the [*S* II] pair, λ 4068 and λ 4076, are enhanced with respect to the *Fe* II lines; H and K are tremendously strong and of nearly equal intensity, while on plates having large numbers of the low-level bright lines H is considerably weaker than K. Although few bright lines are visible, no measurable absorption lines are present.

Continual change seems to be characteristic of the spectrum of UZ Tau. On the other hand, the preceding star of the visual pair, which was the brighter of the two when the duplicity was first discovered, is apparently unaffected by the peculiar behavior of its neighbor and its spectrum shows no certain changes. The mean velocity of the Me companion determined from its emission lines is +16.0 km/sec, which is not in good agreement with −5 km/sec for the variable, as shown in Table 13. This lack of accordance may be due to instability in the atmosphere of the variable and to the effect of absorption components on the position of the emission lines.

Measurements of proper motion and trigonometric parallax are much needed, but near-by comparison stars are few because of heavy obscuration.

TABLE 14

OBSERVATIONS OF XZ TAURI

Plate	Date	Vis. Mag.	Disp.	Emission Lines			Absorption Lines	
				No.	Vel.	Int.	No.	Vel.
					km/sec			km/sec
E350	1941 Nov. 28	12.5	c	39	+48	m	.....	.....
610	1942 Oct. 2	13.5	c	98	+25	m	26	+109
1202	1944 Aug. 28	12.0	c	91	+32	str	.....	.....
Weighted mean	.....	.....	.....	.....	+32	.....	.....	+109

XZ TAURI 042518

The star XZ Tau follows UX Tau by 97 seconds of time in nearly the same declination. Its variability was discovered in 1928 by Mme G. Schajn[42] from an examination of photographs taken at Simeis in the Crimea. The photographic range was estimated to be from 11.3 to 13.5 mag. From the nine plates at her disposal a long period of 260 days was suspected. Observations by M. Esch[43] in the following year indicated that the variations were irregular and that large changes in brightness (9.5–13.2 mag.) occurred within a few days. H. Rugemer[44] also found the changes in light to be irregular, with variations between 10.4 and 13.5 mag.

In the last four years, at times when observations could be made on Mount Wilson, XZ Tau was faint. The three spectrograms obtained (Table 14) indicate that it is one of the most remarkable members of the T Tau group. Even at minimum light, when only low dispersion could be employed, 105 bright lines were measured, the largest number measured on any single plate of the T Tauri series. Observations at maximum light should be most interesting if, as is usually found in stars of the group, the chromospheric lines are stronger and more numerous at maximum than at minimum. Spectrograms in the red and at maximum light will be obtained when opportunity permits.

[42] *A.N.*, **234**, 41, 1928.

[43] *A.N. Beob.-Zirk.*, **11**, 10 (No. 4), 23 (No. 9), 1929.

[44] *A.N.*, **255**, 180, 1935.

No companion star or bright nebulosity has been detected near XZ Tau, which is, however, in the edge of the heavy obscuring cloud which surrounds UX Tau.

GENERAL DISCUSSION OF THE SPECTRA

Only three of the T Tauri stars (T Tau, RY Tau, and UX Tau) have absorption spectra sufficiently well defined to permit a precise determination of the spectral type (Table 18). For RW Aur, UY Aur, and R CrA, rough estimates may be made with the aid of such lines as are available. A variation of three- or four-tenths of a class was found for T Tau and RY Tau. The remaining stars, in which the bright-line spectrum is dominant, have few absorption lines; but, from the distribution of light and the general appearance of the spectrum, we conclude that the physical conditions correspond to those of about type G5. For some stars of the group, selective absorption by surrounding nebulosity may introduce uncertainty. Peculiar features of the spectra such as are mentioned in the preceding descriptions of the individual stars are often so prominent that the usual criteria of classification cannot be employed.

As shown in Plates XII and XIII the intensity of the emission spectrum varies greatly from star to star. When arranged according to the increasing prominence of the emission spectrum, the sequence of the stars is that of Table 15. Although the observations cover

TABLE 15

GREATEST STRENGTH OF EMISSION SPECTRUM

Star	Relative Strength of Emission	Star	Relative Strength of Emission	Star	Relative Strength of Emission	Star	Relative Strength of Emission
UX Tau.....	0	T Tau.....	4	S CrA.....	8	RU Lup.....	10
RY Tau.....	1	R Mon.....	4	RW Aur....	9	UZ Tau.....	10
R CrA.....	2	UY Aur.....	5	XZ Tau.....	9		

a considerable period of time and indicate a marked change in the intensity of emission for each star, the maximum possible strength of the emission spectrum for an individual star may not, thus far, have been observed, and, therefore, the order of the arrangement may not be final.

The changes occurring in the spectra of individual stars are illustrated in Plate XIV. The emission spectrum is usually more prominent at maximum light.

Table 16 is a complete list of all identified bright lines arranged according to the atomic number of the elements. In the successive columns appear the laboratory wave length and intensity from the M.I.T. Table, the electron transitions, the low and high excitation potential, and the maximum relative intensity observed in each of the seven stars showing extensive bright-line spectra. The intensities are on an arbitrary scale and are intended only to give an idea of the relative strengths. An intensity of zero is assigned to lines too faint or indefinite for good measurement. The varying quality of the spectrograms and the difference in the dispersion have made it necessary to adjust the values of the intensities of the lines so that they will be more or less comparable for different plates.

In addition to *H* and *He*, 17 different metallic atoms are represented by more than 160 lines which arise from low levels of excitation. Iron contributes about half the total number of lines. Both neutral and ionized atoms are represented, and a trace of the strongest forbidden lines seems reasonably certain. A large number of additional lines would certainly be found by the use of higher dispersion and by an extension of the search to other spectral regions of shorter or longer wave length.

The line λ 4068.62 [*S* II] is remarkably persistent in the stars with conspicuous emission spectra. Its changes in intensity do not appear to be correlated with the variations

TABLE 16

RELATIVE INTENSITIES OF EMISSION LINES IN T TAURI STARS

LABORATORY		TRANSITION	E.P. (VOLTS)	EMISSION INTENSITY IN STAR							
λ	Int.			T Tau	R Mon	UY Aur	S CrA	RW Aur	XZ Tau	RU Lup	UZ Tau
		H									
3770.63	15	$2^2P^0-11^2D$	10.2–13.4	.....	.....	2	.....	3	1	.....	1
3797.91	20	$2^2P^0-10^2D$	10.2–13.4	.....	.....	2	1	2	3	.....	2
3835.40	40	$2^2P^0-9^2D$	10.2–13.4	.....	.....	5	0	2	3	.....	3
3889.05	60	$2^2P^0-8^2D$	10.2–13.3	2	.....	15	4	4	5	2	4
3970.07	80	$2^2P^0-7^2D$	10.2–13.3	2	.....	4	.....	.....	.....	3	2
4101.74	100	$2^2P^0-6^2D$	10.2–13.2	20	0	35	15	16	15	20	10
4340.46	200	$2^2P^0-5^2D$	10.2–13.0	30	5	40	20	25	30	40	15
4861.33	500	$2^2P^0-4^2D$	10.2–12.7	40	15	40	30	40	40	40	30
6562.82	3000	$2^2P^0-3^2D$	10.2–12.0	50	.....	50	.....	50	.....	50	40
		He I									
4026.19	70	$2^3P^0-5^3D$	20.9–23.9	0	.....	1	1	0	.....	1	....
4471.48	100	$2^3P^0-4^3D$	20.9–23.6	0	.....	3	2	1	2	2	2
5875.62	1000	$2^3P^0-3^3D$	20.9–23.0	.....	.....	.....	.....	1	.....	.....	....
		He II									
4685.75	300	$3^2D-4^2F^0$	48.2–50.8	.....	.....	1	1	.....	.....	0	....
		Na I									
5889.95	9000	$3^2S-3^2P^0$ $\frac{1}{2}-1\frac{1}{2}$	0.0– 2.1	1	.....	.....	.....	.....	.....	1	....
5895.92	5000	$\frac{1}{2}-\frac{1}{2}$	.....	0	.....	.....	.....	.....	.....	1	....
		Mg I									
3829.35	100	$3^3P^0-3^3D$ 0–1	2.7– 5.9	.....	.....	.....	.....	.....	1	.....	....
3832.31	250	1–2	.....	.....	.....	.....	.....	.....	0	.....	0
3838.26	300	2–	.....	.....	.....	.....	.....	.....	1	.....	0
5167.34	100	$3^3P^0-4^3S$ 0–1	2.7– 5.1	.....	.....	.....	.....	1	.....	.....	....
5172.70	200	1–1	.....	.....	.....	.....	.....	2	.....	.....	....
5183.62	500	2–1	.....	.....	.....	.....	.....	3	.....	.....	....
		Al I									
3944.03	2000	$3^2P^0-4^2S$ $\frac{1}{2}-\frac{1}{2}$	0.0– 3.1	.....	.....	.....	.....	1	1	.....	2
3961.53	3000	$1\frac{1}{2}-\frac{1}{2}$	.....	.....	.....	.....	.....	1	1	.....	1

TABLE 16—*Continued*

Laboratory		Transition	E.P. (Volts)	Emission Intensity in Star							
λ	Int.			T Tau	R Mon	UY Aur	S CrA	RW Aur	XZ Tau	RU Lup	UZ Tau
			Si I								
3905.53...	20	$3p^1S - 4S^1P^0$ 0–1	1.9– 5.1	1	.....	0	2	2	2	2	4
			[*S* II]								
4068.62...	.....	$p^3\,^4S^0 - p^3\,^2p^0$ $1\frac{1}{2}$–$1\frac{1}{2}$	0.0– 3.1	1	0	2	2	2	2	2	4
			Ca I								
4226.73...	500	$4^1S - 4^1P^0$ 0–1	0.0– 2.9	0	.....	0	3	2	3	5	4
			Ca II								
3933.67...	600	$4^2S - 4^2P^0$ $\frac{1}{2}$–$1\frac{1}{2}$	0.0– 3.1	40	3	45	15	45	25	20	50
3968.47...	500	$\frac{1}{2}$–$\frac{1}{2}$	.....	35	1	50	20	35	25	15	25
8498.02...	300	$3^2D - 4^2P^0$ $1\frac{1}{2}$–$1\frac{1}{2}$	1.7– 3.1	.....	.....	.....	.....	.....	.....	10	....
8542.09...	1000	$2\frac{1}{2}$–$1\frac{1}{2}$	.....	.....	.....	.....	.....	.....	.....	20	....
8662.14...	1000	$1\frac{1}{2}$–$\frac{1}{2}$	.....	.....	.....	.....	.....	.....	.....	20	....
			Sc II								
4246.83...	80	$a^1D - z^1D^0$ 2–2	0.3– 3.2	.....	.....	0	0	2	1	2	0
4314.08...	50	$a^3F - z^3D^0$ 4–3	0.6– 3.5	.....	0	0	3	2	1	4	4
4320.74...	50	3–2	.....	.....	.....	.....	1	0	0	2	1
4325.01...	50	2–1	.....	.....	.....	.....	0	.....	.....	1	....
4670.40...	100	$b^1D - z^1F^0$ 2–3	1.4– 4.0	.....	.....	.....	1	1	.....	2	....
			Ti II								
3900.54...	30	$a^2G - z^2G^0$ $4\frac{1}{2}$–$4\frac{1}{2}$	1.1– 4.3	.....	.....	.....	.....	.....	1	.....	1
3913.46...	40	$3\frac{1}{2}$–$3\frac{1}{2}$	.....	.....	.....	.....	.....	.....	1	.....	1
4012.39...	35	$a^2F - z^4G^0$ $2\frac{1}{2}$–$2\frac{1}{2}$	0.6– 3.6	.....	.....	.....	0	1	1	0	0
4163.65...	35	$b^2F - x^2D^0$ $3\frac{1}{2}$–$2\frac{1}{2}$	2.6– 5.5	1	.....	1	2	3	.....	2	0
4171.90...	15	$2\frac{1}{2}$–$1\frac{1}{2}$	.....	.....	.....	.....	1	0	.....	1	....
4294.12...	60	$a^2D - z^2D^0$ $2\frac{1}{2}$–$2\frac{1}{2}$	1.1– 4.0	0	.....	.....	2	.....	0	0	1
4337.92...	70	$1\frac{1}{2}$–$1\frac{1}{2}$	.....	1	.....	.....	2	.....	.....	.....	2

TABLE 16—*Continued*

Laboratory λ	Int.	Transition		E.P. (Volts)	Emission Intensity in Star T Tau	R Mon	UY Aur	S CrA	RW Aur	XZ Tau	RU Lup	UZ Tau
					Ti II—*Continued*							
4290.23*	35	$a^4P-z^4D^0$	$1\frac{1}{2}-2\frac{1}{2}$	1.2– 4.0	.....	.....	.....	.....	.....	.....	.....	.....
4300.05	40		$2\frac{1}{2}-3\frac{1}{2}$	.....	1	.....	.....	0	1	1	1	1
4301.93	25		$\frac{1}{2}-1\frac{1}{2}$	.....	0	.....	.....	1	1	.....	2	1
4307.90*	100		$1\frac{1}{2}-1\frac{1}{2}$	.....	.....	.....	.....	.....	.....	.....	.....	.....
4312.87	35		$2\frac{1}{2}-2\frac{1}{2}$	.....	1	.....	0	1	1	1	2	1
4320.96	12		$1\frac{1}{2}-\frac{1}{2}$	.....	0	.....	.....	1	1	0	1	1
4330.71	15		$2\frac{1}{2}-1\frac{1}{2}$	.....	.....	.....	.....	0	1	1	1	0
4399.77	40	$a^2P-z^4D^0$	$1\frac{1}{2}-2\frac{1}{2}$	1.2– 4.0	.....	.....	.....	1	.....	0	3	3
4407.68	2		$\frac{1}{2}-\frac{1}{2}$	.....	.....	.....	.....	1	.....	0	0	0
4395.04	50	$a^2D-z^2F^0$	$2\frac{1}{2}-3\frac{1}{2}$	1.1– 3.9	.....	1	2	3	3	3	5	3
4443.80	80		$1\frac{1}{2}-2\frac{1}{2}$	.....	.....	2	2	2	3	3	6	4
4450.49	12		$2\frac{1}{2}-2\frac{1}{2}$	.....	.....	.....	0	.....	1	1	2	2
4417.72*	40	$a^4P-z^2D^0$	$1\frac{1}{2}-2\frac{1}{2}$	1.2– 4.0	.....	.....	.....	.....	.....	.....	.....	.....
4468.50	80	$a^2G-z^2F^0$	$4\frac{1}{2}-3\frac{1}{2}$	1.1– 3.9	1	2	.....	1	2	1	4	2
4501.27	60		$3\frac{1}{2}-2\frac{1}{2}$	.....	1	2	0	2	2	1	4	2
4529.46	5	$a^2H-z^2G^0$	$4\frac{1}{2}-4\frac{1}{2}$	1.6– 4.3	.....	.....	.....	.....	.....	.....	2	.....
4549.63*	100		$5\frac{1}{2}-4\frac{1}{2}$	.....	.....	.....	.....	.....	.....	.....	.....	.....
4571.98	150		$4\frac{1}{2}-3\frac{1}{2}$	.....	2	.....	1	2	3	4	4	3
4533.97	30	$a^2P-z^2G^0$	$1\frac{1}{2}-2\frac{1}{2}$	1.2– 4.0	1	1	0	1	1	0	3	2
4563.77	100		$\frac{1}{2}-1\frac{1}{2}$	.....	0	.....	1	1	2	1	2	1
4589.95	40		$1\frac{1}{2}-1\frac{1}{2}$	.....	2	1	1	0	1	0	1	1
					Cr I							
4254.35	5000	$a^7S-z^7P^0$	3–4	0.0– 2.9	.....	.....	.....	0	.....	0	1	.....
4274.80*	4000		3–3	.....	0	1	1	2	0	2	2	2
4289.72*	3000		3–2	.....	.....	.....	.....	4	2	3	4	3
					Cr II							
4558.66	20	$b^4F-z^4D^0$	$4\frac{1}{2}-3\frac{1}{2}$	4.1– 6.8	0	.....	0	1	1	1	1	2
4588.22	10		$3\frac{1}{2}-2\frac{1}{2}$	.....	2	.....	0	.....	0	1	1	0
4616.66	4		$1\frac{1}{2}-1\frac{1}{2}$	.....	.....	.....	.....	.....	.....	.....	2	.....
4618.83	6		$2\frac{1}{2}-1\frac{1}{2}$	.....	0	.....	.....	0	.....	1	1	2
4634.09	5		$1\frac{1}{2}-\frac{1}{2}$	.....	1	.....	.....	.....	.....	.....	2	.....
4824.12	4	$a^4F-z^4F^0$	$4\frac{1}{2}-4\frac{1}{2}$	3.9– 6.4	.....	.....	.....	2	1	0	3	2
4848.27	2		$3\frac{1}{2}-3\frac{1}{2}$	.....	.....	.....	.....	0	1	.....	1	2

TABLE 16—*Continued*

Laboratory		Transition		E.P. (Volts)	Emission Intensity in Star							
λ	Int.				T Tau	R Mon	UY Aur	S CrA	RW Aur	XZ Tau	RU Lup	UZ Tau
				Mn I								
4030.76...	500	$a^6S-z^6P^0$	$2\frac{1}{2}$–$3\frac{1}{2}$	0.0– 3.1	.....	.....	.....	.....	0	1	.....	2
				Fe I								
3727.62...	200	$a^5F-y^5F^0$	3–2	0.9– 4.2	.....	.....	.....	.....	1	1	.....	0
3758.24...	700		3–3	.....	.....	.....	.....	.....	2	0	.....	.....
3767.20...	500		1–1	.....	.....	.....	.....	.....	.....	0	.....	0
3787.88...	500		1–2	.....	.....	.....	.....	.....	.....	0	.....	1
3795.00...	500		2–3	.....	.....	.....	.....	.....	.....	1	.....	1
3815.84...	700	$a^3F-y^3D^0$	4–3	1.5– 4.7	.....	.....	.....	.....	2	0	.....	1
3827.82...	200		3–2	.....	.....	.....	.....	.....	1	.....	.....	1
3820.43...	800	$a^5F-y^5D^0$	5–4	0.9– 4.1	.....	.....	1	.....	1	0	.....	2
3825.88...	500		4–3	.....	.....	.....	.....	.....	0	1	.....	1
3840.44...	400		2–1	.....	.....	.....	.....	.....	0	0	.....	0
3849.97...	500		1–0	.....	.....	.....	.....	.....	1	0	.....	0
3872.50...	300		2–2	.....	.....	.....	.....	.....	2	1	.....	1
3878.02*..	400		3–3	.....	.....	.....	.....	.....	.....	.....	.....	.....
3824.44...	150	$a^5D-z^5D^0$	4–3	0.0– 3.2	.....	.....	.....	.....	2	2	.....	1
3856.37...	500		3–2	.....	.....	.....	.....	.....	1	1	.....	1
3859.91...	1000		4–4	.....	.....	.....	1	.....	2	3	.....	3
3878.58*..	300		2–1	.....	.....	.....	.....	.....	2	2	.....	2
3886.28...	600		3–3	.....	.....	.....	.....	.....	3	2	.....	3
3895.66...	400		1–0	.....	.....	.....	.....	.....	1	1	.....	0
3899.71...	15		2–2	.....	.....	.....	.....	.....	1	1	.....	0
3920.26...	500		0–1	.....	.....	.....	.....	.....	.....	1	.....	0
3922.91...	600		3–4	.....	.....	.....	.....	.....	1	2	.....	2
3927.92...	500		1–2	.....	.....	.....	.....	.....	0	1	.....	1
4005.25...	250	$a^3F-y^3F^0$	3–2	1.6– 4.6	.....	.....	.....	1	.....	0	1	2
4045.82...	400		4–4	.....	.....	.....	0	2	2	2	2	3
4063.60...	400		3–3	.....	2	.....	3	5	5	4	5	8
4071.74...	300		2–2	.....	.....	.....	.....	.....	1	.....	1	0
4132.06...	300		2–3	.....	2	.....	1	4	2	3	4	8
4143.87...	400		3–4	.....	0	.....	.....	1	1	1	2	2
4139.92...	40	$a^5F-z^3F^0$	2–2	1.0– 4.0	0	.....	0	0	.....	.....	0	....
4202.03...	400	$a^3F-z^3G^0$	4–4	1.5– 4.4	0	.....	.....	2	2	3	2	2
4250.79...	400		3–3	.....	.....	.....	0	.....	1	2	1	1
4271.76...	1000		4–5	.....	.....	.....	1	1	2	2	4	4
4307.91*..	1000		3–4	.....	2	.....	0	3	2	4	3	2
4325.76...	1000		2–3	.....	2	2	.....	1	1	3	3	3
4282.41...	600	$a^5P-z^5S^0$	3–2	2.2– 5.0	0	.....	0	1	1	1	2	1
4294.13...	700	$a^3F-z^5G^0$	4–4	1.5– 4.4	0	.....	.....	2	.....	1	2	1
4383.55 ..	1000		4–5	.....	3	2	2	5	4	4	6	8
4404.75...	1000		3–4	.....	0	.....	.....	2	1	1	4	2
4415.12...	600		2–3	.....	.....	1	1	2	1	1	2	1

TABLE 16—*Continued*

Laboratory λ	Int.	Transition		E.P. (Volts)	Emission Intensity in Star T Tau	R Mon	UY Aur	S CrA	RW Aur	XZ Tau	RU Lup	UZ Tau
					Fe I—*Continued*							
4375.93...	500	$a^5D-z^7F^0$	4–5	0.0– 2.9	1	1	2	3	2	3	5	5
4427.31...	500		3–4	.....	1	1	1	1	2	2	3	3
4435.15...	70		2–1	.....	.....	.....	.....	1	.....	1	1	1
4461.65...	300		2–3	.....	0	.....	0	1	0	1	2	2
4466.55...	500		1–0	.....	.....	.....	0	0	1	0	3	2
4482.17...	150		1–2	.....	0	0	1	1	2	1	3	2
4494.57...	400	$a^5P-x^5D^0$	2–3	2.2 –4.9	.....	.....	.....	0	.....	.....	1	0
4528.62...	600		3–4	.....	1	.....	0	1	0	0	2	1
					Fe II							
3914.48...	2	$a^4P-z^6D^0$	$2\frac{1}{2}-1\frac{1}{2}$	1.7– 4.8	0	.....	.....	.....	1	1	1	1
3938.29...	2		$2\frac{1}{2}-2\frac{1}{2}$	.....	0	.....	.....	.....	1	1	0	2
4122.64...	4	$b^4P-z^4F^0$	$2\frac{1}{2}-2\frac{1}{2}$	2.6– 5.5	0	0	1	1	1	0	1	1
4178.87...	10		$2\frac{1}{2}-3\frac{1}{2}$	.....	2	2	3	6	4	4	10	12
4258.16...	2		$1\frac{1}{2}-1\frac{1}{2}$	.....	1	0	.....	0	1	.....	2	2
4296.58...	2		$1\frac{1}{2}-2\frac{1}{2}$	.....	1	0	1	2	0	1	2	2
4173.48...	8	$b^4P-z^4D^0$	$2\frac{1}{2}-2\frac{1}{2}$	2.6– 5.5	2	2	3	5	5	5	8	12
4233.17...	100		$2\frac{1}{2}-3\frac{1}{2}$	.....	6	4	5	5	6	6	12	16
4273.32*..	3		$1\frac{1}{2}-\frac{1}{2}$	.....	.....	.....	.....	.....	.....	.....	.....	.....
4303.17...	12		$1\frac{1}{2}-1\frac{1}{2}$	.....	1	3	2	3	2	2	6	6
4351.76...	30		$1\frac{1}{2}-2\frac{1}{2}$	.....	1	3	3	8	4	6	10	20
4385.38...	4		$\frac{1}{2}-\frac{1}{2}$	.....	2	1	0	2	1	1	3	2
4416.82*..	7		$\frac{1}{2}-1\frac{1}{2}$	.....	1	3	3	4	3	3	8	10
4489.18...	2	$b^4F-z^4F^0$	$3\frac{1}{2}-2\frac{1}{2}$	2.8– 5.6	0	2	1	3	2	3	6	4
4491.41...	2		$1\frac{1}{2}-1\frac{1}{2}$	.....	1	2	2	3	2	3	4	4
4515.34...	10		$2\frac{1}{2}-2\frac{1}{2}$	.....	1	1	2	2	2	2	7	4
4520.24...	40		$4\frac{1}{2}-3\frac{1}{2}$	.....	3	2	2	3	3	3	4	5
4555.90...	12		$3\frac{1}{2}-3\frac{1}{2}$	.....	1	2	2	4	3	4	8	6
4629.33...	7		$4\frac{1}{2}-4\frac{1}{2}$	.....	4	3	3	5	5	5	10	12
4666.75...	2		$3\frac{1}{2}-4\frac{1}{2}$	.....	.....	.....	.....	2	0	1	3	3
4508.28...	40	$b^4F-z^4D^0$	$1\frac{1}{2}-\frac{1}{2}$	2.8– 5.6	1	1	1	1	3	1	8	5
4522.63...	60		$2\frac{1}{2}-1\frac{1}{2}$	.....	2	2	2	3	3	3	5	6
4541.52...	2		$1\frac{1}{2}-1\frac{1}{2}$	.....	1	.....	.....	0	0	1	3	2
4549.47*..	100		$3\frac{1}{2}-2\frac{1}{2}$	.....	3	2	2	4	3	3	10	10
4576.33...	3		$2\frac{1}{2}-2\frac{1}{2}$	.....	1	1	0	.....	1	.....	2	2
4583.85...	150		$4\frac{1}{2}-3\frac{1}{2}$	.....	4	4	3	7	5	6	12	15
4620.52...	3		$3\frac{1}{2}-3\frac{1}{2}$	.....	1	.....	1	.....	1	.....	4	5
4731.49...	5	$a^6S-z^4D^0$	$2\frac{1}{2}-3\frac{1}{2}$	2.9– 5.5	0	.....	0	2	1	1	4	3
4923.92...	30	$a^6S-z^6P^0$	$2\frac{1}{2}-1\frac{1}{2}$	2.9– 5.4	6	3	4	4	10	6	10	10
5018.44...	80		$2\frac{1}{2}-2\frac{1}{2}$	.....	5	3	4	3	15	4	6	5
5169.03...	2		$2\frac{1}{2}-3\frac{1}{2}$	.....	5	.....	5	.....	10	.....	6	.....

TABLE 16—*Continued*

Laboratory		Transition		E.P. (Volts)	Emission Intensity in Star							
λ	Int.				T Tau	R Mon	UY Aur	S CrA	RW Aur	XZ Tau	RU Lup	UZ Tau
		Fe II—*Continued*										
5197.59...	10	$a^4G-z^4F^0$	$2\frac{1}{2}-1\frac{1}{2}$	3.2– 5.6	1	.....	2	.....	2	.....	1	....
5234.63...	5		$3\frac{1}{2}-2\frac{1}{2}$	.....	.....	.....	4	.....	3	.....	.....	....
5275.99...	2		$4\frac{1}{2}-3\frac{1}{2}$	.....	.....	.....	2	.....	2	.....	.....	....
5316.61...	150		$5\frac{1}{2}-4\frac{1}{2}$	.....	4	.....	4	.....	2	.....	3	....
		[*Fe* II]										
4243.97...	.....	a^4F-a^4G	$4\frac{1}{2}-5\frac{1}{2}$	0.2– 3.2	1	1	0	1	0	0	.....	1
4359.34...	.....	a^6D-a^6S	$3\frac{1}{2}-2\frac{1}{2}$	0.0– 2.9	.....	1	0	.....	.....	1	.....	1
		Ni I										
3736.81...	300	$a^1D-z^5F^0$	2–2	0.4– 3.7	.....	.....	.....	.....	.....	1	.....	3
3783.53...	500		2–3	.....	.....	.....	.....	.....	.....	0	.....	0
3775.57...	500	$a^1D-z^3D^0$	2–2	0.4– 3.7	.....	.....	.....	.....	1	0	.....	0
3807.14...	800		2–3	.....	.....	.....	.....	.....	.....	1	.....	1
		Sr II										
4077.71...	400	$5^2S-5^2P^0$	$\frac{1}{2}-1\frac{1}{2}$	0.0– 3.0	.....	.....	1	3	3	2	2	4
4215.52...	300		$\frac{1}{2}-\frac{1}{2}$	.....	.....	.....	2	3	3	3	5	5

* Probable blends: λ 3878.58 *Fe* I –λ 3878.02 *Fe* I; λ 4307.91 *Fe* I –λ 4307.90 *Ti* II; λ 4274.80 *Cr* I –λ 4273.32 *Fe* II; λ 4416.82 *Fe* II–λ 4417.72 *Ti* II; λ 4289.72 *Cr* I –λ 4290.23 *Ti* II; λ 4549.47 *Fe* II–λ 4549.63 *Ti* II

of the other bright lines. At times λ 4068 remains practically undiminished when most of the metallic lines have disappeared. The measures support the identification with [*S* II]. The companion line at λ 4076.22 is probably blended with λ 4077.71 *Sr* II and has not been separately observed. These sulphur lines arise from a low metastable level and are frequently found in novae and occasionally in nebulae. None of the other characteristic nebular lines have been observed in these stars.

Distorted Multiplets of *Fe* I

When the emission spectrum appears in the T Tauri stars, λ 4063 and λ 4132 of *Fe* I are much strengthened as compared with the other members of the multiplet $a^3F - y^3F^0$ and are probably affected by some such fluorescent mechanism as that proposed for λ 4202 and λ 4307 of the $a^3F - z^3G^0$ multiplet in Me variable stars.[45] Under

[45] Thackeray and Merrill, *Pub. A.S.P.*, **48**, 331, 1936.

the most favorable conditions, λ 4063 may rival λ 4233 *Fe* II in strength. This phenomenon is unique in the stars of this group and does not occur in the solar chromosphere. The two lines λ 4063 and λ 4132, together with λ 3969, arise from the same upper level of the atom. The latter line has not been observed in emission, possibly because its identity is lost in the complex structure of the region between *H* and *Hε*. All the remaining members of the multiplet have been observed as bright lines of relatively low intensity in the T Tauri stars.[46]

Comparison with the Solar Chromosphere

The most significant characteristic of the spectra of the T Tauri stars is the low-excitation bright-line spectrum which is prominent in most of the stars at certain phases. It occurs with varying intensity in all the stars of the group except RY Tau and UX Tau,

TABLE 17

Comparison of Emission Lines in T Tauri Stars and Solar Chromosphere

Element	Chromosphere			T Tau Stars		Element	Chromosphere			T Tau Stars	
	No. Lines	Mean Intensity	Mean Height	No. Lines	Mean Max. Intensity		No. Lines	Mean Intensity	Mean Height	No. Lines	Mean Max. Intensity
Ca II	2	200	14,000 km	2	50	*Sc* II	4	24	2,220 km	4	2
H	6	160	8,900	6	40*	*Al* I	2	30	2,000	2	2
Sr II	2	70	6,000	2	4	*Fe* II	7	25	1,700	7	12
Ca I	1	40	5,000	1	5	*Ba* II	4	29	1,550	0	.....
Mg I	6	46	4,170	6	1	*Cr* I	3	21	1,500	3	2
He I	11	20	3,840	3	2	*Na* I	2	22	1,500	2	1
He II	1	2	3,500	1	1	*Cr* II	1	15	1,500	1	2
Ti II	21	29	2,410	19	2	*Fe* I	25	13	1,470	21	3

* Mean of four lines (*Hα–Hδ*) only.

which may be considered as rudimentary members of the T Tauri class as far as the spectrum is concerned, showing only *H*, *K*, *Hα*, and *Hβ* in emission.

This bright-line spectrum is quite different from other stellar emission spectra, but its resemblance to that of the solar chromosphere is sufficient to invite a detailed comparison.

The mean heights (> 1000 km) and intensities[47] of chromospheric lines between λ 3750 and λ 6600 are arranged in Table 17 according to height. The numbers of these same chromospheric lines found in the T Tauri stars and their estimated mean maximum intensities (on quite a different scale) are shown in the last two columns of the table. A marked similarity between the emission spectra of the stars and that of the higher levels of the chromosphere is apparent. The bright lines of calcium (H and K) and of hydrogen are outstanding in both. In the stars, as well as in the sun, *Fe* I and *Ti* II have the greatest number of lines of high intensity. The low-excitation *Fe* I lines are more generally represented in emission in these stars than in any other known stellar source, and their maxi-

[46] Since this paragraph was written, George H. Herbig (*Pub. A.S.P.*, **57**, 166, 1945) has reported his observations of this phenomenon in the spectrum of RW Aur and attributed the enhancement of λ 4063 and λ 4132 to populating the y^3F level through the action of λ 3968.47 *Ca* II upon λ 3969.26. The width of the calcium line in the T Tauri stars is more than sufficient to cover the difference in wave length.

[47] S. A. Mitchell, *Ap. J.*, **71**, 11, 1930.

mum strength is relatively greater than in the chromosphere. The *He* I lines are few and decidedly weak in the stars. Only the triplet members, λλ 4026, 4471, and 5875, are certainly present; λ 4685 *He* II was measured in the spectra of three stars, but it is faint; and *Mg* I and *Sc* II are weaker than in the sun. On the other hand, *Fe* II is relatively stronger, and its lines are surpassed in strength only by those of *H* and *Ca* II. The lines λ 4077 and λ 4215 of *Sr* II are well shown but do not have the excessive intensity found in the sun.

The stellar emission lines are much broader than those of the chromosphere, and the strong lines of *H* and *Ca* II often suffer distortion by deep reversals which are not observed in the sun, yet the general resemblance of the spectra leads to the conclusion that they must have their origin under similar physical circumstances. The excitation seems to be somewhat lower in the T Tauri stars than in the solar chromosphere, while in the stars with combination spectra, such as Z And, the excitation is higher.[48]

ABSOLUTE MAGNITUDES AND COLOR INDICES

The spectroscopic absolute magnitudes of T Tau, RY Tau, and UX Tau may be estimated from their absorption lines. The results shown in Table 18 indicate that these

TABLE 18

SPECTRAL TYPES, SPECTROSCOPIC ABSOLUTE MAGNITUDES, AND COLOR INDICES

Star	Spectral Type	M_{sp}	Color Index and Source
RW Aur	dG5	.....	+0.7 mag.; P. P. Parenago, *op. cit.*, **4**, 222, 1933
UY Aur	dG5	.....	
R CrA	F5	.....	+0.97 mag.; C. Payne-Gaposchkin, *Harvard Ann.*, **89**, 193, 1935
T Tau	dG5	+5.0	
RY Tau	dG0	+4.3	+0.93 mag.; O. C. Collins, *Ap. J.*, **86**, 551, 1937
UX Tau	dG5	+5.2	+1± mag.; *Harvard Circ.*, No. 201, 1918
UZ Tau	.....	.....	>+1 mag.; K. Himpel, *A.N.*, **270**, 185, 1940

three stars are dwarfs of the main sequence. For UX Tau and UZ Tau additional evidence may be sought from their visual companions, assuming that they are physically related. The spectral types of both companions are dM3e, and the absolute magnitudes are estimated to be +10.5. If we use 13.3 as the estimated apparent visual magnitude of both companions, $m - M = +2.8$. Applying this modulus to the visual magnitudes (9.9 and 9.2) at maximum of the two variable stars, we obtain values of 7.1 and 6.4, respectively, for their absolute magnitudes, 1.9 and 1.2 mag. fainter than that determined from the spectral lines of UX Tau. On the basis of these data, the variables must be subdwarfs—an inference which does not seem justified. The matter can be harmonized only by concluding that the companions have peculiar spectra, that the stars are not physical pairs, or that general or local obscuration has a greater effect in reducing the visual luminosity of the variable star than that of its fainter and probably redder companion. Both stars are in lanes of heavy obscuration, but no surrounding shells have been observed. The large color indices of Table 18 show a definite color excess, but hardly enough to meet the difficulty.

The spectra of R CrA and R Mon differ considerably from those of other members of the group, and positive evidence of low luminosity is lacking. On the assumption that the

[48] H. H. Plaskett, *Pub. Dom. Ap. Obs.*, **4**, 152, 1928.

changes in the appearance of the attached nebulae result from the passage of light from one part of the nebula to another, the distance of R CrA has been computed by E. P. Hubble[49] and found to be 100 parsecs, which corresponds to a minimum absolute magnitude of +4.7. For the same star, Gaposchkin and Greenstein[50] find from star counts a distance of 150 parsecs, giving a minimum absolute magnitude of +3.9. Elimination of the effect of obscuration on the apparent magnitudes would give brighter absolute magnitudes but probably not sufficient luminosity to rank them among the giants.

A trigonometric parallax of −0".011 relative to near-by comparison stars was found by A. van Maanen[51] for R Mon. This negative result probably indicates that the distant background stars of this field are obscured and that only foreground stars are available for comparison. On account of the presence of obscuring material in the regions surrounding most of the T Tauri stars, the trigonometric method offers little hope for determining distance, absolute magnitude, or proper motion. In some of the fields close comparison stars are completely lacking.

TABLE 19

MEAN RADIAL VELOCITIES OF T TAURI STARS

Star	Emission Lines		Absorption Lines		Abs.−Em.	Star	Emission Lines		Absorption Lines		Abs.−Em.
	No. Plates	Vel.	No. Plates	Vel.			No. Plates	Vel.	No. Plates	Vel.	
RW Aur	9	−25	4	+ 59	+84	RY Tau	4	− 8	9	+ 26.2	+34
UY Aur	10	− 3	6	+ 30	+33	UX Tau	4	+18	8	+ 24	+ 6
R CrA	1	−97	2	− 36	+61	UZ Tau	7	− 5	.....	.....	.....
S CrA	6	−33	.....	.....	.....	XZ Tau	3	+32	1	+109	+67
RU Lup	10	− 6.4	.....	.....	.....						
R Mon	2	+21	1	+ 12	− 9	Weighted mean	.....	.....	.....	.....	+25
T Tau	14	+19.6	14	+ 24.6	+ 5						

No determinations of absolute magnitude, parallax, or color index have been made for RW Aur, UY Aur, S CrA, RU Lup, or XZ Tau. Such observations are needed, but there is no reason to suspect that the physical properties of these stars differ from those of the other members of the group.

Although values of absolute magnitude and distance are made uncertain by the presence of absorbing clouds, the available evidence indicates that the T Tauri stars belong to the main sequence and that their distance is of the order of 100–150 parsecs.

RADIAL-VELOCITY MEASURES

The measures of radial velocity from both emission and absorption lines are summarized in Table 19. The differences (Abs. − Em.) show that in the mean the emission lines are displaced toward the violet with respect to the absorption lines. This result agrees in direction with that found for the irregular Me variables[52] and the Mira stars,[53] but the measured displacement is somewhat greater for the T Tauri stars.

[49] *Mount Wilson Obs., Annual Reports*, p. 252, 1921.

[50] *Harvard Bull.*, No. 904, 1936.

[51] *Mt. W. Contr.*, No. 237, p. 14, 1922.

[52] A. H. Joy, *Mt. W. Contr.*, No. 668; *Ap. J.*, **96**, 165, 1942.

[53] P. W. Merrill, *Mt. W. Contr.*, No. 644; *Ap. J.*, **93**, 380, 1941.

Lack of agreement in the measures of different plates of the same star indicates that the radial velocities may be variable, with a range of 30–40 km/sec. It seems probable that both the emission and the absorption strata are subject to irregular motions but that, in general, the emission layers are rising with respect to the absorbing clouds.

CONCLUDING REMARKS

Only 11 stars have been found which have the qualifications necessary for inclusion in the T Tauri group. The spectral criteria were given high weight. Probably other stars which have similar characteristics exist and will be recognized when competent objective-prism observations can be extended to the faint stars of the Milky Way. However, stars of this class may be expected to be comparatively few because of the peculiar circumstances of their location and their relationship to the galactic absorbing clouds.

Solely on the basis of their light-curves, RR Tau, WW Vul, and perhaps some of the irregular variables in Orion might have been included, but their spectra are of earlier type (A3–F8) and without extensive emission. Other variables, such as Z And and CI Cyg, are similar in some respects but of higher luminosity. Their emitting atmospheres have bright *Ca* II[54] and some faint *Fe* I[55] lines, although, in general, their spectra show lines requiring much higher excitation than that of the T Tauri stars. Their numerous sharp forbidden lines, doubtless, originate in an extended tenuous atmosphere which favors high ionization, while, on the contrary, the presence, in general, of lines of neutral and easily ionized atoms in the T Tauri stars points to a source of considerably lower excitation and higher density. Also, the high-luminosity variables with combination spectra showing strong 4686 *He* II lines are not associated with dark lanes of the Milky Way or with reflection nebulae.

The changes which occur from time to time in the spectra of the T Tauri variables merit more detailed study than can be given in this general survey. They should be definitely correlated with the variation in brightness of the stars. As a result of the higher density of the gases and the smaller dimensions involved, the changes are quite different in nature from those observed in other variable stars. With further observations, the effect of near-by companion stars or of surrounding shells may be investigated. Maximum brightness, which, for some of the stars of the group, bears a resemblance to the outburst of a nova, has not been observed spectrographically. Such extreme activity might furnish a valuable clew to the interpretation of the problem.

[54] P. W. Merrill, *Mt. W. Contr.*, No. 688; *Ap. J.*, 99, 15, 1944.

[55] Swings and Struve, *Ap. J.*, 97, 206, 1943.

PRELIMINARY COLOR INDICES FOR STARS OF LARGE PROPER MOTION. II

WILLEM J. LUYTEN AND MARTIN DARTAYET
University of Minnesota and Córdoba Observatory

ABSTRACT

Approximate color indices are given for 111 stars south of declination −48° having proper motions greater than 0".5 annually and for 514 similar stars with smaller proper motions. Seven new white dwarfs and a number of possible "intermediates" are indicated among these stars.

The present paper is a continuation of a previous article[1] in which we gave provisional color indices for 78 stars south of declination −48° having proper motions in excess of 0".5 annually. Since that time further yellow plates have been taken. All stars within reach of the Córdoba 13-inch *Carte du ciel* telescope were first observed. Subsequently, all remaining stars, viz., those fainter than magnitude 16.0 photographic or too close to the south pole, were observed with the 60-inch telescope at Bosque Alegre. As before, all yellow plates were taken by Dartayet on 103E emulsion with a No. 12 "minus-blue" filter. At the time the program on the brighter stars was completed—during late 1943—there was still considerable risk involved in Atlantic shipping; in order to minimize this risk, the original yellow plates were retained at Córdoba, and lantern-slide positives were shipped to Minnesota. There were compared by Luyten with positive prints of the original blue plates taken at Harvard, and the color indices were determined in the manner described previously. Data obtained in this way for 66 stars, mostly brighter than the sixteenth photographic magnitude, are given in the first part of Table 1, where each star is identified by its LPM number[2] and has its photographic magnitude and total proper motion given, as well as the color index adopted.

The comparisons effected in this way were not entirely satisfactory; and when shipping conditions improved in 1944, it was decided not only to take both blue and yellow plates with the 60-inch telescope but to send both original negatives to Minnesota. The color indices determined for the 47 stars observed in this manner should be somewhat more reliable than those determined from positives only, and the data for these 47 stars are therefore given separately in the second part of Table 1. The two stars LPM 289 and 474 were observed both ways and are therefore listed twice.

2. The six new white dwarfs, LPM 23, 445, 474, 488, 733, and 821, have been announced before,[3] as has the possibility that LPM 428 and 429 are degenerate stars, since they are 7–9 mag. less luminous than main-sequence stars of the same color. The two stars LPM 187 and 759 appear to be definitely whiter than expected—by at least 0.5 mag. While they are probably not genuine white dwarfs, they may well turn out to be "intermediates." The stars LPM 85 and 750 may conceivably also belong to this category.

3. The colors of all stars found in the Bruce Proper-Motion Survey to possess appreciable proper motion, and shown on our present plates, were estimated as in our previous determination of colors of large proper motion stars. Very approximate color indices were thus obtained for 427 stars on the positives from the *Carte du ciel* plates and for 95 more on the plates taken with the 60-inch telescope. Eight stars were common to both

[1] *Ap. J.*, **96**, 55, 1942.

[2] *Pub. Astr. Obs. Minnesota*, **3**, 1, 1940.

[3] *Harvard Announcement Cards*, Nos. 691 and 699, and 712.

lists, and the resulting color indices for 514 different stars are given in Table 2. Since most of these stars are not of any individual interest, they are identified only by their BPM numbers as assigned in the *General Catalogue of the Bruce Proper Motion Survey.*

TABLE 1

COLOR INDICES OF 113 PROPER-MOTION STARS

LPM	Mag.	μ	I.C.	LPM	Mag.	μ	I.C.	LPM	Mag.	μ	I.C.
2.....	15.6	0".53	+1.5	658....	15.7	0.87	+1.4	279....	16.2	0".50	+1.3
4.....	15.0	0.58	+1.6	666....	16.8	0.74	+1.3	289‡...	15.2	0.60	+1.2
54.....	15.1	0.58	+1.3	669....	15.6	0.62	+1.4	290....	16.8	0.60	+1.5
85.....	14.7	1.05	+1.0	684....	14.6	0.54	+1.5	303....	15.8	0.53	+2.0
118.....	16.0	0.62	+1.8	685....	14.7	0.67	+1.6	306§...	16.2	0.50	+1.3
128.....	14.7	0.60	+1.3	686....	15.2	0.70	+1.4	342....	12.4	0.54	+0.9
171.....	15.5	0.66	+1.4	707....	15.3	0.66	+1.2	428....	15.7	1.17	+1.1
185.....	14.6	0.50	+1.4	729....	14.2	0.51	+1.4	429....	17.7	1.17	+1.0
191.....	15.3	0.51	+1.3	737....	14.2	0.61	+1.3	445....	17.4	0.57	+0.2
235.....	15.2	0.57	+1.3	739....	14.2	1.27	+1.5	474....	15.0	0.50	−0.2
287.....	14.5	0.60	+1.2	749....	14.1	0.70	+1.3	484....	16.3	0.79	+1.2
289.....	15.2	0.60	+1.1	750....	14.2	0.50	+1.0	488....	16.1	0.54	−0.3
293.....	16.0	0.77	+1.2	759....	14.3	0.51	+0.6	522....	16.4	0.53	+1.2
309.....	14.8	1.04	+1.2:	774....	15.6	0.57	+1.2	542....	16.1	0.50	+1.3
311.....	14.4	0.53	+1.3	775....	15.0	0.61	+1.3	586....	16.6	0.79	+1.1
326.....	14.8	0.50	+1.2	778....	15.7	0.75	+1.4	589....	16.5	0.65	+1.0
329.....	15.2	0.52	+1.3	788....	16.3	0.52	+1.0	647....	16.1	0.61	+1.6
356.....	15.2	1.65	+1.3	798....	15.6	0.55	+1.8	662....	16.2	0.73	+1.6
359.....	14.5	0.51	+1.3	802....	15.5	0.90	+1.4	665....	16.2	0.65	+1.6
372.....	16.0	0.68	+1.3	804....	15.2	0.52	+1.4	668....	16.5	0.54	+1.6
397.....	16.3	0.81	+1.2	843....	15.4	1.06	+1.6	675....	16.2	0.51	+1.3
418.....	14.2	0.58	+1.1	845....	14.5	0.70	+1.3	694‖...	14.0	1.25	+1.3
431.....	15.2	1.24	+1.1	867....	14.5	0.50	+1.1	708....	17.4	0.64	+1.4
443.....	15.4	0.69	+1.1	871....	14.7	0.58	+1.4	711....	17.5	0.84	+1.9
466.....	14.7	0.52	+1.3	874....	14.1	0.53	+1.4	713....	16.3	0.57	+1.7
471.....	16.2	0.53	+1.3	878....	14.8	0.90	+1.6	723....	16.3	0.54	+1.6
474.....	15.0	0.50	0.0	885....	15.5	0.50	+1.5	732....	17.2	0.64	+1.5
479.....	14.8	0.67	+1.4	902....	14.3	0.71	+1.5	733....	16.2	0.51	−0.3
495.....	14.6	0.55	+1.3					735....	15.7	1.42	+1.7
500*....	16.0	0.70	+0.9+	23....	14.6	0.58	0.0	742....	13.2	0.73	+1.3
516*....	15.0	1.11	+0.8+	74....	14.5	0.55	+2.0	766....	16.3	0.54	+1.9
574.....	15.2	1.14	+1.1	127....	14.5	0.50	+1.5	768....	16.2	0.50	+1.5
576.....	15.5	0.52	+1.3	129....	16.1	0.56	+1.8	775....	15.0	0.61	+1.3
583.....	14.3	0.57	+1.3	141....	16.1	0.61	+1.6	778....	15.7	0.75	+1.6
591.....	15.0	0.63	+1.1	177....	17.7	0.50	+1.7	821....	14.8	0.65	0.0
618.....	14.6	0.50	+1.2	187....	14.7	0.56	+0.6	834....	16.4	0.70	+1.8
642.....	15.1	0.99	+1.2	213....	13.6	1.12	+1.4	838....	17.3	0.78	+2.2
646.....	15.2	0.51	+1.2	262†...	13.6	0.67	+1.2	865....	15.2	0.79	+1.6

* Stars Nos. 500 and 516 lie in heavily obscured regions, and their real color indices are probably much greater than the values given here.

† Has a companion 20".6 in 358°, 16.2 pg, I.C. +0.9.

‡ Has a companion 3".7 in 97°, 17.6 pg., I.C. +0.3:.

§ Has a companion 10".6 in 106°, 17.8 pg, I.C. +0.5:.

‖ Has a companion 12".0 in 15°, 16.6 pg, I.C. +1.4.

It is not yet possible to say whether any of these are physical companions.

Similarly to the procedure followed before, the mean color indices for stars whose reduced proper motion, $H = m + 5 + 5 \log \mu$, lies between given values have been determined; these are given in Table 3. A comparison with the similar values shown in Table 4 of our previous paper indicates that our present color indices average about 0.06 mag.

TABLE 2

COLOR INDICES OF 514 BPM STARS

BPM	I.C. (In Mag.)	BPM	I.C. (In Mag.)	BPM	I.C. (In Mag.)	BPM	I.C. (In Mag.)
133	+1.0	5124	+0.5	7407	+0.8	10494	+0.8
140	0.8	5127	0.9	7418	0.6	10673	0.4
143	1.1	5145	0.5	7448	0.9	10695	1.0
367	1.0	5148	0.9	7452	0.6	10706	0.5
374	1.1	5172	0.4	7464	0.6	10710	0.9
386	0.9	5200	0.8	7472	0.9	10715	0.9
397	1.0	5215	0.9	7477	1.0	10721	0.9
403	0.5	5361	0.8	7480	0.8	10736	0.9
414	0.5	5369	0.5	7550	0.7	10762	0.6
1514	0.7	5380	1.1	7565	1.3	10763	0.4
1533	1.5	5411	1.1	7603	0.9	10770	0.8
1540	0.6	5424	0.4	7613	1.1	10775	1.1
1556	0.6	5429	0.8	7616	1.0	10778	1.2
1957	1.4	5491	0.2	7640	1.1	10787	0.5
2018	1.5	5518	0.6	7647	0.6	10789	0.4
2018a	1.4	5537	1.0	7698	1.0	10792	0.9
2034	1.2	5593	0.9	7780	0.8	10797	0.9
2058	0.9	5670	1.0	8369	1.2	10810	1.2
2240	0.8	5779	0.6	8404	1.1	10858	0.9
2249	0.5	5780	0.7	8418	1.2	10921	1.3
2254	1.1	5782	0.6	8420	0.9	10922	1.3
2278	1.1	5789	0.9	8436	0.0	10966	0.5
2281	1.3	5802	0.5	8870	1.0	10975	0.7
2294	1.6	5803	0.9	9155	1.2	10992	1.1
2313	1.2	5848	0.4	9582	0.5	11100	0.5
2318	1.0	5849	0.7	9594	1.0	11115	1.0
2323	1.2	5854	0.8	9609	0.9	11118	1.5
2328	1.0	5858	0.6	9623	0.8	11123	1.2
2329	1.1	5879	0.7	9633	0.7	11138	1.0
2330	0.4	5882	0.3	9636	1.0	11147	1.2
2332	1.3	5887	0.4	9647	0.9	11176	1.0
2339	1.0	5894	0.7	9650	0.5	11216	0.7
2341	1.1	5903	1.0	9675	1.0	11219	1.2
2373a	1.0	5942	0.7	9767	0.4	11296	1.1
2378	0.9	5999	1.0	9773	0.5	11361	0.7
2382	0.8	6484	0.7	9775	0.4	11382	1.1
2542	0.9	6492	0.5	9783	0.6	11386	1.0
2575	1.0	6501	1.0	9791	1.1	11395	1.0
2601	1.1	6506	1.1	9798	0.5	11420	0.6
2730	1.2	6510	0.7	9803	1.3	11453	1.2
2743	1.8	6656	0.9	9809	0.5	11710	0.7
2860	1.2	6677	1.0	9828	1.0	11748	1.1
3732	1.0	6687	0.7	9889	1.4	11752	1.3
3744	1.2	6769	0.9	9891	1.2	11765	0.9
3756	1.1	6850	0.6	9893	0.3	11774	1.0
3757	1.4	7104	0.5	9898	0.9	11782	1.2
3774	1.7	7137	1.1	9914	1.3	11783	1.2
4161	0.4	7147	0.6	10264	0.8	11798	1.3
4178	0.8	7157	1.2	10376	0.9	11801	1.2
4205	+0.5	7400	+0.8	10487	+0.4	11806	+0.6

TABLE 2—*Continued*

BPM	I.C. (In Mag.)	BPM	I.C. (In Mag.)	BPM	I.C. (In Mag.)	BPM	I.C. (In Mag.)
11857	+0.8	14362	+1.1	15981	+1.3	19013	+1.0
11879	1.2	14378	1.1	15983	1.3	19016	0.4
11890	1.2	14394	0.9	15987	1.0	19019	0.9
12590	1.1	14414	1.2	15988	1.5	19021	0.6
12593	0.9	14685	1.1	15998	0.7	19022	1.3
12640	0.7	14714	1.6	16000	1.4	19024	0.9
12645	1.2	14722	1.4	16097	1.0	19026	1.0
12681	0.6	14723	1.4	16112	1.6	19029	1.1
12682	1.0	14894	1.1	16113	1.1	19033	0.9
12706	0.9	14895	1.4	16120	1.0	19041	0.9
12743	0.2	14902	1.2	16134	1.2	19042	1.1
12745	0.9	14909	1.1	16138	0.5	19053	1.0
12769	1.3	14915	1.3	16140	0.8	19055	0.9
13192	0.8	14922	1.5	16144	1.3	19060	0.9
13239	0.9	14937	1.4	16885	0.4	19068	1.1
13403	1.3	14941	1.4	16897	1.0	19075	0.6
13437	1.4	14957	0.9	16921	1.6	19077	0.9
13447	0.7	14971	1.5	16926	0.5	19078	1.1
13488	1.3	15095	1.1	16935	1.1	19508	1.0
13498	1.4	15096	1.1	16937	1.2	20298	0.9
13512	1.3	15128	1.3	16938	0.7	20312	0.7
13536a*	1.5	15129	1.3	16939	1.1	21425	0.6
13559	1.3	15154	1.4	16940	1.0	21435	0.8
13570	1.2	15205	1.1	16945	0.8	21439	0.6
13590	1.5	15237	1.3	16955	0.5	21443	0.4
13596	1.3	15238	1.3	17445	1.1	21445	0.7
13615	1.4	15250	1.1	17454	1.4	21447	0.6
13617	1.1	15266	0.9	17463	1.0	21475	0.4
13626	1.2	15389	1.2	18167	1.0	21811	0.7
13644	1.4	15395	0.9	18181	1.0	21815	0.3
13649	1.1	15401	1.3	18201	1.2	21822	0.5
13803	1.0	15420	0.5	18219	0.8	21833	0.9
13822	0.5	15447	1.3	18747	1.1	21839	0.7
13824	0.6	15482	0.6	18750	1.2	21840	0.8
13826	1.4	15485	1.0	18752	0.9	21875	0.5
13862	1.2	15526	1.0	18755	0.9	21880	0.5
13872	1.3	15562	1.3	18937	0.9	21890	0.0
13955	0.6	15637	1.0	18941	1.1	21892	0.8
13965	1.4	15638	1.5	18943	0.9	21893	0.9
13973	1.6	15639	1.2	18944	0.6	21894	0.9
13998	0.8	15667a†	1.4	18951	1.2	21898	1.1
14002	0.5	15676	1.1	18974	0.7	21899	0.7
14013	0.7	15689	1.2	18976	1.1	21918	1.0
14144	1.3	15717	1.0	18983	0.6	21927	0.8
14178	1.2	15758	1.4	18987	1.1	21931	1.0
14183	0.9	15938	0.6	18988	0.9	21937	0.8
14187	1.3	15950	0.9	18995	1.0	21960	0.3
14282	1.3	15959	1.0	19003	0.5	21966	0.2
14292	1.0	15968	1.2	19008	1.2	21969	0.6
14309	+1.3	15980	+1.0	19012	+1.0	21979	+1.0

* Listed in the *General Catalogue* as No. 12716; however, its right ascension is 20^h38^m5 instead of 19^h38^m5, and it should be entered as 13536a.

† Omitted from the *General Catalogue*. Its position for 1900 is $23^h38^m8 - 69°43'$, 14^m8, $0''.096$, 185°.

TABLE 2—*Continued*

BPM	I.C. (In Mag.)	BPM	I.C. (In Mag.)	BPM	I.C. (In Mag.)	BPM	I.C. (In Mag.)
21980	+0.9	22335	+0.7	26602	+0.4	26852	+1.3
21981	0.5	22342	0.9	26695	1.2	26994	1.3
21986	1.0	22350	0.8	26698	1.4	27013	1.1
22016	0.7	22364	0.3	26703	0.9	27017	0.9
22026	1.0	22368	0.3	26707	0.8	27034	1.1
22028	0.6	22406	0.2	26708	1.0	27046	1.2
22035	0.5	22416	0.8	26716	1.0	27118	0.6
22061	0.5	22542	0.8	26717	0.9	27144	0.7
22067	1.1	22552	0.9	26721	1.6	27145	1.0
22068	0.7	22567	0.5	26726	1.1	27170	1.0
22069	0.6	22574	0.6	26731	1.0	27172	1.0
22083	1.1	22576	0.5	26735	0.8	27179	1.2
22085	1.1	22585	0.8	26746	1.2	27189	0.6
22087	0.4	22586	0.8	26751	1.0	27586	0.9
22089	0.8	22592	0.7	26752	0.9	27590	1.3
22244	0.8	22608	0.5	26762	0.7	27597	0.8
22248	0.8	22615	0.7	26763	0.9	27603	1.3
22249	1.1	22622	0.5	26771	1.1	27633	0.9
22251	1.0	22631	0.8	26772	1.2	27636	0.7
22258	0.8	22632	0.6	26779	1.2	27640	1.2
22264	0.6	25251	0.5	26783	1.2	28431	0.6
22270	1.0	25255	1.0	26789	1.1	28436	0.7
22283	0.8	25406	1.4	26790	1.0	28444	0.8
22285	0.7	25418	0.9	26797	1.1	28453	+0.3
22296	1.0	25422	1.0	26801	0.9		
22300	0.8	25873	1.2	26803	1.2		
22304	0.7	25901	1.1	26814	0.8		
22308	0.8	25907	0.8	26819	1.1		
22315	0.5	26377	0.1	26839	0.5		
22333	+1.1	26565	+0.6	26850	+0.8		

TABLE 3*

MEAN COLOR INDICES FOR STARS WHOSE REDUCED PROPER MOTIONS LIE BETWEEN GIVEN LIMITS

Limits for *H*	I.C. (In Mag.)	No	I.C. (In Mag.)	No	I.C. (In Mag.)	No
≦ 10.7	+0.72	10	+0.66	29	+0.68	39
10.8–12.2	0.79	60	0.71	106	0.74	166
12.3–13.7	0.82	168	0.74	172	0.78	340
13.8–15.2	0.96	162	0.87	115	0.92	277
15.3–16.7	1.09	85	+1.18	38	1.09	118
16.8–18.2	+1.20	37			+1.21	42

* The second and third columns give the average color index and the number of stars employed in each average for the stars considered in this paper. The fourth and fifth columns give the corresponding data taken from our previous paper, while the sixth and seventh columns give the over-all averages.

redder than the earlier ones but in view of the uncertainties involved, this can hardly be considered as a real systematic difference.

4. Eleven stars included in Table 2 have proper motions larger than 0".3 annually, namely, BPM 5882, 9636, 9898, 10921, 10922, 11798, 11806, 12743, 15988, 16921, and 25901. Further details concerning these stars are given in the catalogue of stars with proper motions between 0".3 and 0".5 annually, and south of declination −50°[4]. It will

TABLE 4

DATA FOR STARS OF SPECIAL INTEREST

BPM	Mag.	μ	I.C. (In Mag.)	BPM	Mag.	μ	I.C. (In Mag.)
5491.....	12.1	0".083	+0.2	19016.....	14.6	0".052	+0.4
5882.....	11.3	.318	.3	21815.....	12.2	.111	.3
5887.....	14.0	.078	.4	21890.....	12.2	.070	.0
8436.....	15.2	.111	.0	21960.....	14.8	.046	.3
9767.....	16.4	.049	.4	21966.....	12.1	.126	.2
9893.....	15.5	.062	.3	22087.....	14.4	.153	.4
10789.....	15.5	.101	.4	22364.....	14.7	.057	.3
11806.....	14.9	.324	.6	22368.....	15.1	.077	.3
12743.....	11.3	.438	.2	22406.....	14.8	.032	.2
13822.....	14.9	.097	.5	26377.....	17.5	0.104:	+0.1
13824.....	16.3	0.113	+0.6				

be noticed that the (very uncertain) low value of 0.3 for the color index of BPM 25901, as given in our earlier paper, is not substantiated by our present observations.

Twenty-one stars appear to be of sufficient individual interest to merit further mention. Data for them are given in Table 4. Five of these may be ordinary red stars situated in obscured regions; others may be high-velocity F or G dwarfs or intermediates. The star BPM 8436 appears to be a genuine white dwarf; it has been announced on *Harvard Announcement Card* No. 699. The star BPM 26377 seems unquestionably white, but reexamination of the measures indicates that the published proper motion is probably in error, most likely due to magnitude error in the measurements.

[4] *Pub. Astr. Obs. Minnesota*, 3, 23, 1940.

THE PHOTOMETRIC ORBIT OF QY AQUILAE

BALFOUR S. WHITNEY
On leave from the University of Oklahoma for service with the Army Air Forces
Received May 26, 1945

ABSTRACT

The color indices at maximum and minimum indicate spectral classes of gG2 and gG9, or dG6 and dK1, respectively. Asymmetries of common forms and undetermined sources are shown in the light-curves. Photographic, photovisual, and visual magnitudes of comparison stars are presented, with a chart of the region. The comparison of the photographic with the visual radii indicates that both components are surrounded by redder gases to a depth of one-fourth or one-fifth of their radii.

This study of QY Aquilae (Ross 268) is based on 910 photographic and 338 visual observations made with the 10-inch reflector at the University of Oklahoma Observatory in 1941 and 1942. The photographic magnitudes of the comparison stars (Table 1) were derived from 17 comparisons with Selected Area 88 for stars brighter than magnitude 14,

TABLE 1

MAGNITUDES OF COMPARISON STARS

Star	m_{pg}	P.E.	m_{pv}	P.E.	m_v	Star	m_{pg}	P.E.	m_{pv}	P.E.	m_v
a.....	12.14	±0.02	10.95	±0.03	11.2	f.....	12.66	±0.02	12.08	±0.02	12.1
b.....	11.46	.03	10.22	.04	10.2	g.....	13.50	.02	12.69	.08	12.7
w.....	11.64	.02	10.99	.03	10.9	k.....	13.57	.02	13.20	.07	13.1
x.....	11.89	.04	11.20	.03	11.1	h.....	14.69	.02	13.65	0.08	13.6
c.....	13.03	.02	12.72	.09	12.4	l.....	14.10	.05	.....	.....	.....
d.....	12.50	.02	12.03	.02	12.0	m....	14.38	.05	.....	.....	.....
e.....	13.32	0.03	11.51	0.03	11.8	n.....	14.39	0.02	.....	.....	.....

and 7 comparisons for the fainter stars. The visual magnitudes were derived from several visual sequences, adjusted to fit the scale of photovisual magnitudes obtained from 8 comparisons with Harvard Standard Regions C 10 and C 11. Stars h and k could be measured on only three of the photovisual plates, and the measures were discordant. Eastman 103–O and 103–G plates (the latter with an Eastman K-2 filter for photovisual magnitudes) were used for most of the work.

Nearly all the photographic measures were made on multiple-exposure plates. The normal exposure times were 2 or 3 minutes during maxima, and from 8 to 16 minutes during primary minima. After more than half of the plates had been measured with a scale of stellar images, 200 of the measures were compared with direct estimates made with the aid of an eyepiece. The distribution of the differences was so nearly normal that the use of the scale was discontinued. Except for these 200, each exposure was measured or estimated only once.

The tabulated visual normal points between $0^p.100$ and $0^p.872$, inclusive (Table 2), are means of 10 observations each. The others are means of 5 observations, except the last, which contains only 3. The tabulated photographic normals between $0^p.077$ and $0^p.913$, inclusive (Table 3), are based on 20 observations, and the remainder on 10 each. However, the normals plotted in the figure contain either 10 photographic or 5 visual observations each. The tabulated residuals were obtained graphically from theoretical curves for complete darkening at the limb.

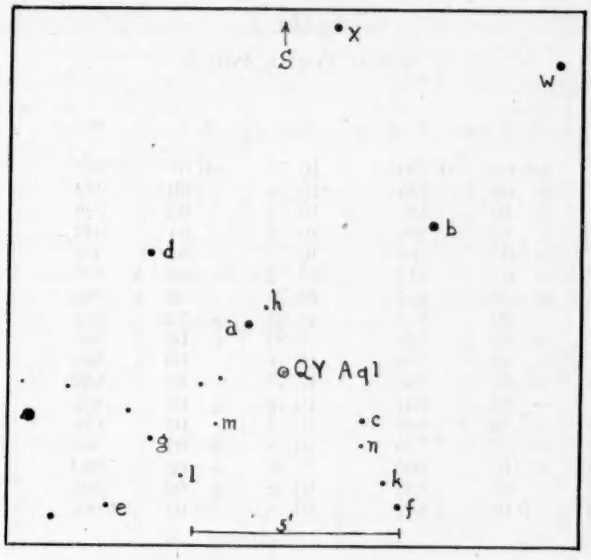

FIG. 1

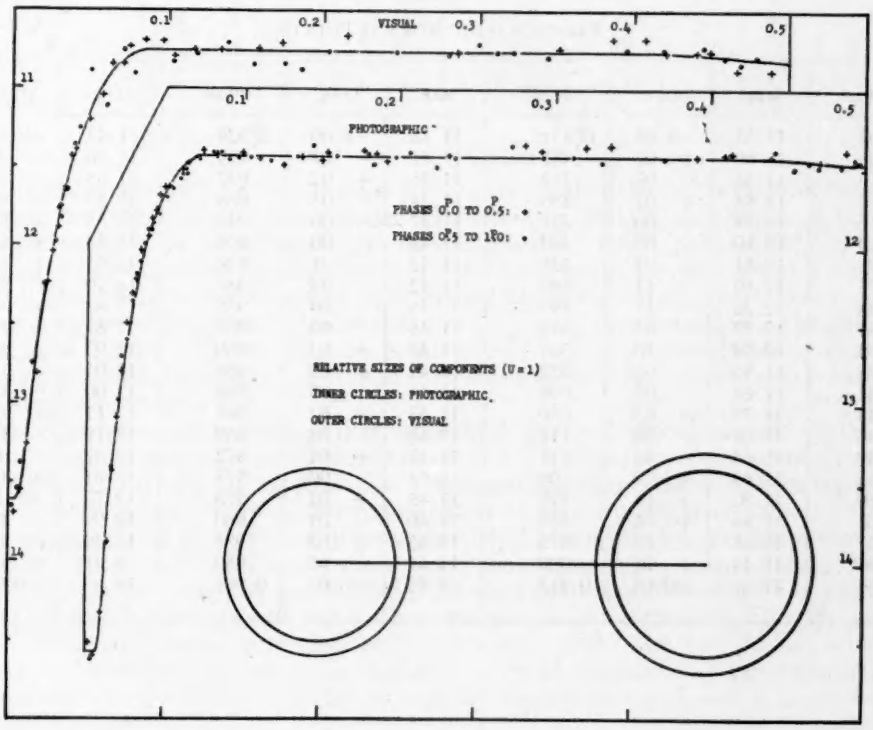

FIG. 2.—The light-curve of QY Aquilae

TABLE 2

VISUAL NORMAL POINTS

Phase	Mag.	O−C	Phase	Mag.	O−C	Phase	Mag.	O−C
0P003	13.70	+0.08	0P100	10.75	−0.01	0P897	10.84	+0.08
.007	13.56	+ .06	.126	10.76	.00	.922	10.91	+ .12
.011	13.27	+ .10	.166	10.73	− .03	.929	10.76	− .07
.017	12.82	+ .12	.250	10.72	− .04	.939	11.12	+ .19
.023	12.24	− .05	.369	10.72	− .04	.950	10.89	− .25
.026	12.05	− .03	.414	10.72	− .04	.957	11.26	− .09
.030	11.89	+ .04	.444	10.76	.00	.960	11.37	− .05
.032	11.76	.00	.477	10.88	+ .12	.964	11.65	+ .07
.035	11.64	+ .02	.526	10.82	+ .06	.966	11.66	.00
.038	11.44	− .06	.548	10.76	.00	.968	11.83	+ .08
.041	11.40	+ .01	.593	10.75	− .01	.969	11.77	− .03
.050	11.21	+ .05	.667	10.78	+ .02	.972	11.98	+ .02
.058	11.05	+ .06	.694	10.74	− .02	.978	12.25	− .10
.064	10.85	− .05	.736	10.78	+ .02	.986	12.75	− .19
.071	10.85	+ .02	.806	10.82	+ .06	.993	13.38	− .12
.075	10.74	− .06	.835	10.85	+ .09	.995	13.55	− .05
0.085	10.70	−0.06	0.872	10.74	−0.02	0.998	13.66	+0.04

TABLE 3

PHOTOGRAPHIC NORMAL POINTS

Phase	Mag.	O−C	Phase	Mag.	O−C	Phase	Mag.	O−C
0P002	14.52	−0.06	0P151	11.43	0.00	0P920	11.42	−0.01
.005	14.60	+ .02	.181	11.41	− .02	.929	11.46	+ .03
.010	14.33	− .07	.212	11.45	+ .02	.937	11.55	+ .08
.013	13.88	+ .02	.286	11.38	− .05	.938	11.52	+ .04
.016	13.43	.00	.327	11.37	− .06	.940	11.55	+ .05
.019	13.10	− .03	.400	11.43	.00	.942	11.58	+ .06
.022	12.81	+ .02	.426	11.42	− .01	.946	11.65	+ .08
.025	12.50	− .11	.480	11.42	− .03	.950	11.70	+ .04
.028	12.32	− .13	.499	11.46	.00	.955	11.81	+ .06
.031	12.22	− .05	.511	11.46	.00	.958	11.87	+ .04
.034	12.04	− .10	.533	11.48	+ .03	.960	11.91	− .01
.038	11.96	− .03	.552	11.44	+ .01	.962	11.91	− .09
.041	11.84	− .05	.609	11.43	.00	.964	12.00	− .07
.044	11.79	− .03	.680	11.45	+ .02	.967	12.11	− .07
.046	11.69	− .04	.718	11.40	− .03	.969	12.19	− .09
.049	11.64	− .04	.771	11.47	+ .04	.972	12.37	− .10
.052	11.63	+ .02	.799	11.43	.00	.975	12.61	− .03
.060	11.52	+ .01	.819	11.45	+ .02	.978	12.72	− .10
.064	11.48	+ .01	.849	11.40	− .03	.980	12.99	− .04
.077	11.41	− .02	.875	11.45	+ .02	.984	13.42	.00
.104	11.44	+ .01	.900	11.44	+ .01	.989	14.21	+ .03
0.131	11.47	+0.04	0.913	11.44	+0.01	0.997	14.63	+0.05

The light-elements used for computing the phases were those published earlier by the writer.[1] At that time, the visual observations had not been reduced.

The first of the observed minima in Table 4 is taken from *Katalog und Ephemeriden veränderlicher Sterne für 1939;* the second and third are from unpublished visual observations by Professor J. O. Hassler at the University of Oklahoma Observatory. The residuals are computed from the elements

$$\text{JD} \odot\ 2430223.6128 + 7.229815 \cdot E .$$

This period is appreciably longer than the one used for computing the phases (7.229617). The earlier period furnishes a better fit for the observations of 1941 and 1942. The systematic trend of the residuals is indicative of a variable period, which is not uncommon for eclipsing variables with asymmetric light-curves.[2]

TABLE 4

OBSERVED MINIMA

JD ⊙	Weight	Type	Epoch	O−C	JD ⊙	Weight	Type	Epoch	O−C
2420000+					2430000+				
6189.37	1	.....	−558	−0^{d}01	259.763	2	p, v	5	+0^{d}001
8517.380	1	v	−236	+ .004	281.450	2	p, v	8	− .001
8806.553	1	v	−196	− .016	295.904	1	p	10	− .007
2430000+					310.375	1	p, v	12	+ .004
165.782	2	p, v	− 8	+ .008	324.825	1	p, v	14	− .005
194.696	2	p, v	− 4	+ .002	548.947	4	p, v	45	− .007
209.168	1	v	− 2	+ .015	556.177	1	p	46	− .007
216.390	1	p, v	− 1	+ .007	563.410	1	p	47	− .004
223.612	4	p, v	0	− .001	570.631	1	p	48	− .013
230.851	2	p, v	+ 1	+ .009	577.873	3	p, v	49	− .001
238.065	1	p, v	+ 2	−0.007	599.558	4	p, v	52	−0.005

Both photographic and visual observations indicate that the star is brighter between primary and secondary minima than between secondary and primary, although the differences between the mean magnitudes are small: 0.015 ± 0.006 (pg) and 0.052 ± 0.012 (vis.) For 0^{d}2 or 0^{P}03 at the beginning of primary minimum, the photographic normals are all lower than the corresponding points on the ascending branch. This was so troublesome in earlier attempts to determine the ratio of the radii that the ascending branch was used alone for the final computations. Small humps midway down both branches of the photographic minimum may have arisen from errors in the magnitudes of two or three of the comparison stars.

For complete and two-thirds darkening at the limb, the algebraic means of the residuals of the photographic normals from the computed curves in primary minimum were −0^{m}016 and +0^{m}008, respectively. The corresponding means, taken without regard to sign, were 0^{m}050 and 0^{m}040. Attempts to reduce these led to negative values of $\cot^2 i$. The mean residual of the ten-point normals outside of either eclipse, taken without regard to sign, was 0^{m}025. For the visual curve the corresponding means were −0^{m}004, −0^{m}018, +0^{m}071, +0^{m}069, and +0^{m}038. (The last value was determined from the five-point normals.) The algebraic and arithmetical means of the residuals from the visual curve for zero darkening in primary minimum were −0^{m}012 and +0^{m}072, respectively. The visual minimum appears to occur later than the photographic by approximately 17 minutes (0^{d}012 ± 0^{d}001). This effect is apparent only in the visual normal points below magnitude 12.5.

[1] *A.J.*, Vol. **50**, No. 6, 1943.

[2] Kopal, *Ann. New York Acad. Sci.*, **41**, 47, 1940.

There are indications that the visual light-curve does not always repeat itself exactly. On JD 2430165 (epoch, −8), a series of 10 estimates in primary minimum indicated a total phase lasting $0^d.088$ or $0^P.012$, of magnitude 13.56 ± 0.04 (mean residual from 5 estimates). Other estimates, at epochs −4, 0, and 1, might have been interpreted in terms of a partial eclipse, with a minimum of about 13.75.

In consideration of the asymmetry of the light-curves and the low weight of the visual curve, the third figures of the photometric elements are of questionable significance.

TABLE 5

	Photographic	Visual
Maximum magnitude	11.429	10.76
Minimum magnitude	14.578	13.62
Luminosity:		
Smaller star	0.945	0.928
Larger star	0.055	0.072

Color indices: At maximum: 0.67; at minimum: 0.96. Spectral Classes:[4] gG2 or dG6; gG9 or dK1.

TABLE 6

	Photographic		Visual		
Limb darkening	$u=1$	$u=2/3$	$u=1$	$u=2/3$	$u=0$
Ratio of radii	0.853	0.804	0.850	0.820	0.710
Radius of larger star	0.237	0.232	0.280	0.285	0.289
Radius of smaller star	0.198	0.186	0.238	0.234	0.205
Inclination	90°	90°	88°.8	87°.4	85°.4
Duration of eclipse (computed)	$0^P.143$	$0^P.134$	$0^P.171$	$0^P.162$	$0^P.163$
Duration of total phase (computed)	$0^d.013$	$0^d.015$	$0^d.007$	$0^d.007$	$0^d.008$
Secondary minimum (computed)	$11^m.471$	$11^m.468$	$10^m.82$	$10^m.81$	$10^m.80$
Ratio of surface brightnesses	24.6	26.6	17.8	19.2	25.6

Mass-ratios (brighter component to fainter) of 1.64 and 1.53 were determined from the photographic and visual elements, respectively, by use of Bethe's expression[3] for the mass-luminosity relation:

$$\log L = \log c + 5.25 \log M - 1.25 \log R .$$

However, since evidence is accumulating that many eclipsing stars do not conform to this relation, these values may not be significant.

The visual radii are approximately one-fifth greater than the photographic for complete darkening, and one-fourth greater for two-thirds darkening (Tables 5 and 6).

I am indebted to the Faculty Research Fund Committee of the University of Oklahoma for a grant used to purchase materials needed for this study.

[3] Quoted by Taylor and Alexander, *Pub. Univ. Pennsylvania, Astr. Ser.*, Vol. 6, Part III, 1940.

[4] Seares and Joyner, *Mt. W. Contr.*, No. 684; *Ap. J.* **98**, 278, 1943.

COMMENTS ON CAPTAIN WHITNEY'S PAPER

Captain Whitney has presented his results so concisely that he has hardly done justice to his own methods. A discussion of his photographic observations with the aid of Merrill's unpublished tables for limb darkening 0.8 leads the writer to almost exactly the same elements: $r_1 = 0.227$, $r_2 = 0.181$, $i = 90°$, and the same computed light-curve. The negative residuals at about the twelfth magnitude and the positive on the other part of the descending branch cannot be removed by any adjustment. The writer attempted to represent the mean of both branches of the observed curve but found that the computed "shoulders" agree with the ascending and disagree with the descending branch—showing this to be forced by the data, independent of any arbitrary choice.

Computation of the ellipticity and reflection effects show that they may be approximately represented by $\Delta m = 0^m01 \cos \theta + 0^m01 \cos 2\theta$. Neglect of them was therefore justified.

With Whitney's mass-ratio, the density of the brighter component comes out 0.025 the sun's and that of the fainter 0.008—entirely normal values.

The visual estimates show very large residuals in some cases and are evidently of a lower order of accuracy. They cannot be even roughly represented by a light-curve derived from the geometrical elements which fit the photographic curve. For example, for half the maximum loss of light ($\alpha = 0.5$) the photographic magnitude is 12.13 and the phase from a freehand light-curve is $\pm$ 0.032 (computed, 0.033). The visual magnitude is 11.44 and phase $\pm$0.040 (freehand curve). So great a systematic difference suggests the desirability of visual observation by some method of higher precision.

Discussion of Captain Whitney's visual observations, as if they alone were available, leads to substantially the elements which he gives.

The difference in inclination between them and the photographic elements can be only a formal result of calculation. Those in the radii—especially of the eclipsing star—appear too great to be of physical significance.

The computed values presumably represent effective radii of sharp-edged disks producing obscuration as nearly equivalent as possible to that of an atmosphere of increasing opacity. Radii 0.285 (vis.) and 0.232 (phot.) would mean that violet light passed with very moderate obscuration at a depth of 18 per cent of the "visual" radius, and over a path 1.16 times this radius, through gases effectively opaque visually.

Further visual observations are greatly to be desired, and also spectroscopic studies.

HENRY NORRIS RUSSELL

PRINCETON UNIVERSITY OBSERVATORY
June 30, 1945

ON THE INTERNAL CONSTITUTION OF STARS OF SMALL MASSES ACCORDING TO BETHE'S LAW OF ENERGY GENERATION

N. R. SEN AND U. R. BURMAN
University College of Science and Technology, Calcutta, India
Received March 1, 1945

ABSTRACT

It is shown that for stars with masses and luminosities similar to those of the sun a satisfactory model may be constructed by associating the Cowling model with Bethe's law of energy generation. From the values of L and M of such stars given by Kuiper, R has been calculated and found to be in good agreement with Kuiper's values, thus lending strong support to the validity of Bethe's law for these stars. The hydrogen abundance of such stars is found to be about 35 per cent; and their central temperatures lie within, or close to, the range of 19–22 million degrees. An empirical formula has been given for calculating the central temperature from L and M of such stars.

It has been found that Bethe's energy-generation law,[1] applied to the convective-radiative model of stars, is in very good agreement with observational results in the case of a star like the sun (with small mass and negligible radiation pressure) when a hydrogen abundance of 35 per cent is assumed. Further, the constitution of such stars is quite satisfactorily given by the Cowling model, in which the convective core contains about 14.5 per cent of the mass and occupies 17 per cent of the radius of the star.[2] A preliminary calculation has convinced us that for these stars of small masses the Cowling-model core is very nearly identical with the energy-generating core of a model constructed strictly according to Bethe's law. The luminosity function also does not differ much in these two models, the discrepancy being limited to about 6 per cent. It is thus reasonable to make use of the Cowling model to study the internal constitution of such stars and to check, as much as possible, the results calculated on the assumption of this model by comparison with observational material. The object of this paper is to examine the results obtained from the Cowling model of stars of small masses in which energy generation takes place according to Bethe's law and to compare them with observational material available to us.

I. CALCULATION OF STELLAR PARAMETERS FROM THE COWLING MODEL

We take the Cowling model to be approximately true for stars of small masses and further assume that energy in them is generated according to Bethe's law. We note that the Cowling model is entirely determined if three parameters are known, as is shown by the following formulae:[3]

$$T_c = 0.9\,\frac{\mu H}{k}\,\frac{GM}{R}, \tag{1}$$

$$\rho_c = \frac{\xi_1^3}{4\pi\psi_1}\,\frac{M}{R^3}, \tag{2}$$

$$Q = \frac{\kappa_0 L}{16\pi}\,\frac{3}{ac}\,\frac{\rho_c^2}{\alpha T_c^{7.5}}, \tag{3}$$

with

$$\alpha^2 = \frac{5k}{8\pi\mu GH}\,\frac{T_c}{\rho_c}. \tag{4}$$

[1] *Phys. Rev.*, **55**, 434, 1939.

[2] *Nature*, **153**, 267, 1944.

[3] S. Chandrasekhar, *An Introduction to the Study of Stellar Structure*, pp. 352–354, Chicago: University of Chicago Press, 1939.

The three parameters may be considered to be M, R, and X, since κ_0 and μ are connected with X by the relations (for negligible *He* content)

$$\kappa_0 = 3.9 \times 10^{25} (1 - X^2) \frac{1}{\bar{t}} \tag{5}$$

and

$$\mu = \frac{2}{1+3X}. \tag{6}$$

The luminosity, according to Bethe's law, is determined by

$$L(r) = \int_0^r 4\pi r^2 \rho \epsilon d r , \tag{7}$$

where

$$\epsilon = \epsilon_0 \rho T^{-2/3} e^{-B/T^{1/3}} \tag{8}$$

and ϵ_0 is a constant, depending on the composition, and

$$B = 56 (2 \times 10^7)^{1/3} .$$

Introducing the variables ξ, θ, and σ, defined by

$$r = a\xi , \qquad T = T_c \theta , \qquad \text{and} \qquad \rho = \rho_c \sigma ,$$

and using the polytropic relation $\sigma = \theta^{3/2} (n = \frac{3}{2})$, we find, after some calculations, that

$$L(\xi) = A \rho_c^{1/2} I(\xi, T_c) , \tag{9}$$

where the luminosity $L = L(\xi_i)$ (ξ_i denoting the value of ξ at the point where the convective core ends), and

$$A = 4\pi\epsilon_0 \left(\frac{5k}{8\pi\mu GH} \right)^{3/2} T_c^{5/6} \tag{10}$$

and

$$I(\xi, T_c) = \int_0^{\xi} \theta^{7/3} e^{-b/\theta^{1/3}} \xi^2 d\xi \qquad \left(b = \frac{B}{T_c^{1/3}} \right). \tag{11}$$

Thus, combining the Cowling model with Bethe's law, we get four equations ([1], [2], [3], and [9]), from which L may be eliminated (by means of eg. ([9])), and three equations obtained involving five quantities: M, R, ρ_c, T_c, and X. These equations can now be solved in terms of two parameters, T_c, and X, say; and thus M, R, and ρ_c can be obtained in terms of these two. Equation (9) then determines $L = L(\xi_i)$. The detailed calculations appear elsewhere.[4] But we may quote here the final formulae. We have

$$L = \frac{B}{\rho_c^{5/2}} , \tag{12}$$

where

$$B = Q \frac{16\pi a c}{3\kappa_0} \left(\frac{5k}{8\pi\mu GH} \right)^{1/2} T_c^8 \tag{13}$$

and

$$\rho_c^3 = \frac{B}{A I(\xi_i, T_c)} . \tag{14}$$

Equations (1) and (2) then determine M and R. In this manner we can construct two-parametric solutions of our equations, giving all the quantities L, M, R, and ρ_c in terms of T_c and X only.

[4] *Indian J. Phys.*, **18**, 212, 1944.

In actual calculations we have to fix the value of the average guillotine factor $\bar{l}$ in equation (5). This is done as follows: We have at our disposal a rigorous integration of the stellar equations, taking Bethe's law into consideration for a central temperature

TABLE 1

SOLUTIONS OF EQUATIONS (1), (2), (3), AND (9) GIVING THE MASS, RADIUS, LUMINOSITY, AND CENTRAL DENSITY FOR STARS WITH ASSIGNED CENTRAL TEMPERATURE AND COMPOSITION

X	$T_c \times 10^{-6}$	$M \times 10^{-33}$	$R \times 10^{-10}$	$L \times 10^{-33}$	ρ_c
0.15.....	19	0.83	4.40	0.38	86.5
	20	1.00	5.01	0.99	70.3
	21	1.18	5.64	2.31	58.1
	22	1.38	6.31	5.21	48.6
0.25.....	19	1.23	5.39	0.76	69.5
	20	1.47	6.14	1.92	56.5
	21	1.75	6.92	4.57	46.6
	22	2.05	7.74	10.32	39.1
0.35.....	19	1.68	6.27	1.25	60.3
	20	2.01	7.13	3.17	49.0
	21	2.38	8.04	7.55	40.4
	22	2.79	8.99	17.06	33.9
0.45.....	19	2.16	7.04	1.88	54.7
	20	2.59	8.02	4.76	44.4
	21	3.06	9.04	11.35	36.7
	22	3.59	10.10	25.64	30.7
0.55.....	19	2.67	7.71	2.67	51.4
	20	3.20	8.78	6.76	41.7
	21	3.78	9.90	16.10	34.5
	22	4.43	11.07	36.38	28.9
0.65.....	19	3.18	8.26	3.65	49.9
	20	3.81	9.40	9.25	40.5
	21	4.51	10.60	22.03	33.5
	22	5.28	11.85	49.77	28.1
0.75.....	19	3.65	8.61	4.91	50.5
	20	4.38	9.80	12.43	41.1
	21	5.18	11.05	29.61	33.9
	22	6.07	12.36	66.88	28.4
0.85.....	19	4.01	8.65	6.60	54.7
	20	4.80	9.85	16.72	44.5
	21	5.66	11.10	39.81	36.7
	22	6.89	12.55	90.00	30.8
0.95.....	19	3.93	7.82	9.61	72.7
	20	4.71	8.90	24.33	59.1
	21	5.57	10.02	57.97	48.8
	22	6.53	11.22	130.95	40.9

of $T_c = 20 \times 10^6$ degrees. The value of $\bar{l}$ is so chosen that for this central temperature the final values of L, M, and R, obtained from the Cowling model, agree as closely as possible with the values obtained from the accurate integrations. This value of $\bar{l}$ turns out to be 6 and has been accepted throughout our present calculations.

II. THE RESULTS OF NUMERICAL CALCULATION

In our numerical work we have taken $T_c = 19$, 20, 21, and 22 million degrees; and for each of these central temperatures calculations have been made for $X = 0.15$, 0.25, 0.35, 0.45, 0.55, 0.65, 0.75, 0.85, and 0.95. Table 1 gives the results of our calculations of L, M, R, and ρ_c, according to the formulae developed above. The highest value of the central temperature considered, viz., $T_c = 22 \times 10^6$ degrees, has been verified to be such that up to about this value neither the radiation pressure nor the opacity due to electron

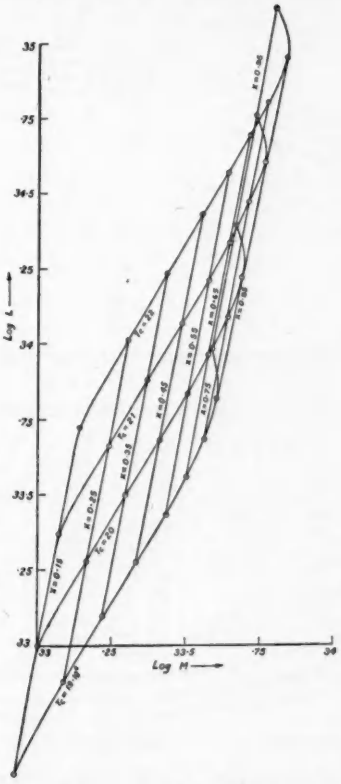

FIG. 1.—The mass-luminosity relation for $X = 0.15$, 0.25, 0.35, 0.45, 0.55, 0.65, 0.75, 0.85, and 0.95 with $Y = 0$ and $T_c = 19$, 20, 21, and 22 million degrees.

scattering plays a significant role. For a central temperature very much below our lowest value, $T_c = 19 \times 10^6$ degrees, the proton-proton reaction of Bethe and Critchfield[5] might contribute a substantial part in the energy generation. Hence we have limited ourselves to this safe temperature range for the present scheme.

From Table 1, Log L and Log M (with L and M in absolute units) have been plotted in Figure 1 for the various central temperatures and hydrogen contents. The plotted points lie on two sets of curves, T_c = constant (from 19 to $22 \cdot 10^6$ K) and X = constant (from 0.15 to 0.95), and determine a narrow lozenge-shaped diagram except for a slight bending of the curves in the upper portion. Two other curves are also plotted with the data taken from Table 1. Figure 2 is an X–Log R (R in absolute units) diagram, while in Figure 3 is plotted ρ_c against X.

[5] *Phys. Rev.*, **54**, 248, 1938.

From these diagrams we can determine all the parameters of a star of which the corresponding point plotted in Figure 1 lies within the lozenge-shaped portion. For instance, the position of this point will give (by interpolation) the values of X and T_c. Figures 2 and 3 will then give the values of R and ρ_c.

From this point of view we have examined some of the stars whose L, M, and R values have been revised by Kuiper.[6] The parameters of those stars whose representative points lie within or near the boundary of Figure 1 have been calculated and given in Table 2.

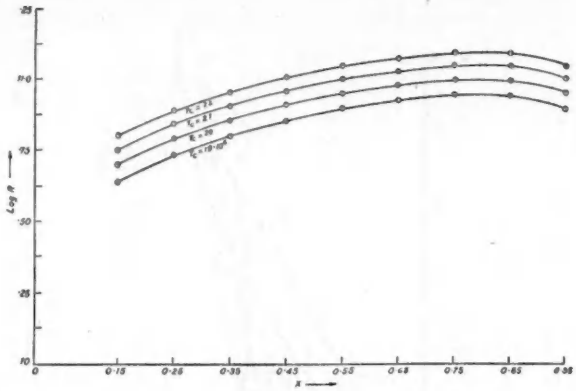

FIG. 2.—The variation of radius with composition for assigned central temperatures

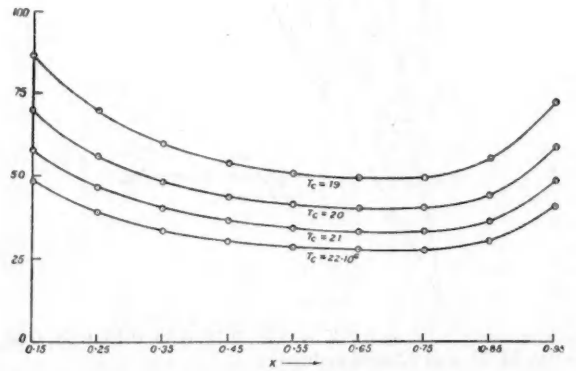

FIG. 3.—The variation of central density with composition for assigned central temperatures

The second, third, and fourth columns of this table give Kuiper's values. The remaining columns have been calculated according to our scheme. We first obtain a value for $R/R_\odot$ of the star, which may be compared with the corresponding observed value (Kuiper) in the fourth column. The agreement is as good as may be expected. Only in the case of the last two stars, viz., α CMi A and ζ Her A, is the agreement not as satisfactory as in the other cases; but such discrepancy in the value of R need not be considered serious—besides, factors other than those we have assumed might also have intervened. The fact that the calculated values of R exceed the observed values only in these two cases (the fact is opposite in all previous cases) is probably significant.

[6] *Ap. J.*, **88**, 486, 1938.

The last three columns give the *calculated* values of X, T_c, and ρ_c, according to our scheme, together with those furnished by the standard-model formulae, these last values being taken from Chandrasekhar's *Stellar Structure* (p. 489). With regard to the stars of Kuiper's table, which are not shown in our Table 2, it has been found that their representative points in Figure 1 (Log L–Log M diagram) all fall much outside the diagram, so that the cases of these stars cannot be considered by the present scheme. For instance, the L-M values of the stars α CMi B, O_2 Eri B, O_2 Eri C, α CMa B, Kr 60 A, and μ Her-$\overline{BC}$ indicate too low central temperatures (very much below 19×10^6 degrees), whereas those for the stars α Aur A, α Aur B, α CMa A, and ζ UMa $\bar{A}$ indicate central temperatures very much higher than 22 million degrees. An extension of our scheme is necessary to include the cases of these stars.

TABLE 2

COMPARISON OF THE CALCULATED AND OBSERVED VALUES OF THE RADII OF SOME STARS AND THE CALCULATED VALUES OF THEIR HYDROGEN CONTENT, CENTRAL TEMPERATURE, AND DENSITY

STAR	$L/L_\odot$ (OBS.)	$M/\odot$ (OBS.)	$R/R_\odot$		X		$T_c \cdot 10^{-6}$		ρ_c	
			(Obs.)	(Calc.)	(Calc.)	(Standard Model)	(Calc.)	(Standard Model)	(Calc.)	(Standard Model)
η Cas A	0.81	0.72	0.81	0.87	0.21	0.25	20.9	20.9	51	100.0
η Cas B	0.07	0.47	0.56	0.62	.23	.34	18.0	17.8	93	19.5
α Cen A	1.26	1.10	1.23	1.15	.37	.36	20.4	17.0	44	45.7
α Cen B	0.37	0.87	0.87	0.91	.36	.43	19.0	17.8	59	100.0
ξ Boo A	0.48	0.87	0.87	0.95	.35	.39	19.5	18.6	54	95.5
ξ Boo B	0.15	0.76	0.80	0.80	.35	.48	18.0	16.2	75	117.5
70 Oph A	0.42	0.89	0.93	0.95	.36	.42	19.3	17.4	55	85.1
70 Oph B	0.14	0.74	0.69	0.77	.36	.50	17.6	17.8	83	166.0
α CMi A	5.76	1.48	1.70	1.38	.36	.31	22.5	17.8	29	23.4
ζ Her A	3.89	0.96	1.95	1.23	0.22	0.12	23.0	13.5	34	9.8

III. DISCUSSION OF THE RESULTS

It is seen from Table 1 that, as the central temperature varies from 19 to 22 million degrees and the hydrogen content from 15 to 95 per cent, the mass of the stellar body varies from $0.4\odot$ to about $3\odot$, its radius from $0.6R_\odot$ to about $2R_\odot$, and the luminosity from 0.1 $L\odot$ to about 33 $L\odot$. It has been shown that for given T_c the four quantities, L, M, R, and ρ_c may be considered as functions of X alone ($Y = 0$). Of these, L happens to be monotonically increasing with X, while M and R have their maximum at $X \sim 0.9$ and 0.8, respectively, and ρ_c has a minimum at $X \sim 0.7$. This behavior is indeed a consequence of neglecting the *He* content and follows easily from theoretical considerations. Thus

$$L \propto X(1+3X)^{3/2}; \qquad M^2 \propto (1+3X)^3 [f(X)]^{1/3}, \tag{15}$$

and

$$R^2 \propto (1+3X)[f(X)]^{1/3}; \qquad \rho_c^3 \propto \frac{1}{f(X)}, \tag{16}$$

where

$$f(X) = X(1-X^2)(1+3X). \tag{17}$$

It may also be noted from Table 1 that for stars of approximately the same mass, as X decreases, R increases. This conclusion was also arrived at by Strömgren by his method of calculation of the hydrogen content. Here we arrive at the same result from the point of view of Bethe's law. Further, as a star of given mass burns hydrogen more and more (X decreases), we find from Table 1, or Figure 1, that its central temperature increases and the central density diminishes. These consequences follow generally from Bethe's law of energy generation.

In Table 2 we note that stars in which energy generation takes place in good or fairly good agreement with Bethe's law have their hydrogen content ranging from about 20 to 40 per cent. This is quite in accordance with Strömgren's conjecture. It is also interesting to note that for the majority of these stars, X is approximately 35 per cent. So far as the central temperature is concerned, the observational material is well distributed between 18 and 23 million degrees, approximately. It is thus permissible to conclude that Bethe's law gives the correct amount of energy generation at least in stars with these ranges of central temperatures. Outside these ranges other factors, which we have previously mentioned, are to be taken into account. A comparison with the standard model of the stars, for which the figures, so far as available, are given in the table, shows that, so far as the central temperature is concerned, there is fairly good agreement in many cases, though discordant results also exist. But as regards the central density, the standard-model values are generally very much higher. There are, however, a few cases where our calculation gives a higher central density, but they systematically correspond to lower central temperatures.

The fairly good uniformity of the variations in L and M with T_c prompted us to obtain an empirical formula for the central temperature. We find that for the temperature range considered (19–22 $\times$ 10^6 K and with L and M near about solar values)

$$T_c = 20 - \tfrac{2}{3}\cdot 0\ (\text{Log}\, M - 33) + 4\ (\text{Log}\, L - 33) \qquad (18)$$

is a very good representation of T_c (in millions of degrees) in terms of Log L and Log M, where M and L are measured in cgs units. When M and L are measured in *solar units*, the corresponding relation is

$$T_c = 20 - \tfrac{2}{3}\cdot 0\ (\text{Log}\, M + 0.30) + 4\ (\text{Log}\, L + 0.58)\,. \qquad (19)$$

This representation can be relied upon, up to a value of $X \sim 0.75$, so long as T_c lies within our limits. A similar representation for X in terms of Log M, and Log L has not, however, been found possible over a wide range in X. One simple formula valid for X in the neighborhood of 35 per cent may, however, be given, but we think it is best to take X from our Log M–Log L diagram (Fig. 1) by simple interpolation.

We have noted that, though Table 1 extends over a wide range in X (15–95 per cent), the observational material available at present is confined within a narrow range of about 20–40 per cent of the hydrogen content. This corresponds to approximately the solar values for the parameters (L, M, and R) and may be significant. Then one has to expect that, for the above ranges of central temperatures, stellar masses and luminosities of the order of solar values only are possible and that their hydrogen content lies within that range. In the future we may obtain further material going outside the narrow range of X (20–40 per cent), with corresponding deviations from solar values. In any case, we note that for central temperatures up to about 22 million degrees, a stellar body of large mass (exceeding $3\odot$) and large luminosity (exceeding $33L\odot$) is inconsistent with Bethe's law. Although we have here limited ourselves to central temperatures up to only 22 million degrees, it appears unlikely that for even higher central temperatures very large stellar masses will be permitted by Bethe's law of energy generation.

IV. CONCLUSIONS

For a given composition, the parameters L, M, R and ρ_c for stars of small masses can be approximately evaluated by the convective-radiative Cowling model, on Bethe's law of energy generation when the central temperature varies from 19 to 20 million degrees. The model fits quite satisfactorily the energy-generation law under the conditions stated. From the observational material available at present, we may conclude that stars whose masses and luminosities do not differ much from those of the sun have their energy generated in accordance with Bethe's law. Further, their central temperatures lie within or close to 19–22 million degrees; and their hydrogen abundance generally is about 35 per cent, though in several cases a low hydrogen content of about 22 per cent has also been calculated. A comparison with the standard model shows that the central temperature of this model is very often in agreement with the model constructed in accordance with Bethe's law, but the standard-model central density is generally too high. As regards the hydrogen content, there is no general agreement, though some agreement is found to exist in several cases.

A STELLAR MODEL WITH A GRAVITATIONAL SOURCE OF ENERGY

MARJORIE HALL HARRISON
Yerkes Observatory
Received June 8, 1945

ABSTRACT

A stellar model consisting of a convective core and an envelope in which the energy generation is of the form $\epsilon \propto T$ is considered. It is found that the convective core extends to a fraction of 0.14 of the radius of the star and incloses 10.5 per cent of the mass. Further, the constants of proportionality in the equations for ρ_c, T_c, P_c, and L differ only slightly from those for the Cowling point-source model.

1. *Introduction.*—In this paper we propose to consider a stellar model with negligible radiation pressure, in which the law of energy generation has the form

$$\epsilon = \epsilon_0 T , \tag{1}$$

where ϵ denotes the energy liberated per gram of the stellar material at temperature T and where ϵ_0 is a constant. The study of such a model has gained renewed interest for stellar structure since it became apparent that the liberation of gravitational energy in consequence of a slow secular contraction of the star must play an important role in discussions relating to stellar evolution.[1] For under circumstances in which a star contracts homologously,[2] the rate of energy liberation is given by

$$\epsilon = -\frac{3\gamma - 4}{\gamma - 1} \frac{1}{R} \frac{dR}{dt} \frac{k}{\mu H} T , \tag{2}$$

where R denotes the radius of the star and the rest of the symbols have their usual meanings.

We should, however, point out that the study of stellar models based on the law (1) or (2) is not new. Indeed, since A. S. Eddington's[3] discussion of the validity of his model "$\kappa\eta$ = constant," it has been generally believed that the standard model on which stars are polytropes of index 3 describes the model $\epsilon \propto T$ very closely. Moreover, Biermann made an exact integration of the equations of equilibrium for a special case, making due allowance for the radiation pressure. But it does not seem that an integration of the important case in which the radiation pressure is neglected in the equation of hydrostatic equilibrium exists. It is the object of this paper to provide such an integration.

2. *The equations of the model.*—In our discussion of the model based on the law (1) we shall suppose that, in the parts of the star where the radiative gradient obtains, the law of opacity is the conventional law of Kramers:

$$\kappa = \kappa_0 \rho T^{-3.5} . \tag{3}$$

With this law the standard equations of equilibrium

$$\frac{k}{\mu H} \frac{d(\rho T)}{dr} = -\frac{GM(r)}{r^2} \rho ; \qquad \frac{dM(r)}{dr} = 4\pi \rho r^2 \tag{4}$$

[1] Cf., e.g., M. Schönberg and S. Chandrasekhar, *Ap. J.*, **96**, 161, 1942.

[2] For a discussion of the conditions under which such a contraction can take place see L. H. Thomas, *M.N.*, **91**, 122 and **619**, 1930.

[3] *The Internal Constitution of the Stars*, pp. 114 ff., Cambridge, England, 1926.

and

$$\frac{dp_r}{dr} = -\frac{\kappa_0 L(r)}{4\pi c r^2}\rho^2 T^{-3.5}; \qquad \frac{dL(r)}{dr} = 4\pi\rho r^2 \epsilon_0 T, \tag{5}$$

valid everywhere except in the convective core at the center, can be reduced to the non-dimensional forms

$$\frac{d(\sigma\theta)}{d\xi} = -\frac{\psi\sigma}{\xi^2}; \qquad \frac{d\psi}{d\xi} = \xi^2\sigma, \tag{6}$$

and

$$\frac{d\theta}{d\xi} = -\frac{Q\lambda\sigma^2}{\xi^2\theta^{6.5}}; \qquad \frac{d\lambda}{d\xi} = \theta\xi^2\sigma, \tag{7}$$

by the transformation

$$r = R\xi; \qquad \rho = \rho_0\sigma; \qquad T = T_0\theta; \qquad M(r) = M\psi; \qquad L(r) = L_0\lambda, \tag{8}$$

with

$$\rho_0 = \frac{M}{4\pi R^3}; \qquad T_0 = \frac{\mu H}{k}\frac{GM}{R} \tag{9}$$

and

$$Q = \kappa_0\epsilon_0\frac{3R^2}{4ac}\frac{\rho_0^3}{T_0^{6.5}} = \kappa_0 L_0\frac{3}{16\pi acR}\frac{\rho_0^2}{T_0^{7.5}}. \tag{10}$$

It is found that, as we approach the center of the configuration along a solution of the equations (6) and (7), the radiative gradient becomes unstable at a determinate point, where the effective polytropic index becomes $\frac{3}{2}$. At this point the convective equations must accordingly replace the radiative, and

$$\sigma = \theta^{3/2}; \tag{11}$$

and the equations (6) can be reduced to the Lane-Emden equation of index $\frac{3}{2}$.

3. *The construction of the model.*—Near $\xi = 1$ the equations (6) and (7) can be approximately integrated. For in the immediate neighborhood of the boundary of the star, $M(r)$ and $L(r)$ remain constant to a high degree of accuracy. Accordingly, letting ψ and λ have their respective boundary values, which we shall denote by ψ_1 and λ_1, the first of the two equations in (6) and (7) can be re-written in the form

$$\frac{d(\sigma\theta)}{d(\theta^4)} = \frac{\psi_1}{\lambda_1}\frac{1}{4Q}\frac{\theta^{3.5}}{\sigma} \tag{12}$$

and

$$\frac{d(\theta^4)}{d\xi} = -\frac{4Q\lambda_1\sigma^2}{\xi^2\theta^{3.5}}. \tag{13}$$

Now let

$$\sigma = \frac{\psi_1^{15}}{2Q^8\lambda_1^{17/4}}S; \qquad \theta = \frac{1}{Q^2}\frac{\psi_1^4}{\lambda_1}t \tag{14}$$

and

$$K = \frac{\psi_1^3}{Q^2\lambda_1}. \tag{15}$$

Introducing these substitutions into equations (12) and (13) and making the further substitutions

$$t = \frac{u^2}{K^2}; \qquad S = z\frac{u^6}{K^7}, \tag{16}$$

we have

$$\tfrac{1}{8} z u \frac{dz}{du} = u - z^2 \tag{17}$$

and

$$\frac{du}{d\xi} = -\frac{K}{8} \frac{z^2}{\xi^2 u^2}. \tag{18}$$

The solutions of equations (17) and (18) satisfying the boundary condition that z and u tend to zero simultaneously are

$$z^2 = \tfrac{16}{17} u\,; \qquad \frac{1}{\xi} = 1 + \frac{17}{4} \frac{u^2}{K}. \tag{19}$$

The corresponding solutions for σ and θ are

$$\sigma = \frac{\lambda_1^{11/4}}{\psi_1^6} \frac{Q^6}{2} z \omega^{12}\,; \qquad \theta = \frac{\lambda_1}{\psi_1^2} Q^2 \omega^4. \tag{20}$$

For any specified value of Q the foregoing equations will enable us to derive σ, θ, and the various other quantities for some value of $\xi < 1$. In practice it is found that these equations provide sufficient accuracy up to $\xi = 0.92$.

For values of $\xi < 0.92$ the solutions thus started will have to be continued by numerical methods. For this purpose it is convenient to introduce the variable

$$x = \frac{1}{\xi} \tag{21}$$

and to re-write equations (6) and (7) in the forms

$$\frac{d(\sigma\theta)}{dx} = \psi\sigma\,; \qquad \frac{d\psi}{dx} = -\frac{\sigma}{x^4} \tag{22}$$

and

$$\frac{d\theta}{dx} = \frac{Q\lambda\sigma^2}{\theta^{6.5}}\,; \qquad \frac{d\lambda}{dx} = -\frac{\theta\sigma}{x^4}. \tag{23}$$

Owing to the nature of the differential equations to be solved, it is found more convenient to do the integration in terms of logarithmic variables. Using an asterisk (*) to denote the logarithm to the base 10, we have

$$\sigma^* = \log \sigma\,; \qquad \theta^* = \log \theta\,; \qquad \psi^* = \log \psi\,; \qquad x^* = \log x\,; \qquad \lambda^* = \log \lambda\,. \tag{24}$$

Let

$$\varphi = \sigma\theta\,; \tag{25}$$

then

$$\varphi^* = \log \varphi = \log \sigma + \log \theta\,. \tag{26}$$

The equations to be integrated then become

$$\left.\begin{aligned}
\frac{d\varphi^*}{dx^*} &= \frac{x}{\varphi}\psi\sigma = 10^{\psi^*+\sigma^*+x^*-\varphi^*},\\
\frac{d\psi^*}{dx^*} &= -\frac{x}{\psi}\frac{\sigma}{x^4} = -10^{-3x^*+\sigma^*-\psi^*},\\
\frac{d\theta^*}{dx^*} &= \frac{x}{\theta^{7.5}} Q\lambda\sigma^2 = Q\,10^{x^*+\lambda^*+2\sigma^*-7.5\theta^*},\\
\frac{d\lambda^*}{dx^*} &= -\frac{\theta\sigma}{\lambda x^3} = -10^{\theta^*+\sigma^*-\lambda^*-3x^*}.
\end{aligned}\right\} \tag{27}$$

It is thus seen that for any specified Q the equations can be integrated, starting from the boundary and going inward. However, as we go along such a solution, a point is generally reached where the radiative gradient breaks down. This point, ξ_i, where the convective gradient sets in is defined by the place where the effective polytropic index

$$n = \frac{1}{Q}\frac{\theta^{6.5}\psi}{\lambda\sigma^2} - 1 \tag{28}$$

TABLE 1

MASS, LUMINOSITY, TEMPERATURE, AND DENSITY DISTRIBUTIONS FOR THE MODEL $\epsilon \propto T$

ξ	ψ	λ	θ	σ
1.0000	1.0000	1.0000	.....	.....
0.9701	1.0000	1.0000	0.0073	.....
0.9410	1.0000	1.0000	.0147	.....
0.9175	1.0000	1.0000	.0212	.....
0.8810	0.9999	1.0000	.0318	0.0063
0.8504	0.9996	1.0000	.0414	0.0145
0.8207	0.9993	1.0000	.0514	0.0272
0.7881	0.9984	1.0000	.0632	0.0538
0.7645	0.9975	0.9999	.0724	0.0842
0.7342	0.9956	0.9997	.0851	0.1410
0.7052	0.9929	0.9994	.0983	0.2258
0.6770	0.9891	0.9991	.1120	0.3455
0.6371	0.9811	0.9981	.1336	0.6093
0.6118	0.9739	0.9971	.1486	0.8594
0.5756	0.9600	0.9948	.1721	1.3783
0.5528	0.9484	0.9927	.1884	1.8424
0.5202	0.9271	0.9885	.2137	2.7585
0.4896	0.9011	0.9825	.2401	3.9917
0.4514	0.8588	0.9716	.2767	6.2392
0.4163	0.8026	0.9566	.3146	9.3058
0.3839	0.7504	0.9373	.3535	13.3010
0.3540	0.6869	0.9135	.3929	18.2850
0.3264	0.6196	0.8858	.4317	24.2826
0.2891	0.5165	0.8382	.4903	34.8168
0.2560	0.4172	0.7868	.5460	46.7441
0.2267	0.3274	0.7354	.5984	59.1696
0.2007	0.2504	0.6875	.6469	71.2087
0.1707	0.1694	0.6329	.7054	85.4250
0.1419	0.1050	0.5854	.7642	98.0942
0.1119	0.0551	0.1966	.8214	109.4
0.0819	0.0227	0.0430	.8682	118.9
0.0519	0.0060	0.0036	.9017	125.9
0.0219	0.0006	.....	.9206	129.8
.....	.....	.....	0.9251	130.8

becomes $\frac{3}{2}$. The solution interior to ξ_i must be described by a Lane-Emden function $\theta_{3/2}$. For an initially arbitrary choice Q, the solution obtained by the integration cannot be fitted to $\theta_{3/2}$. The condition that the fit be made determines Q. Now the conditions at the interface are that the values of the temperature, pressure, and mass of the core should be identical at the interface, along with the condition that the effective polytropic index n attain the value 1.5 at the interface. We then have

$$P(r_i)_c = P(r_i)_e\,; \qquad T(r_i)_c = T(r_i)_e\,; \qquad M(r_i)_c = M(r_i)_e\,; \qquad n = 1.5\,, \tag{29}$$

where P, M, and T denote the total pressure, the mass within the radius r, and the temperature, respectively, and where c refers to the core, e to the envelope, and i to the interface.

Introducing the homology invariant quantities u and v, defined as in Chandrasekhar's *Stellar Structure* (pp. 146 ff.), we have for the conditions at the interface:

$$u_i = \frac{4\pi\rho_e(r_i)\, r_i^3}{M_e(r_i)} = u_e = \left(\frac{\sigma}{\psi}\frac{1}{x^3}\right)_{r=r_i} \tag{30}$$

and

$$v_i = \frac{2}{5}\frac{GM_e(r_i)}{r_i T_e(r_i)}\frac{\mu H}{k} = v_e = \left(\frac{2}{5}\frac{\psi}{\theta}x\right)_{r=r_i}. \tag{31}$$

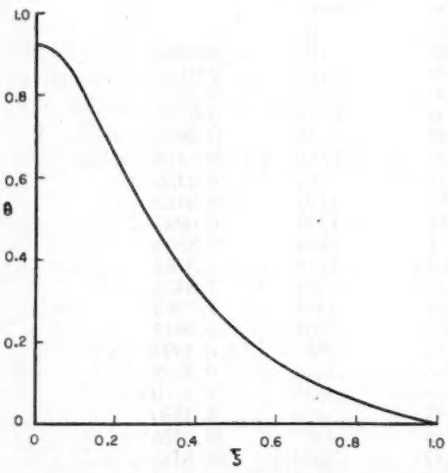

FIG. 1.—The temperature distribution in the model with a gravitational source of energy.

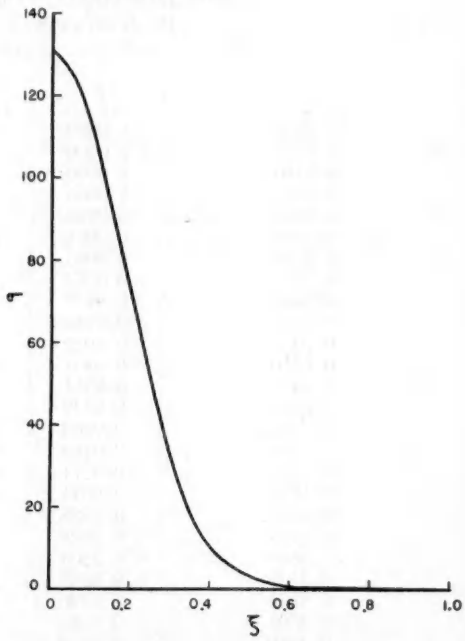

FIG. 2.—The density distribution in the model with a gravitational source of energy.

In terms of logarithms these conditions become

$$\left.\begin{aligned} &\log u_e = \varphi^* - \theta^* - 3x^* - \psi^*\,; \\ \text{and}\quad &\log v_e = -0.397940 + \psi^* + x^* - \theta^*. \end{aligned}\right\} \tag{32}$$

The envelope equations were integrated for values of $\log Q = -5.7265$, -5.85, -5.9, -6, and -7. All calculations were carried out logarithmically to six decimal places. When the point was reached at which the radiative gradient broke down, u_e and v_e were calculated. For the regions of the star inside $r = r_i$ the Fairclough[4] solutions of the Lane-Emden equation of index $\frac{3}{2}$ were used.

4. *Results.*—From the integrations we find that

$$\left.\begin{aligned} \log Q = -5.8864\,; \quad & u_e = 2.6647\,; \quad v_e = 0.3885\,, \\ \xi_i = 0.1419\,; \quad & \psi_i = 0.1050\,; \quad \lambda_i = 0.5854\,, \\ \theta_i = 0.7642\,; \quad & \sigma_i = 98.0942\,; \end{aligned}\right\} \tag{33}$$

and from equation (10)

$$\log \kappa_0 = 24.8379\,. \tag{33'}$$

[4] *M.N.*, **92**, 645, 1931–1932.

By interpolating in the Lane-Emden tables we find that $\theta_i^{3/2} = 0.7501$. This determines the central value of σ. For, we must have[5]

$$\sigma_i = \sigma_c \theta_i^{3/2} . \tag{34}$$

From equation (34) and the known value of $\theta_i^{3/2}$ (= 0.7501)

$$\sigma_c = 130.8 . \tag{35}$$

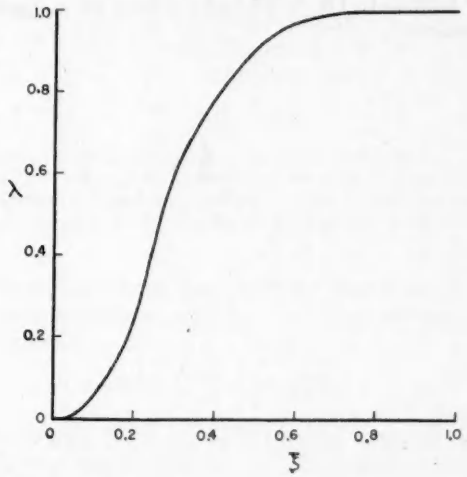

FIG. 3.—The luminosity distribution in the model with a gravitational source of energy

Also, since

$$\bar{\rho} = \frac{M}{\frac{4}{3}\pi R^3} = 3\rho_0 \tag{36}$$

and

$$\rho_c = \rho_0 \sigma_c , \tag{37}$$

we find

$$\rho_c = 43.6\bar{\rho} . \tag{38}$$

Moreover,

$$\sigma_i \theta_i = K \theta_c^{5/3} \theta_i^{5/2} \tag{39}$$

or

$$K = 0.0359 ; \tag{40}$$

and

$$\sigma_c \theta_c = K \sigma_c^{5/3} , \tag{41}$$

or

$$\theta_c = 0.9251 . \tag{42}$$

Finally, we have

$$\left.\begin{aligned} \rho_c &= 43.6\bar{\rho} , \\ T_c = T_0\theta_c &= 0.9251 \frac{\mu H}{k} \frac{GM}{R} , \\ P_c = \frac{k}{\mu H} \rho_c T_c &= 9.625 \frac{GM^2}{R^4} , \\ L &= 6.885 \times 10^{24} \frac{1}{\kappa_0} \frac{M^{5.5}}{R^{0.5}} \mu^{7.5} , \end{aligned}\right\} \tag{43}$$

where L, M, and R are expressed in the corresponding solar units.

[5] S. Chandrasekhar, *An Introduction to the Study of Stellar Structure*, p. 87, Chicago: University of Chicago Press, 1939.

5. *Conclusions.*—It is found that the convective core extends to a fraction 0.14 of the radius of the star and incloses 10.5 per cent of the mass. The march of ψ, λ, θ, and σ for this model is shown in Table 1 (see also Figs. 1, 2, and 3). Further, we notice that the constants of proportionality in equations (43) differ only slightly from those for the Cowling point-source model.

I wish to express my thanks to Dr. S. Chandrasekhar for suggesting this problem and for many helpful discussions.

ON THE CONTINUOUS ABSORPTION COEFFICIENT OF THE NEGATIVE HYDROGEN ION

S. CHANDRASEKHAR
Yerkes Observatory
Received June 25, 1945

ABSTRACT

In this paper it is shown that the continuous absorption coefficient of the negative hydrogen ion is most reliably determined by a formula for the absorption cross-section which involves the matrix element of the momentum operator. A new absorption curve for H^- has been determined which places the maximum at λ 8500 A; at this wave length the atomic absorption coefficient has the value 4.37×10^{-17} cm².

1. *Introduction.*—In earlier discussions[1] by the writer attention has been drawn to the fact that the continuous absorption coefficient of the negative hydrogen ion, evaluated in terms of the matrix element

$$\mu = \int \Psi_d^* (r_1 + r_2) \Psi_c \, d\tau \tag{1}$$

(where Ψ_d denotes the wave function of the ground state of the ion and Ψ_c the wave function belonging to a continuous state normalized to correspond to an outgoing electron of unit density), depends very much on Ψ_d in regions of the configuration space which are relatively far from the hydrogenic core. This has the consequence that the absorption cross-sections are not trustworthily determined if wave functions derived by applications of the Ritz principle are used in the calculation of the matrix elements according to equation (1). This is evident, for example, from Figure 1, in which we have plotted the absorption coefficients as determined by Williamson[2] and Henrich,[3] using wave functions of the forms

$$\Psi_d = \mathfrak{N} \, e^{-\alpha s/2} (1 + \beta u + \gamma t^2 + \delta s + \epsilon s^2 + \zeta u^2) \tag{2}$$

and

$$\left.\begin{aligned} \Psi_d = \mathfrak{N} \, e^{-\alpha s/2} (1 + \beta u + \gamma t^2 + \delta s + \epsilon s^2 + \zeta u^2 + \chi_6 t^4 + \chi_7 t^6 \\ + \chi_8 t^4 u^2 + \chi_9 t^2 u^2 + \chi_{10} t^2 u^4) \, , \end{aligned}\right\} \tag{3}$$

respectively. (In eqs. [2] and [3] $\mathfrak{N}$ is the normalizing factor; and α, β, γ, etc., are constants determined by the Ritz condition of minimum energy,

$$s = r_2 + r_1 \, , \qquad t = r_2 - r_1 \, , \qquad \text{and} \qquad u = r_{12} \, , \tag{4}$$

where r_1, r_2, and r_{12} are the distances of the two electrons from the nucleus and from each other, respectively.) The wide divergence between the two curves in Figure 1 is too large to be explained in terms of only the improvement in energy effected by the wave function (3): it must arise principally from the fact that in the evaluation of the matrix elements according to equation (1) parts of the wave function are used which do not contribute appreciably to the energy integral and are therefore poorly determined. Indeed, this sen-

[1] *Ap. J.*, **100**, 176, 1944; also *Rev. Mod. Phys.*, **16**, 301, 1944.

[2] *Ap. J.*, **96**, 438, 1942.

[3] *Ap. J.*, **99**, 59, 1944.

sitiveness of the derived absorption coefficients to wave functions effecting only relatively slight improvements in the energy makes it difficult to assess the reliability of the computed absorption coefficients. However, in this paper we shall show how these difficulties can be avoided by using a somewhat different formula for the absorption cross-section.

2. *Alternative formulae for evaluating the absorption coefficient.*—It is well known that in the classical theory the radiative characteristics of an oscillating dipole can be expressed in terms of either its dipole moment, its momentum, or its acceleration. There are, of course, analogous formulations in the quantum theory, the matrix element

$$(a \mid z_j \mid b) = \int \psi_a^* z_j \psi_b d\tau \tag{5}$$

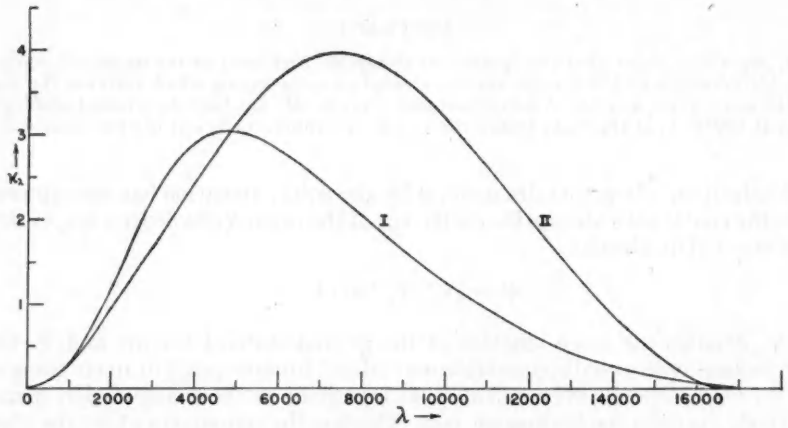

FIG. 1.—A comparison of the continuous absorption coefficient of H^- computed according to formula (I) and with wave functions of forms (2) (curve *I*) and (3) (curve *II*). The ordinates denote the absorption coefficients in units of 10^{-17} cm²; the abscissae, the wave length in angstroms.

for the co-ordinate z_j of the jth electron in an atom being simply related to the corresponding matrix element of the momentum operator or the acceleration. Thus, we have the relations

$$(a \mid z_j \mid b) = \frac{1}{(E_a - E_b)} \int \frac{\partial \psi_a^*}{\partial z_j} \psi_b d\tau = -\frac{1}{(E_a - E_b)} \int \psi_a^* \frac{\partial \psi_b}{\partial z_j} d\tau \tag{6}$$

and

$$(a \mid z_j \mid b) = \frac{1}{(E_a - E_b)^2} \int \psi_a^* \frac{\partial V}{\partial z_j} \psi_b d\tau \tag{7}$$

if all the quantities are measured in Hartree's atomic units and where E_a and E_b denote the energies of the states indicated by the letters a and b and where V denotes the potential energy arising from Coulomb interactions between the particles. More particularly for an atom (or ion) with two electrons, we have

$$\mu_z = \int \Psi_d^* (z_1 + z_2) \Psi_c d\tau , \tag{8}$$

$$\mu_z = -\frac{1}{(E_d - E_c)} \int \Psi_d^* \left(\frac{\partial}{\partial z_1} + \frac{\partial}{\partial z_2} \right) \Psi_c d\tau , \tag{9}$$

and

$$\mu_z = \frac{1}{(E_d - E_c)^2} \int \Psi_d^* \left(\frac{z_1}{r_1^3} + \frac{z_2}{r_2^3} \right) \Psi_c d\tau . \tag{10}$$

While the foregoing formulae are entirely equivalent to each other if Ψ_d abd Ψ_c are exact solutions of the wave equation, they are of different merits for the evaluation of μ_z if approximate wave functions are used. Thus, it is evident that formula (8) uses parts of the

configuration space, which are more distant than relevant, for example, in the evaluation of the energy; similarly, formula (10) uses the wave functions in regions much nearer the origin. It would appear that formula (9) is the most suitable one for the evaluation of μ_z, particularly when wave functions derived by applications of the Ritz principle are used. The calculations which we shall present in the following sections confirm this anticipation; but before we proceed to such calculations, it is useful to have the explicit formulae for the absorption cross-sections on the basis of equations (8), (9), and (10).

In ordinary (c.g.s.) units the standard formula for the atomic absorption coefficient κ_ν for radiation of frequency ν, in which an electron with a velocity v is ejected, is

$$\kappa_\nu = \frac{32\pi^4 m^2 e^2}{3h^3 c}\,\nu v\,|\int \Psi_d^*\,(z_1+z_2)\,\Psi_c\,d\tau\,|^2\,, \tag{11}$$

where m, e, h, and c have their usual meanings. (In writing eq. [11] it has been assumed that the electron is ejected in the z-direction; see eq. [15] below.) By inserting the numerical values for the various atomic constants equation (11) can be expressed in the form

$$\kappa_\nu = 8.561\times 10^{-19}\,(\nu_{\rm at} k\,|\,\mu_z\,|^2)\ {\rm cm}^2\,, \tag{12}$$

where k denotes the momentum of the ejected electron and $\nu_{\rm at}$ the frequency of the radiation absorbed, both measured in atomic units, and where, moreover, the matrix element μ_z has also to be evaluated in atomic units.

If I denotes the electron affinity (also expressed in atomic units)

$$4\pi\nu_{\rm at} = k^2 + 2I\,, \tag{13}$$

and depending on which of the formulae (8), (9), and (10) we use for evaluating κ_ν, we have

$$\kappa_\nu = 6.812\times 10^{-20} k\,(k^2+2I)\,|\int \Psi_d^*\,(z_1+z_2)\,\Psi_c\,d\tau\,|^2\,. \tag{I}$$

$$\kappa_\nu = 2.725\times 10^{-19}\,\frac{k}{(k^2+2I)}\left|\int \Psi_d^*\left(\frac{\partial}{\partial z_1}+\frac{\partial}{\partial z_2}\right)\Psi_c\,d\tau\right|^2, \tag{II}$$

and

$$\kappa_\nu = 1.090\times 10^{-18}\,\frac{k}{(k^2+2I)^3}\left|\int \Psi_d^*\left(\frac{z_1}{r_1^3}+\frac{z_2}{r_2^3}\right)\Psi_c\,d\tau\right|^2. \tag{III}$$

Finally, we may note that if λ denotes the wave length of the radiation measured in angstroms, then

$$\lambda = \frac{911.3}{k^2+2I}\,{\rm A}\,. \tag{14}$$

3. *The continuous absorption coefficient of* H^- *evaluated according to formula (III).*— As we have already indicated, in the customary evaluations of κ_ν according to formula (I) the relatively more distant parts of the wave function are used. It is evident that we shall be going to the opposite extreme in using the wave function principally only near the origin if we evaluate κ_ν according to formula (III). For this reason it is of interest to consider first the absorption coefficient as determined by this formula.

In evaluating κ_ν according to formula (III), we shall use for Ψ_d a wave function of form (3) and for Ψ_c a plane wave representation of the outgoing electron:

$$\Psi_c = \frac{1}{\sqrt{2\pi}}\,(e^{-r_1+ikz_2}+e^{-r_2+ikz_1})\,. \tag{15}$$

(In § 5 we refer to an improvement in Ψ_c which can be incorporated without much difficulty at this stage.) For Ψ_d and Ψ_c of forms (3) and (15) the evaluation of the matrix element

$$\int \Psi_d^*\left(\frac{z_1}{r_1^3}+\frac{z_2}{r_2^3}\right)\Psi_c\,d\tau \tag{16}$$

is straightforward, though it is somewhat involved. We find

$$\left.\begin{aligned}\int\Psi_d^*\left(\frac{z_1}{r_1^3}+\frac{z_2}{r_2^3}\right)\Psi_c d\tau = &-(2048\pi^3)^{1/2}\frac{\mathfrak{N}}{(1+a)^3}\frac{i}{k^2}\left[\sum_{j=-2}^{6} l_j\mathfrak{L}_j^{(a)}\right.\\ &\left.+\sum_{j=-2}^{3}\lambda_j\mathfrak{L}_j^{(1+2a)}-\tfrac{1}{30}\beta(1+a)^4\left\{\sum_{j=-1}^{3}a_jS_j^{(1+2a)}+\sum_{j=-1}^{3}b_jC_j^{(1+2a)}\right\}\right],\end{aligned}\right\}\quad(17)$$

where we have used the following abbreviations:

$$\left.\begin{aligned}\mathfrak{L}_j^{(p)} &= \int_0^\infty e^{-py}\left(k\cos ky-\frac{\sin ky}{y}\right)y^j dy && (j=-2,\,-1,\ldots..),\\ &= (j-1)!\rho^j\{j\rho k\cos[(j+1)\xi]-\sin j\xi\} && (j\geqslant 1),\\ &= \rho k\cos\xi-\xi && (j=0),\\ &= p\xi-k && (j=-1),\\ &= \frac{1}{2}\left(pk-\frac{\xi}{\rho^2}\right) && (j=-2).\end{aligned}\right\}\quad(18)$$

$$\left.\begin{aligned}S_j^{(p)} &= \int_0^\infty e^{-py}y^j\sin ky\,dy && (j=-1,\,0,\ldots..),\\ &= j!\rho^{j+1}\sin[(j+1)\xi] && (j=0,\,1,\ldots..),\\ &= \xi && (j=-1).\end{aligned}\right\}\quad(19)$$

and

$$\left.\begin{aligned}C_j^{(p)} &= \int_0^\infty e^{-py}y^j\cos ky\,dy = j!\rho^{j+1}\cos[(j+1)\xi] && (j=0,\,1,\ldots..),\\ &= \int_0^\infty e^{-py}(e^{ay}-\cos ky)\frac{dy}{y} = \log\left(\frac{p}{p-a}\,|\sec\xi|\right) && (j=-1).\end{aligned}\right\}\quad(20)$$

where

$$\rho=\frac{1}{(k^2+p^2)^{1/2}}\qquad\text{and}\qquad\xi=\tan^{-1}\frac{k}{p};\qquad(21)$$

and

$$\left.\begin{aligned}l_{-2} &= 4q^2\beta,\\ l_{-1} &= 1+q(\tfrac{1}{5}\beta+\delta)+12q^2(\gamma+\epsilon+\zeta)+360q^4(\chi_6+\chi_9)+20{,}160q^6(\chi_7+\chi_8+\chi_{10}),\\ l_0 &= (\delta+\beta)-6q(\gamma-\epsilon)-120q^3(2\chi_6+\chi_9)-5040q^5(3\chi_7+2\chi_8+\chi_{10}),\\ l_1 &= -\frac{\beta}{6q}+(\gamma+\epsilon+\zeta)+24q^2(3\chi_6+\chi_9)+120q^4(45\chi_7+21\chi_8+13\chi_{10}).\\ l_2 &= -\frac{\zeta}{3q}-4q(3\chi_6+2\chi_9)-40q^3(30\chi_7+13\chi_8+12\chi_{10})\\ l_3 &= (\chi_6+\tfrac{7}{3}\chi_9)+4q^2(45\chi_7+29\chi_8+21\chi_{10}).\\ l_4 &= -\frac{\chi_9}{3q}-2q(9\chi_7+12\chi_8+7\chi_{10}).\\ l_5 &= \chi_7+\tfrac{1}{3}^1(\chi_8+\chi_{10}).\\ l_6 &= -\frac{1}{3q}(\chi_8+2\chi_{10}).\end{aligned}\right\}\quad(22)$$

$$\left.\begin{aligned} \lambda_{-2} &= -4\beta q^2\,; & \lambda_1 &= \frac{\beta}{15q}\,, \\ \lambda_{-1} &= -\tfrac{6}{5}\beta q\,; & \lambda_2 &= -\frac{\beta}{30q^2}\,, \\ \lambda_0 &= -\tfrac{1}{5}\beta\,; & \lambda_3 &= \frac{\beta}{30q^3}\,, \end{aligned}\right\} \tag{23}$$

where

$$q = \frac{1}{1+a}\,; \tag{24}$$

and

$$\left.\begin{aligned} a_{-1} &= 6\eta^4\left[4\eta k^2(5a^4 - 10a^2k^2 + k^4) + (a^4 - 6a^2k^2 + k^4)\right], \\ a_0 &= 6\eta^3 a\left[16\eta k^2(a^2 - k^2) + (a^2 - 3k^2)\right], \\ a_1 &= 3\eta^2\left[4\eta k^2(3a^2 - k^2) + (a^2 - k^2)\right], \\ a_2 &= \eta a\,(8\eta k^2 + 1)\,, \\ a_3 &= \eta k^2\,, \end{aligned}\right\} \tag{25}$$

$$\left.\begin{aligned} b_{-1} &= +24\eta^4 ak\left[\eta(a^4 - 10a^2k^2 + 5k^4) - (a^2 - k^2)\right], \\ b_0 &= -6\eta^3 k\left[4\eta(a^4 - 6a^2k^2 + k^4) - (3a^2 - k^2)\right], \\ b_1 &= -6\eta^2 ak\left[2\eta(a^2 - 3k^2) - 1\right], \\ b_2 &= -\eta k\left[4\eta(a^2 - k^2) - 1\right], \\ b_3 &= -\eta ak\,. \end{aligned}\right\} \tag{26}$$

where

$$\eta = (a^2 + k^2)^{-1}\,. \tag{27}$$

Putting $\chi_6 = \chi_7 = \ldots = \chi_{10} = 0$ in the foregoing equations, we shall obtain the formulae which can be used with a wave function of form (2).

By using for the constants of wave functions (2) and (3) the values determined by Williamson and Henrich, the atomic absorption coefficient κ_ν has been computed according to the foregoing formulae for various wave lengths. The results of the calculations are given in Table 1 and are further illustrated in Figure 2. It is seen that, in contrast to what happened when formula (I) was used (cf. Fig. 1), wave function (2) now predicts systematically *larger* values for κ_ν than does wave function (3). The divergence between the two curves must now be attributed to the overweighting of the wave function near the origin, where it is again poorly determined by the Ritz method.

4. *The continuous absorption coefficient of* H^- *evaluated according to formula (II).*— Finally, returning to formula (II), which would appear to have the best chances for determining κ_ν most reliably, the calculations were again carried through for wave functions Ψ_d of forms (2) and (3) and for Ψ_c of form (15). Before we give the results of the calculations, we may note that for Ψ_d of form (3) and for Ψ_c of form (15)

$$\left.\begin{aligned} \int \Psi_d^* \left(\frac{\partial}{\partial z_1} + \frac{\partial}{\partial z_2}\right)\Psi_c\, d\tau = &-(2048\pi^3)^{1/2}\,\frac{\mathfrak{N}}{(1+a)^3}\,\frac{i}{k^2}\left[\sum_{j=-1}^{6} l_j \mathfrak{L}_j^{(a)}\right. \\ &\left. + \sum_{j=-1}^{+1} \lambda_j \mathfrak{L}_j^{(1+2a)} + k^2\left\{\sum_{j=0}^{7} s_j S_j^{(a)} + \sum_{j=0}^{+1} \sigma_j S_j^{(1+2a)}\right\}\right], \end{aligned}\right\} \tag{28}$$

TABLE 1

THE CONTINUOUS ABSORPTION COEFFICIENT OF H^- COMPUTED ACCORDING TO FORMULA III AND WITH WAVE FUNCTIONS OF FORMS (2) AND (3)

λ (A)	$\kappa_\lambda \times 10^{17}$ cm^2		λ (A)	$\kappa_\lambda \times 10^{17}$ cm^2	
	With Wave Function (3)	With Wave Function (2)		With Wave Function (3)	With Wave Function (2)
1000	0.225	0.241	7000	5.173	6.732
2000	0.955	1.010	7500	5.225	7.070
2500	1.459	1.538	8000	5.204	7.333
3000	2.010	2.125	8500	5.106	7.496
3500	2.580	2.752	9000	4.946	7.567
4000	3.139	3.400	9500	4.724	7.536
4500	3.657	4.046	10000	4.453	7.411
5000	4.118	4.676	12000	3.031	5.952
5500	4.505	5.271	14000	1.407	3.355
6000	4.812	5.820	16000	0.149	0.401
6500	5.036	6.310			

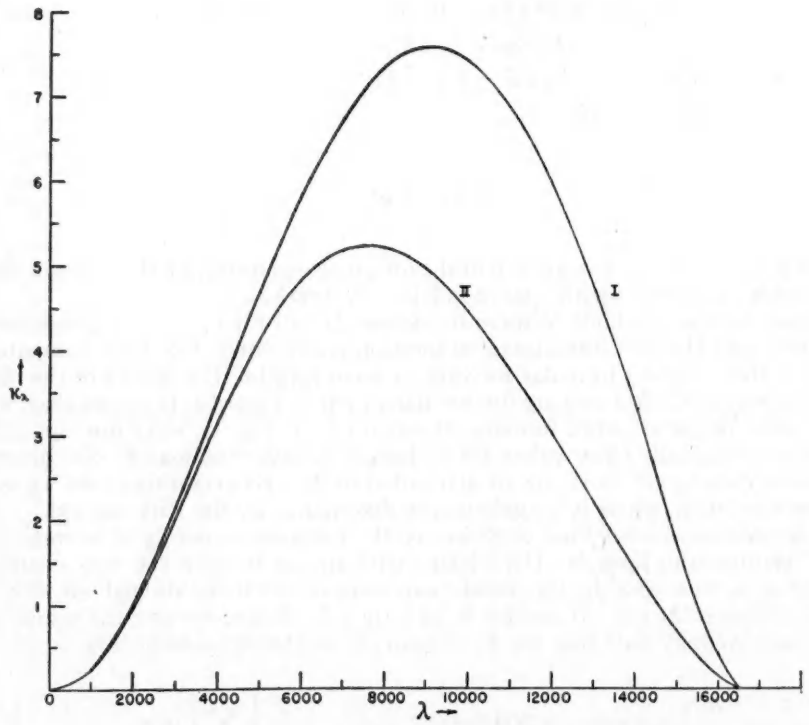

FIG. 2.—A comparison of the continuous absorption coefficient of H^- computed according to formula (III) and with wave functions of forms (2) (curve *I*) and (3) (curve *II*). The ordinates denote the absorption coefficients in units of 10^{-17} cm^2; the abscissae, the wave length in angstroms.

where

$$\left.\begin{aligned} l_{-1} &= 4\beta q^3\,; \quad l_0 = 0\,; \quad l_1 = -\beta q\,. \\ l_2 &= -2q\zeta - 40q^3\chi_9 - 1680q^5(\chi_8 + 2\chi_{10})\,. \\ l_3 &= 16q^2\chi_9 + 960q^4(\chi_8 + \chi_{10})\,. \\ l_4 &= -2q\chi_9 - 80q^3(3\chi_8 + 2\chi_{10})\,. \\ l_5 &= 32q^2(\chi_8 + \chi_{10})\,; \quad l_6 = -2q(\chi_8 + 2\chi_{10})\,, \end{aligned}\right\} \tag{29}$$

$$\lambda_{-1} = -4\beta q^3\,; \quad \lambda_0 = -4\beta q^2\,; \quad \lambda_1 = -\beta q\,, \tag{30}$$

$$\left.\begin{aligned} s_0 &= 4\beta q^2\,, \\ s_1 &= 1 + 3q\delta + 12q^2(\gamma+\epsilon+\zeta) + 360q^4(\chi_6+\chi_9) + 20{,}160q^6(\chi_7+\chi_8+\chi_{10})\,, \\ s_2 &= (\delta+\beta) - 6q(\gamma-\epsilon) - 120q^2(2\chi_6+\chi_9) - 5040q^5(3\chi_7+2\chi_8+\chi_{10})\,, \\ s_3 &= (\gamma+\epsilon+\zeta) + 24q^2(3\chi_6+\chi_9) + 120q^4(45\chi_7+21\chi_8+13\chi_{10})\,. \\ s_4 &= -6q(2\chi_6+\chi_9) - 80q^3(15\chi_7+6\chi_8+5\chi_{10})\,, \\ s_5 &= (\chi_6+\chi_9) + 4q^2(45\chi_7+21\chi_8+13\chi_{10})\,. \\ s_6 &= -6q(3\chi_7+2\chi_8+\chi_{10})\,. \\ s_7 &= \chi_7+\chi_8+\chi_{10} \end{aligned}\right\} \tag{31}$$

and

$$\sigma_0 = -4\beta q^2\,; \quad \sigma_1 = -\beta q\,. \tag{32}$$

Further, in equation (28) the quantities $\mathcal{Q}_i^{(p)}$, $S_i^{(p)}$, and q have the same meanings as in equations (18), (19), (21), and (24).

TABLE 2

THE CONTINUOUS ABSORPTION COEFFICIENT OF H^- COMPUTED ACCORDING TO FORMULA II AND WITH WAVE FUNCTIONS OF FORMS (2) AND (3)

λ (A)	$\kappa_\lambda \times 10^{17}$ cm²		λ (A)	$\kappa_\lambda \times 10^{17}$ cm²	
	With Wave Function (3)	With Wave Function (2)		With Wave Function (3)	With Wave Function (2)
1000.....	0.271	0.270	7000.....	4.174	4.113
2000.....	0.945	0.991	7500.....	4.296	4.080
2500.....	1.335	1.461	8000.....	4.363	3.993
3000.....	1.730	1.955	8500.....	4.372	3.858
3500.....	2.119	2.437	9000.....	4.324	3.682
4000.....	2.498	2.880	9500.....	4.221	3.471
4500.....	2.860	3.265	10000.....	4.065	3.233
5000.....	3.197	3.581	12000.....	2.995	2.108
5500.....	3.504	3.822	14000.....	1.502	0.954
6000.....	3.773	3.989	16000.....	0.167	0.097
6500.....	3.998	4.084			

The absorption cross-sections, as calculated according to formula (II), and the foregoing equations are given in Table 2 and further illustrated in Figure 3. It is seen that, as anticipated, the two curves now do not diverge more than can be reasonably attributed to the betterment of the wave function in consequence of the increased number of parameters used in the Ritz method.

5. *Concluding remarks.*—A comparison of Figures 1, 2, and 3 clearly illustrates the superiority of formula (II) for the purposes of evaluating the continuous absorption coefficient of the negative hydrogen ion. The general reliability of the absorption cross-

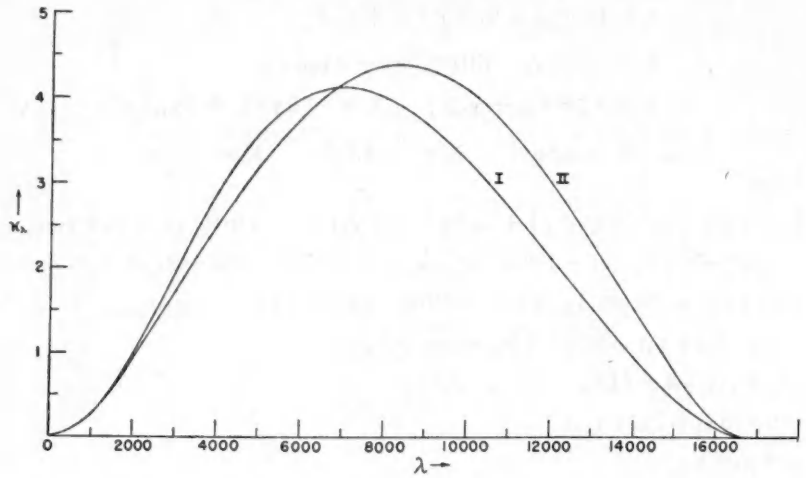

FIG. 3.—A comparison of the continuous absorption coefficient of H^- computed according to formula (II) and with wave functions of forms (2) (curve *I*) and (3) (curve *II*). The ordinates denote the absorption coefficients in units of 10^{-17} cm^2; the abscissae, the wave length in angstroms.

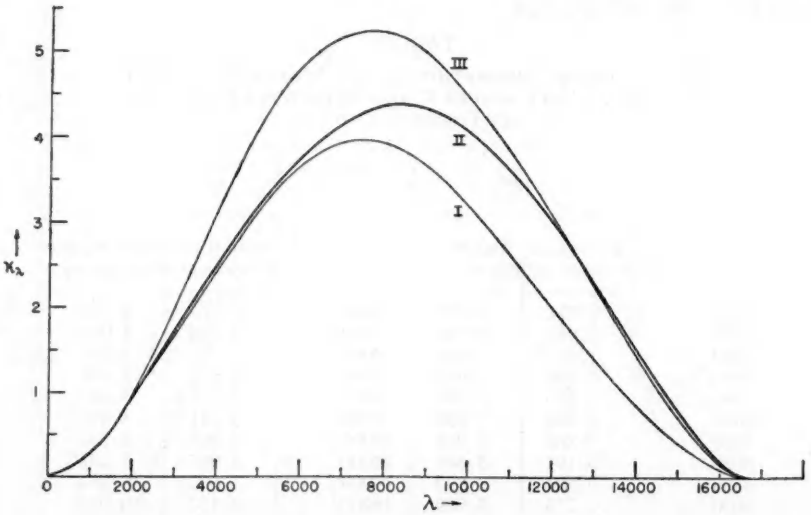

FIG. 4.—A comparison of the continuous absorption coefficient of H^- computed according to formulae (I) (curve *I*), (II) (curve *II*), and (III) (curve *III*) with a wave function of form (3). The ordinates denote the absorption coefficients in units of 10^{-17} cm^2; the abscissae, the wave length in angstroms.

sections derived on the basis of formula (II) and wave function (3) can be seen in another way. In Figure 4 we have plotted κ_ν as given by the three formulae and as obtained in each case with wave function (3). It is seen that, while the cross-sections given by formula (II) agree with those given by formula (I) in the visual and the violet part of the

spectrum ($\lambda < 6000$ A), they agree with those given by formula (III) in the infrared ($\lambda > 12{,}000$ A). This is readily understood when it is remembered that on all the three formulae the absorption cross-sections in the infrared are relatively more dependent on the wave function at large distances than they are in the visual and the violet parts of the spectrum. Accordingly, it is to be expected that, as we approach the absorption limit of H^- at 16,550 A, formula (III) must give less unreliable values than it does at shorter wave lengths; formula (I), of course, ceases to be valid in the infrared. It is also clear that, as we go toward the violet, we have the converse situation.

Summarizing our conclusions so far, it may be said that in the framework of the approximation in which a plane-wave representation of the outgoing electron is used, formula (II), together with wave function (3), gives sufficiently reliable values for the absorption coefficient over the entire range of the spectrum. Attention may be particularly drawn to the fact that the maximum of the absorption-curve is now placed at λ 8500 A, where $\kappa_\lambda = 4.37 \times 10^{-17}$ cm^2.

The question still remains as to the improvements which can be effected in the choice of Ψ_c. As shown in an earlier paper,[4] it may be sufficient to use for Ψ_c the wave functions in the Hartree field of a hydrogen atom. On this approximation we should use (*op. cit.*, eq. [15])

$$\Psi_c = \frac{1}{\sqrt{2\pi}} \left\{ e^{-r_1} \sum_{l=0}^{\infty} \frac{i^l}{k r_2} (2l+1) P_l(\cos \vartheta_2)\, \chi_l(r_2; k) + e^{-r_2} \sum_{l=0}^{\infty} \frac{i^l}{k r_1} (2l+1) P_l(\cos \vartheta_1)\, \chi_l(r_1; k) \right\}, \tag{33}$$

where χ_l is the solution of the equation

$$\frac{d^2\chi_l}{dr^2} + \left\{ k^2 - \frac{l(l+1)}{r^2} + 2\left(1+\frac{1}{r}\right) e^{-2r} \right\} \chi_l = 0, \tag{34}$$

which tends to a pure sinusoidal wave of unit amplitude at infinity. We shall return to these further improvements in a later paper.

It is a pleasure to acknowledge my indebtedness to Professor E. P. Wigner for many helpful discussions and much valuable advice. My thanks are also due to Mrs. Frances Herman Breen for assistance with the numerical work.

[4] *Ap. J.*, **100**, 176, 1944.

THE VELOCITY-CURVES OF SEVEN CEPHEID VARIABLES*

OTTO STRUVE
McDonald and Yerkes Observatories
Received July 14, 1945

ABSTRACT

The radial velocities of V386 Cygni, MW Cygni, VY Cygni, BZ Cygni, TX Cygni, SZ Cygni, and CD Cygni were determined from 113 McDonald Observatory spectrograms, taken in July and August, 1944. The curve for BZ Cyg departs markedly from that determined by Joy on the basis of observations made from 1934 to 1936.

In July and August, 1944, the Cassegrain spectrograph of the McDonald Observatory was used for observing seven faint Cepheid variables in Cygnus, selected by Bart J. Bok and F. J. Heyden of the Harvard Observatory for the purpose of determining the selective absorption in the direction of these stars. The spectral types were communicated to Father Heyden, and some of the astrophysical results secured from them have been discussed elsewhere.[1] The spectrograms have now been measured for radial velocity, and the results are presented in Table 4 and in Figure 1. All seven stars occur in Joy's paper on the "Radial Velocities of Cepheid Variable Stars."[2] For six of them he has given complete velocity-curves; for the seventh—V386 Cyg—he gave only four individual observations but did not represent them by a velocity-curve. The purpose of my new observations was to find whether any appreciable changes had taken place in the velocity-curves of these seven stars since the time of Joy's work.

The observations were obtained with two glass prisms and a 180-mm Schmidt camera, giving a linear dispersion of 76 A/mm at $H\gamma$. The slit was relatively wide, 0.2 mm, but this was reduced by the camera to a width of only 0.036 mm on the film. The star images were trailed over a slit length of 3 mm, so that the spectra were considerably widened. Table 1 gives the observing program. The ranges in photographic magnitude are from Joy's paper. The spectral types have been estimated on the McDonald films.

Table 2 gives a list of 21 standard stars, 39 plates of which were measured by Miss A. Johnson, Miss G. Peterson, or Mrs. M. Carlson. The measures were reduced in the usual way, except that no curvature corrections were applied. The result for each line was then subtracted from the standard radial velocity of the star, as given by Moore's catalogue of radial velocities,[3] and the corresponding corrections with their probable errors were applied to the adopted stellar wave lengths. Asterisks are used to designate those wave lengths which were actually measured in the Cepheids. The corrections are in several cases very large, and the wave lengths adopted differ appreciably from those commonly used. They are, however, best adapted to give results which are consistent with Moore's system of radial velocities.

The phases in Table 4 were computed with the elements given in the same table. The elements for V386 Cyg are due to Father Heyden. The second-order term for TX Cyg, given by Florja and Parenago, was neglected. The new velocity-curves of MW Cyg, VY Cyg, TX Cyg, and CD Cyg agree well with those of Joy, except that in the case of MW Cyg there is a slight horizontal shift in the two curves, suggesting that the period is a

* *Contributions from McDonald Observatory, University of Texas*, No. 112.

[1] Struve, *Observatory*, **65**, 269, 1944.

[2] *Ap. J.*, **86**, 363, 1937.

[3] *Pub. Lick Obs.*, **18**, 1932.

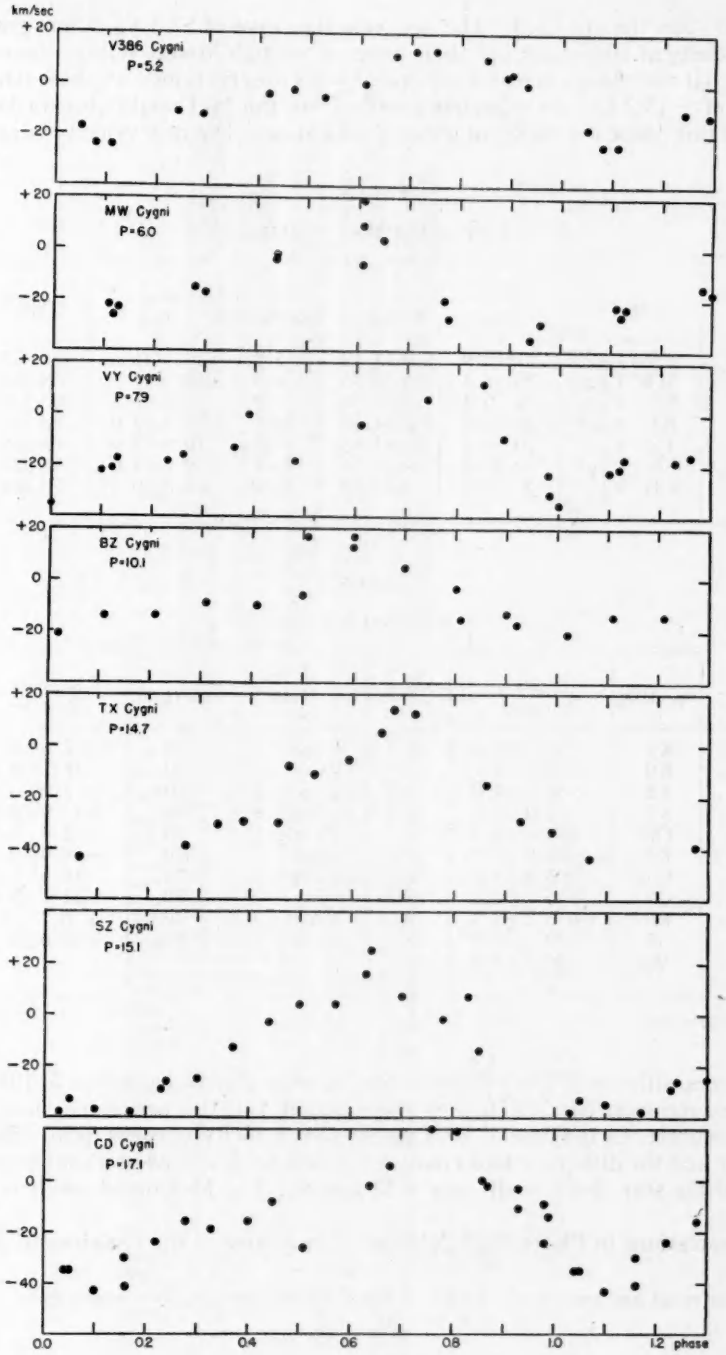

FIG. 1.—Velocity-curves of Cepheid variables

little longer than the one used.[4] The new velocity-curve of SZ Cyg differs greatly from Joy's, especially at maximum, but there were not enough Mount Wilson observations to be certain that the change is real. Only one of Joy's observations—at phase 0.676, giving a velocity of −15.2 km/sec—departs greatly from the McDonald observations, which suggest for this phase a velocity of about +15 km/sec. The new velocity-curve of V386

TABLE 1

LIST OF CEPHEID VARIABLES

No.	Star	α (1900)	δ (1900)	P (In Days)	Mag. Pg.	Sp.	No. of Spectrograms
1	V386 Cyg	$21^h10^m.9$	+41° 18′	5.2	10 –11	F5–G1	16
2	MW Cyg	20 8.4	+32 35	6.0	10 –11	F8–G1	15
3	VY Cyg	21 0.4	+39 34	7.9	10.1–11.3	F6–G1	15
4	BZ Cyg	20 42.6	+44 56	10.1	11.2–12.0	F8–G5	14
5	TX Cyg	20 56.4	+42 12	14.7	10.5–12.4	F5–G6	14
6	SZ Cyg	20 29.6	+46 16	15.1	9.7–11.0	F8–G8	17
7	CD Cyg	20 0.6	+33 50	17.1	9.0–10.5	F8–K0	22

TABLE 2

STANDARD STARS

Name	Sp. (HD)	Standard Velocity	No. of Plates	Name	Sp. (HD)	Standard Velocity	No. of Plates
δ And	K2	− 7.1±0.3	1	α Aqr	G0	+ 7.6±0.1	1
α Cas	K0	− 3.8±0.1	3	ζ Cep	K0	−18.1±0.2	3
α Tau	K5	+54.1±0.0	3	1 Lac	K0	− 7.9±0.3	2
γ Aql	K2	− 2.0±0.1	2	μ Peg	K0	+13.9±0.3	1
γ Cyg	F8p	− 7.6±0.2	2	ι Cep	K0	−12.4±0.2	1
ξ Cyg	K5	−19.9±0.9	2	56 Peg	K0	−26.9±0.4	1
ζ Cap	G5p	+ 3.0±0.3	2	π Cep	G5	−19.6*	1
β Aqr	G0	+ 6.7±0.1	2	ν Peg	G0	−11.5±0.6	1
ϵ Peg	K0	+ 5.2±0.3	3	λ And	K0	+ 6.7*	1
9 Peg	G5	−22.7±0.2	3	ρ Cas	F8p	−42.6±0.3	3
μ Cep	Ma	+20.5±1.0	1				

* Spectroscopic binary.

Cyg disagrees with one of Joy's observations, namely, that of December 5, 1936, after his phases were recomputed with Heyden's new period. But this period may not yet be sufficiently accurate. In the case of BZ Cyg the new velocity-curve is quite different from that of Joy and the difference looks real: it can best be described as a change in the mean velocity of the star. Joy's result was −17 km/sec. The McDonald result is about −4 km/sec.

The illustrations in Plates XVI–XIX give the phases of the variables in days.

[4] A similar result has been obtained by F. J. Heyden from Harvard photometric data.

PLATE XVI

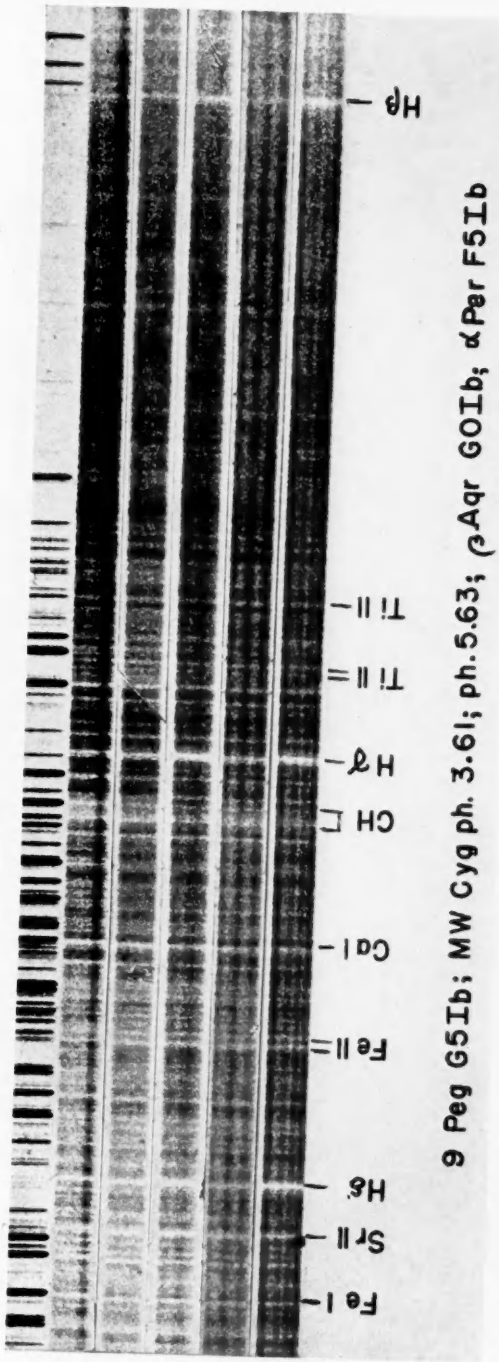

9 Peg G5Ib; MW Cyg ph. 3.61; ph.5.63; ρAqr GOIb; αPer F5Ib

PLATE XVII

9 Peg G5Ib; BZ Cyg ph. 7.15; ph. 9.28; βAqr G0Ib;

αPer F5Ib.

PLATE XVIII

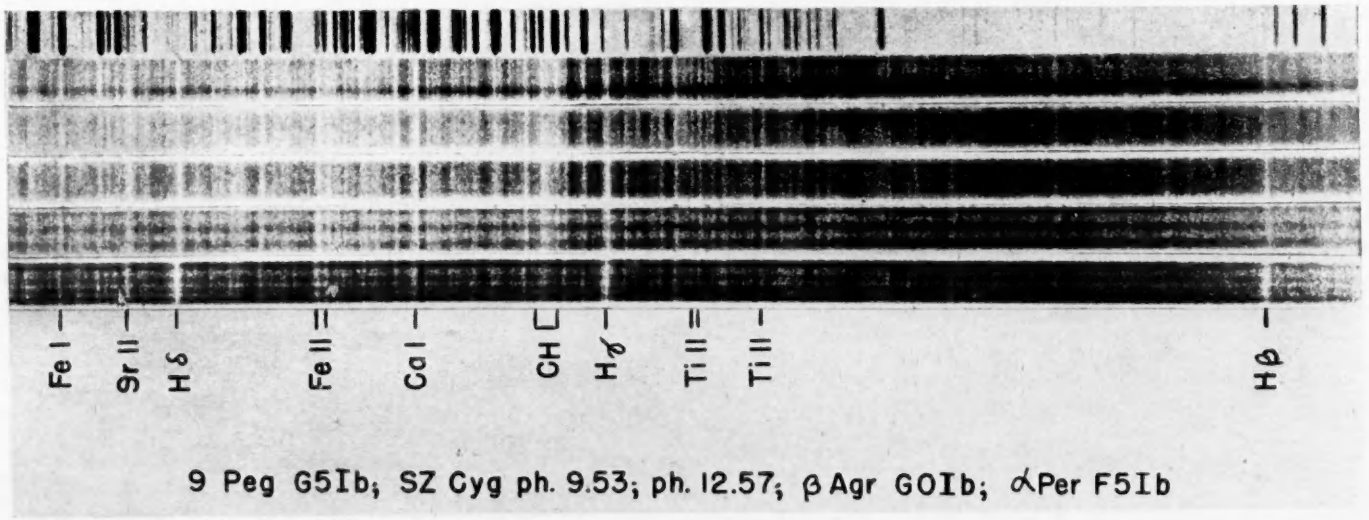

9 Peg G5Ib; SZ Cyg ph. 9.53; ph. 12.57; β Agr G0Ib; α Per F5Ib

PLATE XIX

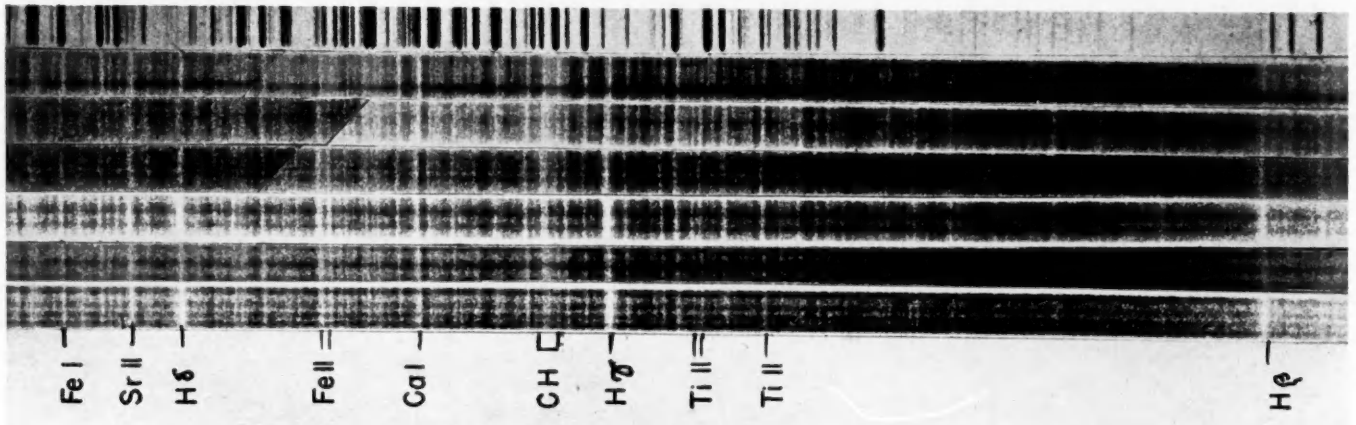

9 Peg G5Ib; CD Cyg ph. 13.76; ph. 15.83; ph. 16.84; β Aqr GOIb;
α Per F5Ib.

TABLE 3

WAVE LENGTHS OF STAR LINES

Preliminary Wave Length	No.	Δλ	Revised Wave Length	P.E.	Note
3997.24	19	+0.70	3997.94 A	±0.05 A	
4005.25	46	+0.42	4005.67	.03	*
4045.82	51	−0.04	4045.78	.02	*
4063.60	52	+0.12	4063.72	.02	*
4067.04			4067.04		†
4071.75	55	+0.19	4071.94	.02	*
4077.71	49	−0.19	4077.52	.02	*
4101.74	49	−0.16	4101.58	.04	*
4127.92	9	+0.50	4128.42	.11	
4143.87	62	−0.40	4143.47	.02	*
4171.90	45	+1.13	4173.03	.04	*
4178.34			4178.34		†
4198.31	14	+0.27	4198.58	.08	
4202.03	28	+0.32	4202.35	.08	
4215.52	69	+0.06	4215.58	.02	*
4226.73	62	+0.10	4226.83	.02	*
4233.16	53	+0.09	4233.25	.03	*
4246.84	30	+0.23	4247.07	.03	
4254.34	44	+0.50	4254.84	.03	
4290.22	67	+0.10	4290.32	.03	*
4314.09	50	+0.46	4314.55	.02	*
4325.77	70	0.00	4325.77	.02	*
4340.47	61	+0.01	4340.48	.03	*
4351.77	73	+0.18	4351.95	.02	*
4374.46	68	+0.61	4375.07	.02	
4383.55	75	+0.60	4384.15	.02	*
4395.05	36	+0.14	4395.19	.03	*
4400.38	44	−0.03	4400.35	.03	*
4404.75	44	+0.26	4405.01	.03	
4415.16	56	+0.49	4415.65	.03	
4435.01	49	+0.34	4435.35	.02	
4443.80	50	−0.69	4443.11	±0.04	*

* Used in Cepheids, as revised.

† Used in Cepheids but not measured in standard stars.

TABLE 4

RADIAL VELOCITIES OF CEPHEID VARIABLES

PLATE G f/2	DATE 1944	U.T.	JD 2431+	PHASE (IN P)	VEL. (IN KM/SEC)
	V386 Cygni Max. = JD 2428066.70 + 5d273661 E				
4549	July 25	11:00	296.96	0.527	− 4.8
56	26	10:30	297.94	.713	+13.1
68	27	10:42	298.95	.904	+ 4.2
78	28	9:43	299.90	.085	−23.7
90	29	11:12	300.97	.288	−12.2
97	30	10:49	301.95	.474	− 1.8
4608	31	11:00	302.96	.666	+10.9
17	Aug. 1	10:29	303.94	.851	+10.2
30	2	11:12	304.97	.046	−16.6
37	3	11:15	305.97	.235	−11.2
42	4	10:12	306.92	.415	− 4.0
50	5	10:48	307.95	.611	+ 0.2
74p	11	11:18	313.97	.753	+12.9
79	12	9:19	314.89	.927	− 0.3
90	13	9:12	315.88	.114	−23.5
4712	17	11:10	319.97	0.889	+ 2.6
	MW Cygni Max. = JD 2425173.40 + 5d9550 E				
4534p	July 21	7:40	292.82	0.611	+ 9.1
37p	23	9:14	294.88	.957	−28.8
51	26	5:35	297.73	.435	− 4.3
63	27	6:02	298.75	.606	− 5.8
73	28	5:54	299.75	.774	−19.7
85	29	6:31	300.77	.945	−34.6
92	30	5:57	301.75	.111	−22.2
4603	31	5:29	302.73	.275	−15.3
13	Aug. 1	5:33	303.73	.443	− 1.5
25	2	5:32	304.73	.611	+19.4
32	3	5:33	305.73	.779	−26.6
45	5	5:39	307.74	.116	−26.5
69	11	6:28	313.77	.129	−22.6
77	12	7:06	314.80	.302	−17.1
97	14	8:34	316.86	0.648	+ 4.2
	VY Cygni Max. = JD 2423497.14 + 7d856956 E				
4555	July 26	9:24	297.89	0.846	+11.6
67	27	9:41	298.90	.975	−31.4
77	28	8:44	299.86	.097	−22.4
89	29	10:26	300.93	.233	−18.0
96	30	9:59	301.92	.359	−12.9
4607	31	9:55	302.91	.485	−18.0
16	Aug. 1	9:16	303.89	.610	− 3.7
29	2	10:13	304.93	.742	+ 5.9
40	4	7:56	306.83	.984	−22.7
49	5	9:43	307.90	.121	−20.7
73	11	10:25	313.93	.888	− 9.0
78	12	8:10	314.84	.004	−34.6
89	13	8:26	315.85	.132	−16.9
96	14	7:32	316.81	.255	−16.2
4701	15	9:23	317.89	0.392	− 0.3

TABLE 4—*Continued*

PLATE G *f*/2	DATE 1944	U.T.	JD 2431+	PHASE (IN *P*)	VEL. (IN KM/SEC)
	BZ Cygni Max. = JD 2426674.10 + 10d1416 E*				
4553	July 26	7:25	297.81	0.915	−17.2
65	27	7:43	298.82	.015	−21.2
76	28	7:36	299.82	.113	−13.6
87	29	8:13	300.84	.214	−14.4
94	30	7:48	301.82	.311	− 9.1
4605	31	7:26	302.81	.408	−10.2
15	Aug. 1	7:57	303.83	.509	+16.7
27	2	7:33	304.81	.605	+16.8
34	3	7:46	305.82	.705	+ 5.0
41	4	9:04	306.88	.810	−14.8
47	5	7:39	307.82	.902	−13.2
71	11	8:18	313.85	.497	− 5.8
80	12	9:17	314.89	.600	+13.1
99	14	11:09	316.96	0.804	− 3.3
	TX Cygni Max. = JD 2422290.94 + 14d70791 E				
4554	July 26	8:50	297.87	0.387	−28.9
66	27	8:40	298.86	.454	−29.4
79	28	10:43	299.95	.528	−11.2
88	29	9:21	300.89	.592	− 4.8
95	30	8:59	301.87	.659	+ 4.7
4606	31	8:42	302.86	.726	+12.3
28	Aug. 2	8:52	304.87	.863	−15.3
35	3	8:58	305.87	.931	−29.2
39	4	7:01	306.79	.993	−32.8
48	5	8:48	307.87	.067	−43.4
61	8	9:34	310.90	.273	−39.0
64	9	7:28	311.81	.335	−30.1
72	11	9:23	313.89	.476	− 7.9
98	14	9:50	316.91	0.681	+13.9
	SZ Cygni Max. = JD 2426399.22 + 15d111056 E				
4535p	July 21	9:13	292.88	0.846	−13.7
39	24	11:00	295.96	.050	−33.4
52	26	6:24	297.77	.170	−38.4
64	27	6:56	298.79	.238	−25.9
75	28	6:46	299.78	.303	−24.9
86	29	7:16	300.80	.371	−13.2
93	30	6:46	301.78	.435	− 3.3
4604	31	6:21	302.76	.500	+ 4.0
14	Aug. 1	6:34	303.77	.567	+ 3.6
26	2	5:28	304.73	.631	+15.6
33	3	6:43	305.78	.700	+ 7.1
43	4	11:09	306.96	.778	− 2.0
46	5	6:33	307.77	.832	+ 6.7
59	8	5:35	310.73	.028	−37.9
63	9	5:41	311.74	.095	−36.9
70	11	7:18	313.80	.231	−28.7
4711	17	9:41	319.90	0.635	+24.6

TABLE 4—*Continued*

Plate G *f*/2	Date 1944	U.T.	JD 2431+	Phase (in *P*)	Vel. (in Km/Sec)
	CD Cygni Max. = JD 2421501.04 + 17^d.071343 E				
4538	July 24	9:54	295.91	0.761	+19.5
50	26	4:39	297.69	.865	− 0.4
62	27	5:24	298.72	.926	−11.1
72	28	5:22	299.72	.984	−23.9
74	28	6:20	299.76	.986	−14.0
84	29	6:01	300.75	.045	−35.2
91	30	5:32	301.73	.102	−42.7
4602	31	4:57	302.71	.159	−30.0
12	Aug. 1	5:00	303.71	.218	−24.2
24	2	5:01	304.71	.277	−16.2
31	3	4:43	305.70	.334	−18.7
38	4	6:27	306.77	.397	−15.8
44	5	5:03	307.71	.452	− 8.4
58	6	6:19	308.76	.514	−25.6
60	8	7:56	310.83	.635	− 2.5
62	9	4:37	311.69	.685	+ 5.5
68	11	5:47	313.74	.806	+19.0
76	12	6:22	314.77	.866	− 2.1
88	13	7:42	315.82	.927	− 3.0
95	14	6:51	316.79	.984	− 9.2
4700	15	7:53	317.83	.045	−35.2
10	17	8:16	319.84	0.163	−40.9

* An improved period of 10.14122 days was published by Soloviev after the completion of this paper (*Astr Circ. Ac. Sc. Soviet Union*, No. 38, 1945).

PHYSICAL PROCESSES IN GASEOUS NEBULAE

XVIII. THE CHEMICAL COMPOSITION OF THE PLANETARY NEBULAE

LAWRENCE H. ALLER[1] AND DONALD H. MENZEL[2]
Harvard College Observatory
Received June 4, 1945

ABSTRACT

Bowen and Wyse's conclusion that the chemical composition of the planetary nebulae is essentially the same as that of the sun is substantiated by a more detailed treatment of the same problem in which an attempt has been made to estimate the relative abundances of the lighter elements. For hydrogen, helium, and carbon, which are represented only by permitted lines of the recombination spectrum, we have estimated mean relative abundances of 1000, 100, and 0.6. The abundance of hydrogen follows from the intensity of the continuous spectrum at the limit of the Balmer series. An estimate of the abundance of ionized helium is provided by the observed line intensities and the theory given by Goldberg. The singlets are stronger than they should be, according to Goldberg's theory; and we may interpret the discrepancies between observations and theory by supposing that collisional excitations and de-excitations of the atoms in the high 2^3S and 2^1S metastable levels play a role in fixing the population of the high-energy levels. The abundances of the *C* III and *C* IV ions have been evaluated from the recombination lines of *C* II and *C* III with the aid of approximate wave functions calculated by Slater's rules and of *b*-factors estimated from the hydrogenic case. The *O* III abundance in NGC 7009, as estimated from the *O* II recombination lines, appears to agree with that found from the green nebular lines, thus removing the discrepancy suggested by Wyse.

We have estimated the abundances of the other ions from their forbidden lines and, with the exception of *O* III, from approximate collisional cross-sections. To calculate the numbers of atoms of any kind, we must make some estimate of their distribution among various stages of ionization. This step, which has to be made empirically, seems to introduce the greatest share of the uncertainty in the final results. The average abundances of nitrogen, oxygen, fluorine, neon, sulphur, chlorine, and argon are found to be 0.2, 0.25, 0.0001, 0.01, 0.036, 0.002, and 0.0015, respectively—all on the basis of hydrogen as 1000. Comparisons with the compositions of the solar atmosphere and that of τ Scorpii are discussed. It was not possible to estimate the contribution of the metals. The possible effects of stratification and of the bright-line radiation of the central star are briefly discussed.

I. INTRODUCTION

Perhaps one of the most difficult of astrophysical problems is the determination of the absolute abundances of the various elements composing a planetary nebula. To some extent this difficulty arises from the different mechanisms by which the nebular radiations are produced. Thus, atoms represented by forbidden lines are favored by a factor of a thousand fold over those that show only permitted (recombination) lines. To a greater extent uncertainties arise from the fact that only one ion of a given element may be observable while the nonobservable ions may be in the majority.

In previous papers of this series[3] we have shown how to derive the abundances of hydrogen ions and *O* III ions in planetary nebulae from intensity measures of the Balmer and green nebular lines. The results indicate about ten thousand times as many hydrogen ions as *O* III ions in the planetary nebulae, despite the fact that the green nebular lines (N_1 and N_2) are often of the order of ten times as strong as $H\beta$.

[1] Now of Indiana University, Bloomington, Indiana.

[2] Now serving as lieutenant commander, United States Navy, on leave of absence from Harvard University.

[3] Series of papers entitled "Physical Processes in Gaseous Nebulae" appearing in the *Astrophysical Journal:* I, **85**, 330, 1937; II, **86**, 70, 1937; III, **88**, 52, 1938; IV, **88**, 313, 1938; V, **88**, 423, 1938; VI, **89** 587, 1939; VII, **90**, 271, 1939; VIII, **90**, 601, 1939; IX, **91**, 307, 1940; X, **92**, 408, 1940; XI, **93**, 178, 1941; XII, **93**, 195, 1941; XIII, **93**, 230, 1941; XIV, **93**, 236, 1941; XV, **93**, 244, 1941; XVI, **94**, 30, 1941; XVII, **94**, 436, 1941. The papers of this series are referred to in the text as papers I, II, III, etc.

The estimation of the abundances of the other ions from their spectral lines is a much more difficult problem. In the first place, with the exception of neutral and ionized helium, we have only rough guesses of the transition probabilities of the permitted lines of the various ions observed in the gaseous nebulae. Reasonably good transition probabilities are available from recent calculations[4] for most of the forbidden lines. So far, cross-sections for the collisional excitation of forbidden lines are available only for *O* III. The theory of the statistical equilibrium of low-lying metastable levels presents no essential difficulties. The number of such levels is small; and one can solve for the populations in the various levels in terms of the collisional cross-sections, the transition probabilities, and the temperatures and densities of the electron gas. We possess fair estimates of all the quantities but the cross-sections. If we can get some idea of the latter, we can work out the relative abundances of the various types of ions.

The next section of this paper will be devoted to estimates of the target areas for the excitation of metastable levels and to the application of these target areas in connection with transition probabilities of the forbidden lines and the appropriate equations of statistical equilibrium to calculations of ionic abundances. Once the target areas have been agreed upon, the calculation of ionic abundances proceeds as in the case of *O* III.

The third section considers the recombination spectra of ionized carbon, ionized oxygen, and helium. Here, again, necessary atomic parameters are not known except for helium, and the transition probabilities of permitted lines have been estimated with the aid of the *LS*-coupling hypothesis and radial quantum integrals derived with the aid of Slater's rules.[5] The abundance of *O* III in NGC 7009, estimated from the recombination *O* II lines, agrees well with that estimated from the green nebular lines, thus removing the discrepancy suggested by Wyse.[6]

The fourth section of the paper is concerned with the problem of ionization in a planetary nebula subjected to radiation from a hot central star. The simultaneous appearance of ions representing a considerable range in ionization potential shows that it is not possible to explain the planetary nebulae as shells of gas exposed to black-body radiation. Stratification of the nebular layers, the filamentary structure exhibited by many planetaries and suspected in most of them, combined with the probable bright-line character of the ultraviolet spectrum of the central star—all conspire to introduce considerable complexities into the problem.

Finally, from the calculated abundances of the various ions we estimate the actual abundances of the various elements that make up the planetary nebula. Since we observe only one or two stages of ionization for most elements, we have to estimate the contribution to the total from the unobserved lines. An empirical procedure seems best here; and the method actually employed introduces the assumption that the ratio of the abundance of the ions in successive stages of ionization—e.g., the ratio of *O* II/*O* III, *Ne* III/*Ne* IV, etc.—depends only on the ionization potentials involved and not at all on the type of ion. From such ratios, for a given nebula, curves giving the estimated distribution of the atoms in various stages of ionization may be constructed; and it is with the aid of these curves that the final abundances are estimated.

That the above procedure introduces an appreciable uncertainty in the estimated composition of the nebula is obvious enough, but the difficulty that one encounters here is fundamental. Only a few of the ions of each kind of atom are observed, and we must extrapolate somehow to take account of the others. Further observations and identifications of fainter lines will help us here. Especially desired are observations or identifications of ions of higher ionization potential than *Ne* V, so that we may estimate, with a higher degree of certainty than is possible at present, the proportion of very highly ionized atoms.

[4] Pasternack, *Ap. J.*, **92**, 129, 1940; see also Paper XI of series.

[5] Slater, *Phys. Rev.*, **57**, 36, 1930.

[6] *Ap. J.*, **95**, 356, 1942.

In the end it turns out, as Bowen and Wyse have suggested,[7] that the composition of the planetary nebulae is essentially the same as that of the sun. More accurately, it would be better to word the result as follows: A mass of gas, similar in composition to the sun and expanded to the size and density of a planetary nebula and exposed to dilute high-temperature radiation, would give exactly the same kind of a spectrum as the planetaries are observed to give, in so far as our present knowledge of atomic structure and absorption coefficients permit us to predict. Wyse and Bowen's conclusion is confirmed by this independent and more detailed theoretical treatment of the problem.

II. ABUNDANCES OF IONS ESTIMATED FROM THEIR FORBIDDEN LINES

The method of evaluating ionic abundances from the intensities of their forbidden lines is well illustrated by the case of *O* III, which has been treated in a previous paper.[8] The additional data needed were the electron temperature and density. If the latter could be calculated from the intensity of the Balmer continuum at the series limit, the former could be found from the ratio of λ 4363 to the green nebular lines.

The application of these theoretical considerations to any ion possessing a ground configuration with metastable terms is straightforward. Let A denote the ground level of the ion and B the upper level of the observed transition AB. The number of collisional excitations from A to B will be given by

$$\mathfrak{F}_{AB} = 8.54 \times 10^{-6} \frac{N_A N_e}{T_e^{1/2}} \frac{\Omega(AB)}{\varpi_A} e^{-\chi_{AB}/kT}, \tag{1}$$

and the number of collisions of the second kind (superelastic collisions) will be

$$\mathfrak{F}_{BA} = 8.54 \times 10^{-6} \frac{N_B N_e}{T_e^{1/2}} \frac{\Omega(AB)}{\varpi_B}, \tag{2}$$

where χ is the excitation potential of B with respect to A, where $\tilde{\omega}_A$ and $\tilde{\omega}_B$ are, respectively, the statistical weights of levels A and B, and where $\Omega(AB)$ is the target area factor to be calculated by wave mechanics.

Our present discussion is confined to transitions arising between the terms of the ground p^2, p^3, and p^4 configurations. The formulae of papers XIII and XVI of this series may be applied immediately to a discussion of the p^2 and p^4 configurations. For the statistical equilibrium of the p^3 configuration we shall derive slightly modified expressions.

Unfortunately, target areas for the collisional excitation of ions other than *O* III are not available, so that we have had to resort to an approximate treatment of the problem. Accordingly, rough target areas have been estimated according to the following scheme:

1. The target areas for a p^4 configuration are taken to be the same as for a p^2 configuration. In this approximation *Ne* III has the same cross-section as *O* III.

2. For a p^3 configuration the ratio $\Omega_{AB}/\tilde{\omega}_A\tilde{\omega}_B$ is taken as a constant for all transitions. (Within a factor of 2 this condition is fulfilled for *O* III.) For *O* II we have arbitrarily taken $\Omega = 10$ for the $^4S - {}^2D$ transition and $\Omega = 15$ for the $^2D - {}^2P$ auroral transition.

Thus the target areas for the p^2 and p^4 configurations are all taken to be the same as those of *O* III. Admittedly, this approximation is a crude one, but we suspect it will give the correct order of magnitude. The target areas are taken to be independent of Z in this treatment, although we have also carried out a calculation in which we have supposed the target area to be proportional to Z^2 for the larger values of Z. It seems very unlikely that the dependence on Z can be as severe as Z^2, but the effect of Z on the target area is

[7] *Lick Obs. Bull.*, **19**, 1, 1939.

[8] See Paper XVI. Equations are referred to by number and paper; thus XII-7 means eq. (7) of Paper XII of the nebular series.

very difficult to see until further calculations have been made. For the main discussion we shall neglect any variation of Ω with Z but shall occasionally refer to the results of the earlier calculations in which it was supposed that Ω was proportional to Z^2. The values of Ω computed from the above approximation are collected in Table 1.

TABLE 1*

ATOMIC PARAMETERS FOR THE CALCULATION OF ABUNDANCES FROM FORBIDDEN LINES

NEBULAR TRANSITIONS

Ion	Config.	χ	ν_0/ν	ΣA	j
N II	p^2	1.89	1.31	0.0030	0.086×10^3
F II	p^4	2.58	0.956	.064	1.87
Ne III	p^4	3.19	0.776	.275	8.05
S III	p^2	1.33	1.88	.092	2.69
F IV	p^2	3.07	0.808	.109	3.19
Cl IV	p^2	1.59	1.56	.28	8.20
Ne V	p^2	3.69	0.672	.42	12.3
A V	p^2	1.92	1.29	0.73	21.4

AURORAL TRANSITIONS

Ion	Config.	χ	$\lambda/4363$	A_{8D}	f
N II	p^2	4.04	1.315	2.2	0.99
S III	p^2	3.32	1.411	5.6	.86
Cl IV	p^2	4.00	1.216	6.6	0.71

NEBULAR TRANSITIONS

Ion	Config.	χ	ν_0/ν	$\bar{A}$	ξ
O II	p^3	3.31	0.75	0.00008	9.13
Cl III	p^3	2.23	1.11	.0042	491
S II	p^3	1.84	1.35	.0014	164
A IV	p^3	2.62	0.95	0.0136	1590

TRANSAURORAL TRANSITION

Ion	Config.	χ	$\bar{A}$	ξ
S II	p^3	3.04	0.26	5×10^4

* The target area $\Omega = 10$ for nebular transitions in p^3 and $\Omega = 6$ for the transauroral transition.

Let us first turn our attention to the nebular $^3P - {}^1D$ transitions in p^2 or p^4 configurations. The relation between the number of atoms in the ^3P term and the surface brightness H_n (in magnitudes per square minute of arc) of the nebular images may be written in the form analogous to XVI-6:

$$N_P = 3.36\times10^{19}\frac{T_e^{1/2}e^{\chi/kT_e}}{N_e D(1-\beta)}(2.512)^{-H_n}\frac{\Omega_0}{\Omega}\frac{\nu_0}{\nu} = C\frac{T_e^{1/2}}{N_e}\frac{e^{\chi_{PD}/kT_e}}{D(1-\beta)}(2.512)^{-H_n}, \quad (3)$$

where C is a constant that depends on the ion involved, the target area, and the frequency; where χ_{PD} is the excitation potential of the ^1D level, D depends on the thickness of the nebular shell and its outer radius A, in accordance with the expression

$$D = 3d\left(1 - \frac{d}{A} + \frac{d^2}{3A^2}\right) \tag{4}$$

(cf. XII-7); and where β is the fraction of atoms excited to the ^1D level that are collisionally de-excited. It is given by

$$\beta = \frac{\mathfrak{F}_{DP}}{\mathfrak{F}_{DP} + F_{DP}} = \frac{1}{1 + \dfrac{\Sigma A_{DP_i}}{3.42 \times 10^{-5}} \dfrac{T_e^{1/2}}{N_e} \dfrac{\Omega_0}{\Omega}} = \frac{1}{1 + \dfrac{jT_e^{1/2}}{N_e}}, \tag{5}$$

defining j. Here $\mathfrak{F}_{DP}$ represents the number of collisional de-excitations of the ^1D level (superelastic collisions) and F_{DP} the number of radiative transitions; Ω_0 denotes the target area for the nebular transition in the O III atom. If we write the abundance of the O III ion as (cf. XVI-6)

$$N_0 = 3.38 \times 10^{19} \frac{T_e^{1/2} e^{\chi_0/kT_e}}{N_e D(1-\beta_0)} (2.512)^{-H_0} \tag{6}$$

and recall that the last factor is simply proportional to the sum of the intensities of the two forbidden lines, we obtain for the ratio of the abundance of any ion, p, to that of doubly ionized oxygen

$$\frac{N_p}{N_0} = \frac{I_p}{I_0} \frac{\nu_0}{\nu} e^{(\chi - \chi_0)/kT_e} \frac{(1-\beta_0)}{(1-\beta)} \frac{\Omega_0}{\Omega}, \tag{7}$$

where the subscript zero refers to the data for the O III atom and the green nebular lines.

Likewise for the auroral transition in the O III atom, one may write a similar expression (cf. Paper XIII) by noting that in this case the ^1S level is fed almost entirely by collisional excitations from the ground level. Of the atoms entering the ^1S level, the fraction $f = A_{SD}/(A_{SD} + A_{SP})$ goes to produce the auroral line, provided the collisional de-excitation of the ^1S level is negligible in comparison with the radiative de-excitations. Hence we may write an expression of the form

$$N_P = 1.65 \times 10^{20} \frac{e^{\chi_{PS}/kT_e}}{Df} \frac{\Omega_0}{\Omega} \frac{\lambda}{4363} \frac{T_e^{1/2}}{N_e} (2.512)^{-H_n}, \tag{8}$$

where the wave length λ is expressed in angstrom units. We now find the ratio of the number of ions to the number of O III ions to be given by

$$\frac{N_P}{N_0} = \frac{4.88}{f} \frac{\Omega_0}{\Omega} \frac{\lambda}{4363} \frac{I_p}{I_0} e^{(\chi_{PS} - \chi_0)/kT_e} (1 - \beta_0). \tag{9}$$

Table 1 gives the necessary atomic data for the calculation of N_P from H_n, T_e, and N_e. The values for the Einstein A's have been taken from the work of Pasternack, checked in many cases with the help of the tables or formulae of Shortley's work (Paper XI).

For some atoms, e.g., S II or N II, both the auroral (λ 5755 of N II) and the nebular (λ 6548 and λ 6584 of N II) lines are strong; and it is possible to estimate N_P in two ways. If the velocity distribution is reasonably Maxwellian, a comparison of these values should provide an estimate of the error of our approximate collisional cross-sections. The auroral

lines tend to give somewhat higher abundances than the nebular lines, but the ratios are not constant and fluctuate widely from nebula to nebula. Thus the values of Table 2, based principally on the intensity measures of Wyse, with additive measures of brighter lines by one of us, show discrepancies ranging up to a factor of 3, apparently not correlated with the electron temperature.

Let us now turn to the case of the p^3 configuration. There are three terms to be considered here: a ground $^4S_{3/2}$ term and higher $^2D_{3/2,5/2}$ and $^2P_{1/2,\,3/2}$ levels. We shall have to

TABLE 2*

IONIC ABUNDANCES DETERMINED FROM FORBIDDEN LINES

NEBULA	N I	N II		O II	O III	Ne III	Ne V	S II		S III	Cl III	Cl IV	A IV	A V
		Nebular	Auroral					Nebular	Transauroral					
NGC 7027	0.037	0.224	0.58	0.1	1.11	0.055	0.063	0.0093	0.0121	0.177	0.0028	0.0281	0.0054	0.0094
NGC 6572	.046	.108	.32	0.44	0.78	.076	.....	.0022	.008	.072	.0020	.....	.0038	.....
NGC 6826	.....	.....	.....	0.05	0.34	.031	.....	.....	.....	.....	.....	.....	.....	.....
NGC 6543	.....	.67	.....	1.14	2.16	.35	.....	.....	.....	.....	.....	.....	.....	.....
IC 418	.046	.17	.16	2.1	0.072	.0024	.....	.0065	.006	.028	.0017	.....	.....	.....
NGC 7662	.....	.011	.023	0.25	1.05	.0075	.0171	.0017	.0032	.035	.0011	.030	.011	.0014
NGC 7009	.....	.063	.057	0.48	1.28	.0145	0.0034	.0052	.0072	.052	.0037	0.044	.0066	.....
NGC 6741	.026	.207	.43	.....	0.69	.053	.....	.....	.011	.15	.0048	.....	.006	.003
NGC 2440	0.012	.054	0.11	0.02	0.10	.0095	.....	0.0005	.0018	.015	0.0005	.....	.....	.....
NGC 2165	.....	.046	.....	.....	0.73	.059	.....	.....	.0084	.048	.....	.....	.0064	0.0015
IC 5217	.....	0.032	.....	.....	0.67	0.064	.....	.....	0.0072	0.045	.....	.....	0.0054	.....

* From the fluorine lines observed by Wyse in NGC 7027 and NGC 7662 we estimated the abundance of the *F* II ion to be 3×10^{-4} in NGC 7027 and 1.6×10^{-4} to be the abundance of the *F* IV ion in NGC 7662. All abundances refer to numbers of ions per cm³ in the nebula. The *O* II abundances are computed on the basis of a weighted mean *A*-value of 7.2×10^{-5}, as determined from the Hartree field for *O* II (called "case *B*" in text).

consider the statistical equilibrium of these possible levels of the atom. For convenience we shall indicate the various terms and levels by the accompanying notation.

Abbreviation	Term
S	^4S
D	^2D
P	^2P

Abbreviation	Level
S	$^4S_{3/2}$
d	$^2D_{3/2}$
d'	$^2D_{5/2}$
p	$^2P_{1/2}$
p'	$^2P_{3/2}$

The number of atoms entering the d level by collisional excitation from the ground level and by radiative cascade from the P term will equal the number leaving by collisional and radiative processes:

$$\left.\begin{aligned}\frac{8.54\times10^{-6}}{T_e^{1/2}}\frac{N_sN_e}{\varpi_s}\Omega_{sd}e^{-\chi_{sD}/kT_e}+N_pA_{pd}+N_{p'}A_{p'd}\\ =\frac{8.54\times10^{-6}}{T_e^{1/2}}\frac{N_dN_e}{\varpi_d}\Omega_{sd}+N_dA_{ds}\end{aligned}\right\}\quad(10)$$

with a similar equation for d'. In these expressions we neglect the superelastic collisions which transfer atoms from P to D, since we shall suppose that the population of the P term is very small.

The number of atoms entering the P term by collision from the ground term must equal the number lost by superelastic collisions to the D or S terms and the radiative transitions. Thus for the p level we have

$$\left.\begin{aligned}\frac{8.54\times10^{-6}}{T_e^{1/2}}\frac{N_eN_s}{\varpi_s}\Omega_{sp}e^{-\chi_{sp}/kT_e}=\frac{8.54\times10^{-6}}{T_e^{1/2}}\frac{N_pN_e}{\varpi_p}[\Omega_{sp}+\Omega_{Dp}]\\ +N_P(A_{pd}+A_{pd'}+A_{ps}),\end{aligned}\right\}\quad(11)$$

with a similar expression for p'. We have neglected collisional and radiative transitions between p and p' and between d and d'. If the electron density is such that we can neglect the collisional de-excitations of the p levels in comparison with the radiative de-excitations, we may write for the level d:

$$\left.\begin{aligned}\frac{8.54\times10^{-6}}{T_e^{1/2}}\frac{N_sN_e}{\varpi_s}\Big\{\Omega_{sd}e^{-\chi^{SD}/kT_e}+e^{-\chi_{sp}/kT_e}\Big[\Omega_{sp}\Big(\frac{A_{pd}}{A_{pd}+A_{pd'}+A_{ps}}\Big)\\ +\Omega_{sp}\Big(\frac{A_{p'd}}{A_{p'd}+A_{p'd}+A_{p's}}\Big)\Big]\Big\}=\frac{8.54\times10^{-6}}{T_e^{1/2}}\frac{N_dN_e}{\varpi_d}\Omega_{sd}+N_dA_{ds},\end{aligned}\right\}\quad(12)$$

with a similar expression for d'. We may neglect the second term on the left side unless $\Omega_{Sp}>>\Omega_{Sd}$ or χ_{SP} is relatively small and T_e is large. Thus our expressions become even simpler, for it turns out that we can neglect the existence of the ^{2}P term altogether in calculating the equilibrium of the ^{2}D term. Of the N_D atoms in the ^{2}D term, let us *now* use d to denote the fraction in the $^2D_{3/2}$ level and d' the fraction in the $^2D_{5/2}$ level, with $d+d'=1$. The equation of statistical equilibrium for the ^{2}D term is then

$$\left.\begin{aligned}\frac{8.54\times10^{-6}}{T_e^{1/2}}\frac{N_sN_e}{\varpi_s}[\Omega_{sd}+\Omega_{sd'}]\,e^{\chi/kT_e}=\frac{8.54\times10^{-6}}{T_e^{1/2}}N_DN_e\\ \times\Big\{\frac{d}{\varpi_d}\Omega_{sd}+\frac{d'}{\varpi_{d'}}\Omega_{sd'}\Big\}+N_D[dA_{ds}+d'A_{d's}].\end{aligned}\right\}\quad(13)$$

If collisional de-excitations are more important than radiative transitions in depopulating the ^{2}D level, we may suppose that the populations of the two levels of the ^{2}D term are proportional to their statistical weights. In that case, $d=0.4$ and $d'=0.6$. If we let

$$\Omega_{Ab}+\Omega_{Ab'}=\Omega_{AB}\,,\quad(14)$$

and recall that $\tilde{\omega}_s=4$, $\tilde{\omega}_d=4$, and $\tilde{\omega}_{d'}=6$, we obtain

$$\left.\begin{aligned}N_S=0.4N_D\Big(1+\frac{0.4A_{ds}+0.6A_{d's}}{\Omega_{sD}}\,1.17\times10^6\frac{T_e^{1/2}}{N_e}\Big)\,e^{\chi/kT_e}\\ =0.4N_D\Big[1+\xi\frac{T_e^{1/2}}{N_e}\Big]e^{\chi/kT_e},\end{aligned}\right\}\quad(15)$$

where ξ depends on atomic constants only. The factor in parentheses is essentially b_S/b_D; it is a measure of the deviation from thermodynamic equilibrium. As N_e increases, $b_S/b_D\to1$, and

$$\frac{N_D}{N_s}=\frac{\varpi_D}{\varpi_s}\frac{b_D}{b_s}\,e^{-\chi/kT_e}\quad(16)$$

reduces to Boltzmann's law. The uncertainty in Ω will introduce but a small error in the computed value of N_S if N_e is sufficiently large and the A's are sufficiently small and adequately known. Otherwise the error will be directly proportional to the error in Ω and that in A.

The surface brightness of the planetary in the light of a forbidden line will be given by

$$S_\lambda=840\,(2.512)^{-H_\lambda}=\tfrac{1}{3}DN_D\,(dA_{dS}+d'A_{d'S})\,h\nu=\tfrac{1}{3}DN_D\bar{A}\,h\nu\,,\quad(17)$$

where H_λ is the surface brightness in magnitudes per square minute of arc. We thus obtain

$$N_S=\frac{1.01\times10^3}{A\,h\nu}\frac{b_s}{b_D}\frac{e^{\chi/kT_e}}{D}(2.512)^{-H_\lambda}=C_3\frac{b_s}{b_D}\frac{e^{\chi/kT_e}}{D}(2.512)^{-H_\lambda},\quad(18)$$

where C_3 depends only on atomic parameters. Table 1 gives the ion, the adopted A-values, the excitation potential χ, ξ, and f.

The transauroral $^4S - {}^2P$ transition is observed in S II; and for this line a similar theory yields

$$N_s = 1.28 \times 10^{15} \frac{e^{\chi_{sp}/kT_e}}{D} \left(\frac{b_s}{b_p}\right) (2.512)^{-H_\lambda} . \tag{19}$$

Except for *NGG* 2440 and 6572 the values of N_S for S II computed from the transauroral lines agree with those found from the nebular lines to within a factor of about 2.

The close O II pair at 3726.16 and 3728.91, corresponding to the $^4S_{3/2} - {}^2D$ transition, are second in importance only to the green nebular lines. These lines are observed in most planetary nebulae, in the diffuse nebulae of the Milky Way, and in emission nebulosities in external galaxies, but not in the novae.

Pasternack gives Einstein A-values for the $^4S_{3/2} - {}^2D_{3/2}$ and $^4S_{3/2} - {}^2D_{5/2}$ lines as 0.00011 and 0.0014, respectively. Since the statistical weights of the two ^2D levels are respectively 6 and 4, we should expect the relative intensities of these lines to be

$$\frac{6 \times A_{3729}}{4 \times A_{3726}} = 1.9 ,$$

in favor of the λ 3729 line. Actually, just the opposite is observed. The $^4S - {}^2D$ transition comprises both magnetic dipole and electric quadrupole components, whose strengths may be computed by the methods of Paper XI. For O II Shortley's paremeter, $\chi = 0.0153$, and the magnetic dipole strengths are given by

$$\left.\begin{aligned} S_m\,(^2D_{5/2} - {}^4S_{3/2}) &= \tfrac{2}{2}\tfrac{5}{4}\tfrac{5}{3}\chi^4 = 5.63 \times 10^{-9} \\ &\text{and} \\ A_m\,(^2D_{5/2} - {}^4S_{3/2}) &= 4.82 \times 10^{-7} \\ S_m\,(^2D_{3/2} - {}^4S_{3/2}) &= \tfrac{3}{9}\tfrac{0}{7}\tfrac{2}{2}\tfrac{5}{5}\chi^4 = 17.05 \times 10^{-8} \\ &\text{and} \\ A_m\,(^2D_{3/2} - {}^4S) &= 2.19 \times 10^{-5} . \end{aligned}\right\} \tag{20}$$

Similarly for the quadrupole transitions, we have

$$A_q\,(^2D_{5/2} - {}^4S_{3/2}) = 14.05 \times 10^{-5} s_q^2 , \qquad A\,(^4S_{3/2} - {}^2D_{3/2}) = 9.08 \times 10^{-5} s_q^2 , \tag{21}$$

where s_q depends upon the radial quantum wave functions according to the expression

$$s_q = \tfrac{2}{5} \int r^2 R\,(nl)\, d\,r , \tag{22}$$

where r is in atomic units. The total Einstein A coefficient is

$$A = A_q + A_m \tag{23}$$

for any given transition; and if we let $s_q = 1$, we obtain Pasternack's value. If we use the Hartree self-consistent field radial wave function, we find $s_q = 0.73$; and the resultant A-values are

$$A\,(^2D_{5/2}, {}^4S_{3/2}) = 7.45 \times 10^{-5} \qquad \text{and} \qquad A\,(^2D_{3/2}, {}^4S_{3/2}) = 6.8 \times 10^{-5} , \tag{24}$$

which give relative intensities of 1.64—again in contradiction to the observations.

A third of the possible procedures is to adopt the observed intensity ratio of the λ 3729 to λ 3726 lines (2 is a sufficiently accurate value for illustrative purposes) and calculate

the required values of the A's with the utilization of s_q as an adjustable parameter. Thus,

$$A\ (^2D_{3/2}, {}^4S_{3/2}) = 3A\ (^2D_{5/2}, {}^4S_{3/2})\ ;$$

and, since $A = A_q + A_m$, we obtain $s_q = 0.257$ and finally

$$A\ (^2D_{3/2}, {}^4S_{3/2}) = 2.78 \times 10^{-5} \quad \text{and} \quad A\ (^2D_{5/2}, {}^4S_{3/2}) = 0.93 \times 10^{-5}\ , \quad (25)$$

values considerably smaller than those found by Pasternack. These considerations illustrate the extreme sensitivity of the A-values to the outer portions of the radial wave functions. It is quite possible that the wave function may be inaccurate enough in this region of large r to account for the discrepancy.[9]

In view of the approximate character of the available target areas and transition probabilities, our results for *O* II are of a decidedly tentative character. We have computed the abundance of singly ionized oxygen on the basis of two assumptions concerning the weighted mean value of A, viz., assumption A, $s_q = 0.257$, and $A = 1.67 \times 10^{-5}$, which gives the correct intensity ratio but has no justification in quantum mechanical calculations; and assumption B, with $s_q = 0.73$, and $A = 7.19 \times 10^{-5}$, as calculated from the best available Hartree function but which, unfortunately, does not give the correct intensity ratio of the two components of the line.

Assumption A gives us a lower limit to the transition probability and therefore an upper limit to the abundance of ionized oxygen. Probably the results found from assumption B are more nearly of the correct order of magnitude.

Many years ago Wright[10] found an infra-red line at λ 7325 in NGC 7027. This line is the unresolved $^2P - {}^2D$ (auroral) pair of [*O* II] at λ 7319 and λ 7330. Wyse, however, did not observe these lines, and no intensity measures are available; so we cannot include them in our present study. On the basis of the excitation potentials and transition probabilities we would expect the intensity of this pair to be of the same order of magnitude as that of λ 4363 of [*O* III] for comparable abundances of *O* II and *O* III.

Unless the target areas for collisional excitation of neutral nitrogen are very small, i.e., $\Omega << 10$, we can probably get a good estimate of the abundance of this atom by simply supposing that the population of the ^2D term is given by Boltzmann's law and by calculating the number of metastable atoms from the intensities of their forbidden lines. Here again, unfortunately, the same objections that apply to the transition probabilities in *O* II are valid; if spin-orbit interactions are important in ionized oxygen, they are also important in neutral nitrogen. The scatter in the abundance of nitrogen as derived from the forbidden lines may represent actual variations in nitrogen content rather than effects of ionization or excitation. Where the [*N* II] lines are strong, they are nearly always accompanied by neutral nitrogen. Conversely, when they are weak, as in NGC 7662, NGC 7009, or IC 5217, the [*N* I] lines are missing.

In most elements we observe two successive stages of ionization; but neon deserves special comment, since, although the lines of *Ne* III and *Ne* V have been found in great strength in a number of planetaries, the auroral lines of *Ne* IV at λ 4714 and λ 4720 have not been found (the nebular lines fall in the inaccessible ultraviolet). Our equations of equilibrium reveal that with an electron temperature of 10,000° K, an electron density of 10^4, and an excitation potential of 7.7 volts, these lines should be about ten thousand times fainter than the *Ne* III lines. Their absence is thus easy to understand. Intensities of the *Ne* V lines in NGC 6741, 2440, 2165, or IC 5217 were not available.

The precision of our abundance determination could be improved were better esti-

[9] A refined treatment of the λ 3727 transition probabilities is being undertaken by C. W. Ufford and one of us. In this treatment the spin interaction of one electron with the orbit of another electron is being taken into account following a suggestion by J. H. Van Vleck. Calculations are at present in progress and should yield improved values of the transition probabilities eventually.

[10] *Pub. A.S.P.*, **32**, 64, 1920.

mates of the collisional cross-sections and transition probabilities available. Probably our results are correct in so far as orders of magnitude are concerned. As we shall see, the chief uncertainty of our attempted quantitative analysis comes not so much from poor knowledge of the relevant physical parameters, in many cases, as from the distribution of the atoms of a given element among the various stages of ionization. In the calculation of abundances, it is therefore not correct simply to add together the observed numbers of ions of each element. Such a procedure will give the right answer only for hydrogen and helium, since, as we shall see presently, the number of neutral hydrogen and helium atoms in the luminous body of a planetary nebula is very small. We would obtain too small an abundance of the other atoms, such as argon or oxygen, which can exist in six or eight stages of ionization. If we count only the number of observed ions of these atoms, we may get more or less correct relative abundances, but our absolute values will be in error by factors as high as 10 or more.

III. ABUNDANCES ESTIMATED FROM RECOMBINATION LINES

Permitted lines of helium, carbon, and oxygen in various stages of ionization are observed in the gaseous nebulae. Presumably these are recombination lines. Electrons are recaptured on high levels; and, as they cascade downward in energy, the atoms emit the ordinary permitted lines of the spectrum. Only for hydrogen and helium are the transition probabilities known, so that one may work out a theory of statistical equilibrium for these atoms. Hydrogen has been discussed in detail earlier in this series, and Goldberg has worked out the theory of statistical equilibrium for neutral helium.

The treatment of ionized helium follows at once from that of hydrogen; we may carry Menzel and Baker's tables from Paper III of the nebular series[3] directly over to the problem at hand. Since

$$X_n = \frac{hRZ^2}{n^2 kT_e} = \frac{hR}{n^2 k\left(\frac{T_e}{Z^2}\right)}, \tag{26}$$

we need only call the arguments of the tables $4T_e$ instead of T_e; e.g., the solution for *He* II at $T_e = 80{,}000°$ K is equivalent to that of hydrogen at 20,000°. Unfortunately, the tables do not contain entries for the physically interesting case of $T_e = 10{,}000°$ K. The strongest line of ionized helium is λ 4686, the first line of the Paschen series for which $n' = 3$, $n'' = 4$, $g = 0.768$, and $Z = 2$ in the usual expression (I-9)

$$E_{n'n} = N_i N_e \frac{KZ^4 b_n}{T_e^{3/2}} g \frac{2hRZ^2}{n'^3} e^{hRZ^2/n^2 kT_e} \tag{27}$$

for the amount of energy radiated per cubic centimeter per second. Here[11] $K = 3.20 \times 10^{-6}$, R is the Rydberg constant, and b_n is a number that measures the departure of the nth state from its population in thermodynamic equilibrium. Hence,

$$E_{4,3} = 3.92 \times 10^{-18} \frac{N_i N_e}{T_e^{3/2}} b_4 e^{X_4}; \tag{28}$$

and the number of doubly ionized helium atoms is, accordingly,

$$b_4 N_i = 6.43 \times 10^{20} \frac{T_e^{3/2}}{N_e D} e^{-X_4} (2.512)^{-H}. \tag{29}$$

If we knew b_4, we could find N_i at once; but, unfortunately, this quantity is not immediately available. One procedure is to assume Baker and Menzel's case *B* and to extra-

[11] The value of K in Paper I is incorrectly given.

polate b_4 from their table. In this way we have obtained $b_4 = \frac{1}{200}$, which is probably correct in so far as the order of magnitude is concerned. An alternative approach is to employ some of the higher lines of the Pickering series, alternate members of which are blended with the Balmer series and others of which are confused with lines of other elements. Convenient Pickering lines are λ 4542 and λ 5411, which Wyse has measured in a number of nebulae. The upper level of the first transition is $n = 9$; that of the second is $n = 7$. We obtain

$$b_9 N_i = 1.48 \times 10^{22} \frac{T_e^{3/2}}{N_e D} e^{-X_9} (2.512)^{-H_\lambda}$$

and

$$b_7 N_i = 7.19 \times 10^{21} \frac{T_e^{3/2}}{N_e D} e^{-X_7} (2.512)^{-H_\lambda}. \tag{30}$$

In all cases we have extrapolated b_n from Menzel and Baker's table for case *B*, obtaining $b_4 = 0.005$, $b_7 = 0.08$, and $b_9 = 0.125$. The resultant N_i's from λ 4686[12] and λ 4542 are usually in good agreement, in view of the precision of the measurements and the assumption that the b's are the same in all the nebulae. The N_i's obtained from λ 5411 are usually larger than those obtained from the other two lines. The assigned values of b may be in error, or Wyse's intensity estimates in the visual region may be on a slightly different scale from those in the photographic region.

The recombination lines of neutral helium are frequently strong in the planetary nebulae, indicating that helium is the most abundant element there, next to hydrogen. Ambarzumian[13] first treated the problem of the helium nebula and noted the interesting effects due to the high metastable levels 2^1S and 2^3S.

Since an ionized helium atom may recapture an electron in either a singlet or a triplet term the downward cascading electron will remain in the singlet or in the triplet system. Intercombination lines are virtually forbidden, since almost strict *LS* coupling obtains in helium.

Atoms in the high normal n^1P levels may cascade directly to the ground level with the emission of lines of the principal series, or they may linger on the way, dropping to n^1S_0, etc. If they reach the 2^1S_0 level, they find themselves in a metastable state. If there are no collisional de-excitations, the mean lifetime of this state is determined by the probability of the simultaneous emission of two photons. Breit and Teller,[14] on this basis, estimate that the lifetime of the 2^1S level is about the same as that for the 2s level of hydrogen, for which they find a lifetime of 0.14 second. The two quanta formed in this process escape from the nebula as part of the continuous radiation field. Accordingly, quanta of the principal series in helium suffer a fate somewhat different from that of the Lyman quanta in hydrogen. Consider, for example, the $1^1S - 3^1P$ transition. From 3^1P the atom may return to 1^1S, restoring the original quantum, or to 3^1S, thence to 2^1P, and on to 2^1S or 1^1S; or it may go to 2^1S directly. Quanta of the types $3^1S - 3^1P$, $2^1S - 3^1P$, and $2^1P - 3^1S$ escape from the nebula without further reabsorptions unless the metastable level is very heavily populated. By such a process, quanta of the principle series are degraded into low-frequency line quanta and continuous radiation from the double photon $2^1S - 1^1S$ transition.

On the other hand, all electrons recaptured on triplet levels cascade ultimately to the 2^3S level. According to Breit and Teller, the probability of the spontaneous emission of two photons is very much smaller (perhaps by a million fold) than in the case of 2^1S, so

[12] There is no evidence for any self-reversal of λ 4686 in the nebulae, although such self-reversal is quite apparent in such objects as Wolf-Rayet stars.

[13] *Pulkovo Bull.*, **13**, No. 3, 1933; *M.N.*, **93**, 50, 1932.

[14] *Ap. J.*, **91**, 215, 1940.

that it seems likely that in the case of a planetary nebula the bulk of the de-excitations of the 2^3S level take place by collision.

Ambarzumian treated the 2^3S level as rigorously metastable, in which case the $2^3S - 2^3P$, λ 10,830 transition plays the role of Lyman alpha and the $2^3S - 3^3P$, λ 3889 line the role of Lyman beta. Monochromatic nebular images in the λ 10,830 line would be very interesting. Unfortunately, the λ 3889 line is confused with $H\zeta$ of hydrogen, from which it cannot be separated.

More recently, Goldberg has treated the problem of the statistical equilibrium of neutral helium. Although he formally investigates an eight-state helium atom, he was able to allow somewhat for the variation of the continuous absorption coefficient with frequency and for the infinite number of discrete levels. In solving the equations of statistical equilibrium for the b's he used the results of his previous calculations of the f-values and treated the 2^1S and 2^3S levels as rigorously metastable. His treatment is based on purely radiative processes and takes no account of collisional effects or the possibility of the $2^1S - 1^1S$ transition.

In Table 3 we have summarized the results of the calculations of the helium abundances from two singlet lines, λ 4143 and λ 4388, and two triplet lines, λ 4471 and λ 5876. Goldberg's theory predicts a very great weakening of the singlet lines with respect to the triplets. For example, the relative intensities of λ 4143 and λ 4471 for an electron temperature of 10,000° K and a central star temperature of 50,000° K is predicted to be 0.013, while the observed intensity ratio is 0.16 for NGC 7662, according to the observations of Wyse. We find, on reference to the table, that the N_i's calculated from the singlets are some eight or ten times larger than the N_i's calculated from the triplets. So large a discrepancy can scarcely be attributed to any scale error in Wyse's intensities. We are inclined to look for an explanation in collisional and radiative effects not taken into account by Goldberg's treatment.

Collisions of electrons with atoms in the metastable ^1S and ^3S levels affect the populations of these and the higher levels in the following ways. In the first place, there may be superelastic collisions resulting in the de-excitation of ^1S and ^3S. For slow electrons, i.e., those with energies in the range from 0 to 5 volts, the cross-section for the de-excitation of the triplet is much greater than that of the singlet level, because the $^1S - {}^3S$ transition represents an effect of electron exchange and will be particularly important at low electronic energies. In the second place, inelastic collisions may excite atoms to the higher permitted levels from the metastable ones, and this effect would tend to make the b's larger than predicted by Goldberg's theory. Thirdly, although no radiative transitions between the singlet and triplet systems ever take place, collisional transitions are likely to be quite frequent, because the slow electronic velocities favor electron-exchange processes.

Accordingly, changes in density throughout the nebula ought to produce marked changes in the populations of the helium levels and in the resultant spectrum. Thus, in helium the effects of density fluctuations should be apparent in one stage of ionization, whereas, in general, density effects are apparent only in considering more than one stage.

We are inclined to attribute the strengthening of the singlets with respect to the triplets primarily to radiative processes. The singlet levels can be populated by direct transitions from the ground level; and if the radiation from the central star is rich in the resonance helium lines or if the nebula is of sufficient optical thickness to permit the building-up of an appreciable radiation density in the helium lines, radiative excitation may play the dominating role in producing the strong singlet lines. In our abundance calculations we have supposed this to be the case and have estimated the quantity of helium from the triplet lines. The resulting abundances may be too low if the collisional de-excitation of the 2^3S level is important.

When we turn to the radiative processes involved in recombination in more complex atoms, we are confronted with two very great difficulties. First, we must know the transi-

tion probabilities for jumps between all the upper levels and between the higher levels and the ground level. Second, we must use these parameters to calculate the statistical equilibrium for each level. Only then can we take the intensity of a given recombination line and infer the abundance of the ion which is gaining an electron.

Actually, we have not been able to carry this program through for any atom, and the best we can utilize is a rather approximate substitute. Wave functions for the excited and

TABLE 3

ABUNDANCES OF SINGLY AND DOUBLY IONIZED HELIUM FROM RECOMBINATION LINE INTENSITIES

ABUNDANCES OF SINGLY IONIZED HELIUM FROM He I LINES

Nebula	Singlets				Triplets			
	λ 4143		λ 4388		λ 4471		λ 5876	
	b_nN_i	N_i	b_nN_i	N_i	b_nN_i	N_i	b_nN_i	N_i
NGC 7027	256	3700	427	6150	184	750	306	1250
NGC 6572	463	5050	576	6300	261	1000	360	1450
IC 418	225	2250	462	4620	85	210	93	370
NGC 7662	525	4200	500	4000	197	580	143	420
NGC 7009	490	4900	585	5800	202	700	370	730
NGC 6741	.....	.....	.....	.....	49	220	260	1200
NGC 2440	134	1340	110	1100	42	120	68	190
NGC 2165	.....	.....	206	3420	76	370	68	330
IC 5217	1200	11000	800	7000	220	670	270	840

ABUNDANCES OF DOUBLY IONIZED HELIUM FROM He II LINES

Nebula	λ 4686		λ 5411		λ 4542	
	b_4N_i	N_i	b_7N_i	N_i	b_9N_i	N_i
NGC 7027	3.30	660	180	2300	80	640
NGC 6572	0.05	10	8	100	.....	.....
NGC 7662	6.2	1200	200	2500	170	1300
NGC 7009	1.3	260	130	1700	60	460
NGC 6741	1.1	210	100	1000	46	370
NGC 2440	12.0	230	90	1100	47	370
NGC 2165	1.0	210	30	380	78	600
IC 5217	0.75	150	35	440	.....	.....

ground levels of carbon and oxygen in various stages of ionization could be derived by Hartree's method or by some variation method, but such calculations are likely to be time-consuming. As a first rough approach to the problem, we have employed, for the evaluation of the radial quantum integrals, the wave functions calculated in the manner suggested by Slater. The Slater functions often give good approximations to the energies of the excited levels, but they neglect the loops and nodes of the wave functions, and the calculation of transition probabilities may suffer as a consequence. It seems likely, however, that they are definitely better than the hydrogenic functions, since they do take some account of the screening by the inner electrons.

The number of atoms in a level j is given by

$$N_j = b_j \frac{N_i N_e}{T_e^{3/2}} \frac{h^3}{(2\pi m k)^{3/2}} \frac{\varpi_j}{\varpi_i} e^{I_j/kT_e}, \tag{31}$$

where $\tilde{\omega}_j$ is the statistical weight of level j; $\tilde{\omega}_i$ is the statistical weight of the ion; and $I_j = I_0 - \chi_j$, where I_0 is the ionization potential and χ_j is the excitation potential of the level j. Now

$$N_j = \frac{2.52 \times 10^3}{DAh\nu} (2.512)^{-H_\lambda},$$

so that we obtain the general formula

$$b_j N_j = \frac{(2\pi m k)^{3/2}}{h} \frac{2.52 \times 10^3}{Ah\nu} \frac{\varpi_i}{\varpi_j} \frac{T_e^{3/2}}{N_e D} (2.512)^{-H_\lambda} e^{-I_j/kT_e}. \tag{32}$$

Consequently, if we can evaluate b_j, we can find N_j. In our preliminary reconnaissance, about the best we can do is to adopt the b's from the analogous hydrogenic problem. Accordingly, it is to be kept in mind that the abundances estimated from one or two lines are likely to be very approximate, clearly because of the necessity of making shaky assumptions about the b's. One cannot simply adopt the hydrogenic b's for the same n with any degree of assurance, because in complex atoms the l degeneracy is removed and there may be terms of several multiplicities and L-values arising from each configuration. Finally, configuration interaction may enter, and there may be deviations from LS coupling.

Carbon is represented only by its recombination lines. In the case of *O* II there is only the λ 4267 line corresponding to the $3d^2D - 4f^2F$ transition, for which we have derived $A = 3.18 \times 10^8$. The intensity of this line gives us an estimate of b_4 multiplied by the number of *C* III ions; and if we adopt hydrogenic b_4's, the number of *C* III atoms turns out to be of the same order of magnitude as the number of *O* III atoms. In a similar fashion we have estimated the abundance of the *C* IV ion from the λ 4187 recombination lines of *C* III with $b_5 = 0.10$.

Wyse has observed lines of *C* IV in a number of planetaries, indicating that four-times ionized carbon atoms must exist in such objects as NGC 7662 and NGC 7027. Unfortunately, for such highly ionized atoms we have no reliable means of estimating the b's, and consequently it is not possible to estimate the abundances of these ions. In particular, the λλ 5800–5813 *C* IV pair arises from a level 25 volts below the ionization limit, and $b_3 N_i$ turns out to be of the order of 10^{-12}; but b_3 is probably also very small, so we cannot guess the number of *C* V ions.

The permitted *O* II lines observed by Wyse in NGC 7009 are of particular interest because they allow an independent estimate of the *O* III abundance. Wyse believed he found a serious discrepancy between the abundance of *O* III ions calculated from the forbidden lines and that obtained from the recombination spectrum. He assumed the rate of capture to depend on Z^2 (it should have been Z^4, according to I-24) and compared the spectrum with that of hydrogen. It is not clear just what approximations one should make to treat carbon as a hydrogenic atom in view of the high order of degeneracy among the energy-levels of the latter. The radial wave functions must differ considerably, although by adjusting the effective Z-values some improvement may be effected.

As an alternative procedure we have computed the transition probabilities of the *O* II ions observed in NGC 7009 with the aid of Slater wave functions and the assumption of LS coupling. These computed A-values and Wyse's intensity measures enable one to estimate $b_n N_{O\,III}$ (see Table 4). Since we had no knowledge of b_n, we plotted $b_n N_{O\,III}$ against the excitation potential (see Fig. 1). Notice that, as the excitation potential increases, b_n increases. The circle in the upper right-hand corner indicates the estimate of

O III determined from the green nebular lines; it was placed on the diagram at the ionization limit, where $b_n = 1$. These data suggest to us that there is no discrepancy between the number of *O* III ions calculated from the green nebular lines and the number found

TABLE 4*

THE RECOMBINATION SPECTRUM OF O II IN NGC 7009

Transition	s	S	log A	χ	I	log $b_n N(O\,III)$
$p^2 3p - p^2 3d(^3P)$						
4072 $^4D - ^4F$	0.24	168	8.27	28.57	0.7	−1.61
4132 $^4P - ^4P$	.14	30	7.55	28.71	0.3	−0.98
4153 $^4P - ^4P$	.15	.....	7.41	28.70	0.4	−0.90
4156 $^4P - ^4P$	.15	.....	7.59	28.71	0.3	−1.03
4397 $^2D - ^2D$	.56	15	7.61	28.94	0.3	−1.07
$p^2 3p - p^2 3d(^1D)$						
4185 $^2F - ^2G$	.43	108	8.28	31.18	0.3	−0.60
4190 $^2F - ^2G$	.56	.....	8.30	31.18	0.3	−0.82
4873 $^2P - ^2D$	.60	21	7.64	31.24	1.0	0.70
$p^2 3p - p^2 4f$						
4284 $^4D - ^4F$	.04	374	8.50	31.62	0.3	0.37
4295 $^4P - ^4D$	.11	227	8.75	31.58	0.3	−0.65
4304 $^2P - ^4D$	.40	.....	9.02	31.57	0.4	−1.09
4609 $^2D - ^2F$	.58	168	8.85	31.00	0.4	−0.90
$p^2 3s - p^2 3p\ (^3P)$						
4318 $^4P - ^4P$	.29	12	7.67	25.74	0.4n	−2.94
4590 $^2D - ^2F$	.58	14	8.07	28.24	0.3n	−1.90
4598 $^2D - ^2F$	0.40	.....	8.02	28.24	0.30	−1.84

* The first column gives the various lines and term designations grouped according to configuration and parentage; s is the fraction of the strength of a multiplet radiated by a given line; S is the strength of the multiplet; log A is based on approximated wave functions; χ is the excitation potential; and I is taken from the work of Wyse.

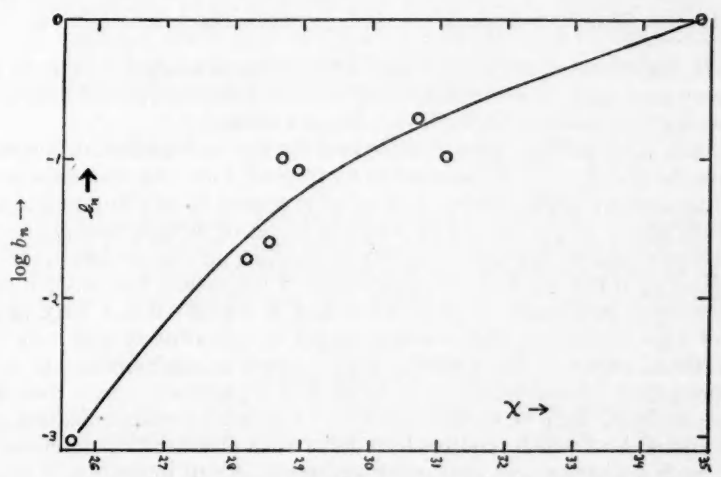

FIG. 1

from the recombination spectrum—a result especially satisfying in view of the approximate character of the A-values, the weakness of the lines, and the fact that target areas for *O* III may be in error by a factor of 2 or 3.

IV. IONIZATION AND STRATIFICATION

The calculated atomic abundances of the observable ions of hydrogen, helium, carbon, nitrogen, oxygen, fluorine, neon, sulphur, chlorine, and argon are summarized in Tables 2 and 5. The observational data for the weaker lines and for the lines in the visual region have been taken from the work of Wyse; for the stronger lines in the ordinary and photographic regions of the spectrum, from the investigations by one of us.[15] These tables also include the adopted electron densities and temperatures, and it will be noticed that they are somewhat different from the previously published values in some cases. For the objects observed by Wyse, for which no data on the Balmer continuum were available, we have estimated the electron density from the intensity of $H\beta$ in the manner indicated in Paper XII.

Most of the hydrogen in the luminous regions of the planetaries is ionized, so that the electron density which is equal to the ion density is essentially the density of hydrogen itself, since this gas is the most important constituent of gaseous nebulae. The estimates of ionized helium and doubly ionized helium follow from their recombination lines and

TABLE 5

ABUNDANCES ESTIMATED FROM RECOMBINATION LINES

Nebula	Hydrogen	*He* II	*He* III	C III	C IV
NGC 7027	5.9×10^3	750	650	1.08	0.3
NGC 6572	10.5	1030	10	1.2	.2
NGC 6826	4.5	181	.....	.....	.....
NGC 6543	11.7	415	.....	.....	.....
IC 418	11.0	210	.....	0.84	.....
NGC 7662	13.2	580	1200	2.12	0.2
NGC 7009	20.4	700	350	2.6	.....
NGC 6741	2.2	222	300	.....	.....
NGC 2440	1.5	120	300	0.3	.....
NGC 2165	2.4	366	300	0.7	.....
IC 5217	4.4	674	150	1.0	.....

are uncertain, for reasons previously cited. The carbon abundances, it is to be emphasized, are very uncertain. For the remaining ions, forbidden lines and approximate collisional cross-sections provide us with abundance estimates.

We find that, if we add up the contributions for the various ions of a given element and compare the result with the number of hydrogenic ions, the abundances tend to be somewhat less than we might expect. The nebulae appear to be composed of 90 per cent hydrogen with nearly 10 per cent of helium and traces of oxygen, carbon, and nitrogen, etc. The answer is that we have not been fair in counting up the number of the more complex ions. Hydrogen can exist in only one stage of ionization, but oxygen can exist in eight. Accordingly, we should try to take account of the fact that a large percentage of the atoms of a given element may reside in stages of ionization of which we have no direct observational evidence. Our problem is to choose a suitable method of apportioning the ions among the various stages of ionization, and it promises to be a complicated one. To illustrate, in NGC 7027 we observe lines of *N* I which have an ionization potential of 14.46 volts and of *Ne* V which requires that *Ne* IV with an ionization potential of 97 volts be ionized. Such a distribution among the various stages of ionization is scarcely to be expected in a nebula of uniform density, with no marked radial stratification and exposed to high-temperature black-body radiation. Several possible explanations suggest themselves.

[15] See Paper XIV of this series.

The planetaries are certainly not of uniform density or symmetrical structure. It seems very likely that local regions of high or low relative density may exist here and there throughout the nebula, thereby favoring fluctuations of the ionization. A nebula possessing a distinct filamentary structure may exhibit quite a different spectrum from a uniform nebula of the same mean density. Within the filaments the degree of ionization may tend to be smaller because of the higher density, the auroral lines may become more prominent with respect to the nebular lines, and the recombination lines may be especially favored. In the low-density regions, on the other hand, most radiations will be weakened; but those of highly ionized atoms may actually become enhanced, and the larger volume may compensate for the effects of a weaker emission per unit volume. In addition, the various filaments may be exposed to different radiation fields, so that the effects can become quite complicated.

Further, as Swings[16] has pointed out, the central stars of the planetaries probably do not radiate like black bodies in the ultraviolet; rather intense emission lines may be scattered throughout this region of the spectrum. We would certainly expect such ultraviolet emission lines in the Wolf-Rayet stars, and such lines may even exist in the nuclei showing continuous spectra. Within the nebula itself originate intense emission lines of Ly α, the λ 303 resonance line of *He* II, etc.; these may also play roles in ionization processes. The quantitative character of this radiation field is quite unknown; we shall be lucky if we can infer its general properties qualitatively.

The nebulae which show a symmetric type of stratification—e.g., small images of ionized helium and large *O* II images—present no essential difficulty. Many years ago Bowen[17] called attention to the fact that the high-frequency quanta would be rapidly absorbed by the nebula and that the radiation reaching the outer portions of the shells would be incapable of doubly ionizing helium or quadruply ionizing neon, for example. The general qualitative features are well understood; the details may offer some interesting problems.

Let us now develop the ionization formula for a complex atom exposed to dilute high-temperature radiation. First we shall obtain the relation between the capture coefficient for an electron of velocity v and the continuous absorption coefficient a_ν involved in the photoelectric ejection of an electron with velocity v. Since these are atomic parameters, we may evaluate them with the aid of the principle of detailed balancing in thermodynamic equilibrium; i.e., the number of ionizations in the frequency interval $d\nu$ will equal the number of captures from a velocity interval dv, viz.,

$$\frac{N_1 4\pi I_\nu a_\nu (1 - e^{-h\nu/kT})\, d\nu}{h\nu} = f(v)\, v\sigma dv N_i N_e , \tag{33}$$

where the negative absorptions (stimulated emissions) are taken into account by the factor in parentheses on the left. Here a_ν is the absorption coefficient; σ is the target area for capture; and ν is related to the velocity of the free electron by $h\nu = \chi + \frac{1}{2}mv^2$; $hd\nu = mvdv$. The velocity distribution $f(v)$ of the free electrons is given by Maxwell's law:

$$f(v) = 4\pi \left(\frac{m}{2\pi kT}\right)^{3/2} v^2 e^{-(mv^2/2)/kT} , \tag{34}$$

while for I_ν Planck's law obtains. Then we have

$$\frac{N_i N_e}{N_1} = \frac{8\pi a_\nu}{c^2}\, e^{-h\nu/kT} \frac{\nu^2 m}{h} \left(\frac{2\pi kT}{m}\right)^{3/2} \frac{1}{4\pi} \frac{e^{[1/kT](h\nu-\chi)}}{\sigma v^3} . \tag{35}$$

[16] *Ap. J.*, **95**, 112, 1942.

[17] *Ap. J.*, **67**, 1, 1928.

If we compare this expression with the ionization formula for thermodynamic equilibrium, we find that

$$\frac{2m\nu^2}{c^2 h\nu^2}\frac{a_\nu}{\sigma}\left(\frac{2\pi kT}{m}\right)^{3/2} e^{-\chi/kT} = \frac{(2\pi mkT)^{3/2}}{h^3}\frac{\varpi_e\varpi_i}{\varpi_1} e^{-\chi/kT}, \tag{36}$$

whence we derive the relation between a_ν and σ

$$\frac{a_\nu}{\sigma} = \frac{m^2v^2c^2}{\nu^2h^2}\frac{\varpi_e\varpi_i}{2\varpi_1}, \tag{37}$$

which holds quite generally and is not influenced by the state of the assembly or by how far it deviates from thermodynamic equilibrium.

In a planetary nebula nearly all the ionization will take place from the ground level, so that the number of ionizations

$$\int_{\chi_1}^{\infty} N_1 \frac{4\pi I_\nu a_\nu}{h\nu}\, d\nu = \frac{8\pi N_1}{c^2}\int_{\nu_1}^{\infty} \frac{\nu^2 W_{1\kappa} a_\nu}{\nu_1 (e^{h\nu/kT_1} - 1)}\, d\nu \tag{38}$$

will equal the number of captures upon all of the bound levels, viz.,

$$\sum_j \int_0^{\infty} N_{ij} N f(v)\, v\sigma_j dv = \sum_j \int_0^{\infty} \frac{N_{ij}N_e}{T_e^{3/2}} 4\pi \left(\frac{m}{2\pi k}\right)^{1/2} e^{-(mv^2/2)/kT}\sigma_j v^2 dv. \tag{39}$$

Except at the very lowest velocities, most of the recaptures will take place upon the ground level. Accordingly, we shall neglect the captures upon the higher levels in our preliminary study of the problem; this corresponds to taking only the first term in $\Sigma S_n/n^3 = G_{T_e}$ (cf. Paper V). We may change our variable of integration from v to ν, noting that $\chi_1 = h\nu_1$ and $v = 0$ for the ionization limit. If we substitute for σ in terms of a_ν and equate the resultant expression to the number of ionizations from the ground level, there results

$$\frac{N_i N_e}{N_1} = \frac{(2\pi mkT_e)^{3/2}}{h^3}\frac{\varpi_e\varpi_i}{\varpi_1} e^{-\chi/kT_e} \frac{\displaystyle\int_{\nu_1}^{\infty} \frac{W_{1\kappa}\nu^2 a_\nu}{(e^{h\nu/kT_1} - 1)}}{\displaystyle\int_0^{\infty} e^{-h\nu/kT_e}\nu^2 a_\nu d\nu}. \tag{40}$$

If $a_\nu \sim 1/\nu^2$, the ratio of the integrals reduces simply to

$$\overline{W}\frac{T_1}{T_e}\frac{e^{h\nu/kT}}{(e^{h\nu_1/kT_1} - 1)},$$

where $\overline{W}$ is the mean dilution factor.

Bates[18] has calculated a_ν for the neutral atoms *C*, *N*, *O*, *F*, and *Ne* from the Hartree wave functions. Goldberg and Aller have calculated a_ν for oxygen in various stages of ionization with the aid of an analytic representation of the Hartree wave functions. For other light atoms Hartree fields were not available, and approximate Slater functions have been utilized for the ground levels. The resultant absorption coefficients are probably no more than qualitatively correct. All these calculations show that for complex atoms the absorption coefficient does not fall off hydrogenically as ν^{-3}, as many writers have assumed, but may even rise for a distance beyond the series limit. Thus the absorption coefficient of oxygen reaches a maximum a little above the series limit at $\tilde{\nu} = 160{,}000$ and then falls off gradually with frequency. On the other hand, the absorption

[18] *M.N.*, **100**, 25, 1940.

coefficient of ionized and doubly ionized oxygen falls off monotonically with increasing frequency. In general, the continuous absorption coefficient tends to become more nearly hydrogenic as one goes to higher and higher stages of ionization.[19]

If the central stars of the planetary nebulae radiated essentially as black bodies and if the nebulae were so tenuous that the atoms throughout were exposed to dilute blackbody radiation, the precise character of the absorption coefficient would not play too great a role in determining the ionization; variations of a_ν according to ν^{-1}, ν^{-2}, or ν^{-3} would make but little difference in the results. If, however, the radiation impinging upon a typical volume element of the nebula is not simply dilute temperature radiation but is distorted by stellar emission lines and by emission lines arising in the nebula, the character of the absorption coefficient may assume considerable importance. For example, the absorption coefficient of oxygen falls off much more slowly with frequency than that of hydrogen. Consequently, line radiation far beyond the Lyman limit will be much more effective in ionizing oxygen than in ionizing hydrogen.

Aside from the purely geometrical aspects of the problem, W will be determined by (1) the nature of the initial radiation from the star and (2) the effect of absorption in the nebula itself upon the radiation from the central star.

As previously remarked, the central stars of the planetary nebulae are frequently stars of the Wolf-Rayet type, showing strong lines of helium, carbon, and oxygen, or helium and nitrogen, or sometimes lines of all of these elements. Swings[16] has suggested that the ultraviolet spectra of these stars in the region λλ 30–912 contain great numbers of intense lines of the aforementioned atoms. He calls attention to the fact that helium radiation from the stars at λλ 256.31, 243.02, and 237.33 may be absorbed by *C* III and *N* IV atoms, while, on the other hand, the coincidence of the ionization potentials of *O* III and *He* II cuts down the ionization of *O* III, owing to the fact that helium is much more abundant than oxygen. Thus, in NGC 6543 Swings finds fairly strong permitted lines of *C* III and *N* III in recombination, while those of *O* III are missing.[20]

In other planetaries, particularly certain high-excitation objects such as NGC 7009, NGC 3242, or NGC 7662, the nuclei exhibit apparently continuous spectra with no certain evidence of emission lines. We are ignorant of the ultraviolet spectra of these objects; but we reasonably might suppose that, if they contained strong ultraviolet emission lines, some emission lines ought to be found in the astronomically accessible regions. In any case, it does not seem safe to postulate the existence of strong emission lines in the ultraviolet spectra of all planetary nebulae.

We may illustrate the effects of the continuous absorption of radiation from the central star radiating as a black body by considering a hydrogen shell which, however, contains enough other atoms to lower the electron temperature to about 10,000° K in the manner indicated in Paper XVI. We have treated the problem of the transfer of radiation in the Lyman continuum in Paper II of this series. The method there employed essentially amounted to using a solution of the type suggested by Ambarzumian with an additional correction function, $R(\nu)$, which depended on the dilution factor W and the electron temperature T_e. It turned out that the correction function was too large to be treated as a perturbation, and the problem had to be solved by successive approximations. This treatment took no account of possible inelastic collisions with foreign atoms; the electron temperature was supposed to depend on the character of the radiation field

[19] The reason for the nonhydrogenic behavior of the absorption coefficient is that an outer electron in a partially filled 2p or 3p shell is incompletely screened by its neighbors. Such an electron will move in a field, $Z - \sigma$, where σ, which is a measure of the screening, is less than $(N - 1)$, where N is the number of electrons in the ion. On the other hand, if a 2p electron is raised to a d level, it will move in a nearly hydrogenic field of charge $Z - (N - 1)$. Consequently, in calculating the transition from the bound 2p to the free ɛd level, one cannot employ the same value of $Z - \sigma$ in the initial and final wave functions. For a fuller discussion of this and related points see Bates (*op. cit.*).

[20] *Ap. J.*, **92**, 289, 1940.

to which the volume element was subjected, in accordance with the conditions described in Paper V. Actually, as we have seen, the electron temperature of a planetary nebula is nearly constant at about 10,000° K. Accordingly, the theory of transfer of radiation in the Lyman continuum will have to be examined from a new point of view.

Consider an interval $d\nu$ at ν in the ultraviolet continuum. The absorption of energy at this frequency will depend roughly on $1/\nu^3$, since $a_\nu \sim 1/\nu^3$; but the emission of energy in this interval will depend on the number of electrons of velocity v (such that $h\nu = \chi + \frac{1}{2}mv^2$) that are captured per second. The number with the required velocity v will be determined by Maxwell's law and electron temperature T_e. Since the latter is in the neighborhood of 10,000° K, there will be very few high-velocity electrons with energies of the order of 4 or 5 volts; and consequently the captures from this velocity region will be very few. Thus, energy will be returned to the continuum only in frequencies near the series limit; and at frequencies corresponding to but a few volts beyond the series limit, the radiation will simply be extinguished by the nebula. In other words, radiation is piled up at the low-frequency end of the Lyman continuum at the expense of energy absorbed at the higher frequencies. Since the absorption coefficient is greatest at the lower-frequency end of the range, the over-all effect is to increase the rate at which the ultraviolet radiation is extinguished in the nebula. An approximate treatment of the equations of the problem shows that on the inner boundary of the nebula there is a concentration of radiation near the series limit. This "Lyman limit excess" gradually falls to a very small value near the outer boundary of the nebula, where the hydrogen is nearly all in the neutral condition. A more exact treatment of this problem, possibly by the methods being developed by Chandrasekhar, might be of great value in interpreting the observed nebular images. We must recall that in actual practice the ultraviolet radiation field is depleted not by one type of atoms but by several types. Probably neutral and ionized helium play important roles in this connection.

We shall now illustrate how the densities of the neutral atoms of hydrogen and singly ionized helium may be evaluated from the sizes of the nebular images. As an example, let us consider NGC 7009. If we adopt Berman's distance estimate,[21] the main portion of the nebula has a radius of 1.25×10^{17} cm and a shell of thickness 3.7×10^{16} cm. The absorption coefficient of hydrogen at the limit of the Lyman series is

$$a_\nu = \frac{2^5\pi^2\epsilon^6 RZ^4}{3\sqrt{3}\,ch^3}\frac{1}{\nu^3} = 5.0 \times 10^{-18}\left(\frac{\nu_1}{\nu}\right)^3$$

per atom. At an optical depth of about 3, extinction will be fairly complete; the portions of the nebula beyond this point will not contribute much to the luminosity of the nebular images. If N is the average number of neutral hydrogen atoms per unit volume, then

$$3 \backsim 5 \times 10^{-18} \times 3.7 \times 10^{16} \times N\ ,$$

or $N \sim 20$. Similarly, the thickness of the ionized helium shell is of the order of 2.5×10^{16} cm, $a_\nu = 1.25 \times 10^{-18}$, and $N \sim 100$ for an optical depth of 3. An independent calculation of the upper limit of the *He* II abundance gave for this nebula $N = 800$. Our elementary calculation has taken no account of the re-emission of radiation near the series limit, nor of the fact that the optical depth of 3 at the series limit corresponds to a somewhat smaller optical depth near by. Our calculation of N thus gives us a lower limit to the value of this quantity, but it does not seem likely that our estimates are in error by more than a factor of 2 or 3 from this cause.

In any case, these calculations justify the assumptions we have made to the effect that the hydrogen in the luminous portions of a planetary nebula is nearly all ionized. Hence the masses of the luminous portions calculated on the basis of this assumption seem justified. An examination of slitless spectrograms of a number of planetaries reveals

[21] *Lick Obs. Bull.*, **18**, 57, 1937.

that the outer edges of the hydrogen images are often fairly sharp. This shows that toward the boundary of the luminous portion the ionizing radiation becomes depleted over a short distance in the manner indicated by Strömgren[22] and that the gas becomes neutral. As the number of neutral atoms increases, the opacity to the ionizing radiation rises in proportion, and the nebula shows a sharp boundary. With a hydrogen density of about 6×10^3 atoms/cm^3 we see that an optical depth of about 3 can be attained in 10^{14} cm if the hydrogen is neutral. Thus, within a distance amounting to only a few per cent of the nebular radius, hydrogen can change from a condition of high ionization to an almost neutral condition.

The stratification effects for other atoms provide an interesting study. Slitless spectrograms obtained thirty years ago by Wright[23] showed that in many objects of complicated structure the main body of the nebula is surrounded by a faint extended envelope or shell shining with the λ 3727 radiation of [*O* II]. Presumably, radiation escaping from the inner shells has ionized oxygen in these outer regions. Since the ionization potential of neutral oxygen is almost the same as that of hydrogen, we might expect oxygen to be ionized in the regions where hydrogen is ionized and neutral where hydrogen is neutral. The absorption curve for oxygen, however, reaches a maximum at about λ 625 and then falls slowly to half its maximum value at λ 310; and it is still 30 per cent of its maximum at λ 170, which corresponds to an excitation potential of 74 volts. On the other hand, the absorptivity of hydrogen falls off as ν^{-3}, and therefore hydrogen is relatively transparent to radiations in the far ultraviolet while oxyen still absorbs energy appreciably. Thus it is not entirely surprising that oxygen is ionized at greater distances from the nucleus than is hydrogen.

Another point that should be stressed in discussing stratification in the planetary nebulae is the lack of radial symmetry often apparent in their structures. A glance at slitless spectra of NGC 7009, for example, shows that the λ 3727 radiation is concentrated at the ends of the spindle, whereas the λ 4686 radiation is strongest near the broader portions of the spindle. Any detailed discussion of stratification effects must take these irregularities into account. In the ansae of NGC 7009 the degree of excitation is much less than in the main body of the nebula, although even here much *O* III remains. In fact, if we suppose $N_e \sim 10^3$ and $T_e \sim 8000°$ K for the ansae, we obtain $N_{O\,II}/N_{O\,III} \sim 2$, which is nearly the same value as that for the main body of the planetary.

Line radiation is likely to play an important role in the ionization of atoms in the nebular shell; so we shall develop here the fundamental formulae for the problem. Detailed applications must wait until we have definite knowledge of line radiation intensities in the nebular shell. If an atom is excited from a ground 2p configuration to an excited nd configuration, the frequency of the absorbed radiation may be expressed in the form

$$\nu = RZ^2\left(\frac{1}{n_0^{*2}} - \frac{1}{n^2}\right),$$

where we choose n_0 in such a way as to reproduce the term value of the ground level. We suppose that the upper levels may be represented as hydrogenic; i.e., $T = RZ^2/n^2$. Transitions to the continuum may be represented by

$$\nu = RZ^2\left(\frac{1}{n_0^{*2}} - \frac{1}{\kappa^2}\right) = R\left(\frac{\chi}{\chi_H} + \frac{Z^2}{\kappa^2}\right),$$

where we have replaced n by $i\kappa$ and where χ is the ionization potential of hydrogen. If we let $\chi' = \chi/\chi_H$, the frequency of the bound-free transitions will be

$$\nu = R\chi'\left(1 + \frac{Z^2}{\chi'\kappa^2}\right).$$

[22] *Ap. J.*, **87**, 526, 1939.

[23] *Pub. Lick. Obs.*, **13**, 193, 1918.

Since the relation between the absorption coefficient a_ν and the oscillator strength f is

$$\int a_\nu d\nu = \frac{\pi e^2}{mc} f ,$$

we may formally express a_ν as $(\pi e^2/mc)(df/d\nu)$. Just to the redward side of a series limit there will be Δn lines of mean oscillator strength f per unit frequency interval, whereas just to the violet side the f-value per unit frequency interval will be $f\Delta\kappa$, and the f-value corresponding to the ν-interval $d\nu$ will be $df = fd\kappa$, while

$$a_\nu = \frac{\pi e^2}{mc}\frac{df}{d\nu} = \frac{\pi e^2}{mc}\frac{df}{d\kappa}\frac{d\kappa}{d\nu} = \frac{\pi e^2}{mc} f \frac{d\kappa}{d\nu} .$$

Now

$$d\nu = -\frac{2RZ^2}{\kappa^3} d\kappa ,$$

so that

$$a_\nu = \frac{\pi e^2}{mc} f \frac{\kappa^3}{2RZ^2} ,$$

where

$$f = \frac{1}{(2j'+1)} \frac{8\pi^2 m\nu}{3h} \frac{a^2}{4l^2-1} S\rho^2$$

can be calculated if the radial quantum integral ρ is known.

If the atom is exposed to intense radiation over an interval $\Delta\nu$, the amount of energy absorbed will be

$$a_\nu I_\nu \Delta\nu = \frac{\pi e^2}{mc} \frac{f\kappa^3}{2RZ^2} I_\nu \Delta\nu ,$$

and the amount of energy absorbed by N atoms exposed to a series of monochromatic sources will be

$$\frac{\pi e^2}{mc} \frac{1}{2RZ^2} \Sigma f \kappa^3 I_\nu \Delta\nu .$$

The order of magnitude of $\Delta\nu$ as suggested by equation (XVI-12) is about 1×10^{11}. In the case of *O* II an elementary calculation shows that an increase of energy in such a line as λ 303 of *He* II by a factor of 10^4 above the value to be expected from only the geometrical dilution may exert a controlling effect upon the ionization. Thus, photoelectric ionization by line absorption may very well be an important factor in controlling the ionization of the shell.

It should be clear from the foregoing that a theoretical calculation of the ionization in a gaseous nebula becomes a virtually hopeless task. The chief stumbling block is the unknown radiation field within the nebula; but, even if this were predictable, the interlocking effects of different radiations and stratification would render the problem one of forbidding complexity.

If we know the temperature of the central star and the electron density, it should be possible to take ions of the same atom in successive stages of ionization and work out empirical dilution factors. We have done this for the *O* III/*O* II ratio. The calculated W, of course, depends very critically on the assumed stellar temperature and varies, in the cases considered, from 10^{-13} to 10^{-16}. Upon using the *Ne* III/*Ne* V ratios we found that the same central star temperature gave very different dilution factors, and the attempt to calculate ionization from the theoretical formulae was abandoned.

V. ESTIMATES OF TOTAL ABUNDANCES

The final step in the calculation of abundances is to devise some ways of guessing the contribution from the unobserved ions. We have seen that there is no sound theoretical procedure for calculating these contributions, and we shall have to proceed in some purely empirical fashion. We feel reasonably confident that the abundances of various ions deduced from their forbidden lines and given in Table 5 are of the right order of magnitude, but the final step in determining the composition seems necessarily uncertain.

Our method of taking into account the variation of ionization among ions of different ionization potential is as follows: Let A_1 and A_2 denote the abundances of two ions of the same element in successive stages of ionization, and let χ_1 and χ_2 denote their ionization potentials. Then we shall suppose that A_2/A_1 gives us the ratio of the abundances of two ions of any kind with ionization potentials χ_1 and χ_2; i.e., we get a segment of the curve relating abundance with ionization potential. Other pairs of ions give other segments; and when these segments are fitted together by a vertical displacement on the relative-abundance–χ diagram, we get a curve which will tell us how we may expect the ions of a given element to be distributed among their various stages of ionization.

For example, the relative abundances of *O* II and *O* III suggest the relative degree of ionization of atoms of 13.5 and 34.9 volts, ionization potential, the relative numbers of *Ne* III and *Ne* V ions, the relative degrees of ionization of ions of 40.5 and 97 volts, etc. Thus, for NGC 7027 we get the accompanying table relating ionization and ionization

Ionization Potential (Volts)	Relative Ionization	Ionization Potential (Volts)	Relative Ionization
0 (neutral)	0.01	50	0.68
10	0.023	60	.52
20	0.13	70	.42
30	0.81	80	.37
40	1.00	100	0.28

potential. Neutral atoms fall at zero; singly ionized atoms, at the first ionization potential; etc. Thus the relative abundance of *Ne* II is taken as 0.18 (ionization potential of *Ne* I is 21.5 volts); that of *Ne* III is 1.0 (I.P. = 40 volts); that of *Ne* IV is 0.48 (I.P. of *Ne* III is 63 volts); etc. From the relative ionization graphs for each nebula we can calculate the distribution of ions of each element among the various stages of ionization, and therefore the fraction contributed by the observed ions to the total.

Unfortunately, there is a considerable scatter in the points which serve to determine the graphs. In the first place, the abundances derived from approximate target areas may be in error by a factor of 2 or 3 or even more. In the second place, the assumption that the ionization varies smoothly with ionization potential, as assumed in our graphs, cannot be correct if the central star has strong bright lines in its ultraviolet spectrum. Hence the relative proportions of successive ions of a given element may be very different from what we would expect from the graph.

The resultant abundances are listed in Table 6. In some cases, where the discrepancy is particularly bad, we have tabulated the results from two different ions of the same atom. The second of the difficulties listed above may be the dominating trouble here. In most other cases, both ions of a given element give reasonably concordant values. The figures in parentheses are those obtained from a previous calculation, in which it was presumed that the target area for the collisional excitation of the metastable levels varied as Z^2 for the more highly stripped ions. In general, the older calculations give the same order of magnitude as the newer ones, suggesting that effects of selection, ionization, etc., introduce a larger uncertainty than ignorance of the correct target areas.

The scatter in the relative abundances of Table 6 probably arises from the unavoidable approximations and effects of selection more than from variations in chemical composition. For carbon we have had to rely on recombination lines entirely and have given greater weight to *C* III than to *C* IV because of the greater uncertainty in the *b*-factor for the latter. The results for nitrogen are based primarily on the *N* II ion, and in many cases the ratio of total to observed ions is very large. The spread of the computed oxygen abundances, which have been calculated from the intensities of the green nebular lines and good target areas, is less than the spread of the computed abundances of other elements. The relative ionization curves indicate that for oxygen the *O* III ions contribute a large

TABLE 6*

THE COMPOSITION OF THE PLANETARY NEBULAE

Nebula	*He*	*C*	*N*	*O*	*F*	*Ne*	*S*	*Cl*	*A*
NGC 7662...	135	1.06	0.018	0.33	0.00003	0.0016	0.006	0.0087	0.003
	.....	.....	.....	.....	.....	0.0078	0.033	.....	0.0001
	(154)	(0.9)	(0.03)	(0.31)	(0.00009)	(0.02)	(0.02)	(0.0025)	(0.0005)
NGC 6741...	237	.....	1.9	0.63	.....	0.05	0.29	0.009	0.008
	.....	.....	.....	.....	.....	.....	.....	.....	0.003
NGC 7027...	240	0.73	1.34	0.42	0.0012	0.02	0.27	0.013	0.0023
	.....	.....	.....	.....	.....	.....	.....	0.044	.....
	(260)	(0.81)	(1.48)	(0.7)	(0.00008)	(0.04)	(0.21)	(0.006)	(0.0009)
NGC 2440...	280	0.82	0.92	0.18	.....	0.015	0.058	0.0021	0.0014
NGC 7009...	52	0.34	0.018	0.16	.....	0.002	0.010	0.014	0.0012
	.....	.....	.....	.....	.....	.....	.....	0.001	.....
	(56)	(0.3)	(0.02)	(0.25)	.....	(0.002)	(0.007)	(0.0012)	(0.00035)
NGC 6572...	100	0.18	0.08	0.12	.....	0.022	0.016	0.0004	0.0015
	(103)	(0.21)	(0.09)	(0.28)	.....	(0.064)	(0.016)	(0.0003)	(0.0011)
IC 418...	19	0.12	0.025	0.19	.....	.....	0.004	0.0003	.....
	(25)	(0.20)	(0.095)	.....	.....	.....	(0.009)	(0.0002)	.....

* This table gives the number of atoms of a given kind per thousand hydrogen atoms. In some cases the abundances calculated on the basis of two ions of the same atom disagreed significantly; so we give both results. The figures in parentheses refer to results of an earlier calculation, in which the abundances of the various ions were calculated on the basis of different assumptions about the target area Ω for collisional excitation of the metastable levels.

share of the total in most planetaries. Hence the oxygen abundances ought to be fairly well established as of the order of from 10^{-3} to 10^{-4} that of hydrogen. The data for fluorine are very scanty, and the corrections for ionization are very large and uncertain. Neon turns out to be less abundant than we might have anticipated from the work of Unsöld on τ Scorpii. Argon, the next in line of the noble gases, is of the order of ten times less abundant than neon, while sulphur seems comparable in amount. The forbidden lines of chlorine and argon are both very weak.

When we compare the different nebulae, we notice a considerable scatter in the relative contributions of the various elements. For example, in NGC 7027 the abundances of nearly all elements seem unusually high with respect to hydrogen, the Balmer continuum of which seems unusually weak for such a bright nebula. It may be that a greater proportion of atoms of a given element are represented by observable ions than we anticipated; and until this matter is further investigated, we cannot distinguish between this and the possibility that hydrogen is actually less abundant there.

We have attempted no abundance estimates for the metals, since the corrections for ionization would be so uncertain as to render the results quite meaningless. The target areas are unknown even though we may have transition probabilities.

The "average composition" of a planetary nebula, essentially obtained by taking a geometric mean of the abundances in Table 6, may be compared with the results obtained for the solar atmosphere by Menzel and Goldberg[24] and for the atmosphere of τ Scorpii by Unsöld. (See Table 7.)

The uncertainties in all methods are very great; but the abundances of carbon, nitrogen, and oxygen, with respect to hydrogen, in τ Scorpii seem, nevertheless, very similar to the results for the sun or the gaseous nebulae. For helium, nitrogen, oxygen, and sulphur the agreement between the solar and nebular abundances is surprisingly good. The discrepancy of a factor of 10 for carbon is easily understandable because our estimates are ultimately based on a single recombination line of *C* II. The discrepancy for neon

TABLE 7

COMPARISON OF THE AVERAGE COMPOSITION OF A PLANETARY NEBULA WITH THE COMPOSITIONS OF THE SUN AND τ SCORPII

Element	Relative Numbers of Atoms		τ Scorpii
	Planetary Nebula	Sun	
Hydrogen	1000.0	1000.0	1000.0
Helium	100.0	222.0	175.0
Carbon	0.6	0.04	0.17
Nitrogen	0.2	0.12	0.3
Oxygen	0.25	0.37	1.0
Fluorine	0.0001	.....	.....
Neon	0.01	.....	1.1
Sulphur	0.036	0.037	.....
Chlorine	0.002	.....	.....
Argon	0.0015	.....	.....

probably arises from other causes. It may be that τ Scorpii is richer in neon content than the average star or that conditions are particularly suitable for the excitation of neon lines.

Thus the conclusion of Bowen and Wyse that the chemical composition of the gaseous nebulae is essentially the same as that of the sun appears to be substantiated by an independent and more elaborate theoretical treatment of the same problem. We have attempted to use the splendid observational material obtained by Wyse to deduce the abundances of a number of ions which are not observable in the sun.

It would seem that further progress along these lines cannot be made until improved observational and theoretical material is available. The identifications of additional ions, especially those having higher ionization potential than does *Ne* V, would be very helpful in estimating the distribution of the various ions among different stages of ionization. Target areas for various ions ought to be computed; such calculations are in progress at present for *O* II.

This paper completes the series of articles entitled "Physical Processes in Gaseous Nebulae."

[24] *Atoms, Stars, and Nebulae*, Philadelphia: Blakiston, 1942.

REVIEWS

Cosmogony of the Solar System. By V. G. FESSENKOFF. (In Russian.) Moscow and Leningrad: Academy of Sciences of the U.S.S.R., 1944. Pp. 112. R. 5.00.

This book consists of six chapters: (i) "The Structure of the Solar System; Planets and Asteroids"; (ii) "The Zodiacal Light"; (iii) "The Scale of the Solar System and Its Relation to the System of the Stars"; (iv) "The Physical Properties of the Planets; Planets without Atmospheres; Planets with Atmospheres"; (v) "The Age of the Solar System"; and (vi) "The Origin of the Solar System; The Hypotheses of Kant and of Laplace; The Theory of Jeans and Jeffreys; How Was the Solar System Really Formed?"

The presentation is popular and avoids the use of mathematics. The first three chapters are especially elementary and are not quite consistent with the much greater demands upon the reader's training made by the rest of the book. Thus, a reader who must be told how a planet differs from a fixed star (p. 3) can hardly be expected to understand why the principle of conservation of angular momentum should render untenable the nebular hypothesis of Laplace (p. 85) or why in Bethe's carbon cycle the atom of C_{12} reappears at the end of the reaction (p. 72). But the last three chapters are stimulating in the extreme. They comprise nearly four-fifths of the book and reflect the highly individualized interests of the author.[1]

In some respects the treatment resembles that of H. N. Russell's famous little book, *The Solar System and Its Origin*, of which Fessenkoff makes occasional use, as, for example, in the discussion of the angular momentum per unit mass in relation to the original theory of a close encounter. But in many other respects Fessenkoff's treatment is new, as in the case of his conclusion that the zodiacal light is formed by particles of recent origin and cannot be considered a remnant of an original nebula; or it digests material which has not yet been applied in this form to cosmogony—as is his discussion of the velocities of escape from the sun, required, according to recent computations by Parijsky, to produce closed orbits around the sun, in the event of the close passage of another star.[2]

The original nebular hypothesis by Kant is presented with more than the customary amount of detail, and its influence upon the later meteoric theory of Ligondès and the planetesimal hypothesis of Moulton and Chamberlin is briefly traced. The work of Laplace is discussed somewhat less thoroughly, as are the various objections to it. The author rejects all theories which require the building-up of planets from a uniform medium of small particles, because he believes that they contradict the discontinuity of structure inside the earth, established by Wiechert in 1907. He also rejects the various theories which depend upon the encounter or close passage of another star, largely because of the small probability of such an event. He does not mention such recent work as that of Spitzer and of Whipple on the effect of interstellar matter upon the formation of a star or that of Hoyle and Lyttleton on mass accretion in cosmic dust or in gas clouds. Nor could he have been acquainted with Weizsäcker's recent theory, published in 1943 in the *Zeitschrift für Astrophysik*.

The last section of the sixth chapter presents Fessenkoff's own views. He assumes that the sun

[1] The reviewer remembers a stimulating colloquium which took place about thirty years ago at the observatory of the University of Kharkov in southern Russia, at which Professor Fessenkoff and others presented a review of Poincaré's book *Leçons sur les hypothèses cosmogoniques*. Fessenkoff had then recently returned from Paris, where he had worked for several years on his dissertation, entitled *La lumière zodiacale*. Some years earlier he had made an extensive series of visual observations of the surface features of Jupiter and had published a memoir on the structure of this planet. This work probably determined the evolution of his scientific interests. He is now a member of the Academy of Sciences of the U.S.S.R. and editor of the *Astronomical Journal of the Soviet Union*.

[2] A few minor errors may be corrected: On p. 6: the discovery of Pluto was made by Tombaugh at the Lowell Observatory, using a 13-inch photographic refractor, not a reflector. On p. 9: the discovery of the fifth satellite of Jupiter by Barnard was made at the Lick Observatory, not at Yerkes. On p. 37: the idea of formaldehyde snow on Venus has been abandoned by Wildt. On p. 73: there is something wrong with the labeling of his Figure 21, illustrating the carbon cycle.

was originally a stable star of low density, whose rotation was not excessive. Periods of stability, during which the energy was generated by different nuclear mechanisms, were separated by periods of rapid contraction, during which the angular rotation increased to the extent of causing instability. In order to re-establish stable conditions, the star underwent fission, with the creation of a double (or multiple) star of mass ratio of not more than about 0.001. Fessenkoff does not consider this ratio improbable, and he believes that recent observational evidence has tended to fill in the gap between typical double stars and typical planetary systems.[3] The original planet moved in an approximately circular orbit whose diameter was of the order of ten times the diameter of the sun. Tidal action is invoked to increase the size of the orbit to its present value. Taken as a whole, this section is too short and much too lacking in mathematical verification fully to satisfy the reader.

About a year ago the *Scientific Monthly* reprinted a famous article by T. C. Chamberlin on the method of multiple hypotheses in scientific research. This method, so admirably suited to the study of many geological problems, has found a particularly fertile field of application in cosmogony, and Fessenkoff makes use of it to the fullest extent. We observe the present condition of the solar system, and we find a number of regularities which cannot be due to chance. We do not, as a rule, observe the evolutionary processes in action which have given rise to these regularities. But we do possess one great advantage over the geologists: we can observe other stars, in different stages of their evolution; and while we cannot, with our present equipment, obtain much useful information concerning any possible planetary systems of other stars, we can at least make use of a large volume of information pertaining to the central bodies of any such systems. It seems to the reviewer that this method of approach has not been sufficiently used in cosmogonical studies. Some of the oldest hypotheses (Laplace) and some of the most recent (Weizsäcker, Fessenkoff) attribute the origin of the planets to the rapid rotation of a parent-body or of a nebulous mass around it. But Fessenkoff does not mention the rotational velocities of the stars. The present equatorial rotational velocity of the sun is quite slow—of the order of 2 km/sec—and is so far below the critical velocity, of about 400 km/sec, required to cause rotational instability at the equator that we are of necessity faced with the question: "Did the sun have a very rapid angular rotation before the planets were formed?" Since we cannot answer this question directly, we must have recourse to observations of other stars. But we do not definitely know how the stars evolve, and it would be dangerous to choose a sequence, that uses for its criterion the spectral type or the luminosity of the stars and to assume that this sequence has an evolutionary significance. But we do know that the vast majority of the stars of the solar type, which are not close binaries, have very slow rotations. The sun is in this respect, as in so many others, a typical G-type star of the main sequence. On the other hand, the majority of stars of spectral classes B, A, and early F have rapid rotational velocities; and some of them may even now be close to rotational instability. The transition, at about spectral class F5, in the average rotational velocity, as we pass from the early classes to the later ones, is very sudden and does not resemble the gradual changes observed in most (but not all) physical characteristics. Since we do not definitely know whether early-type stars change into late-type stars, we cannot go much further. But it is suggestive that, on the one hand, we are certain that rapid rotations among the single stars of solar type are extremely rare or absent, while, on the other hand, we discern no obvious correlation between rotational velocity, within, say, the main-sequence stars of class A, and other physical characteristics—mass, luminosity, etc.—such as might be expected to exist if angular momentum can be lost by a star without change in spectral type. The possibility exists that in some unknown manner rapidly rotating stars of early type are transformed into slowly rotating stars of later type, through the creation of a planetary system which takes with it a large fraction of angular momentum of the original star.

To this limited extent the observational facts tend to support Fessenkoff's idea that planetary systems are formed by rapidly rotating stars and result in the transfer of a large amount of angular momentum from the original star to the planets. In this connection it may be recalled that Kreiken many years ago remarked that, if the angular momenta of the planets were combined with that of the sun, the resulting equatorial velocity would be comparable to the larger values observed by the reviewer and by Elvey in stars of early type (about 120 km/sec).

Fessenkoff does not elaborate upon the actual physical process which, in his opinion, permits

[3] Fessenkoff mentions Holmberg's work but does not refer to recent papers by Strand, Reuyl, Van de Kamp, and others. He points out that observational selection favors the discovery of double stars having mass ratios of the order of one.

the rapidly rotating star to get rid of most of its angular momentum by transferring it to the planets. His discussion of the traditional stages of development culminating in the breakup of a pear-shaped body is sketchy and leaves the reader in doubt as to how this mechanism can lead in some cases to the formation of a double star and in others to the formation of a planetary system. Then, of course, there remain unanswered the various objections which have been raised, by Moulton, MacMillan, and others, to the original fission theory.

The observations have given us no certain indication that pear-shaped bodies are now in existence in the universe. The only resemblance to such bodies we have is in the case of close binaries having common envelopes of nebulous matter (β Lyrae). But the breakup may take relatively little time, so that the lack of observational confirmation has little significance. On the other hand, we seem to have quite definite indications that in some early-type stars rotational breakup leads to the formation of very tenuous gaseous rings or shells (Pleione). In close binaries, where instability is favored by tidal action, the existence of these rings has been demonstrated by the periodical eclipses of the two lobes of the rings (RW Tauri, SX Cassiopeiae, etc). The amount of matter contained in these rings is much too smal to produce anything like a planetary system, even if all of it should condense. So far as we can tell, the rings are unstable, and they often disintegrate completely within a few years after their formation. These considerations may not apply to stars with expanding shells, like P Cygni, the Wolf-Rayet stars, the novae, etc.; but no one has ever evoked the process of rotational breakup to explain the attendant phenomena of these groups of stars.

Fessenkoff correctly points out that the formation of equatorial rings, as considered by Jeans in the case of stars which are greatly concentrated toward their centers, cannot relieve the star of a sufficient amount of angular momentum to guarantee its stability during the intervals of contraction. Such a star would remain unstable as long as the contraction lasts, and it would—continuously or discontinuously—shed equatorial rings. The star could not be transformed into a slowly rotating body, and consequently this process could not have produced the solar system. But we can hardly conclude, as Fessenkoff does, that therefore the origin of the planets *must* have been by the process of fission.

It may be best at this time to admit that we do not know by what means the planetary system became endowed with the large amount of angular momentum it now possesses. Tempting, as it is, to follow the processes to their origin, there is some danger in the resulting oversimplification of what a star really is.

O. STRUVE

Yerkes Observatory